Investigating the link between defective DNA end-processing and human neurological disease

A thesis submitted to the University of Sussex for the degree of Doctor of Philosophy

By

John J Reynolds

January 2011

Declaration

I hereby declare that this thesis has not been and will not be submitted, in whole or in part to another University for the award of any other degree.

John J Reynolds

Acknowledgements

"I love deadlines. I like the whooshing sound they make as they fly by."

Douglas Adams

Whilst searching for an appropriate quotation to use at the front of my thesis I happened upon this one by Douglas Adams and felt compelled to include it. This quotation quite succinctly and irreverently sums up a time of unexpected difficulties that coincided with the final months of my PhD. There were many moments during the writing of this thesis when its completion was utterly unimaginable and it is with a not insubstantial amount pleasure and relief that I submit the completed version.

There are many people who are intricately linked to this work that I would like to acknowledge. Firstly I have to thank my supervisor Professor Keith Caldecott for his guidance, support and understanding throughout the completion of both my laboratory work and my thesis. All the members of the Caldecott lab, both past and present, as well as fellow scientists and students at the Genome Damage and Stability Centre have also offered indispensable help over the years, especially Stuart, who doesn't realise how much he is appreciated and without whom the lab would certainly be a poorer place. My family and friends also deserve recognition for sticking by me. Particular mention has to be made to both Helen and Ross for so many fun and memorable moments over the years and also to Sean and Julie who especially deserve thanks for housing me in the final months. Lastly I cannot finish this acknowledgement without mentioning the vending machine in the JMS café, without which I would surely have succumbed to hunger during the many late evenings I have spent in the laboratory.

And now for the science bit.

University of Sussex

John J Reynolds

Doctor of Philosophy Biochemistry

Investigating the link between defective DNA end-processing and human neurological disease

Summary

DNA single-strand breaks (SSB) are the most commonly occurring type of DNA damage arising in a cell and they are repaired by rapid repair pathways collectively termed single-strand break repair (SSBR). Recently several rare hereditary neurodegenerative disorders with mutations in genes associated with SSBR, spinocerebellar ataxia and axonal neuropathy-1 (SCAN1), ataxia oculomotor apraxia-1 (AOA1) and microcephaly with early onset seizures and developmental delay (MCSZ), have been discovered. A striking aspect that these disorders have in common is that they are all caused by mutations in end-processing factors. The majority of SSBs that arise via endogenous damage have 'dirty' termini and require end-processing to restore DNA ends with conventional 'ligatable' chemistry. Another common feature of these end-processing enzymes is their association with XRCC1, a scaffolding protein that is a core component of SSBR. Complete loss of XRCC1 is embryonically lethal and the conditional deletion of XRCC1 in the developing mouse brain leads to persistent DNA damage, cerebellar interneurons loss and abnormal hippocampal function resulting in behavioural abnormalities such as seizures and episodic epilepsy. Taken together these observations suggest that neural cells are exquisitely sensitive to defects in chromosomal SSBR. In my thesis, I will describe biochemical and cellular data on lymphoblastoid and fibroblast cell lines derived from patients with mutations in the end-processing factors aprataxin (APTX is mutated in AOA1). I will include data showing that aprataxin is required for the short-patch SSBR of abortive ligation intermediates *in vitro* and that repair arrests in AOA1 cell lines due to insufficient levels of non-adenylated DNA ligase.

Contents

List of Figures

List of Tables

Abbreviations

(6-4)PP	=	6-4 photoproducts
3meA	=	3-methyladenine
7meG	=	7-methylguanine
8-oxo-G	=	8-hydroxyguanine
α,β	=	3'-α,β unsaturated aldehyde
Ade	=	Aldehyde
Alkaline comet assay	=	Alkaline single-cell agarose-gel electrophoresis
AMP	=	adenosine monophosphate
AOA1	=	ataxia oculomotor apraxia
AP site	=	Apurine/Apyramidine
APH	=	Aphidicolin
APS	=	Ammonium persulfate
APTX	=	Aprataxin
AT	=	Ataxia Telangtiectasia
ATLD	=	Ataxia telangtiectasia - like disorder
ATM	=	Ataxia telangtiectasia mutated
ATP	=	Adenosine triphosphate
BIR	=	Break induced recombination
BER	=	Base excision repair
BLM	=	Bloom's syndrome protein
bp	=	Base pair
BRCT	=	Breast cancer associated protein 1 C-terminal domain
CΔ5	=	Deletion of the 5 most C-terminal amino acids in Chlorella Virus DNA ligase
Ci	=	Curie
CHK2	=	Checkpoint kinase 2

CHO	=	Chinese hamster ovary
cDNA	=	Cloned DNA
CK2	=	Casein kinase 2
cm	=	Centimetre
CPD	=	Cyclobutane pyrimidine
CPT	=	Camptothecin
C-terminus	=	Carboxyl terminus
CTBP	=	C-terminal Binding Protein
CtIP	=	CTBP interacting protein
CV Ligase	=	Chlorella Virus DNA ligase
DDB	=	DNA damage binding heterodimer
DDR	=	DNA damage response
ddH_2O	=	double distilled H_2O
ddTTP	=	Dideoxythymadine triphosphate
DMSO	=	Dimethyl sulfoxide
DNA	=	Deoxynucleic acid
DNA PK	=	DNA dependent protein kinase
DNA PKcs	=	DNA dependent protein kinase catalytic subunit
dNTP	=	Deoxynucleotide triphosphate
DPBS	=	Dulbecco's phosphate buffered saline
dRP	=	5’-deoxyribose phosphate
DSB	=	Double strand break
DSBR	=	Double strand break repair
DTT	=	Dithiothreitol
dTTP	=	Deooxythymadine triphosphate
E.coli	=	*Escherichia coli*
ECL	=	Enhanced chemiluminescence
EDTA	=	Ethylenediaminetetraacetic acid

EGTA	=	Ethylene glycol tetraacetic acid
ERCC1	=	Excision repair cross-complementing 1
EXO1	=	Exonuclease 1
FCS	=	Foetal calf serum
FEN1	=	Flap endonuclease 1
FHA	=	Fork-Head Associated Domain
Gy	=	Gray
^{3}H	=	Tritium (hydrogen-3)
H2A	=	Histone H2A
H2AX	=	Histone H2A variant X
γH2AX	=	Histone H2A variant X phosphorylated on S139
H_2O_2	=	Hydrogen peroxide
HCl	=	Hydrochloric acid
HDR	=	Homology directed repair
HECT domain	=	Homologous to the E6-associated protein carboxyl terminus
HERC2	=	Hect domain and RCC1-like domain containing 2
HINT	=	Histidine triad nucleotide-binding protein
His	=	Histidine
HIT	=	Histidine Triad Domain
HJ	=	Holiday junction
HNT3	=	Histidine triad Nucleotide-binding 3
hr	=	Hour
HR	=	Homologous recombination
hTERT	=	Human telomerase reverse transcriptase
IMAC	=	Immobilised metal affinity chromatography
IPTG	=	Isopropyl β-D-1-thiogalactopyranoside
IR	=	Ionising radiation
kan	=	Kanamycin
Kb	=	Kilobase

KCl	=	Potassium chloride
LB	=	Luria-Bertani medium
L	=	Litre
LCL	=	Lymphoblastoid cell line
LigI	=	DNA ligase I
LigIIIα	=	DNA ligase III α
M	=	Molar
MCSZ	=	Microcephaly, early-onset, intractable seizures and developmental delay
MDC1	=	Mediator of DNA damage checkpoint protein 1
MEF	=	Mouse embryonic fibroblasts
$MgCl_2$	=	Magnesium chloride
µg	=	Microgram
µl	=	Microlitre
µm	=	Micrometre
µM	=	Micromolar
ml	=	Millilitre
MLS	=	Mitochondrial localisation signal
mg	=	Milligram
min	=	Minute
MMS	=	Methyl methanesulfonate
mM	=	Millimolar
MPG	=	N-methylpurine-DNA glycosylase
Mre11	=	Meiotic recombination 11
MRN	=	Mre11/Rad50/Nbs1
MRX	=	Mre11/Rad50/Xrs2
mtLigIIIα	=	Mitochondrial LigIIIα
MYH	=	*MutY* homolog
NAD(P)H	=	Nicotinamide adenine dinucleotide phosphate

NBS1	=	Nijmegen breakage syndrome 1
NEIL1	=	Endonuclease VIII-like 1
NEIL2	=	Endonuclease VIII-like 2
Ni	=	Nickel
ng	=	Nanogram
NLS	=	Nuclear localisation signal
nM	=	Nanomolar
N-terminus	=	Amino-terminus
nt	=	Nucleotide
NTase	=	nucleotidyltransferase
NTA	=	Nitrilotriacetic acid
NTH1	=	Endonuclease III homolog
OB-fold	=	oligonucleotide binding
OD	=	Optical density
OGG1	=	8-oxoguanine DNA glycosylase
OH	=	Hydroxyl
ORF	=	Open reading frame
P	=	Phosphate
p53	=	Tumour protein 53
PAGE	=	Polyacrlyamide gel electrophoresis
PAR	=	Poly(ADP-ribose)
PARG	=	Poly(ADP-ribose) glycohydrolase
PARP1	=	Poly(ADP-ribose) polymerase 1
PBS	=	Phosphate buffered saline
PCNA	=	Proliferating cell nuclear antigen
PG	=	Phosphoglycolate
pI	=	Isoelectric point
PIKK	=	Phosphoinositide-3-kinase-related protein kinase

PLD	=	Phospholipase D
PMSF	=	Phenylmethanesulfonylfluoride
PNK	=	Polynucleotide kinase phosphatase
Polβ	=	DNA polymerase beta
Pol δ/ε	=	DNA polymerase delta/epsilon
Polι	=	DNA polymerase iota
Polλ	=	DNA polymerase lambda
ppi	=	Pyrophosphate
RAD50	=	Radiation sensitive 50
Rad27	=	Radiation sensitive 27
RCC1	=	Regulator of Chromosome Condensation 1
RPA	=	Replication protein A
ROS	=	Reactive oxygen species
RNA	=	Ribonucleic acid
RNF8	=	Ring finger protein 8
RNF168	=	Ring finger protein 168
rpm	=	Rotations per minute
s	=	Second
SAM	=	S-adenosylmethionine
SCAN1	=	Spincocerebellar axonal neuropathy 1
SDS	=	Sodium dodecyl sulphate
SDSA	=	Synthesis dependent strand annealing
siRNA	=	Small interfering RNA
SMUG1	=	Single-strand-selective monofunctional uracil DNA glycosylase
S-phase	=	Synthesis phase
Spo11	=	SPOrulation 11
SSA	=	Single-strand annealing
SSB	=	Single-strand break

SSBR	=	Single-strand break repair
TAE	=	Tris base, Acetic acid, EDTA
TBE	=	Tris base, Boric acid, EDTA
TBST	=	Tris-buffered saline and Tween 20
TDG	=	Thymine-DNA glycosylase
TDP1	=	Tyrosyl-DNA phosphodiesterase 1
TDP2	=	Tyrosyl-DNA phosphodiesterase 2
TdT	=	terminal deoxyribonucleotidyltransferase
TEMED	=	Tetramethylethylenediamine
TOP1	=	DNA topoisomerase 1
TOP2	=	DNA topoisomerase II
U	=	unit
Ub	=	Ubiquitin
UNG	=	Uracil- N-glycosylase
UV	=	ultraviolet
UVDE	=	Ultraviolet DNA endonuclease
V	=	Volt
V(D)J recombination	=	Variable (Diverse) Joining recombination
v/v	=	Volume per volume
VZ	=	Ventricular zone
SVZ	=	Subventricular zone
W	=	Watt
WT	=	Wild type
w/v	=	Weight per volume
XLF	=	XRCC4-like factor
XP	=	Xeroderma pigmentosum
XPA	=	Xeroderma pigmentosum complementation group A
XPF	=	Xeroderma pigmentosum complementation group F

XRCC1	=	X-ray cross complementing 1
XRCC4	=	X-ray cross complementing 4
Xrs2	=	X-Ray Sensitive 2
ZnF	=	Zinc finger motif

CHAPTER ONE

Introduction

1.1 DNA damage and repair

The DNA in our cells is under constant attack from DNA damaging agents which are a continuing threat to genomic integrity (Lindahl, 1993, Ward, 1998). Maintenance of genomic integrity is of fundamental importance to the continuing survival of the cell and without the multitude of DNA repair pathways that exist, the cell would very quickly accumulate lethal DNA aberrations and would cease to function. A large variety of DNA damage can occur from three main sources. The first common source of DNA damage is environmental. Ultraviolet (UV) radiation that is a component of sunlight is a major source of exogenous DNA damage and induces bulky lesions, such as cyclobutane pyrimidine dimers (CPD) and 6-4 photoproducts ((6-4)PP) that distort the DNA double helix (Hoeijmakers, 2001). Exogenous genotoxic agents, such as polycyclic aromatic hydrocarbons that can be found in cigarette smoke and heterocyclic amines found in over-cooked foods, can also damage DNA and induce bulky adducts (Hoeijmakers, 2001). A third source of exogenous DNA damage is ionising radiation (IR) in the form of either γ-rays or X-rays which induce DNA breaks, both DNA single – strand breaks (SSB) and double – strand breaks (DSB), and base damage via the production of hydroxyl (OH) radicals (Ward, 1975, Ward et al., 1987, Ward, 1998). A large source of naturally occurring ionising radiation is radon, a radioactive gas that emanates from uranium-containing soil and porous rock (Al-Zoughool and Krewski, 2009, Bissett and McLaughlin, 2010).

The second source of DNA damage are endogenous (by)products of cellular metabolism. Reactive oxygen species (ROS) such as superoxide anions, OH radicals and hydrogen peroxide can induce a staggeringly large variety of oxidative DNA lesions (Cadet et al., 2003, Sander et al., 2005, Beckman and Ames, 1997, Evans, 1997). Endogenous ROS are generated during a number of cellular processes such as during the electron transfer chain, when “leaked” electrons encounter oxygen, in the immune response, when phagocytic cells produce an oxidative burst to kill virally or bacterially infected cells and during lipid peroxidation in peroxisomes (Evans, 1997, Cooke et al., 2003). The large amount of ROS generated by the cell means that a high level of oxidative DNA damage can be measured in normal tissues at any time.

A third source of DNA damage is the tendency of some chemical bonds in DNA to spontaneously disintegrate under physiological conditions. Nucleotide residues can hydrolyse, leading to abasic (AP) sites and the spontaneous deamination of cytosine, adenine, guanine or 5-methylcytosine can result in uracil, hypoxanthine, xanthine and thymidine respectively (Lindahl, 1993).

The consequences of unrepaired DNA lesions are generally deleterious. DNA replication or transcription can become blocked as polymerases are unable to bypass bulky DNA lesions caused by exposure to UV light or polycyclic aromatic hydrocarbons. The accumulation of unrepaired bulky adducts can lead to cell-cycle arrest and/or cell death. Some DNA lesions are particularly mutagenic, such as oxidative 8-hydroxyguanine (8-oxo-G) which can pair with cytosine or adenine with equal affinity, potentially resulting in a GC →TA point mutation (Shibutani et al., 1991, Akbari and Krokan, 2008). The accumulation of damage-induced point mutations is a driving factor in oncogenesis as it can lead to deregulation of the cell cycle as the result of either the loss of tumour-suppressor genes or the untimely activation of oncogenes (Hoeijmakers, 2001, Kastan and Bartek, 2004, Stratton et al., 2009). DSBs are considered to the most genotoxic lesion that can arise and if left unrepaired or repaired inappropriately can lead to a variety of chromosomal aberrations and/or mis-segregation of chromosomes during mitosis (Hoeijmakers, 2001). SSBs, although not considered to be genotoxic themselves, can be converted into DSBs by collision with a replication or transcription fork (Kuzminov, 2001, Hoeijmakers, 2001, Kouzminova and Kuzminov, 2006).

The examples briefly discussed here show that a variety of adverse outcomes can result from DNA damage and serve to highlight the importance of the accurate repair of DNA for cell survival. As there is a very large variety of DNA lesions that can arise, there are also numerous over-lapping DNA response and repair pathways that have evolved in all organisms to maintain genome stability. The ultimate function of these genome maintenance pathways is the accurate transmission of genetic information to subsequent generations.

1.2 DNA Single Strand Breaks

DNA single-strand breaks (SSB) are discontinuities in one strand of the DNA sugar phosphate backbone and are the most commonly occurring type of DNA lesion in the cell. It has been estimated that as many as 10,000 SSBs can arise in a single cell per day (Lindahl and Nyberg, 1972, Lindahl, 1993, Sander et al., 2005, Ward, 1998, Caldecott, 2001, Beckman and Ames, 1997). Although SSBs are not considered to be particularly genotoxic themselves, if left un-repaired and allowed to convert into DSBs via collision with replication or transcription machinery, the sheer volume of breaks would quickly overwhelm the DSBR capacity of the cell (Kuzminov, 2001, Deckbar et al., 2007). As a consequence of this cells have evolved rapid and efficient repair pathways collectively single-strand break repair (SSBR) (Reviewed in detail in (Caldecott, 2008)).

There are a number of different sources of endogenous SSBs. SSBs can arise directly from the disintegration of oxidized sugars following attack on the sugar-phosphate backbone of DNA by ROS (Ward et al., 1987, Ward, 1998). This is the biggest source of SSBs owing to the creation of large amounts of ROS during normal cellular metabolism (Beckman and Ames, 1997, Evans, 1997, Cadet et al., 2003, Sander et al., 2005). SSBs created in this manner are usually associated with a single nucleotide gap resulting from base loss and typically possess "damaged" DNA termini. These are termini that have different chemistry from the conventional 3'-hydroxl and 5'-phosphate moieties that are required for DNA ligation. It has been estimated that ~70% of 3' termini of ROS induced SSBs possess a 3'-phosphate and ~30% possess a 3'-phosphoglycolate (Ward, 1998, Caldecott, 2001). The 5' termini of these SSBs usually contain an undamaged 5' – phosphate although a small percentage possess a 5'-hydroxyl.

SSBs can also arise indirectly as the result of the enzymatic processing of damaged bases during the base excision repair pathway (BER). Base damage is another consequence of ROS induced DNA damage and it is thought that up to 20% of the total DNA damage induced by ionising radiation is comprised of oxidized bases (Von Sonntag, 1987, Demple and DeMott, 2002). Indeed over 70 types of oxidative base and sugar products can be generated (Sander et

al., 2005). 8-hydroxyguanine (8-oxo-G) is a commonly occurring oxidative lesion and is the most frequently used marker for oxidative base damage (Figure 1.1A) (Kasai et al., 1984, Lindahl, 1993, Sander et al., 2005). As mentioned above this oxidative lesion is particularly mutagenic as adenine can be inserted opposite an 8-oxo-G lesion with the same frequency as cytosine during DNA replication and can result in a GC →TA point mutation (Figure 1.1B) (Shibutani et al., 1991).

Alkylation of DNA is another important source of base damage (Sedgwick et al., 2006). S-adenosylmethionine (SAM) is the donor of methyl groups during cellular enzymatic methylation events (Figure 1.2A) (Sedgwick et al., 2006, Barrows and Magee, 1982). SAM has a very high transfer potential and is a source of spontaneous DNA methylation. It has been shown that SAM induces the same base adducts as the alkylating agent methyl methanosulfonate (MMS) (Rydberg and Lindahl, 1982). Two noteworthy products arising from the methylation of DNA are 7-methylguanine (7meG) and 3-methyladenine (3meA) (Figure 1.2B). 3meA is considered to be genotoxic as it blocks both RNA and DNA polymerase activity (Sedgwick et al., 2006).

A third source of base damage is the spontaneous deamination of cytosine to uracil which can result in the mis-incorporation of adenine and can result in a CG→TA point mutation (Figure 1.3). It has been estimated that spontaneous cytosine deamination events can occur 60-500 times in a cell per day (Krokan et al., 2002, Barnes and Lindahl, 2004). Additionally cytosine deamination can be caused by ROS induced oxidative damage resulting from ionising radiation (Bjelland and Seeberg, 2003). Apurinic/apyramidinic sites (AP) sites result from the intrinsic instability of DNA in aqueous solution and are a major source of endogenous SSB. It has estimated that in each cell per day 2000-10000 depurination events occur (Lindahl and Nyberg, 1972, Lindahl, 1993).

A final source of endogenous SSBs is via the abortive action of the enzyme topoisomerase 1 (Top1). Top1 relaxes supercoiled duplex DNA during transcription and DNA replication by nicking one strand of the DNA double helix and allowing it to unwind (Roca, 1995, Wang,

2002). A transient cleavage complex is formed, in which Top1 becomes covalently linked via a 3' phosphotyrosyl bond to the DNA, before the nick is resealed. These nicks are usually resealed rapidly and are not a source of endogenous SSBs. However if a DNA or RNA polymerase collides with Top1 before the nick is resealed, then the cleavage complex can become trapped as a Top1-SSB, probably due to the misalignment of the 5'-OH, and the SSB cannot just be religated (Pommier et al., 2003). The Top1 inhibitor camptothecin (CPT) increases the half-life of the cleavage complexes and is used to experimentally increase the level of Top1-SSBs (Pourquier et al., 1997). Top1-SSBs can also become trapped if the cleavage complex occurs in the close proximity of another DNA lesion (Pourquier et al., 1997).

1.3 DNA single strand break repair

As described above SSBs can either arise directly from the fragmentation of damaged sugars, indirectly during the removal of damages bases in base excision repair (BER) or as the result of abortive Top1 activity. However, despite the variety of ways SSBs can occur, they are all repaired in overlapping repair pathways collectively termed single-strand break repair (SSBR) (reviewed in (Caldecott, 2008)). Most SSBR pathways proceed through four stages of repair; detection of the break, end-processing of damaged termini, gap-filling and DNA ligation (Figure 1.4, 1.5 and 1.6).

1.3.1 Detection

Detection of direct SSBs is achieved by the enzyme poly(ADP-ribose) polymerase 1 (PARP1) (D'Amours et al., 1999, Kim et al., 2005) (Figure 1.4). PARP1 has a very high affinity for DNA breaks and upon binding it catalyses the polymerisation of long branched chains upon itself and other target molecules (Benjamin and Gill, 1980, Weinfeld et al., 1997, Bramson et al., 1993). Once autoribosylated the PARP1 molecule disassociates from the break (Ferro and Olivera, 1982, Zahradka and Ebisuzaki, 1982) and is rapidly targeted by the enzyme poly(ADP-ribose) glycohydrolase (PARG) which catalyses the degradation of the poly(ADP-ribose) polymers, allowing PARP1 to be recycled (Cortes et al., 2004, Fisher et al., 2007).

PARP1 has been shown to have an important role in stimulating rapid SSBR as the depletion, deletion or inhibition of PARP1 results in decreased rates of repair of global SSBs (Fisher et al., 2007, Le Page et al., 2003, Godon et al., 2008). Importantly depletion of PARG imparts a similar SSBR defect (Fisher et al., 2007). One way in which PARP1 could be facilitating rapid SSBR is by stimulating the rapid accumulation of downstream SSBR factors. PARP1 is known to interact with, and is required for the rapid accumulation of foci at sites of oxidative damage, of the core SSBR protein X-ray cross complementing protein 1 (XRCC1) (Caldecott et al., 1996, El-Khamisy et al., 2003, Masson et al., 1998). XRCC1 does not appear to have any enzymatic activity but has an essential role in cells, as evidenced by the fact that *Xrcc1-/-* mice do not survive past embryonic day 6.5 (Tebbs et al., 1999, Tebbs et al., 2003). Additionally four Chinese hamster ovary cell lines (CHO) that harbour mutations in XRCC1 display hypersensitivity to DNA damaging agents and exhibit global SSBR defects (Caldecott, 2003b).

XRCC1 contains three domains; an N-terminal domain and two BRCT domains, and also contains putative PAR binding motifs (Caldecott, 2003b). It interacts with numerous components of SSBR and it is thought that it helps facilitate rapid repair by acting as a molecular scaffold for the various repair factors involved and helps to organise the downstream steps of SSBR (Figure 1.4) (Caldecott, 2003b, Caldecott, 2003a). Confirmed partners of XRCC1, other than PARP1, include DNA polymerase β (Polβ) (Caldecott et al., 1996, Kubota et al., 1996, Luo et al., 2004), polynucleotide kinase phosphatase (PNK) (Whitehouse et al., 2001, Luo et al., 2004), aprataxin (APTX) (Clements et al., 2004, Luo et al., 2004), AP endonuclease 1 (APE1) (Vidal et al., 2001) and DNA ligase IIIα (LigIIIα) (Caldecott et al., 1994, Caldecott et al., 1995, Nash et al., 1997). XRCC1 has also been shown to stimulate the activities of a number of its interacting partners (Whitehouse et al., 2001, Mani et al., 2007, Lu et al., 2010, Marsin et al., 2003, Campalans et al., 2005).

Detection of base damage is achieved in a different manner to direct SSBs. Altered bases cause minor perturbations in the DNA helix which are recognised and cleaved by distinct DNA glycosylases (Figure 1.5). Ten DNA glycosylases have been identified to date and each recognises and excises specific damaged bases (Reviewed in (Robertson et al., 2009)). There are two types of glycosylase; mono-functional and bi-functional glycosylases (Figure 1.7) (a list

of known DNA glycosylases and their substrates is presented in Table 1.1). Both types catalyse the cleavage of an N-glycosidic bond, releasing the damaged base and creating an AP site (Lindahl, 1974). AP sites generated by mono-functional glycosylases are then cleaved by AP endonuclease I (APE1) to produce a SSB with a 3'-OH and a 5'-dRP (Demple et al., 1991). Bi-functional glycosylases possess an additional AP lyase activity and cleave the abasic site themselves in either a β elimination or βδ elimination reaction, resulting in SSBs containing single nucleotide gap with a 5'-P and a 3'-αβ unsaturated aldehyde or 3'-P respectively (McCullough et al., 1999, O'Connor and Laval, 1989, Hegde et al., 2008).

PARP1 has been seen accumulating at sites of base damage, although it is not thought that PARP1 plays the same role in the repair of indirect SSBs produced during BER as it does in the repair of direct SSBs (Durkacz et al., 1980). XRCC1 has been shown to interact with the DNA glycosylases OGG1, NEIL1, NEIL2 and MPG as well as APE1 (Vidal et al., 2001, Marsin et al., 2003, Campalans et al., 2005, Das et al., 2006) and it is thought that SSBs arising during the initial stages of BER are simply relayed to the next step in SSBR and would not require the action of PARP1 to be detected. It is also not currently clear whether PARP1 plays a role in the detection of TOP1-SSBs.

1.3.2 End – processing

As mentioned previously, the majority of SSBs possess "damaged" termini. For successful DNA ligation to occur the conventional 3'-OH and 5'-P chemistries have to be restored and as a consequence a large variety of DNA end-processing factors have evolved to repair the different chemistries arising at damaged DNA breaks (the structures of the different chemistries that arise at the termini of damaged SSBs are shown in Figures 1.8 and 1.9, and the enzymes that are involved in processing them are detailed in Table 1.2). DNA breaks with damaged termini are considered to be cytotoxic as they could lead to the production of collapsed replication or transcriptions forks. Repair of the 3' terminus is also thought to be particularly crucial as a damaged 3' terminus would not support DNA polymerase activity if left unrepaired and could lead to the continued blockage and prevention of replication fork restart. The importance of DNA end-processing is highlighted by the observation that three human neurological disorders

associated with mutations in SSBR proteins have been discovered to be caused by defects in end-processing factors. These three factors are APTX, TDP1 and PNK as and are mutated in ataxia oculomotor apraxia 1 (AOA1), spinocerebellar ataxia with axonal neuropathy 1 (SCAN1) and microcephaly, early-onset, intractable seizures and developmental delay (MCSZ) respectively (Date et al., 2001, Moreira et al., 2001, Takashima et al., 2002, Shen et al., 2010)

An end-processing factor that is particularly worthy of attention is PNK, a bi-functional protein that possesses both 3' phosphatase and 5' kinase activity (Jilani et al., 1999, Karimi-Busheri et al., 1998, Whitehouse et al., 2001, Bernstein et al., 2005b). PNK contains an N-terminal FHA domain, through which it interacts with CK2 phosphorylated XRCC1 and XRCC4, and phosphatase and kinase catalytic domains (Loizou et al., 2004, Whitehouse et al., 2001, Bernstein et al., 2005b). PNK is considered to be a critical protein in SSBR due to the sheer volume of SSBs possessing a 3'P that can potentially arise in a cell per day. 3'-P termini, which is a major substrate for PNK, arises at approximately 70% of direct SSBs induced by ROS (Figure 1.4), at SSBs created indirectly via the excision and cleavage of base damage by a bi-functional DNA glycosylase in a βδ elimination reaction (Figure 1.5 and 1.7) and following TDP1 activity during the repair of TOP1-SSBs (Figure 1.6) (Caldecott, 2001, Ward, 1998, O'Connor and Laval, 1989, Interthal et al., 2001). This critical role is further underlined by the observation that mutations in PNK result in the human developmental disorder MCSZ (Shen et al., 2010). PNK also acts to repair termini harbouring a 5'-OH, which can also arise as the result of ROS induced sugar fragmentation or following TDP1 activity although it is not thought that the 5' kinase activity of PNK plays as large a role in SSBR as its 3' phosphatase activity (Ward, 1998, Caldecott, 2001, Interthal et al., 2001). In support of this PNK has both a higher affinity for and a greater activity on 3'-phosphorylated substrates than on DNA substrates with a 5'-OH (Dobson and Allinson, 2006).

APE1 is an important SSBR factor that is involved in the repair of both direct and indirect SSBs (Figure 1.4 and 1.5). In addition to its AP lyase activity, it has also been shown to repair 3'PG termini (Demple et al., 1991, Chen et al., 1991, Demple and Harrison, 1994, Winters et al., 1992, Winters et al., 1994), and to a lesser extent, 3'P termini (Chen et al., 1991, Demple and Harrison, 1994, Izumi et al., 2000). SSBs possessing 3'-PG termini are another common type of

lesion that requires processing. 3'-PG arise at approximately 30% of direct SSBs induced by ROS (Ward, 1998, Caldecott, 2001). APE1 is essential in mammalian cells and *Ape1*$^{-/-}$ mice do not survive past embryonic day 4-5 (Xanthoudakis et al., 1996, Izumi et al., 2005). Studies have also demonstrated that conditional inactivation of APE1 in living cells leads to an accumulation of both SSBs and AP sites (Izumi et al., 2000, Izumi et al., 2005, Mitra et al., 2007).

Polβ is a member of the X-family of polymerases and is an important end-processing factor in the repair of indirect SSBs. It is contains two separate domains; a small N-terminal dRP lyase domain and a larger polymerase domain and as mentioned previously it forms an interaction with XRCC1 (Beard and Wilson, 2000, Marintchev et al., 2000, Breslin and Caldecott, 2009). AP sites cleaved by APE1 possess 5'dRP termini which are repaired by the AP lyase activity of Polβ in a reaction mechanism that involves the production of a Schiff base intermediate, a reaction intermediate in which an active site lysine becomes covalently attached to the DNA (Piersen et al., 1996, Sobol et al., 2000, Matsumoto and Kim, 1995). This AP lyase activity has been shown to be the critical activity for Polβ as the hypersensitivity of *Polβ*$^{-/-}$ MEFs to DNA alkylating agents can be rescued by expression of only the N-terminal dRP lyase domain (Sobol et al., 2000).

APTX is a member of the Hint-like histidine triad (HIT) superfamily (Brenner, 2002, Kijas et al., 2006). APTX interacts with CK2 phosphorylated XRCC1 and XRCC4 via a N-terminal FHA domain as shown by yeast-two hybrid analysis and co-immunoprecipitation (Sano et al., 2004, Clements et al., 2004, Luo et al., 2004, Date et al., 2004, Gueven et al., 2004). It has been shown that APTX and PNK bind to the same CK2 phosphphorylated cluster on XRCC1, S518/T519/T523, and are present in two mutually exclusive complexes (Luo et al., 2004). APTX has also been reported to co-immunoprecipitate with PCNA (Hirano et al., 2007), PARP1 and p53 (Gueven et al., 2004).

APTX catalyses the release of AMP groups covalently linked to 5'-phosphate termini of a DNA SSB or DSB (Ahel et al., 2006, Rass et al., 2008). Release of the 5'-AMP is achieved via a two-step reaction in which the AMP becomes transiently linked to a histidine residue within the

active site (Rass et al., 2008). Adenylated nicks are produced as a normal intermediate during ligation by an ATP-dependant DNA ligase, and an stable abortive ligation intermediate can arise if a ligase has prematurely attempted to ligate a SSB with a 3' terminus other than a 3'OH (the reaction mechanism of mammalian ligases is described in detail later in section 1.3.4.1). Mutations in APTX result in the neurodegenerative disorder AOA1, which suggests that abortive ligations could be occurring at sufficient frequency within a cell to cause problems if left unrepaired (Date et al., 2001, Moreira et al., 2001). It has also been proposed that APTX can remove 3'P and 3'PG, although this activity is orders of magnitude less efficient than the adenylate hydrolysis activity (Takahashi et al., 2007b).

TDP1 is the end-processing factor that is responsible for the repair of abortive TOP1-SSBs (Figure 1.6) (Interthal et al., 2001, El-Khamisy et al., 2005). TDP1 has tyrosyl-DNA phosphodiesterase activity and cleaves the phosphodiester bond linking the active site tyrosine residue of TOP1 with the 3' terminus of DNA in TOP1-SSBs in a reaction mechanism that involves the transient formation of a covalent enzyme-DNA intermediate (Interthal et al., 2001). Removal of the TOP1 results in a DNA nick possessing a 3'-P and a 5'-OH and therefore requires further processing by PNK. It should also be noted that TDP1 has been reported as being able to repair a 3'-PG (Zhou et al., 2005, Inamdar et al., 2002). A single mutation in TDP1 has been shown to be the cause of the neurodegenerative disorder SCAN1 (Takashima et al., 2002). This is intriguing as defects in both APTX and TDP1 result in neurodegeneration and both are involved in the repair of DNA damage arising from abortive enzymatic activity.

1.3.3 Gap – filling

As the majority of SSBs are associated with a missing base, a gap-filling step usually follows end-processing. At this stage of SSBR the pathway splits into two sub-pathways; short-patch repair, in which a single nucleotide is incorporated into the gap (Dianov et al., 1992), and long-patch repair, in which a repair patch of 2-12 nucleotides is synthesised, displacing a 5' single-stranded flap which is cleaved by flap endonuclease 1 (Frosina et al., 1996, Klungland and Lindahl, 1997, Kim et al., 1998, Mosbaugh and Linn, 1983, Singhal et al., 1995).

Early studies involving the reconstitution of short-patch repair of damaged bases using recombinant human proteins and cell-free extracts from *Polβ*$^{-/-}$ MEFs suggested an important role for Polβ in short-patch repair (Singhal et al., 1995, Sobol et al., 1996, Nealon et al., 1996, Kubota et al., 1996, Klungland and Lindahl, 1997, Karimi-Busheri et al., 1998, Fortini et al., 1998, Winters et al., 1999, Fortini et al., 1999, Dianov et al., 1999, Whitehouse et al., 2001, Podlutsky et al., 2001b, Pascucci et al., 2002, Dianova et al., 2004, Vens et al., 2007). Quiescent *Polβ*$^{-/-}$ MEFs exhibit sensitivity to γ-irradiation, although this sensitivity is not evident in cycling *Polβ*$^{-/-}$ MEFs (Vermeulen et al., 2007b, Vermeulen et al., 2008).

It is important to note that there is some Polβ independent short-patch repair seen in the *Polβ*$^{-/-}$ MEF extracts showing that there is functional redundancy at the level of DNA polymerase choice in short-patch repair (Braithwaite et al., 2005b). DNA polymerase λ (Polλ), also a member of the same X-family of polymerase, has significant sequence homology with Polβ and also has 5'dRP lyase activity (Garcia-Diaz et al., 2000, Nagasawa et al., 2000, Garcia-Diaz et al., 2001, Garcia-Diaz et al., 2002). It has been shown that Polλ can carry out single nucleotide incorporation during short-patch repair in the absence of Polβ (Garcia-Diaz et al., 2001, Braithwaite et al., 2005a, Braithwaite et al., 2005b, Braithwaite et al., 2010). Another potential polymerase that could add to the functional redundancy within short-patch repair is Pol ι, a member of the Y- family of polymerases. The Y-family polymerases are low-fidelity polymerases which are involved in the bypass of DNA lesions during translesion synthesis (Reviewed in (Prakash et al., 2005)). Like both Polβ and Polλ, Polι has 5'dRP lyase activity and can also carry out single nucleotide incorporation in the absence of Polβ (Bebenek et al., 2001, Prasad et al., 2003, Vens et al., 2007). Additionally Polι depleted human fibroblasts are hypersensitive to hydrogen peroxide (Petta et al., 2008).

A number of polymerases have been implicated in long-patch repair. It has been suggested that Polβ can carry out strand displacement synthesis during long-patch repair in a reaction that is stimulated by the presence of PARP1 and FEN1 (Dianov et al., 1999, Prasad et al., 2001, Prasad et al., 2000, Liu et al., 2005, Balakrishnan et al., 2009). On the other hand it has also been suggested that Polβ is only responsible for the initiation of synthesis and other polymerases carry out the strand displacement reaction (Parlanti et al., 2004, Podlutsky et al.,

2001a, Dianov et al., 2001, Dianov et al., 1999). Experiments using extracts from *Polβ*$^{-/-}$ MEFs, however, show that Polβ is not the only polymerase that can operate in long-patch repair and it has been shown that the replicative polymerases DNA polymerase δ and ε (Polδ/ε) can also carry out strand displacement synthesis in a reaction that is dependent on the presence of proliferating cell nuclear antigen (PCNA) (Dresler and Lieberman, 1983a, Dresler and Lieberman, 1983b, DiGiuseppe and Dresler, 1989, Frosina et al., 1996, Klungland and Lindahl, 1997, Stucki et al., 1998, Fortini et al., 1998, Pascucci et al., 1999, Matsumoto et al., 1999, Dogliotti et al., 2001, Parlanti et al., 2004, Parsons et al., 2007). Additionally it has also been suggested that Polλ also operates during long-patch repair which adds further potential redundancy to long-patch repair (Brown et al., 2011).

It is thought that it is the nature of the DNA lesion which determines which sub-pathway of SSBR is used. An example of this is in the presence of a reduced AP site that is resistant to the AP lyase activity of Polβ which is repaired by a FEN1 dependent long-patch repair pathway as short-patch repair would be unable to repair the lesion (Matsumoto et al., 1994, Matsumoto and Kim, 1995, Klungland and Lindahl, 1997, Miller and Chinault, 1982b, Miller and Chinault, 1982a). Another observation that has been made is that *in vitro* different sub-pathways are utilised depending on the glycosylase that initiates BER (Fortini et al., 1999). Finally it has also been proposed that cellular concentrations of ATP could also determine sub-pathway choice in a mechanism that is regulated by XRCC1 and LigIIIα (Petermann et al., 2003, Petermann et al., 2006). In this model short-patch repair would be favoured in conditions with lower levels of cellular ATP.

1.3.4 DNA Ligation

Following gap-filling, the final stage of SSBR is DNA ligation. This is achieved in mammalian cells by two DNA ligases; DNA Ligase III α (LigIIIα) and DNA Ligase I (LigI) (Figure 1.10) (Reviewed in (Ellenberger and Tomkinson, 2008a)). LigIIIα is the ligase that is predominantly associated with short-patch repair (Brookman et al., 1994, Caldecott et al., 1994, Caldecott et al., 1995, Cappelli et al., 1997, Winters et al., 1999, Sleeth et al., 2004). LigIIIα is one of three polypeptides that is generated by the *LIG3* gene; which include the nuclear version that

interacts with XRCC1 (LigIIIα), a mitochondrial version of LigIIIα (mtLigIIIα), which differs to the nuclear version only with the presence of an N-terminal mitochondrial localisation signal (MLS), and a germ-line specific isoform that lacks the C-terminal BRCT that is generated by an alternative splicing event called LigIIIβ which lacks the C-terminal BRCT domain (Lakshmipathy and Campbell, 1999, Perez-Jannotti et al., 2001, Mackey et al., 1997).

The nuclear LigIIIα protein consists of two distinct DNA binding modules. The first is comprised of an N-terminal ZnF motif and an internal DNA binding domain and the second contains the catalytic core (Cotner-Gohara et al., 2008). The ZnF domain allows LigIIIα to act as a nick sensor and, although dispensable for simple nick ligation, is required for the efficient repair of SSBs in the presence of abnormal secondary structure of DNA or other DNA lesions (Caldecott et al., 1996, Mackey et al., 1999, Taylor et al., 2000b). The second module consists of the nucleotidyltransferase (NTase) domain and oligonucleotide binding (OB-fold) domain and a C-terminal BRCT domain. The BRCT motif of LigIIIα forms a constitutive interaction with the second BRCT domain of XRCC1, and although recombinant LigIIIα is stable *in vitro*, this interaction is required for stability of the ligase *in vivo* (Caldecott et al., 1994, Caldecott et al., 1995, Nash et al., 1997, Taylor et al., 1998, Dulic et al., 2001). LigIIIα also has the ability to ligate DSBs, which requires both the N-terminal ZnF and the catalytic core (Cotner-Gohara et al., 2008).

While LigIIIα is usually associated with short-patch repair, LigI is thought of as the ligase that is involved in long-patch repair (Karimi-Busheri et al., 1998, Matsumoto et al., 1999, Pascucci et al., 1999, Prasad et al., 1996, Winters et al., 1999, Sleeth et al., 2004). An interaction between LigI and PCNA has also been shown to be crucial to its role in long-patch repair (Levin et al., 1997, Levin et al., 2000). Aside from its role in SSBR, LigI also has an essential role in the maturation of Okazaki fragments during DNA replication (Waga and Stillman, 1998). Like LigIIIα, LigI has a central region consisting of a DNA binding domain, an NTase domain and an OB-fold, however the ZnF and BRCT domains are unique to LigIIIα which likely reflect the different roles of the ligases. It is important to note that the roles of the two ligases in the different sub-pathways has largely been demonstrated using *in vitro* repair assays and two recent studies have in which XRCC1 and LigIIIα were inactivated in the mouse nervous system

has challenged the current dogma of which ligases are involved in short-patch and long-patch repair (Simsek et al., 2011, Katyal and McKinnon, 2011, Gao et al., 2011). In these studies it was shown that the essential function of LigIIIα was its role in mitochondrial repair and LigI was implicated as the main DNA ligase in XRCC1-mediated SSBR. Indeed, LigIIIα-deficient cells were found to exhibit normal or near-normal rates of SSBR following oxidative DNA damage while LigI-deficient cells exhibited delayed rates of SSBR (Gao et al., 2011). It is likely that the simple model of different ligases functioning seperately in short-patch repair and long-patch repair is untrue and that the roles of LigIIIα and LigI in SSBR are more overlapping than previously thought.

1.3.4.1 Reaction mechanism of mammalian ligases

DNA ligases are nucleotidyltransferases (NTases) that utilise a high energy cofactor to catalyse phosphodiseter bond formation in a universal three-step reaction mechanism that includes an intermediate in which the 5' terminus of the nick becomes adenylated (Figure 1.11) (Olivera et al., 1968, Harvey et al., 1971, Weiss et al., 1968b, Gumport and Lehman, 1971, Lehmann, 1978). Under certain circumstances, such as a premature attempt to ligate a SSB with a damaged 3' terminus, the ligation reaction will stall and a stable abortive ligation intermediate will persist (Shuman, 1995, Sriskanda and Shuman, 1998c, Ahel et al., 2006). The discovery of the neurodegenerative disorder AOA1, a disease caused by mutations in APTX, suggests that adenylated SSBs could be physiologically relevant lesions in cells (Date et al., 2001, Barbot et al., 2001).

All eukaryotic ligases use ATP as a cofactor and contain six highly conserved NTase motifs. Details of the reaction mechanism have been elucidated from extensive functional and structural studies using the DNA ligase of the *Chlorella* Virus PBCV-1 (CV Lig) (Ho et al., 1997). This is the smallest known eukaryotic ATP-dependant DNA ligase and although it consists of only the catalytic core it can almost fully compensate the loss of both *S.cerevisiae* DNA ligases, Cdc9p and Lig4p, *in vivo* making it an appropriate model system for studying DNA ligation (Sriskanda et al., 1999).

In the first step of DNA ligation, the ligase reacts with ATP to form a ligase-adenylate intermediate in which AMP is covalently linked to the active-site lysine via a phosphoamide bond (Olivera et al., 1968, Harvey et al., 1971, Weiss et al., 1968b, Gumport and Lehman, 1971, Lehmann, 1978). This reaction is very energetically favourable and the ligase-adenylate intermediate is stable in the absence of a DNA substrate. The majority of DNA ligases, including LigIIIα, have a significantly higher affinity for a nicked or broken DNA duplex than an intact duplex (Sekiguchi and Shuman, 1997, Caldecott et al., 1996, Sriskanda et al., 1999). This is described as nick sensing and the covalent lysine-AMP adduct is a crucial part of this as the AMP forms contacts with the 5'P termini of a nick, allowing a ligase adenylate to bind tightly to broken DNA (Sekiguchi and Shuman, 1997, Sriskanda and Shuman, 1998a, Odell et al., 2000, Odell et al., 2003, Nair et al., 2007b). Mutations in the critical active site lysine that forms the covalent bond with AMP abolishes both ligase adenylation and nick sensing, whereas mutations that preserve ligase adenylation but prevent the downstream stages of ligation do not affect nick sensing (Sriskanda and Shuman, 1998a).

This mechanism ensures that only an adenylated ligase primed for ligation will bind to a DNA nick and will prevent competition with a non-adenylated ligase. It has also been shown that a ligase will not bind to an un-ligatable nick with a 5'OH, allowing the ligase to possess a degree of proof-reading ability for the suitability of a nick (Sekiguchi and Shuman, 1997, Sriskanda and Shuman, 1998a, Odell et al., 2000, Odell et al., 2003, Tomkinson et al., 2006, Nair et al., 2007b). This ability to proof-read the suitability of a nick is, however, not perfect as a ligase will still adenylate a 5'dRP and does not seem to be able to differentiate between this and a 5'P (Rass et al., 2007a).

The second step of ligation is the activation of the 5'P by adenylation of the DNA (Olivera et al., 1968, Harvey et al., 1971). During this step the oxygen of the 5'P attacks the phosphorus of the AMP, dispelling the lysine and transferring the adenylate group onto the 5'P, forming an AMP-DNA intermediate (Odell et al., 2003, Nair et al., 2007b). This is facilitated by a conformational change in the ligase and a possible reconfiguration of metal ions in the active site (Odell et al., 2003, Nair et al., 2007b). It has been proposed that the 3'-OH participates in binding of the catalytic metal ions required for the reaction and that this could act as another

checkpoint to dissuade the ligase from prematurely adenylating an un-ligatable nick (Nair et al., 2007b).

The final step of ligation is the reformation of the phosphodiester backbone (Lehmann, 1978). During this step the non-adenylated ligase catalyses the nucleophilic attack of the 5'AMP by the 3'OH, displacing the AMP and joining the two polynucleotides by formation of a phosphodiester bond (Odell et al., 2000, Sriskanda and Shuman, 2002b, Sriskanda and Shuman, 2002a, Crut et al., 2008, Nair et al., 2007b). This step is very rapid, and the rate of phosphodiester resynthesis is much faster than the adenylation of the DNA (Crut et al., 2008). Less data is available about this step of ligation as it is so rapid and the only crystal structure of a non-adenylated ligase bound to adenylated DNA used nick with a 3'dideoxynucleoside rather than a 3'OH to block phosphodiester formation and could have disrupted metal ion coordination in the active site (Pascal et al., 2004).

1.3.5 Replication-coupled single strand break repair

The SSBR pathways described above are very rapid and seem to operate throughout the cell cycle and are therefore described as 'global SSBR' (Reviewed in (Caldecott, 2008)). However there is some evidence that alternate SSBR pathways operate at different times throughout the cell cycle, specifically during S-phase. It has been shown that XRCC1 co-localises with PCNA at replication foci (Fan et al., 2004) and a complex consisting of APE1, UNG2, XRCC1 and Polβ replicative Polα, Pol δ /ε and DNA ligase 1 co-associates with DNA replication proteins in human cycling cells (Parlanti et al., 2007, Otterlei et al., 1999). Additionally it has been shown that the BRCT domains within XRCC1 have a role in the repair of SSBs during S-phase (Taylor et al., 2000a). It is possible that a core SSBR complex associates with the replication fork during S-phase and deals with any SSBs that are encountered. This hypothetical pathway has been termed replication-coupled SSBR (RC-SSBR) (Figure 1.12) (Caldecott, 2008, Caldecott, 2001, Caldecott, 2003b). It is considered likely that this hypothetical pathway would resemble long-patch repair due to the fact that many of the proteins involved in long-patch repair, such as Polδ/ε, PCNA, FEN1 and LigI, are also core components of the replication machinery. It has also been suggested that this pathway could operate in conjunction with the double-strand

break repair pathway homologous recombination (HR) due to the fact that SSBs converted into DSBs upon collision with the replication fork are substrates for HR (Kouzminova and Kuzminov, 2006, Kuzminov, 2001). This also raises the possibility that the structure specific nucleases that operate during HR could also play a role in RC-SSBR. One of the attractions of this hypothetical pathway is that the presence of this pathway could explain the lack of cancer predisposition in SSBR defective disorder as any unrepaired SSBs encountered by the replication fork would be repaired by RC-SSBR and would not become a permanent block to replication.

1.3.6 SSBs and Transcription

The survival of the cell depends on not just the accurate replication of the genome, but also on the unperturbed transcription of the many coding and regulatory regions within the genome and therefore DNA lesions located within these transcribed regions of the genome can result in a number of deleterious effects. Transcribing past the damage can result in mutations due to base misinsertions opposite the lesion, the presence of the lesion can affect the rate of transcription, altering the expression level of the damaged gene, and finally transcription can be completely blocked, leading to loss of the transcript (Zhou and Doetsch, 1994, Saxowsky and Doetsch, 2006, Tornaletti, 2009).

The role of dedicated repair pathways, such as transcription-coupled repair (TCR) in the recognition and repair of specific transcription blocking lesions, such as cyclobutane pyrimidines (CPD) and intrastrand crosslinks, is already well established and is described later in Section 1.6 (Tornaletti, 2009, Nouspikel, 2009, Lagerwerf et al., 2011). Indeed there are human disorders, such as the microcephalic cockayne syndrome, which are associated with defects in the repair of DNA lesions in transcribed genes, highlighting the cytotoxicity of unrepaired transcription-blocking lesions (Lehmann, 2003). There is evidence that SSBs can also block RNA polymerases and that SSBR has a role in protecting against transcription blocking DNA damage, although this is not as well established as TCR.

It is known that collision with transcription machinery converts Top1 cleavage complexes into abortive Top1-SSB (Kroeger and Rowe, 1989, Bendixen et al., 1990, Wu and Liu, 1997). Indeed a significant portion of the accumulating abortive Top1-SSBs seen in TDP1-defective cell lines following incubation with camptothecin (CPT), a Top1 poison that increases the half-life of Top1 cleavage complexes, is dependent on the presence of active transcription as shown by their disappearance upon incubation with the RNA polymerase inhibitor α-amanitin (Miao et al., 2006, El-Khamisy et al., 2005). Additionally, CPT-induced SSBs still accumulate in TDP1-defective cell lines in the presence of the replication inhibitor aphidicolin showing that TDP1 dependent SSBR has a role in protecting the cell against transcription blocking lesions (Miao et al., 2006, El-Khamisy et al., 2005). The DNA glycoslysase NEIL2 has also been shown to associate with RNA polymerase II and to preferentially repair oxidised bases within transcibed genes, further supporting a role for SSBR in the repair of transcription-blocking lesions (Banerjee et al., 2011).

1.4 DNA Double Strand Breaks

DNA double strand breaks (DSB) are discontinuities in both strands of the DNA double helix and can arise from both endogenous and exogenous sources. Although rare lesions, it is estimated that only 10 spontaneous DSBs arise per cell per day based on experiments performed on early passage primary human fibroblasts (Lieber et al., 2003, Lieber and Karanjawala, 2004, Martin et al., 1985), DSBs are considered to be particularly genotoxic lesions and a single unrepaired DSB can be sufficient to induce apoptosis (Rich et al., 2000). Failure to repair the breaks correctly can lead to chromosomal rearrangements, including translocations and deletions, chromosomal miss-segregation during mitosis and/or cell death (Hoeijmakers, 2001).

Like SSBs, DSBs can be generated directly if the attack of free radicals on the sugar-phosphate backbone of the DNA double helix, results in the disintegration of two closely located oxidised sugars on anti-parallel strands of the DNA double helix (Ward et al., 1987, Ward, 1998). Ionising radiation is a major source of DSBs as the IR particles create localised clusters of ROS as they pass through the cell, predominantly from water, increasing the chance that two

closely spaced lesions will arise. Indeed, unlike hydrogen peroxide which induces one DSB for every ~2000 SSBs, IR generates one DSB for every 25 - 40 SSBs (Friedberg EC et al., 2006, Ward et al., 1987, Ward, 1998).

Endogenous DSBs can arise from a number of sources; as the result of the abortive activity of type II DNA topoisomerases which transiently nick both strands of the duplex, by the collision of a replication fork with a SSB during DNA replication, forming a one ended DSB, or from mechanical stress on chromosomes such as during chromosomal segregation in mitosis (Adachi et al., 2003, Friedberg et al., 2006, Kuzminov, 2001, Hoeijmakers, 2001, Kouzminova and Kuzminov, 2006).

1.5 Double strand break repair

The accurate repair of DSBs is vital to the survival to the cell and an intricate network of signalling cascades and double-strand break repair (DSBR) pathways have evolved to ensure unrepaired breaks do not persist to threaten genomic stability. Mammalian cells have evolved two major double-strand break repair (DSBR) pathways to deal with DSBs; non-homologous end-joining (NHEJ), an efficient DSBR pathway that operates throughout the cell cycle but is particularly importance during the G1 and early S phases of the cell cycle, and homologous recombination (HR), a repair pathway that predominantly operates during late S –phase and G2 (Reviewed in (Hartlerode and Scully, 2009, Lieber, 2010). In addition there are a number of DSB sensors that can detect and signal the presence of a DSB to facilitate its rapid repair. In this section I will discuss the two main DSBR pathways, NHEJ and HR, and detail DSB signalling by the protein kinase ataxia telangiectasia mutated (ATM).

1.5.1 Non-homologous end-joining

NHEJ is an efficient error-free DSBR pathway that aims to accurately religate the ends of a DSB with no loss of genetic information (Figure 1.13) (Hartlerode and Scully, 2009, Mahaney et al., 2009, Lieber, 2010). As NHEJ does not require a homologous sequence for accurate repair it

operates throughout the cell cycle and is of particular importance during G0, G1 and early S-phase when a sister chromatid is not available for use as a donor template (Takata et al., 1998, Sonoda et al., 2006, Delacote and Lopez, 2008).

NHEJ is initiated by the rapid binding of the Ku70/80 heterodimer to both ends of the DSB. Upon binding to the DSB, Ku70/80 forms a ring-like structure that encircles the DNA and translocates inwards, making the ends of the DNA accessible to other DNA repair factors such as DNA dependent protein kinase (DNA PK) (Walker et al., 2001, Yoo and Dynan, 1999). The recruitment of the catalytic subunit of the DNA PK (DNA PKcs) then occurs in the presence of both Ku and DNA to for the active holoenzyme DNA PK (Jin et al., 1997, Uematsu et al., 2007, Suwa et al., 1994). The activated DNA PK then loads onto the exposed DNA termini on both sides of the DSB and interacts across the break to form a 'synaptic complex' (DeFazio et al., 2002). This 'synaptic complex' acts to tether the ends of the DSB to each other and to offer protection against unwanted processing by nucleases. The assembly of the DNA PKcs/Ku/DSB synaptic complex also stimulates the kinase activity of DNA PK, resulting in the disassociation of DNA-PK from the break and allowing access of other repair factors to the DNA ends (Meek et al., 2007). The poly (ADP) ribose polymerase protein PARP3 also has a role in DSB signalling and is activated upon induction of a break, ribosylating itself and other substrate proteins such as histones (Rulten et al., 2011, Rulten et al., 2008, Iles et al., 2007).

The next stage of NHEJ is the processing of the DNA termini at the ends of the DSB to restore conventional ligatable 3'OH and 5'P. Like SSBs, DSBs can have a multitude of different chemistries and structures at the DNA ends, depending on the source of the damage, and therefore require a diverse set of end-processing enzymes to repair. Artemis is key NHEJ end-processing factor that is reported to possess a number of different repair activities, including 5' → 3' exonuclease and 3'PG processing activity and the ability to resolve DNA hairpins (Ma et al., 2002, Ma et al., 2005, Povirk et al., 2007). Artemis is recruited to DSBs via an interaction with DNA PKcs, and it seems likely that Artemis is involved in multiple aspects of NHEJ (Ma et al., 2002).

Another processing factor that is likely to have a role in NHEJ is PNKP. As discussed in section 1.3.2, PNKP plays a very important role in SSBR in the processing of SSBs induced by a variety of DNA damaging agents aided by an interaction with XRCC1 (Jilani et al., 1999, Karimi-Busheri et al., 1998, Whitehouse et al., 2001, Bernstein et al., 2005b). PNKP also interacts with CK2 phosphorylated XRCC4 and it is believed that it performs a similar role in the processing of DSBs during NHEJ (Ward, 1998, Chappell et al., 2002, Bernstein et al., 2005a, Koch et al., 2004, Karimi-Busheri et al., 2007, Mani et al., 2010, Segal-Raz et al., 2011). Similarly, APTX is another end-processing factor that interacts with both CK2 phosphorylated XRCC1 and XRCC4 and has been shown to remove adenylate groups from the 5' termini of both SSBs and DSBs, and has also been implicated in DSBR (Clements et al., 2004, Rass et al., 2007a).

Another end-processing factor that has a potential role in NHEJ is tyrosyl-DNA phosphodiesterase 2 (TDP2), a protein that resolves damage arising from abortive topoisomerase 2 (Top2) activity. Top2 induces DSBs in a reaction mechanism that involves an intermediate in which the topoisomerase becomes covalently linked to the 5'termini of the break via a phosphotyrosyl bond (Wang, 2002, Nitiss, 2009b, Nitiss, 2009a). Normally this is a very transient intermediate and the DSB is rapidly resealed in the final stage of the reaction, but under certain circumstances, such as in the presence of Top2 poisons, a stable DSB with Top2 linked to the 5' termini can form which requires processing to resolve. Tdp2 is a recently identified phosphodiesterase that cleaves 5' - phosphotyrosyl bonds and has been shown to repair Top2 – DSBs (Zeng et al., 2011, Cortes Ledesma et al., 2009). Tdp2 generates clean ligatable DNA ends and it is very likely that it functions during NHEJ to promote the error-free repair of abortive Top2 – DSBs. Finally Ku has also been reported to possess 5'-dRP/AP lysase activity, suggesting a role in the processing of DNA ends in addition to its main role in NHEJ (Roberts et al., 2010).

Often the processing of DSBs leads to the creation of DNA gaps, which require the action of a DNA polymerase to repair. The DNA polymerase X family of polymerases have been implicated in carrying out gap-filling during NHEJ, including polymerases μ and λ, which interact with Ku and XRCC4/LigIV, and terminal deoxyribonucleotidyltransferase (TdT), which interacts with Ku, (Nick McElhinny and Ramsden, 2004, Mueller et al., 2008).

Once the DNA termini have been processed, and any gaps have been filled, the final stage of NHEJ is DNA ligation. Ligation of the DSB is carried out by DNA LigIV in a complex with XRCC4 (Critchlow et al., 1997, Grawunder et al., 1997, Sibanda et al., 2001, Grawunder et al., 1998a, Grawunder et al., 1998b). Like XRCC1, XRCC4 has no enzymatic activity but has a critical role in NHEJ, acting as a scaffolding protein to facilitate the recruitment of repair factors to the site of the break (Mari et al., 2006). The recruitment and stability of XRCC4-LigIV at the DSB is mediated by interactions with Ku70/80, DNA PK and the ADP-ribose binding protein, aprataxin and PNK- like factor (APLF) (Mehrotra et al., 2011, Rulten et al., 2011, Rulten et al., 2008, Macrae et al., 2008, Iles et al., 2007, Mari et al., 2006, Costantini et al., 2007, Nick McElhinny et al., 2000). XRCC4 –like factor (XLF) is another factor that is recruited to DSBs via an interaction with Ku70/80 and functions to stimulate NHEJ (Ahnesorg et al., 2006, Yano et al., 2008). XLF is similar in structure to XRCC4 and facilitates rapid end-joining by stimulating the DNA ligation and promoting the re-adenylation of LigIV following end-joining (Gu et al., 2007, Tsai et al., 2007, Lu et al., 2007, Wu et al., 2007, Riballo et al., 2009, Hammel et al., 2011).

1.5.2 Homology directed repair

A series of pathways in operation in cells that use a homologous sequence from an undamaged donor template to repair a DSB are collectively called homology directed repair (HDR) (Figure 1.14) (Paques and Haber, 1999, Hartlerode and Scully, 2009). These pathways are of particular importance during the late S-phase and G2 phases of the cell cycle owing to the existence and close proximity of sister chromatids (Delacote and Lopez, 2008, Sonoda et al., 2006).

The Mre11-Rad50-NBS1 (MRN) complex plays a critical role in the early response to DSBs during HDR (Williams et al., 2007). Amongst its many roles it is thought that two MRN complexes carry out a similar function during HDR to the DNA PKcs/Ku/DSB synaptic complex in NHEJ by tethering the ends of a DSB together via homodimerisation of the Rad50 subunit (Hopfner et al., 2002, Williams et al., 2008, Lavin, 2007). Following detection of the break, the DNA ends are resected in a 5’ → 3’ direction to generate 3’ ssDNA overhangs with a 3’OH. MRN, in co-operation with CtIP, has been shown to initiate DNA resection by trimming of the

DNA ends (Sartori et al., 2007, Huertas and Jackson, 2009, You et al., 2009b, Nicolette et al., 2010a, Paull, 2010b, Coleman and Greenberg, 2011, Mimitou and Symington, 2008). The bulk of end resection is then carried out by two nucleases, DNA2 and EXO1, in combination with the helicase BLM (Nimonkar et al., 2011, Cejka et al., 2010, Zhu et al., 2008, Mimitou and Symington, 2008). Another factor which has been implicated in the regulation of DNA resection is BRCA1 (Coleman and Greenberg, 2011).

The ssDNA generated by resection is rapidly bound by the ssDNA binding protein RPA which melts the DNA's secondary structure (Sung and Klein, 2006). RPA is then displaced from the ssDNA by the Rad51 recombinase with the help of the mediator proteins BRCA1/BARD1 and BRCA2/DSS1 to form a Rad51 nucleofilament which carries out the strand invasion and homology search steps of HDR (Sy et al., 2009, Zhang et al., 2009, Wong et al., 1997, Pellegrini et al., 2002, San Filippo et al., 2006). Strand invasion occurs by the capture of the intact duplex by the Rad51 nucleofilament which forms a D-loop intermediate, where the 3' termini of the invading strand is primed for DNA synthesis. It is at this stage that various hypothesised pathways of HDR diverge (Figure 1.14).

In the synthesis-dependent strand-annealing model (SDSA), following DNA synthesis and D-loop migration, the newly synthesised invading strand is displaced and anneals back to the second resected end of the break (West, 2003, Paques and Haber, 1999, Hartlerode and Scully, 2009). In the homologous recombination (HR) pathway, the resected second DNA end is captured by the migrating D-loop, forming double holiday-junctions (HJ) (Paques and Haber, 1999, Hartlerode and Scully, 2009). These double HJs are then resolved enzymatically by a number of structure – specific endonucleases (Wu and Hickson, 2003, Chen et al., 2001, Rass et al., 2010, Svendsen and Harper, 2010). Depending on the orientation of resolution this can lead to either a crossover or non-crossover in event (Paques and Haber, 1999, Hartlerode and Scully, 2009).

Single-strand annealing (SSA) is an error prone HDR pathway that can occur when a DSB arises between two direct repeats (Paques and Haber, 1999, Hartlerode and Scully, 2009). Resection

of the DNA ends uncovers the repeats, generating two complementary single strands that anneal together. The resulting DNA flaps generated are excised and the DNA nicks are ligated. Finally break – induced recombination (BIR) occurs when a one-ended DSB invades the intact duplex, forming a recombination induced replication fork (Paques and Haber, 1999, Hartlerode and Scully, 2009). This could be a particularly important repair pathway during DNA replication as a way of restarting a collapsed replication fork caused when an elongating fork collides with a SSB (Kuzminov, 2001).

1.5.3 ATM dependent DNA double strand break signalling

Ataxia telangiectasia mutated (ATM) is a member of phosphatidylinositol 3-kinase-related kinases (PIKK) family of serine/threonine protein kinases, which includes DNA PK, and plays a critical role in the coordination of events that take place during DSB sensing and repair (Figure 1.15). ATM is rapidly recruited to DSBs and immediately phosphorylates serine 139 on the histone variant H2AX to produce γH2AX (Burma et al., 2001). The ATM activity is partially dependent on the presence of MRN, another DSB sensor that rapidly accumulates at sites of damage, and it is thought that these two DSB sensors act in concert to promote a complete and efficient DNA damage response and repair (Uziel et al., 2003, Lavin, 2007, Williams et al., 2007).

Following the formation of γH2AX, the adaptor protein mediator of DNA damage checkpoint protein 1 (MDC1) is recruited to the break via its BRCT repeats and is phosphorylated by ATM (Stucki and Jackson, 2004, Lukas et al., 2004). MDC1 binds to the phosphorylated histone and is thought to act as a protein platform to help stabilise DDR proteins at the break. It also helps to propagate the spreading of the γH2AX signal, recruiting more ATM to the break via its FHA domain, which in turn phosphorylates H2AX further away from the break (Lou et al., 2006). H2AX phosphorylation can spread for up to 1-2 megabases around the DSB, which is important for sustaining the DDR (Celeste et al., 2002, Harper and Elledge, 2007).

A cascade of ubiquitin modification at sites of DSBs adds another layer to the DNA damage response (DDR). The E3 ubiquitin ligase ring finger protein 8 (RNF8) interacts with phosphorylated MDC1 at the break and ubiquitinates H2A and γH2AX at the site of the break (Huen et al., 2007, Kolas et al., 2007, Mailand et al., 2007). A second and third E3 ligase are then recruited to the break, RNF168 via a ubiquitin interacting motif, binds to the ubiquinated histones and, HERC2, interacting with the FHA domain of RNF8, to stimulate further ubquitination around the break (Doil et al., 2009, Stewart et al., 2007, Bekker-Jensen et al., 2010). The spreading of the ubiquitin chains leads to the recruitment of RAP80, BRCA1 and 53BP1 (Huen et al., 2007, Kolas et al., 2007, Lavin, 2008). 53BP1 plays an important that role in the DNA damage response, although precisely what that role is has yet to be discerned.

1.6 Nucleotide excision repair

Nucleotide excision repair (NER) is one of the most versatile DNA repair pathways within mammalian cells (Figure 1.16) (Nouspikel, 2009). It recognises and repairs a wide range of DNA lesions, including bulky DNA adducts that result in the distortion of the DNA double helix. Bulky, helix distorting adducts can be caused by exposure to UV light, in particular UVB radiation which is a component of sunlight, resulting in the formation of photodamage within DNA (Cadet et al., 2005a, Douki and Cadet, 2001). Cyclobutane pyrimidines (CPD) and (6-4) pyrimidine photoproducts ((6-4)PP) are the most commonly occuring type of lesion (Figure 1.17) (Cadet et al., 2005b). Other types bulky DNA adducts that are repaired by NER include DNA lesions induced by polycyclic aromatic hydrocarbons which are commonly found in air, food and drinking water as well as in tobacco smoke (Perera et al., 2005).

NER achieves its versatility by excising a short patch of DNA surrounding the lesion, bypassing the need for specific DNA repair enzymes. There are two pathways that operate within NER; global genome NER (GGR), which recognises and repairs DNA adducts that cause major distortions of the double helix anywhere in the genome, and transcription coupled repair (TCR), which repairs transcription blocking lesions (Gillet and Scharer, 2006, Tornaletti, 2009, Nouspikel, 2009).

There are two major damage detection complexes involved in GGR. The XPC complex is involved in the recognition of lesions that cause major distortions in the double helix, such as (6-4)PPs (Kusumoto et al., 2001, Sugasawa et al., 2001, Araki et al., 2001). However the XPC complex is unable to recognise lesions which only cause small distortions in the double helix, such as CPDs and recognition of these lesions is performed by the XPE complex (also known as the DDB complex) (Kim et al., 1995, Payne and Chu, 1994). In TCR, the lesion is only recognised when it is encountered by an elongating RNA polymerase, which causes stalling of the transcription bubble (Payne and Chu, 1994). CSA and CSB are two proteins that are recruited to the site of the stalled transcription complex and are required for efficient TCR (Tu et al., 1997, Tijsterman et al., 1997, Tu et al., 1998, Tantin, 1998). Following detection of the lesion, the GGR and TCR pathways converge and are mechanistically identical.

The next stage of NER is the unwinding of the DNA helix to form a bubble around the lesion. This is carried out by the transcription factor TFIIH, a large complex consisting of 10 subunits, including the two ATP-dependent DNA helicases XPB and XPD, which have opposing 3' → 5' and 5' → 3' helicase activities respectively (Tapias et al., 2004, Tantin, 1998, Drapkin et al., 1994). It is at this stage that the proteins XPA, XPG and the ssDNA binding protein RPA are recruited via interactions with TFIIH (Araujo et al., 2001, Volker et al., 2001). XPA is absolutely essential for NER to take place although its precise role has not yet been determined (Tanaka et al., 1990, Gillet and Scharer, 2006, Park and Choi, 2006). One potential role it could perform is damage verification to ensure that RPA coats only the undamaged DNA strand, allowing proper assembly of the pre-incision complex (Hermanson-Miller and Turchi, 2002, Sugasawa et al., 1998). The coating of RPA on the undamaged DNA strand is essential for the incision and repair synthesis stages (Mu et al., 1995, Coverley et al., 1992, Guzder et al., 1995). The final protein to be recruited to the pre-incision complex is ERCC1-XPF via an interaction with XPA (Li et al., 1995a, Saijo et al., 1996, Park and Sancar, 1994, Nagai et al., 1995, Li et al., 1994).

Following formation of the denaturation bubble and assembly of the pre-incision complex, dual incisions are made at the 3' and 5' ends of the bubble at the ssDNA-dsDNA junction by the structure-specific endonucleases XPG and ERCC1-XPF respectively (O'Donovan et al., 1994,

Sijbers et al., 1996, Park et al., 1995, Matsunaga et al., 1995). Following excision, the gap is filled by the replicative polymerases Pol δ and Pol ε in association with PCNA, and the remaining nick is ligated by the XRCC1-LigIII complex (Popanda and Thielmann, 1992, Shivji et al., 1992, Moser et al., 2007).

1.7 Mismatch repair

Canonical Watson-Crick base pairing, in which A pairs with T and G pairs with C, is an inherent feature of the structure of double stranded DNA and allows for the error-free duplication and maintenance of genetic information (Watson and Hayes, 1953). However, alternative configurations of base-pairing, called DNA mismatches can occur. DNA mismatches can involve non-Watson-Crick combinations of bases, including G-T, A-C, A-A, G-G, A-G, C-T, C-C and T-T, the pairing of undamaged bases with damaged bases, such as of 8-oxo-G with A or O6meG with C, mismatches arising loops from small nucleotide insertions or deletions or mismatches arising between undamaged bases and uracil (Li, 2008, Kunz et al., 2009). DNA mismatches that arise as the result of base damage are generally repaired by specific DNA glycosylases during BER (Table 1.1) while other types of DNA mismatch are recognised and repaired by a highly conserved repair pathway called DNA mismatch repair (MMR) (Figure 1.18) (Li, 2008, Kunz et al., 2009).

In human MMR, recognition of base-base mismatches post replication is achieved via the activity of the two heterodimers, MSH2-MSH6 and MSH2-MSH3 (Kunkel and Erie, 2005). Once a base mismatch is recognised, this leads to the recruitment of the MLH1/PMS2, resulting in the formation of a ternary complex which is crucial for the completion of MMR in human cells (Kunkel and Erie, 2005). It is thought that PCNA also plays a role in the recruitment of MMR proteins in the vicinity of a replication fork via interactions with MSH6 and MSH3 (Hsieh and Yamane, 2008). An essential aspect of MMR is that the nascent DNA strand containing the mismatch can be discriminated from the parental strand which contains the correct base. Post replication, a newly synthesised DNA strand contains discontinuities due to the presence of DNA primer ends and unprocessed Okazaki fragments and in eukaryotes MMR is directed

towards whichever strand contains discontinuities in the proximity of the mismatch (Hsieh and Yamane, 2008, Li, 2008, Kunz et al., 2009).

Once the MMR machinery has been assembled at the site of damage, a nick is introduced 5' to the mismatch in a PCNA dependent manner by PMS2, then the nicked strand is degraded by the 5' → 3' exonuclease EXO1 (Hsieh and Yamane, 2008, Genschel et al., 2002). The single-stranded gap is then rapidly bound by RPA, which helps facilitate Polδ or Polε dependent DNA synthesis, and finally the resulting DNA nick is ligated by DNA Ligase I (Zhang et al., 2005, Li, 2008).

1.8 DNA Damage Response and Human Genetic Disease

As described above, the large variety of DNA lesions that can arise in cells are repaired by over-lapping DNA response and repair pathways that function to maintain genome integrity. The importance of these pathways in the maintenance of human health is highlighted by the existence of human genetic diseases which are caused by defects in many of these pathways (Table 1.3). There are three main classes of symptoms that are associated with defective responses to DNA damage, including pre-disposition to cancer and deficiencies of the immune system and nervous system (Jackson and Bartek, 2009, Hoeijmakers, 2001, Hoeijmakers, 2007, McKinnon, 2009, McKinnon and Caldecott, 2007).

Cancer is a disease that is fundamentally linked to genomic instability (Negrini et al., 2010). DNA damage that results in mutations, either by faulty repair or replication errors, can lead to the loss of tumour-suppressor genes or the improper activation of oncogenes, triggering uncontrolled cellular proliferation and the development of malignant cells (Stoler et al., 1999, Hoeijmakers, 2001, Stratton et al., 2009). In fact many lymphoid tumours are linked with specific chromosomal translocations involving proto-oncogenes (Schlissel et al., 2006). Furthermore, defects in DNA repair pathways or the deregulation of DNA damage response pathways can contribute to a 'mutator phenotype' in which enhanced mutation rates speed the progression of malignancy, such as the link between inherited defects in MMR and

predisposition to colorectal and endometrial carcinomas (Hoeijmakers, 2001, Jiricny, 2006). Indeed the fact that most carcinogens are DNA damaging agents further highlights the link between cancer and DNA damage (Hoeijmakers, 2001).

Defects in many other DNA damage signalling and repair pathways have also been linked with cancer. Mutations in *BRCA1* and *BRCA2*, which impart defects in the homologous recombination DSBR pathway, strongly predispose to breast cancer (Venkitaraman, 2002). Defective NER, in particular the global genome NER pathway, leads to pronounced UV-sensitivity and a very high incidence of skin cancer. Additionally mutations in proteins that form part of the DNA DSB signalling cascade, such as ATM and Nbs1, also impart susceptibility to cancer (Chun and Gatti, 2004, Varon et al., 1998).

The link between immunodeficiency and defects in DNA repair pathways arises due to essential roles specialised DNA repair pathways have in the development of the vertebrate immune system (Dudley et al., 2005). Core members of the NHEJ pathway perform direct roles in the production and diversification of the antigen receptors expressed on B- and T-lymphocytes in a pathway called V(D)J recombination (Hartlerode and Scully, 2009). Consistent with this role, various immunodeficient human disorders are caused by mutations in proteins involved in DSB signalling and repair. Deficiencies in Ku70/80, LigIV, Artemis, RNF168, ATM, Mre11 and XLF all lead to disorders associated with severe immunodeficiency (Gu et al., 1997, Zhu et al., 1996, Moshous et al., 2001, Stewart et al., 2007, Bohgaki et al., 2011, Stewart et al., 2009, Stewart et al., 1999, Chun and Gatti, 2004, Buck et al., 2006a). Additionally multiple DNA repair pathways are also thought to be involved in class switch recombination, another specialised DNA repair pathway involved in the production of antibodies (Dudley et al., 2005).

Finally, defective DNA repair can also lead to disorders of the nervous system. There are two main types of neuropathology presentation that is linked to defective DNA repair; primary microcephaly and progressive neurodegeneration (McKinnon, 2009, O'Driscoll and Jeggo, 2008). Primary microcephaly is a clinical term which is used to describe reduced head size,

defined as head circumference 3 standard deviations below the mean, which presents from birth (O'Driscoll and Jeggo, 2008). The underlying cause of the reduced head circumference is a reduction in total brain volume, as the outward pressure of the developing brain is the driving force for the expansion of the head and skull. An early period of rapid proliferation of neuronal progenitor cells in the ventricular (VZ) and subventricular zones (SVZ) that line the ventricles of the developing brain is critical for the development of the huge amount of neurons that comprise the mature nervous system (Bayer et al., 1991, Chan et al., 2002). Once these neuronal progenitors have replicated, cells destined to become neurons exit the cell cycle, differentiate and migrate away from the VZ and SVZ towards the cortical plate (Bayer et al., 1991, Chan et al., 2002, Carmichael and Woods, 2006). Due to the rapid proliferation that the neuronal progenitors undergo, they are likely to be heavily reliant on DNA repair pathways to prevent replication-associated DNA damage (Barnes et al., 1998, Gao et al., 1998). Additionally, these neuronal progenitors also seem to have a low threshold of DNA damage that is required to induce apoptosis (Hoshino and Kameyama, 1988, Narasimhaiah et al., 2005, Hoshino et al., 1991). Therefore defects in DNA repair could lead to an increased rate of apoptosis in the proliferating progenitors due to high levels of replication stress, resulting in a reduction in the total numbers of neurons in the developing brain, and consequently giving rise to microcephaly (Gatz et al., 2011). Microcephaly is common feature amongst defective DNA repair disorders, with defects in NHEJ, NER, SSBR, and MRN dependent DSB signalling all resulting in microcephalic disorders (Shen et al., 2010, Varon et al., 1998, O'Driscoll et al., 2001, Buck et al., 2006a, Reed et al., 1965, Mimaki et al., 1986, Jaspers et al., 2007, Lehmann, 2003).

The other type of neuropathology that can arise from defective DNA repair is the progressive neurodegeneration of the adult brain. Neurodegenerative disorders usually present after birth and are typically associated with the progressive degeneration of specific regions of the brain such as the cerebellum (Date et al., 2001, Moreira et al., 2001). The progressive degeneration of the adult brain is thought to be due to the accumulation of DNA lesions in post mitotic lesions. Neurons are highly active cells and generally exhibit high levels of mitochondrial respiration, and also have a reduced capacity to neutralise reactive oxygen species, leading to elevated levels of oxidative DNA damage in neurons (Weissman et al., 2007, Barzilai, 2007). Additionally, the adult brain also has a limited capacity for cellular regeneration and post

mitotic neurons, being in G0, would lack the DNA repair pathways that operate during S-phase and G2, such as HR (Rass et al., 2007b). Therefore, due to the increased oxidative stress, the adult brain would be sensitive to the loss of any the remaining DNA repair pathways, which could lead to the gradual accumulation of unrepaired DNA lesions. The accumulating DNA lesions could potentially interfere with the transcription machinery, leading to cell dysfunction or apoptosis (Ljungman and Lane, 2004). Defects in ATM and Mre11 dependent DSB signalling, SSBR and NER can all result in disorders characterised by progressive neurodegeneration of the cerebellum (Chun and Gatti, 2004, Taylor et al., 2004, Date et al., 2001, Moreira et al., 2001, Stewart et al., 1999).

1.8.1 Ataxia Telangiectasia/Ataxia Telangiectasia – Like Disorder

Ataxia telangiectasia (A-T) is a rare, autosomal recessive disorder characterised by progressive cerebellar ataxia, neurodegeneration, radiosensitivity, cell-cycle checkpoint defects, genome instability and a predisposition to cancer (Boder and Sedgwick, 1958). Ataxia is characterised by a lack of coordination of muscle movement that affects movement, speech and balance and is typically caused by dysfunction of the cerebellum. AT was discovered to be caused by mutations in the gene ataxia-telangiectasia mutated (ATM), named after the disorder (Savitsky et al., 1995). As described earlier in section 1.5.3, ATM is a serine/threonine protein kinase that plays a critical role in DSB sensing and repair (Kastan and Lim, 2000). A-T is considered to be the archetypal DDR-defective disorder as it provided one of the first direct links between DNA damage and neurodegeneration.

The primary symptom of A-T, and the most debilitating aspect of the disease, is early onset, progressive neurodegeneration which results in prominent ataxia and dysarthria, which are symptoms of cerebellar dysfunction (Boder and Sedgwick, 1958). Indeed by the age of 10, magnetic resonance imaging of A-T patients reveal that the cerebellum has lost much of its volume and the patients are usually wheelchair bound by this age (Tavani et al., 2003, Chun and Gatti, 2004). It has been shown that ATM is required for DNA damage induced apoptosis in the nervous system which suggests that ATM functions to eliminate neurons that possess

DNA damage and the absence of ATM may result in the persistence of DNA lesions eventually resulting in cell loss and neurodegeneration (Lee et al., 2000, Sekiguchi et al., 2001).

Ataxia-telangiectasia like disorder (A-TLD) is caused by hypomorphic mutations in Mre11 and has a neuropathological presentation which is very similar to A-T, although with a delayed onset and lacking the symptoms of telangiectasia and cancer predisposition (Stewart et al., 1999). The clinical overlap between these two syndromes could be explained by the overlapping roles that ATM and MRN play in sensing and signalling DSBs. ATM activity is partially dependent on the presence of the MRN complex and it is believed they act in concert to promote an efficient DDR (Uziel et al., 2003, Lavin, 2007, Williams et al., 2007). In contrast, mutations in NBS1, another component of the MRN complex, result in Nijmegen breakage syndrome (NBS), which presents with microcephaly and lacks the neurodegenerative symptoms common to A-T and A-TLD (Varon et al., 1998). How two different clinical presentations can arise from mutations in two proteins within the same complex could be potentially be explained due to the ATM-independent roles that MRN performs, such as the involvement of NBS1 in ATR signalling and HR (Stiff et al., 2005, Hopfner et al., 2002, Williams et al., 2008, Lavin, 2007, Nicolette et al., 2010a, Paull, 2010b). Therefore mutations in Mre11 that lead to A-TLD could be the result of a defect in the ATM-dependent role of MRN, while mutations in NBS1 could cause deficiencies in ATR signalling and/or HR.

1.9 DNA single strand break repair disorders

1.9.1 Ataxia oculomotor apraxia 1

AOA1 is the most common form of autosomal recessive ataxia in Japan and the second most common in Portugal. It clinically presents with early onset ataxia, oculomotor apraxia, cerebellar atrophy and axonal motor neuropathy (Figure 1.19) (Date et al., 2001, Moreira et al., 2001, Shimazaki et al., 2002a, Le Ber et al., 2003, Sekijima et al., 2003, Tranchant et al., 2003, Amouri et al., 2004, Criscuolo et al., 2004, Habeck et al., 2004, Criscuolo et al., 2005, Duquette et al., 2005, Ito et al., 2005, Mahajnah et al., 2005, Quinzii et al., 2005, Tsao and Paulson, 2005, Palau and Espinos, 2006, Shahwan et al., 2006, Baba et al., 2007, Ferrarini et al., 2007, Zuhlke et al., 2007, D'Arrigo et al., 2008, Liu and Narayanan, 2008, Salvatore et al., 2008,

Sugawara et al., 2008, Yoon et al., 2008, Anheim et al., 2010, Tada et al., 2010). As mentioned above, ataxia is characterised by a lack of coordination of muscle movement affecting movement, speech and balance, while oculomotor apraxia is an inability to control eye movements, both of which result from cerebellar dysfunction. Onset of AOA1 occurs between early childhood and adolescence and patients can be severely disabled and wheel chair-bound by later life (Aicardi et al., 1988, Barbot et al., 2001, Tachi et al., 2000, Gascon et al., 1995). An interesting feature of this disorder is that although it shares a number of neurological symptoms with other DNA repair defective disorders, such as ataxia-telangiectasia, it lacks any of the other extraneurological features such as immunodeficiency or cancer pre-disposition (Table 1.3). As mentioned previously it is caused by mutations in the gene *APTX*, a member of the Hint-like histidine triad (HIT) superfamily which consist of adenosine 5'-monophosphoramide hydrolyases (Brenner, 2002, Bieganowski et al., 2002a, Krakowiak et al., 2004a, Seidle et al., 2005, Kijas et al., 2006). APTX also possess a divergent zinc finger motif (ZnF) and an amino-terminal fork-head associated domain that has homology with the amino-terminus of PNK (Barbot et al., 2001).

The *in vitro* substrate for APTX has been discovered and well characterised. APTX catalyses the release of adenylate groups covalently linked to 5'-P termini of a DNA SSB or DSB (Ahel et al., 2006, Rass et al., 2007a, Rass et al., 2008). Cell-free extracts prepared from *APTX*$^{-/-}$ DT40 cells or *APTX*$^{-/-}$ mouse cortical astrocytes lack the ability to repair a 5'AMP-SSB indicating that this activity is unique to APTX in mammalian cells (Ahel et al., 2006). Also cell-free extracts prepared from *APTX*$^{-/-}$ mouse cortical astrocytes are defective in full repair assays which measure short patch SSBR of an adenylated SSB *in vitro* (Ahel et al., 2006). Adenylated nicks are produced as a normal intermediates during ligation by an ATP-dependant DNA ligase, and an stable abortive ligation intermediate can arise if a ligase has attempted to ligate a SSB with a 3' terminus other than a 3'OH. Thus APTX has been proposed to play a role in SSBR as a way of resetting an abortive ligation and allowing repair to continue.

Consistent with its association with SSBR and DSBR machinery overexpressed EGFP-tagged APTX has also been shown to co-localise with XRCC1 at sites of heavy ion-induced damage and laser irradiation (Gueven et al., 2004, Jakob et al., 2005, Harris et al., 2009, Gueven et al.,

2007). Heavy-ion irradiation introduces complex localised DNA damage and it is very likely that both SSBs and DSBs are present at the sites of damage. It has also been reported in a number of different studies that APTX defective cells exhibit sensitivity to DNA damaging agents. Transformed lymphoblastoid cell lines (LCL) and primary fibroblasts have been reported to show sensitivity to treatment with the alkylating agent MMS and the oxidising agent H_2O_2, although this was very mild in the case of the fibroblasts (Gueven et al., 2004, Clements et al., 2004). In the same study Clements et al demonstrated that the AOA1 primary fibroblasts showed a mild sensitivity to X-rays while the LCLs were not sensitive to γ-ionising radiation in the Gueven et al study (Gueven et al., 2004, Clements et al., 2004). siRNA mediated knock-down of APTX in HeLa cells has also been shown to confer sensitivity to MMS (Luo et al., 2004).

AOA1 primary fibroblasts were also reported to show sensitivity to buthionine-(S,R)-sulfoximine (BSO), an inhibitor of the synthesis of the ROS scavenger glutathione (Hirano et al., 2007). This sensitivity is rescued by addition of the anti-oxidants decylubiquinone or all-trans-retinol (Hirano et al., 2007). Importantly it has been shown that deleting Hnt3, the saccharomyces cerevisae homolog of APTX, in an *apn1Δ apn2Δ* (3' end-processing factors) or a *rad27Δ* (FEN1) background conferred sensitivity to H_2O_2 and MMS. Taken together these data provide support for an important role for APTX in the promotion of cellular survival following alkylating or oxidative damage (Daley et al., 2010).

The evidence for a global SSBR defect in AOA1 cell lines, however, has proved somewhat inconsistent. Several studies have reported that APTX defective cell lines show normal rates of SSBR upon treatment with H_2O_2 or MMS when measured by comet assay or NAD(P)H depletion assay (Gueven et al., 2004, Reynolds et al., 2009, El-Khamisy et al., 2009). A single study has reported that AOA1 cell lines show reduced repair of CPT lesions by comet assay but as CPT treatment would result in the increase in SSBs containing a non-adenylatable nick with a 5'OH it is again unclear how this fits in with the role of APTX in SSBR (Mosesso et al., 2005). It is possible that this defect is due to a 3' processing defect but in the presence of highly efficient 3' phosphatase activity of PNK this seems unlikely (Takahashi et al., 2007b).

Additionally two studies have reported an increased level of oxidative damage persists in AOA1 cells. They demonstrated that there is an elevated level of 8-oxo-G staining in AOA1 cells compared to a control cell lines using an anti-8-oxo-G antibody (Hirano et al., 2007, Harris et al., 2009). They also attempted to show elevated levels of 8-oxo-G staining in a post-mortem slice from an AOA1 patients cerebellum compared to an unrelated age-matched control (Hirano et al., 2007). However it is unclear how the loss of APTX leads to an increase in 8-oxo-G as this is type of DNA damage has not been shown to be a substrate for APTX. The processing of any potential abortive ligations would be downstream of the recognition and excision of 8-oxo-G by OGG1.

Interestingly, a genetic approach in which *APTX*$^{-/-}$ *TDP1*$^{-/-}$ double knockout mice where generated, showed that *APTX*$^{-/-}$ *TDP1*$^{-/-}$ astrocytes exhibited a synergistic decrease in rates of global SSBR compared to either of the single mutants (El-Khamisy et al., 2009). This was observed for the repair of both hydrogen peroxide and MMS induced damage. It is possible that in the *APTX*$^{-/-}$ single mutant, the level of unrepaired adenylated breaks could be too small to detect. The increase in blocked 3' termini due to the loss of TDP1 in the double mutant may result in the increase of abortive ligations above the threshold level of detection. Another possibility is that APTX-independent pathways that use the 3' terminus, such as long-patch repair, could function to repair the adenylated SSBs in *APTX*$^{-/-}$ cells and could be blocked in the double mutant.

APTX has been proposed to play a role in SSBR following DNA damage as a way of resetting an abortive ligation and allowing repair to continue. This offers a possible explanation for the clinical presentation of AOA1 as unrepaired adenylated SSBs could accumulate in post-mitotic neurons leading to blocked transcription and eventually cell death.

1.9.2 Spinocerebellar ataxia with neuronal neuropathy 1

The neurodegenerative disorder SCAN1 was discovered to be caused by a mutation in TDP1 (Figure 1.20) (Takashima et al., 2002). SCAN1 is an adult onset autosomal recessive ataxia which is characterised by spinocerebellar ataxia and, intriguingly, like AOA1 lacks any extraneurological features. SCAN1 has a later age-of-onset than AOA1 and seems to have a milder clinical presentation. To date nine SCAN1 patients, from a single family, have been discovered, each possessing the same H493R point mutation (Takashima et al., 2002).

TDP1 is phosphodiesterase that can selectively hydrolyse a phosphotyrosyl linkage at the 3' termini of DNA SSBs or DSBs (Yang et al., 1996, Interthal et al., 2001). In eukaryotic cells these linkages arise as the result of abortive topoisomerase 1 activity which leads to DNA breaks with a TOP1 peptide covalently linked to the 3' terminus of a SSB (Pommier et al., 2003). The H493R mutation found in SCAN1 patients resides within one of the HKD catalytic active sites within the phosphodiesterase domain and results in an approximately 25-fold reduction in activity as well as causing the accumulation of the TDP1-DNA covalent intermediate (Interthal et al., 2005, Walton et al., 2010). Thus the combination of accumulating TDP1-DNA adducts together with unrepaired Top1-SSBs would interfere with replication and transcription, potentially leading to progressive neuronal cell death and neurodegeneration.

SCAN1 cell lines have been shown to accumulate more DNA breaks in the presence of the Top1 inhibitor camptothecin than WT control cells using the alkaline comet assay (El-Khamisy et al., 2005) . Levels of these breaks did not decrease when subsequently incubated in drug – free media (El-Khamisy and Caldecott, 2006). Interestingly only half of these breaks where dependent on replication, suggesting that collision with the transcription machinery was responsible for as many abortive Top1-SSBs as with collision with replication machinery (El-Khamisy and Caldecott, 2006). This is important as the clinical presentation of SCAN1 is restricted to post-mitotic neurones which are highly transcriptionally active and could potentially possess a high level TOP1-SSBs and therefore a higher dependence on TDP1 than other cell types (Flangas and Bowman, 1970, Sarkander and Uthoff, 1976).

SCAN1 cell lines also displayed defective SSBR of oxidative damage induced by hydrogen peroxide and γ-rays (Katyal et al., 2007, El-Khamisy et al., 2007, El-Khamisy et al., 2005). This could either reflect an increase in abortive topoisomerase activity due to the close proximity of oxidative DNA lesions to the cleavage complex or it could reflect a defect in the processing of oxidative DNA breaks as TDP1 has been shown be able to process a 3'-PG and a number of other 3' adducts (Zhou et al., 2005, Inamdar et al., 2002).

Importantly *TDP1*$^{-/-}$ mice display a progressive decrease in cerebellar size which is consistent with the clinical presentation of the disease although the mice do not seem to exhibit any obvious ataxic phenotype (Katyal et al., 2007). SCAN1 is a relatively late onset disorder and it is possible that the mice do not live long enough to display these symptoms. Alternatively the ataxia in SCAN1 individuals could be due to the extra TDP1-SSBs that are generated as a result of the neomorphic H493R mutation (Interthal et al., 2005). Together the data provides strong evidence for the critical role of TDP1 in SSBR in maintaining neuronal integrity and preventing cerebellar degeneration.

1.9.3 Microcephaly, early-onset, intractable seizures and developmental delay

Very recently a third human neurological disorder associated with defective SSBR has been discovered. MCSZ is a developmental disorder characterised by microcephaly, infantile-onset seizures, developmental delay and variable behavioural problems, especially hyperactivity, and is caused by mutations in PNK (Figure 1.21) (Shen et al., 2010). It is striking that mutations arising in PNKP result in a developmental defect presenting with severe microcephaly while mutations in APTX and TDP1 result in a progressive cerebellar degeneration. Additionally MCSZ does not seem to display any neurodegeneration, although like the other disorders it also lacks any extraneurological symptoms. It is also important to note that this is the first human disorder associated with defective DNA repair that presents with seizures, which is intriguingly close to the pathology of mice that have a targeted deletion of XRCC1 (Lee et al., 2009).

Seven families with individuals suffering from MCSZ have been discovered so far. These individuals harbour four different mutations in PNK (Shen et al., 2010). L176F and E326K are point mutations within highly conserved residues of the phosphatase domain and T424Gfs48X and exon15Δfs4X are mutations within the kinase domain that produce truncated PNKP due to premature stop codons resulting from frameshifts. The frameshift within T424Gfs48X is the result of 17bp duplication within exon14 in the kinase domain, resulting in a 471 amino acid polypeptide of which the last 48 residues are out of frame. The frame-shift within exon15Δfs4X mutation arises due to a 17bp deletion within intron 15 that leads to mRNA transcript lacking exon 15, and resulting in a polypeptide of 436 amino acids of which the last 4 residues are out of frame (Shen et al., 2010). All of the mutations resulted in at an approximately 10-fold reduction in total levels of PNK protein. Importantly lymphoblastoid cell lines (LCL) derived from MCSZ patients displayed reduced rates of SSBR of both hydrogen peroxide and camptothecin induced DNA damage, consistent with previous data using a stable PNK knock down in human cells (Shen et al., 2010, Rasouli-Nia et al., 2004).

As mentioned previously PNK is a particularly important protein in SSBR due to its role in the repair of 3'-P termini. SSBs harbouring 3'-P termini arise at the majority of direct SSBs induced by ROS and this could provide an explanation for the differences in the clinical presentations of MCSZ with AOA1 and SCAN1 (Ward, 1998). It is thought that abortive ligations and TOP1-SSBs arise only rarely and therefore may not accumulate to sufficient levels to interfere with the developing nervous system. However oxidative lesions that require processing by PNK arise thousands of times per cell per day (Ward et al., 1987). Defective PNK activity would therefore present the rapidly dividing neuronal stem cell progenitors in developing brains with a huge quantity of unrepaired SSBs which would rapidly be converted into DSBs and would ultimately lead to cell death.

1.9.4 DNA Ligase I Deficiency

Mutations in DNA ligase I have been discovered within an individual suffering from stunted growth, sun-sensitivity and severe immunodeficiencies was discovered to possess mutations within DNA Ligase I alleles (Barnes et al., 1992). So far this has been the only documented case

of a Ligase I deficiency. This individual possessed two point mutations in different alleles of Ligase I, E566K and R771W, both of which reside within the active site of the protein intermediate and seem to disrupt the formation of the ligase-adenylate intermediate (Barnes et al., 1992). A fibroblast cell line established from the patient, 46BR, was shown to be hypersensitive to a wide range of DNA damaging agents including alkylating agents, cross-linking agents, ionising radiation, PARP inhibitors and UV (Simmonds et al., 1982, Squires and Johnson, 1983, Teo et al., 1983a, Teo et al., 1983b, Henderson et al., 1985, Lehmann et al., 1988, Lonn et al., 1989).

The types of DNA lesions induced by these chemically unrelated DNA damaging agents would require different DNA repair pathways to correct, implicating ligase I in pathways as diverse as BER, SSBR, NER, and interstrand crosslink repair (Caldecott, 2008, Nouspikel, 2009, Deans and West, 2011). In conjunction with its role in DNA repair, DNA ligase I also has a core role in DNA replication in the maturation of Okazaki fragments (Waga and Stillman, 1998). Consistent with this role, the 46BR cell line exhibits a reduced rate of joining of Okazaki fragments (Henderson et al., 1985, Lehmann et al., 1988, Lonn et al., 1989). Although DNA LigI is implicated in SSBR, the symptoms associated with ligase I deficiency are unlikely to be caused by the loss of any one pathway but instead a combination of defects in DNA replication and the repair of a variety of DNA lesions.

1.9.5 SSBs and Neurological Dysfunction

The existence of three human disorders associated with defective repair of SSBs, AOA1, SCAN1 and MCSZ, suggest that the SSBR has a crucial role in the maintenance of human health (Shen et al., 2010, Date et al., 2001, Moreira et al., 2001, Takashima et al., 2002). A striking similarity between the disorders is that they are all caused by mutations in DNA end-processing enzymes. APTX removes an adenylate group from the 5' of DNA, TDP1 cleaves the phosphor-tyrosyl linkage between the 3' terminus of DNA and a top1 peptide and PNKP repairs SSBs with 3'-phosphate and 5'-hydroxly termini (Ahel et al., 2006, Interthal et al., 2001, Takashima et al., 2002, Jilani et al., 1999, Karimi-Busheri et al., 1998, Whitehouse et al., 2001, Bernstein et al., 2005b). The end-processing stage of SSBR is enzymatically diverse as a large number of

different chemistries can arise at SSBs depending on the source of damage, requiring a number of mechanistically distinct activities to repair (Section 1.3.2). Thus there is likely to be less redundancy amongst the components of end-processing than during gap-filling or DNA ligation, as the later stages of SSBR utilise a number of DNA repair enzymes that possess similar mechanistic activities. This means that SSBR is potentially more susceptible to the loss of an end-processing factor, particularly if the defective protein possesses a unique activity.

Another striking similarity between the disorders is the presentation of pronounced neuropathology in the absence of extraneurological symptoms that are common to other DNA repair defective disorders, such as cancer predisposition and immunodeficiency. This suggests that neurons are exquisitely sensitive to defects in SSBR. The absence of extraneurological symptoms present in these three disorders could be due to a combination of factors. There is evidence for a hypothetical role S-phase specific role for XRCC1 in the repair of SSBs encountered by the replication fork, in the replication-coupled SSBR pathway, and it has been suggested that this pathway could operate in conjunction with HR and therefore involve the structure specific nucleases that operate during HR (Figure 1.12) (Caldecott, 2008, Caldecott, 2001, Caldecott, 2003b). The presence of this pathway could explain the lack of cancer predisposition in SSBR defective disorder as any unrepaired SSBs encountered by the replication fork would be repaired by RC-SSBR and would not become a permanent block to replication. Finally there is no evidence for a role of SSBR in development of the vertebrate immune, explaining the lack of immunodeficiency in AOA1, SCAN1 and MCSZ.

There is, however, a very important difference between the neuropathologies that present in AOA1, SCAN1 and MCSZ. While both AOA1 and SCAN1 are neurodegenerative disorders that are associated with progressive degeneration and atrophy of the cerebellum after birth, MCSZ presents with primary microcephaly from birth, but exhibits no evidence of subsequent degeneration. The different presentations likely reflects that the loss of APTX and TDP1 primarily effect post-mitotic neurones while mutations in PNKP have a greater impact upon the developing brain.

The sensitivity of post-mitotic neurons to the loss of APTX and TDP1 could be due to a number of factors. This first is that post-mitotic neurones could be more dependent on APTX and TDP1 dependent SSBR due to the absence of alternate end processing factors or redundant repair pathways. For example, long-patch repair, which could function in the absence of APTX to repair adenylated SSBs, is thought to be attenuated in post-mitotic neurones due to the down-regulation of replication factors (Cam et al., 2004). Additionally homologous recombination and other DNA repair pathways that operate during S-phase and G2 would not be in operation in the G0 phase of post-mitotic neurons (Delacote and Lopez, 2008, Sonoda et al., 2006, Caldecott, 2008, Rass et al., 2007b).

Another possibility is that post-mitotic neurones are exposed to a higher level of oxidative stress than other tissue types due to the high oxygen demand of the nervous system. Neurons are highly active cells and exhibit high levels of mitochondrial respiration together with a reduced capacity to neutralise reactive oxygen species, which will lead to high levels of oxidative DNA damage (Weissman et al., 2007, Barzilai, 2007). This would place a higher load on the SSBR pathways in post-mitotic neurones that repair oxidative DNA damage. Post mitotic neurones are also highly transcriptionally active which, in combination with the high level of oxidative stress, could mean that post-mitotic neurones possess a high level of transcription associated DNA damage and would, again, be more dependent on the SSBR pathways than other cell types (Flangas and Bowman, 1970, Sarkander and Uthoff, 1976). The accumulation of unrepaired SSBs and collapsed transcription forks in AOA1 and TDP1 could ultimately lead to a higher occurrence of neuronal cell death in individuals suffering from the disease. Finally the nervous system has a very limited regenerative capacity which would mean that it would be highly sensitive to progressive cell death and any brain tissue lost through degeneration would not be replaced.

Together these factors provide a potential explanation for why post-mitotic neurones are sensitive to mutations in APTX and TDP1. However, in contrast, MCSZ presents with severe microcephaly from birth and there is no evidence of any subsequent neurodegeneration (Shen et al., 2010). As described earlier, the generation of the huge numbers of neurons that

comprise the adult brain is dependent on a critical period of proliferation of neuronal stem cell progenitors (Bayer et al., 1991).

Due to the highly metabolic status of the developing brain, oxidative DNA damage induced by ROS produced by cellular metabolism would be a very significant source of DNA damage, a large proportion if which would be substrates for PNK. Therefore the proliferating neuronal stem cells are likely to be heavily dependent on PNK-dependent SSBR and defects in PNK could lead to a significant increase in the numbers of unrepaired oxidative SSBs and DSBs in the rapidly replicating neuronal progenitors, and in combination with the low threshold for undergoing apoptosis, leading to an increased rate of apoptosis. This would result in a reduction in the total numbers of neurons in the developing brain, and could consequently give rise to microcephaly. Indeed this has been suggested to also be the case for the incidence of microcephaly linked to defective repair of DSBs via the non-homologous end-joining pathway (O'Driscoll et al., 2001, Buck et al., 2006b, Gatz et al., 2011).

The absence of microcephaly in AOA1 and SCAN1 could reflect the potential rarity of the DNA lesions that APTX and TDP1 repair. It is possible that these rare lesions would not accumulate in enough numbers to impact upon the neuronal progenitors in the VZ and SVZ of the developing brain, whereas PNKP substrates would be amongst the most commonly arising DNA lesions. However the absence of neurodegeneration in MCSZ is more difficult to explain, as PNKP-dependent SSBR would also be defective in post-mitotic neurons which are subject to a high oxidative load. This could potentially be explained by the observation that post-mitotic neurons are much less sensitive to DNA damage that the neuronal progenitors in the VZ and SVZ of the developing brain (Hoshino and Kameyama, 1988, Narasimhaiah et al., 2005, Hoshino et al., 1991). As MCSZ cell lines have residual levels of PNKP, approximately 5-10%, there could be a low level of PNKP activity that is sufficient for the post-mitotic neurons, which can tolerate more DNA damage, but which is insufficient for the neuronal progenitors which are very sensitive to damage (Shen et al., 2010).

1.10 General aim of thesis

The first major aim of this thesis was to further investigate the short-patch repair defect of adenylated SSBs exhibited by APTX defective cell extracts *in vitro*. Prior to this study it has been shown that APTX defective cell extracts are unable to repair adenlyated SSBs *in vitro*, however the precise nature of this defect has not been shown. Additionally it has not been clear whether a DNA strand defect is responsible for the AOA1 disease as conflicting data exists for the presence of a chromosomal SSBR defect in APTX defective cells. To attempt to provide an answer for why this discrepancy exists between the biochemical and cellular data, it was the aim of this study to determine the precise stage at which the repair of abortive ligation intermediates AOA1 extracts failed *in vitro* and what the nature of the failure was. This was carried out using *in vitro* repair assays with a combination of recombinant DNA repair proteins and whole cell extracts prepared from AOA1 cell lines. The second major aim of this thesis was to use this knowledge to investigate whether APTX – independent repair pathways existed for the resolution of abortive ligation intermediates in living cells, and thereby proposing a hypothesis for the lack of a consistent DNA repair defect in AOA1 cells. To test this, the polymerase inhibitor aphidicolin was used investigate the impact of inhibiting Polδ and Polε dependent long-patch repair on the rates of SSBR in AOA1 cells following oxidative DNA damage.

CHAPTER TWO

Materials and Methods

2.1 General Chemicals and Equipment

All chemicals were obtained from VWR, Fisher Scientific or Sigma unless otherwise stated. All enzymes were obtained from Roche or New England Biolabs unless otherwise stated. All cell culture media was obtained from Gibco® Invitrogen Cell Culture and cell culture flasks, dishes and cryovials from Nunc.

All centrifugation steps, with the exception of cell culture, were carried out using a Beckman GS – 15R centrifuge using S4180, F0630 and F24020H rotors or a Sigma 1-13 micro centrifuge. All cell culture centrifugation steps were carried out using a Denley B5400 centrifuge or a Hettich Rotina refrigerated centrifuge.

2.2 Preparation of Plasmid DNA Constructs

2.2.1 DNA constructs

The sources of all bacterial expression plasmid DNA constructs used in this thesis are detailed in table 2.1.

2.2.2 Preparation of Plasmid DNA

Plasmid DNA was prepared by first transforming chemically competent DH5α *E.coli* cells with 0.2µg - 2µg of the appropriate plasmid. Plasmid DNA was incubated with 50µl of chemically competent DH5α cells for 30min on ice before heat shocking for 45 seconds at 42°C and then cooling on ice for 5 min. 1ml of LB was added to the transformation mixture which was incubated at 37°C for 1 hour with shaking at 220rpm. The transformation mixture was plated onto LB agar plates containing 50µg/ml ampicillin or kanamycin and incubated at overnight at 37°C. Single colonies were picked and used to inoculate 5ml (mini-preparation) or 100ml (midi preparation) LB containing 50µg/ml of the appropriate antibiotic. These cultures were then incubated overnight at 37°C on a shaker at 220rpm. Plasmid DNA was then extracted by

alkaline lysis according to manufacturer's specifications using Quiagen DNA extraction kits (QIAprep® Miniprep Kit and QIAGEN® Plasmid Midi Purification Kit).

2.2.3 Quantification of DNA concentration in solution

The concentration of DNA in solution was quantified by measuring the absorbance at 260 and 280nm in quartz cuvettes. The ratio of 260/280 absorbance was used to determine the purity of the DNA solution. A ratio of 1.8 or greater indicated that the preparations were free from contaminations. The concentration was confirmed in parallel by analysing the DNA solution by DNA agarose gel electrophoresis and comparing to a linear DNA molecule of known concentration.

2.2.4 DNA agarose gel electrophoresis

Agarose gels (0.8 – 1% w/v) were prepared by dissolving Ultrapure Electrophoresis Grade Agarose (Invitrogen) in 1xTAE buffer (0.4M Tris Acetate and 1mM EDTA pH8.0). 2µg/ml ethidium bromide was added to the agarose gel mix and the gel was poured. DNA samples were loaded onto the agarose gel in type II loading buffer (1 x concentration: 0.04% w/v bromophenol blue, 0.04% w/v xylene cyanol FF, 2.5% w/v ficoll (Type 400 from Pharmacia)) in distilled water. DNA was subjected to electrophoresis at 80V for 45min. 1 Kb Plus DNA Ladder (Invitrogen) was electrophoresed in parallel and used as a size marker. DNA was visualised by UV illumination (The Imager UV Transilluminator Appligene Inc QBiogene).

2.2.5 Restriction enzyme digestion of DNA

DNA of the appropriate concentration (0.5µg - 5µg) was incubated with 1-2U of appropriate restriction enzyme for 1 hour at 37°C. Complete digestion of the DNA determined by comparison to an undigested control sample by agarose gel electrophoresis. If appropriate, DNA fragments were purified using Qiagen QIAquick® Gel Extraction Kit and the DNA concentration was quantified as described above.

2.2.6 DNA ligation

Prior to ligation, digested vector DNA was dephosphorylated with 1U calf intestine alkaline phosphatase for 1 hour at 37°C and purified using the Qiagen QIAquick® Gel Extraction Kit. DNA ligation reactions were set up according to Sambrook and Russell (Sambrook and Russell, 2001) at vector to insert ratios of 1:0, 1:1 and 1:3. Reactions were incubated with 1U of T4 DNA ligase (Roche) overnight at 16°C in a total volume of 10µl. 5µl of the ligation reaction was transformed into chemically competent DH5α as described above in section 2.2.3. Plasmid DNA was extracted by alkaline lysis according to manufacturer's specifications using Quiagen DNA extraction kits (QIAprep® Miniprep Kit). The presence of the insert and correct orientation was confirmed by digestion of the plasmid by restriction digest and analysis by agarose gel electrophoresis.

2.2.7 DNA sequencing

Plasmid DNA was sequenced by GATC Biotech using standard primers or gene-specific primers.

2.3 Analysis of cellular extracts and recombinant protein by SDS-PAGE and immunoblotting

2.3.1 SDS- Polyacrylamide Gel Electrophoresis (SDS-PAGE)

10% resolving (10ml final volume: 4ml ddH_2O, 3.3ml 30% acrylamide/bisacrylamide (37.5:1) mix (Flowgen), 2.5ml 1.5M Tris pH 8.8, 0.1ml 10% SDS, 0.1ml 10% APS, 4µl TEMED) and 5% stacking (4ml final volume: 2.7ml ddH_2O, 0.67ml 30% acrylamide/bisacrylamide (37.5:1) (Flowgen) 0.5ml, 0.5ml 1M Tris pH6.7, 40µl 10% SDS, 40µl 10% APS, 4µl TEMED) polyacrylamide gels (PAGE) were prepared according to Sambrook and Russell (Sambrook and Russell, 2001). Protein samples (purified recombinant protein, bacterial and mammalian cell extract) were denatured by incubating in SDS loading buffer (1x concentration: 50mM Tris pH8.0, 2% w/v SDS, 10% w/v glycerol, 0.1% w/v bromophenol blue 200mM DTT) at 94°C for

5min. The denatured samples were briefly centrifuged at full speed and aliquots were separated on SDS-PAGE using Precision Plus Protein Prestained Duel Colour Standards (BioRad) as markers. Electrophoresis was carried out using Mini Protean 3 apparatus (BioRad) in 1x running buffer (25mM Tris, 250mM glycine, 0.01% w/v SDS) at 150V for 60min. Total protein was visualised by staining in coomassie brilliant blue solution (0.25% w/v coomassie brilliant blue G-250 (BioRad, 50% v/v methanol, 10% v/v acetic acid) for 30min and destaining (10% v/v methanol, 10% v/v acetic acid) and dried.

2.3.2 Immunoblotting of proteins

Total protein was transferred from polyacrylamide gels to nitrocellulose membrane (H-Bond C Extra Membrane GE Healthcare) by wet transfer using Protean 3 Mini Trans-Blot Cell (BioRad) in 1x Towbin buffer (20mM Tris, 150mM glycine, 10% v/v methanol) at 100V for 90min or 10V for 999min. Successful transfer was determined by non-permanent staining of total protein on the membrane with 0.1% w/v Ponceau S in 5% acetic acid. The stain was removed by washing in 1x TBST (10mM Tris, 140mM sodium chloride, 0.1% v/v Tween 20, pH 7.9). Membranes were blocked by incubation with 5% (w/v) non-fat milk in 1xTBST for 1 hour and then washed briefly in 1xTBST. Membranes were then incubated in primary antibody under the appropriate conditions (Table 2.2), washed in 1xTBST (1x 15min, 1x 10min and 2x 5min) and finally incubated in the appropriate secondary antibody (Table 2.3). The membranes were washed again as described for the primary antibody and incubated in enhanced chemiluminescence (ECL) western blotting detection reagent (GE Healthcare) for 1 minute and developed on autoradiography blue sensitive film (GRI) using Xograph Compact 4 automatic X-ray film processor.

2.4 Overexpression and purification of recombinant human proteins from *E.coli*

2.4.1 Overexpression of recombinant proteins in *E.coli* strain BL21 (DE3)

The appropriate bacterial expression vector was transformed into chemically competent BL21 (DE3) *E.coli* cells. 0.2µg - 2µg plasmid DNA was incubated with 50µl of chemically competent

BL21 (DE3) cells for 30min on ice before heat shocking for 45 seconds at 42°C and then cooling on ice for 5min. 1ml of LB was added to the transformation mixture which was subsequently incubated at 37°C for 1 hour with shaking at 220rpm. The transformation mixture was plated onto LB agar plates containing 50µg/ml ampicillin or kanamycin and incubated at overnight at 37°C. Single colonies were picked and used to inoculate 10ml starter culture consisting of LB containing 50µg/ml of the appropriate antibiotic and the culture was incubated overnight at 37°C on a shaker at 220rpm.

The starter culture was centrifuged at 4,800 rpm for 20 min, resuspended in fresh LB media and diluted into a large scale 500ml culture to a final OD_{600} 0.01. The culture was incubated at 30°C until OD_{600} 0.6 was reached and a 1ml pre-induction sample was taken for analysis. For the expression of proteins using the pET16b vector, 1mM IPTG was added and the culture was incubated for a specified time and temperature (details of the appropriate incubation conditions for different proteins are contained in Table 2.4). A 1ml post induction sample was taken for analysis and the culture was harvested by centrifugation at 5,000 rpm for 20min. The pellet was washed once in PBS and stored at -20°C. Aliquots of the 1ml pre- and post-induction samples were analysed by SDS-PAGE.

The ORF of human Polβ was contained within the heat- inducible expression vector pLW11 and protein expression was induced by incubation of *E.coli* containing the bacterial expression vector at 42°C for 4 hours (Sobol et al, 1996). Pre- and post- induction samples were obtained and analysed as described above.

2.4.2 Preparation of clarified cell extract from *E.coli*

Bacterial cell pellets containing overexpressed recombinant were resuspended in 20ml sonication buffer (25mM Tris-HCl (pH7.0), 0.5M NaCl, 10% glycerol, 1mM DTT, 1mM imidazole (pH8.0) and 1mM PMSF). Crude cell extract was prepared by sonicating the resuspended cell pellet at 30% power for ten times 30 seconds bursts followed by a 30 second cooling period. The soluble and insoluble material was separated by spinning at 14,000 rpm for 20min at 4°C.

The supernatant was retained, snap frozen in liquid nitrogen and stored at -80°C. 100µl aliquots of the soluble and insoluble material were retained for anaylsis by SDS-PAGE.

2.4.3 Purification of His-tagged APTX, PNK and LigIIIα proteins from *E.coli*

Human recombinant Histidine-tagged APTX, PNK and LigIIIα were purified from *E.coli* extract using the method below.

2.4.3.1 Purification of His-tagged APTX, PNK and LigIIIα by immobilised metal affinity chromatography (IMAC)

Human recombinant His-tagged APTX, PNK and LigIIIα were overexpressed in BL21 (DE3) *E.coli* cells as described (section 2.4.1) using the expression vectors pB352-hAPTX, pET16b-hPNK and pET16b-hLigIIIα respectively (Table 2.4). The first purification step was immobilised metal affinity chromatography (IMAC) on Ni-NTA agarose beads (first described in Porath et al. 1975). In IMAC, metal ions (Ni^{2+}) are bound to a metal chelating group (NTA) immobilised on agarose beads. The Ni^{2+} ions form interactions with imidazole side-chains present within histidine residues, retaining any histidine containing proteins on the beads. To take advantage of this proteins are fused to tags consisting of six or ten histidine residues, allowing the recombinant protein to bind to the Ni^{2+} on the column with high affinity. Proteins are eluted from the beads with a buffer containing an excess of free imidazole, which out-competes the interaction of the histidine side chains with the column.

A Ni-agarose column with a 5.0ml bed volume was prepared by loading 1ml Ni-NTA Agarose resin (Qiagen) onto a Bio-Rad PolyPrep column and washing with 10 column volumes of sonication buffer (25mM Tris-HCl, 0.5M NaCl, 10% glycerol, 1mM DTT, 1mM imidazole (pH8.0)). 20ml clarified *E.coli* extract containing His-tagged recombinant protein was loaded onto the Ni-NTA agarose column at 4°C. All subsequent steps were also carried out at 4°C. The column was washed three separate times with 10 column volumes of sonication buffer containing 20mM, 40mM and 80mM imidazole respectively. His-tagged protein was then eluted with 5 column volumes of sonication buffer containing 250mM imidazole and 0.5ml

elution fractions were collected. Aliquots of the column load, flow through, washes and elution fractions were analysed by SDS-PAGE.

2.4.3.2 Purification of His-tagged APTX, PNK and LigIIIα by cation exchange chromatography

IMAC elution fractions containing either His-APTX, His-PNK or His-LigIIIα were subsequently purified by cation exchange chromatography using a 1.6-ml POROS column on a BioCAD ® Sprint Perfusion Chromatography System (Applied Biosystems, United Kingdom). The column was washed with 20 column volumes of ice cold high salt buffer (25mM Tris-HCl, 1M NaCl, 10% glycerol, 1mM DTT) and then 20 column volumes of ice cold low salt buffer (25mM Tris-HCl, 0.1M NaCl, 10% glycerol, 1mM DTT). Prior to washing, the high and low salt buffers were filtered through a 0.22µm filter unit. pH strongly affects the charge characteristics of a protein and the affinity of the target protein for the column. This effect is expressed by the isoelectric point (pI) of a protein, which describes the pH at which a molecule has a net charge of zero. The purification of different proteins was carried out at different pH to optimise the yield (Table 2.5). All buffers and protein solutions were kept on ice.

Peak elution fractions from IMAC (section 2.4.3.1) were pooled, loaded onto the cation exchange column and washed with 10 column volumes low salt buffer. His-APTX was eluted with a salt gradient from 0.1M NaCl to 1M NaCl over 15 column volumes. 1ml elution fractions were collected. Aliquots of the column load, flow through and elution fractions were analysed by 10% SDS PAGE and peak fractions were dialysed into storage buffer (25mM Tris-HCl, 150mM NaCl, 10% glycerol, 1mM DTT) using a D-Tube™ Dialyzer (Novagen). The protein concentration of the final dialysed fractions was quantified by the Lowry method using the *DC* Protein Assay (BioRad) with BSA used as a protein standard. The dialysed fractions were aliquoted, snap frozen in liquid nitrogen and stored at -80°C.

2.4.4 Purification of Polβ from *E.coli* by cation exchange chromatography

Recombinant Polβ was purified by cation exchange chromatography using 1.6-ml POROS cation and anion exchange columns on a BioCAD ® Sprint Perfusion Chromatography System

(Applied Biosystems, United Kingdom). Consecutive anion and cation exchange columns were set up in a circuit and washed with 20 column volumes of ice cold high salt buffer (25mM Tris-HCl, 1M NaCl, 10% glycerol, 1mM DTT, (pH7.5)) and then 20 column volumes of ice cold low salt buffer (25mM Tris-HCl, 0.1M NaCl, 10% glycerol, 1mM DTT, (pH7.5)). Prior to washing, the high and low salt buffers were filtered through a 0.22µm filter unit. All buffers and protein solutions were kept on ice.

Bacterial clarified extract containing recombinant human Polβ was prepared as previous described (section 2.4.2) and loaded onto the ion exchange columns. The columns were washed with 10 column volumes of low salt buffer and the anion exchange column was removed from the circuit. Polβ was eluted from the cation exchange column with a salt gradient from 0.1M NaCl to 1M NaCl over 15 column volumes and 1ml elution fractions were collected. Aliquots of the column load, flow through and elution fractions were analysed by 10% SDS PAGE and peak fractions were dialysed into storage buffer (25mM Tris-HCl, 150mM NaCl, 10% glycerol, 1mM DTT) using a D-Tube™ Dialyzer (Novagen). The protein concentration of the final dialysed fractions was quantified by the Lowry method using the *DC* Protein Assay (BioRad) with BSA used as a protein standard. The dialysed fractions were aliquoted, snap frozen in liquid nitrogen and stored at -80°C.

2.4.5 Purification of His-tagged Chlorella Virus DNA ligase from *E.coli* by immobilised metal affinity chromatography (IMAC)

Recombinant wild-type His-tagged DNA ligase from Chlorella Virus and a C-terminally truncated Chlorella Virus DNA ligase mutant (CΔ5) were overexpressed in BL21 (DE3) *E.coli* cells as described (section 2.4.1) using the expression vectors pET16b- PBCV- Ligase and pET16b- PBCV- CΔ5 respectively (Table 2.4). The His-tagged Chlorella Virus DNA ligase proteins were purified by immobilised metal affinity chromatography (IMAC) on Ni-NTA agarose beads. A Ni-agarose column with a 5.0ml bed volume was prepared by loading 1ml Ni-NTA Agarose resin (Qiagen) onto a Bio-Rad PolyPrep column and washing with 10 column volumes of ice

cold sonication buffer (25mM Tris-HCl (pH8.0), 0.5M NaCl, 10% glycerol, 1mM DTT, 1mM imidazole (pH8.0)).

20ml clarified *E.coli* extract containing His-tagged recombinant protein was loaded onto the Ni-NTA agarose column at 4°C. All subsequent steps were also carried out at 4°C. The column was washed three separate times with 10 column volumes of sonication buffer containing 20mM, 40mM and 80mM imidazole respectively. His-tagged protein was then eluted with 5 column volumes of sonication buffer containing 250mM imidazole and 0.5ml elution fractions were collected. Aliquots of the column load, flow through, washes and elution fractions were analysed by SDS-PAGE. Peak elution fractions were dialysed into storage buffer (25mM Tris-HCl (pH8.0), 150mM NaCl, 10% glycerol, 1mM DTT) using a D-Tube™ Dialyzer (Novagen). The protein concentration of the final dialysed fractions was quantified by the Lowry method using the *DC* Protein Assay (BioRad) with BSA used as a protein standard. The dialysed fractions were aliquoted, snap frozen in liquid nitrogen and stored at -80°C.

2.5 *In Vitro* Single-Strand Break Repair Assays

2.5.1 Urea polyacrylamide gel electrophoresis (Urea PAGE)

Urea polyacrylamide gels were prepared using the SequaFLOWGel Sequencing Kit (Flowgen Bioscience) using a 21cm x 40cm Sequi-Gen GT Sequencing Cell (Bio-Rad). Radiolabelled DNA was denatured by heating to 90°C in formamide loading buffer (1x concentration: 30% formamide, 0.04% w/v bromophenol blue) and was separated on 15% urea polyacrylamide gels (50ml total volume: 30ml SequaGel Concentrate, 15ml SequaGel Diluent, 5ml SequaGel Buffer, 400µl 10% APS, 20µl TEMED). Prior to loading of the DNA samples, the polyacrylamide gel was pre-run by carrying out electrophoresis at 45W for 45 min. Denatured DNA samples were then loaded and electrophoresis was carried out in 1xTBE (90mM tris, 90mM boric acid, 2mM EDTA) at 45W for 90 – 180 min. After electrophoresis the polyacrylamide gel was incubated in 10% acetic acid 10% methanol for at least 20 min, dried and exposed to a Phosphor Screen (GE Healthcare). Radiolabelled DNA was detected by phosphorimaging using a Storm™ phosphoimager (GE Healthcare) and visualised by ImageQuant TL software (GE Healthcare).

2.5.2 Native polyacrylamide gel electrophoresis (Native PAGE)

15% native polyacrylamide gels were prepared using 40% acrylamide/bis-acrylamide (19:1) solution and 1xTBE. DNA samples were loaded onto the native acrylamide gel in type II loading buffer (1 x concentration: 0.04% w/v bromophenol blue, 0.04% w/v xylene cyanol FF, 2.5% w/v ficoll (Type 400 from Pharmacia)) in distilled water. Electrophoresis was carried out using Mini Protean II apparatus (Bio-Rade) in 1xTBE at 80V for 2 hours. After electrophoresis the polyacrylamide gels were incubated in 10% acetic acid 10% methanol, dried and exposed to Phosphor Screens (GE Healthcare). Radiolabelled DNA was detected by phosphorimaging using a Storm™ phosphoimager (GE Healthcare) and visualised by ImageQuant TL software (GE Healthcare).

2.5.3 Preparation of a model oxidative SSB substrate *in vitro*

Double stranded oligonucleotide duplexes harbouring a SSB with a 1 nucleotide gap were prepared by annealing 17mer and 25mer oligonucleotides to a complimentary 43mer oligonucleotide backbone. An oligonucleotide duplex containing a nick instead of a gap could be prepared by substituting the 17mer oligonucleotide with an 18mer. Additionally a duplex containing a SSB that mimicked an oxidative break with a 3'-phosphate could also be prepared by using a 17mer with a 3' phosphate modification. Unless otherwise stated all other termini contain an OH. All oligonucleotides used in this thesis are detailed in Table 2.6 and were obtained from Eurofins MWG Operon.

To prepare a SSB substrate in which repair of the 5' termini could be visualised, the 25mer was first radiolabelled on the 5' termini by incubating the oligonucleotide with γ^{32}P ATP and T4 PNK (Roche) in a total volume of 40µl for 60 min at 37°C. Unincorporated radionucleotides were then removed by applying the reaction to an illustra MicroSpin™ G-25 Columns (GE Healthcare) and centrifuging according to manufacturer's specifications. To prepare a SSB substrate in which repair of the 3' termini could be visualised, the 17mer was radiolabelled. To radiolabel a 17mer harbouring a 3' phosphate modification, T4 PNK 3' phosphatase free

mutant (Roche) was used to prevent processing of the 3' termini. The success of the radiolabelling was determined by analysing the reaction products by 15% urea PAGE.

The radiolabelled oligonucleotides were annealed to a two-fold molar excess of unlabelled oligonucleotides in by incubating 95°C for 5 min and then incubating successively at 70°C, 50°C, 37°C, and room temperature for 10 min each before placing on ice. A control sample lacking either the 17mer or 25mer was annealed in parallel. The annealed products were fractionated by 15% native PAGE.

2.5.4 Preparation of 5'-AMP abortive ligation intermediates *in vitro*

To prepare a 5'-AMP abortive ligation intermediates in vitro, an oxidative SSB substrate was adenylated using T4 DNA ligase. The 25mer (25µM) was radiolabelled on the 5' termini by incubating with 1U T4 DNA ligase and γ^{32}P ATP in a volume of 40µl for 1 hour at 37°C. Unincorporated radionucleotides were removed using an illustra MicroSpin™ G-25 Columns and the ^{32}P radiolabelled 25mer was annealed (11.25µM) to a two-fold excess of unlabelled 17mer 3'-P (22.5µM) and 43mer (22.5µM) in Buffer EB (Qiagen). The annealed oxidative SSB was then adenylated by incubating 7.5µM of the oligonucleotide duplex with 1U of T4 DNA ligase (Roche) for 30°C for 1 hour in 25mM tris-HCL (pH7.5), 130mM KCl, 1mM DTT, 10mM $MgCl_2$, and 1mM ATP. A mock adenylated control lacking T4 DNA ligase was prepared by incubated 7.5µM of the oxidative SSB with ligase storage buffer (20 mM Tris-HCl (pH 7), 60 mM KCl, 1 mM EDTA, 5 mM DTT, 50% glycerol (v/v)). The efficiency of the adenylation reaction is not 100% and there is always some unadenylated ^{32}P-25mer present necessitating purification of the AMP-^{32}P-25mer by denaturing gel extraction using the Crush and Soak method.

The reaction products were fractionated by 15% urea PAGE and the position of the adenylated and mock adenylated 25mer oligonucleotides was determined by autoradiography using blue sensitive film. The AMP-^{32}P-25mer and ^{32}P-25mer were excised from the gel and the DNA was eluted from the acrylamide by crushing the gel slice and incubating overnight at room

temperature in 2x volume crush and soak buffer (300mM sodium acetate, 1mM EDTA (pH 8.0)). The resulting slurry was centrifuged at high speed and the supernatant retained. 1µl of Pellet Paint® NF Co-precipitant (Merck Biosciences) was added to the supernatant followed by 2 x volume of ice cold absolute ethanol. The solution was incubated at -80°C overnight and the DNA pelleted by centrifugation at 14,000 rpm for 20min at 4°C. The pellet was washed twice with ice cold 70% ethanol, air dried and the purified DNA resuspended in 30µl Buffer EB (Qiagen).

The purity of the purified AMP-^{32}P-25mer and ^{32}P-25mer oligonucleotides were determined by analysing by 15% denaturing PAGE. The concentration of the purified oligonucleotides was determined by quantifying the intensity of the AMP-^{32}P-25mer and ^{32}P-25mer bands using ImageQuant TL software (GE Healthcare) and relating it to the intensity of a known quantity of the pre-gel extracted ^{32}P-25mer. The final adenylated and mock adenylated substrates containing a 1 nucleotide gap were prepared by annealing the purified AMP-^{32}P-25mer and ^{32}P-25mer to a 2x molar excess of unlabelled 43mer and 17mer as previously described and analysing by 15% native PAGE. A substrate containing an adenylated nick was prepared by substituting the 17mer for the 18mer oligonucleotide.

2.5.4.1 Preparation of a dual radiolabelled 5'-AMP abortive ligation intermediate *in vitro*

An adenylated SSB substrate containing a ^{32}P radiolabel on the radiolabel of both the 17mer and 25mer oligonucleotides was prepared. The 17mer 3'-P and 25mer were ^{32}P radiolabelled with T4 PNK 3' phosphatase free and annealed to a 2x fold molar excess of the unlabelled 43mer. The annealed duplex was then adenylated and mock adenylated as previously described. The substrates were separated on 15% native PAGE and the fully annealed duplexes were purified from the partially annealed duplexes by gel extraction using the crush and soak method as described in section 2.5.4. The purity of the final purified adenylated and mock adenylated duplexes were determined by analysis by 15% native PAGE and 15% urea PAGE and the concentration of the substrates were determined as described above.

2.5.5 *In vitro* repair of adenylated SSB substrates by whole cell extracts

For reactions involving whole cell extracts, 25nM of adenylated SSB substrate was incubated with the indicated concentrations of whole cell extract for 60 min at 30°C in reaction buffer containing 25mM HEPES (pH8.0), 130mM KCl, 1mM DTT, 10mM $MgCl_2$, 100µM deoxynucleoside triphosphates (dNTPs) and 1mM ATP unless otherwise stated. 1000x fold molar excess of competitor oligonucleotide (Table 2.6) was added to the reactions to suppress non-specific nuclease activity. Reactions were stopped by addition of 1/3 volume of formamide gel loading buffer (90% formamide, 0.12% w/v bromophenol blue) and denaturing by incubation at 90°C for 5 min. Reaction products were separated by 15% urea PAGE gels and visualised by phosphorimaging as described previously.

2.5.6 *In vitro* repair of SSBs by recombinant proteins

For reactions involving recombinant proteins, 100nM of adenylated SSB substrate was incubated with the indicated concentrations of recombinant proteins for 60 min at 30°C in reaction buffer containing 25mM tris-HCL (pH7.5), 130mM KCl, 1mM DTT, 10mM $MgCl_2$, 100µM dNTPs and 1mM ATP unless otherwise stated. Reactions were stopped by addition of 1/3 volume of formamide gel loading buffer (90% formamide, 0.12% w/v bromophenol blue) and denaturing by incubation at 90°C for 5 min. Reaction products were separated by 15% urea PAGE gels and visualised by phosphorimaging as described previously.

2.5.7 *In vitro* ligase adenylation assay

Ligase adenylation was assayed by incubating 100ng DNA ligase with 5 µM α^{32}P ATP, 10nM ATP, 25mM HEPES (pH8.0), 130mM KCl, 1mM DTT and 10mM $MgCl_2$ at 30°C for 5 min. Reactions were stopped by addition of SDS loading buffer (1x concentration: 50mM Tris pH8.0, 2% w/v SDS, 10% w/v glycerol, 0.1% w/v bromophenol blue 200mM DTT) and reaction products were fractionated by SDS PAGE. Proteins were visualised by coomassie brilliant blue staining as described previously followed by destaining in 10% methanol 10% acetic acid. The acrylamide gel was dried and adenylation of the ligase was visualised by phosphorimaging as described previously.

2.6 Mammalian Cell Culture

Sources and genotypes of mammalian cell lines employed in experiments within this thesis are detailed in Table 2.7.

2.6.1 Maintenance of mammalian cell lines

All mammalian cell lines were incubated in a humidified atmosphere with 5% carbon dioxide at 37°C. The primary fibroblast cell lines FD105 and 1BR were maintained as monolayers in MEM supplemented with 15% (v/v) foetal calf serum (FCS), 100units/ml penicillin, 100Mg/ml streptomycin and 2mM L-glutamate. The hTERT immortalised fibroblast cell lines FD105 M20 hTERT, FD105 M21 hTERT and 1BR M20 hTERT were maintained in the same media containing 0.3µg/ml puromycin and 300µg/ml G418. The cultures were passaged every 2-4 days to maintain them in logarithmic growth phase. Cells were washed with PBS and incubated in 1x trypsin (250mg/ml trypsin in PBS) for 5min. Cells were shaken into suspension, washed with fresh media and an appropriate volume transferred into a fresh flask with fresh media.

The lymphoblastoid cell lines (LCL) MT1 and MT6 were maintained in suspension in RPMI supplemented with 10% (v/v) foetal calf serum (FCS), 100units/ml penicillin, 100mg/ml streptomycin and 2mM L-glutamate. Cells were passaged every 1-3 days by diluting in fresh media to maintain them in logarithmic growth phase at no greater than $1x10^6$ cells/ml.

For long term storage cells were pelleted by centrifugation at 1,500rpm for 3min and resuspending in fresh media containing 10% DMSO to a density of 5.0- $7.5x10^6$ cells/ml. 1ml aliquots were transferred to cryotubes and cooled slowly to -80°C before storage in liquid nitrogen. Cultures were regenerated by quickly thawing a frozen aliquot at 37°C and subsequently adding to fresh media in fresh flask (10ml media in a $75cm^2$ flask for fibroblasts or 5ml media in a $25cm^2$ flask for lymphoblastoid cell lines). The hTERT immortalised

fibroblasts were incubated in drug free medium for 24 hours before replacing with selection media.

2.6.2 Preparation of total cellular protein extracts

Cell pellets were lysed in 1x SDS loading buffer (50mM Tris pH8.0, 2% w/v SDS, 10% v/v glycerol, 0.1% w/v bromophenol blue, 200mM DTT) at 94°C at a cell density of 0.5- $2x10^6$ cells/µl. Total protein extracts were separated by SDS-PAGE and transferred onto nitrocellulose for immunoblotting.

2.6.3 Preparation of cell free protein extracts

$7.5x10^6$ cells were harvested by centrifugation at 1,500 rpm and washed in 3xPBS. Cell pellets were lysed by incubation with 0.2ml cell lysis buffer (20 mM Tris-HCl (pH 7.5), 10 mM EDTA, 1 mM EGTA, 100 mM NaCl, 1% Triton X-100 and 1/100 dilution of protease inhibitor cocktail (Sigma)) on ice and cell free extracts were prepared by centrifuging at 13,000rpm for 20min at 4°C. The supernatant was retained and the protein concentration quantified by the Lowry method using the *DC* Protein Assay (BioRad) with BSA used as a protein standard. Cell free extracts were aliquoted and stored at -80°C.

2.6.4 Preparation of quiescent fibroblasts

To render human fibroblasts quiescent, cells were cultured in complete media (MEM supplemented with 15% FCS) until confluence. For hTERT immortalised fibroblasts, cells were seeded in a $75cm^2$ flask and grown until confluent. Complete media was then replaced with serum- free media (MEM supplemented with 0.1% FCS) and cells were incubated for seven days. 24 hours prior to experimentation, on day six, media containing antibiotic selection was removed and the cells were incubated in drug free media. For primary fibroblasts $6x10^5$ cells were plated in 60mm culture dishes in complete media and grown until confluence. Complete media was then replaced with serum – free media and incubated for 28 days. Media was replaced with fresh media every 7 days.

2.7 DNA Replication Assays

2.7.1 ^{3}H-thymidine incorporation in the presence or absence of aphidicolin

^{3}H-thymidine incorporation was used as a measure of DNA replication synthesis in cycling and quiescent fibroblasts in the presence or absence of aphidicolin. For quiescent fibroblasts, $1x10^{5}$ cells were seeded in duplicate into a 6 well dish and allowed to adhere by incubation at 37°C for 4hrs. Cells were then incubated with complete media containing 0.02µCi/ml ^{14}C-thymidine for 48hrs, at which point the cells had achieved confluence. The cells were washed in PBS three times and then incubated in serum-free media (MEM supplemented with 0.1% FCS) for seven days. Following this cells were incubated with serum-free media containing 50µM APH or an equal volume of DMSO for 60 min at 37°C. ^{3}H-thymidine was added to the cells to a final concentration of 20µCi/ml in the presence of APH or DMSO and incubated for 3 hours at 37°C.

For cycling fibroblasts, $0.5x10^{5}$ cells were seeded in duplicate into a 6 well dish and allowed to adhere for 4 hours. Cells were then incubated with complete media containing 0.02µCi/ml ^{14}C-thymidine for 48hrs and subsequently chased for 4 hours in complete media lacking the radionucleotide. Following this cells were incubated with complete media containing 50µM APH or an equal volume of DMSO for 60 min at 37°C. ^{3}H-thymidine was added to the cells to a final concentration of 20µCi/ml in the presence of APH or DMSO and incubated for 3 hours at 37°C.

Cells were washed in PBS three times and harvested and lysed by scrapping in 2% SDS. 100µl was spotted in duplicate onto filter paper, which was then incubated in 5% trichloroacetic acid for 5 min and then in 70% ethanol for 5min. The filters were dried overnight, incubated in 1ml Ecoscint™ A (National Diagnostics) and the ^{3}H and ^{14}C signal was counted by liquid scintillation counting. ^{3}H-thymidine counts were normalised to ^{14}C-thymidine counts and the data was plotted graphically.

2.8 Cellular DNA Strand-Break Repair Assays

2.8.1 Alkaline Single-Cell Agarose Gel Electrophoresis (Alkaline Comet Assay)

The alkaline comet assay was used to measure the rate of repair of DNA strand breaks in mammalian cells after treatment with DNA damaging agents.

2.8.1.1 Preparations

For cycling primary and hTERT immortalised fibroblasts, cells were seeded into a 75cm^2 flask and cultured until approximately 50% confluence. 24 hours prior to treatment of the hTERT immortalised fibroblasts, media containing antibiotic selection was removed and the hTERT fibroblasts were incubated in drug – free media. Quiescent primary and hTERT immortalised fibroblasts were prepared as previously described in section 2.6.4. On the day of the experiment, cells were trypsinised and resuspended in fresh media to a cell density of 2x10^5 cells/ml.

Agarose slides were prepared by coating frosted slides (Fisher) with 0.6% (w/v) ultrapure electrophoresis grade agarose (Invitrogen) dissolved in PBS. 150µl 0.6% agarose was spread under a coverslip in duplicate to prepare two mini agarose gels per slide and stored at 4°C for at least 60 min until use.

2.8.1.2 Cell treatments, repair and cell harvesting

Before treatment a 1ml mock treated sample was removed and kept on ice. For treatment by exposure to γ-rays, cells were irradiated in suspension in complete media on ice. After treatment, cells were incubated at 37°C for a desired repair period and harvested by centrifuging at 1,500 rpm at 4°C and resuspending in 1ml ice cold PBS. Untreated and no repair samples were harvested in the same manner as repair samples. For dose response assays, cells were irradiated with increasing doses of γ-rays and samples were immediately harvested. All samples were retained on ice until plating.

2.8.1.3 Cell plating, cell lysis and electrophoresis

200µl of the cell suspensions were mixed with 200µl of 1.2% low melting point agarose (Sigma) and 150µl of the mixture was quickly spread over the 0.6% mini agarose gels on frosted slides (described in section 2.8.1.1) on ice. Slides were maintained at 4°C in the dark for the remainder of the assay. Cells were lysed by immersing in ice cold lysis buffer (2.5M sodium chloride, 100mM EDTA, 10mM Tris, 1% DMSO, 1% Triton-X-100, pH10) for 60 min. Slides were washed three times with ice cold ddH_2O and DNA was denatured by incubating slides in alkaline electrophoresis buffer (50mM sodium hydroxide, 1mM EDTA, 1% DMSO) for 45 min. The DNA was subjected to electrophoresis for 25 min at 25V and then subsequently neutralised by incubating in 0.4M Tris pH7.0 for 30 min.

2.8.1.4 Nucleic acid staining and scoring

DNA was stained with SYBR green (1:10000 dilution) and visualised by fluorescent microscopy (Nikon Eclipse E400) at 20x magnification. Comet tail moment for 100 cells per sample was determined using Comet Assay IV software (Perceptive Instruments). The average tail moment and scatter graphs of tail moments were calculated plotted for each repair time point.

2.8.1.5 Pre-treatment of cells with aphidicolin

For comet assays in the presence of aphidicolin, the cells were either pre-treated with 50µM APH (stock 30mM in DMSO) in complete media or with equal volume of DMSO for 60 min at 37°C. The cells were then irradiated and allowed to repair in the presence of APH or DMSO. The comet assay was performed as described above.

CHAPTER THREE

A defect in short-patch SSBR in AOA1 cell extracts

3.1 Introduction

AOA1 is an autosomal recessive ataxia that clinically presents with early onset ataxia, oculomotor apraxia, cerebellar atrophy and axonal motor neuropathy and is caused by mutations in the gene *APTX* (Barbot et al., 2001, Date et al., 2001). APTX has been shown to resolve abortive ligation intermediates *in vitro* by catalysing the release of adenylate groups covalently linked to 5' phosphate terminus of a DNA SSB or DSB (Ahel et al., 2006, Rass et al., 2007a, Rass et al., 2008). Whole cell extracts prepared from *APTX*$^{-/-}$ DT40 cells or *APTX*$^{-/-}$ mouse primary cortical astrocytes lack AMP-DNA hydrolase activity and are unable to perform short-patch SSBR on an *in vitro* substrate modelling an abortive ligation of an oxidative SSB (Ahel et al., 2006). APTX has been proposed to play a role in SSBR following DNA damage as a way of resetting an abortive ligation and allowing repair to continue (Figure 3.1).

3.1.2 Aims of this chapter

So far all the *in vitro* data on the role of APTX in repairing aborted ligation intermediates has been presented using recombinant proteins and cell free extracts from *APTX*$^{-/-}$ DT40 cells or *APTX*$^{-/-}$ mouse cortical astrocytes (Ahel et al., 2006, Rass et al., 2007a, Rass et al., 2008). The aim of this chapter is to determine if whole cell extracts prepared from human AOA1 disease cell lines are also defective in the short-patch SSBR of abortive ligation intermediates. To achieve this lymphoblastoid cell lines (LCL) derived from an individual with AOA1 were cultured and whole cell extracts from these cells were prepared. A model substrate of an abortive ligation of an oxidative SSB was prepared *in vitro* using ^{32}P radiolabelled oligonucleotides and AOA1 and WT whole cell extracts were compared for their ability to repair an abortive ligation intermediate *in vitro*.

3.2 Results

To measure short patch SSBR *in vitro* a double stranded oligonucleotide duplex harbouring a SSB was prepared by annealing 17mer and 25mer oligonucleotides to a complimentary 43mer oligonucleotide backbone resulting in an oligonucleotide duplex that contains a 1 nucleotide gap and non-complementary 3' overhangs (Figure 3.2 A). The 3' termini of the 17mer oligonucleotide (17mer-P) possess a 3'-phosphate terminus, mimicking the most common type of 3' termini that arises from oxidative DNA damage (Ward, 1998, Ward et al., 1987, Caldecott, 2001). To visualise the substrate the 5' termini of the 25mer was radiolabelled using γ^{32}P ATP and T4 PNK prior to annealing. Unless otherwise stated all other termini contain an OH.

3.2.1 Preparation of 5'-AMP abortive ligation intermediates in vitro

To prepare 5'-AMP abortive ligation intermediates in vitro, an oxidative SSB substrate was adenylated using T4 DNA ligase. A schematic detailing the preparation of the 5'-AMP substrate is presented (Figure 3.2 B). To prepare the model abortive ligation intermediate substrate, the 5' termini of the 25mer was first radiolabelled by incubating with 1U of T4 PNK and γ^{32}P ATP at 30°C for 1 hour. The unincorporated nucleotides were removed using spin-column chromatography. The radiolabelled ^{32}P-25mer was then annealed into a double stranded duplex by mixing with a 2x molar excess of unlabelled 43mer and 17mer-P and heating the mixture to 94°C for 5 min followed by cooling slowly to room temperature. The substrate was then adenylated by incubation with 1U of T4 DNA ligase at 30°C for 1 hour, or mock adenylated in the absence of ligase. The 5'- adenylated ^{32}P-25mer product of this abortive ligation reaction, which arises because the ligation reaction is prevented from going to completion due to the presence of the 3'P on the 17-mer and the 1 nucleotide gap, is shown in Figure 3.3A. The adenylated 25mer (AMP-^{32}P-25mer) was then separated from the non-adenylated 25mer (^{32}P-25mer) by 15% denaturing PAGE, recovered by gel extraction (Figure 3.3B), and re-annealed with the 17mer and 43mer to create the final adenylated substrate (Figure 3.3C).

To confirm the substrate was fully annealed the oligonucleotide duplexes were fractionated by 15% native PAGE (Figure 3.3 C). The fully annealed oligonucleotide duplex (lane 1) was readily

distinguished from a control partially annealed duplex lacking the 17mer (Figure 3.3 C, lane 2) and from the single stranded AMP-^{32}P-25mer (lane 3). This final substrate contains a SSB with a 1 nucleotide gap, a 3'P and a 5'AMP. It has been estimated that ~70% of SSBs produced by ROS have a 3'P so this substrate is a good model of an abortive ligation of an oxidative SSB (Caldecott, 2001). This substrate is also useful for measuring short-patch SSBR as the position of the ^{32}P radiolabel on the 5' of the 25mer means that long-patch SSBR events will not be detected. If gap filling extended past incorporation of a single nucleotide, a 5' flap containing the ^{32}P radiolabel would be generated. Cleavage of this 5' flap by FEN1 would result in loss of the label. Thus only repair involving short-patch SSBR would result in the ^{32}P radiolabel being incorporated into a ligation product.

3.2.2 Overexpression and purification of His-tagged APTX in *E.coli*

To investigate the role of APTX in the repair of abortive ligation intermediates *in vitro* recombinant APTX was purified to homogeneity by two successive rounds of chromatography. Human APTX cDNA is present within the expression vector pB352 under the control of the T7 promoter and carries an N-terminal 6x histidine-tag (Clements et al., 2004). Expression of APTX was induced by addition of 1mM IPTG to a 500ml culture at OD_{600} 0.6 and incubation at 30°C for 3hrs. After induction of protein the cells were harvested and lysed by sonication. Clarified extract was prepared by pelleting the insoluble material by centrifugation and retaining the supernatant. His-APTX was then purified by immobilised metal affinity chromatography (IMAC) on a column prepared using nickel-nitrilotriacetic acid (Ni-NTA) agarose beads (first described in (Porath et al., 1975)). The clarified extract was loaded onto the column, washed three times and eluted in sonication buffer containing 250mM imidazole. Aliquots of the column load, flow through and elution fractions were analysed by 10% SDS-PAGE (Figure 3.4 A). His-APTX bound tightly to the Ni-NTA agarose column and was significantly depleted in the flow through. It eluted over four fractions following addition of elution buffer containing 250mM imidazole, peaking in the second fraction (Figure 3.4 A). A number of contaminating proteins co-purified with His-APTX. These most likely reflected contaminating histidine-rich *E.coli* proteins and were subsequently removed by cation exchange chromatography.

Cation exchange was chosen because the isolelectric point (PI) of APTX is 9.27, and is therefore a basic protein at neutral pH. Peak His-APTX fractions from IMAC were (1 & 2) were pooled and loaded onto a cation exchange column. His-APTX bound tightly to the column and was undetectable in the flow through (Figure 3.4 B). Following extensive washing His-APTX was eluted with a salt gradient (NaCl) from 0.1M to 1M and aliquots of elution fractions analysed by 10% SDS PAGE (Figure 3.4 B). His-APTX eluted in a sharp peak at approximately 300-400mM NaCl. Fractions 26 and 27 were pooled, dialysed into storage buffer, quantified by Bradford assay and 500ng of this material analysed by SDS-PAGE and coomassie blue staining (Figure 3.4 C).

3.2.3 AOA1 whole cell extracts display defective short-patch SSBR of an abortive ligation intermediate *in vitro*

To determine if human AOA1 cells have the ability to repair an abortive ligation intermediate *in vitro*, the lymphoblastoid cell lines (LCL) cell lines MT6 (AOA1) and MT1 (WT) were employed. MT6 is a cell line derived from an individual that is homozygous for a whole genomic deletion of *APTX* (Reynolds et al., 2009). $7.5x10^6$ cells from each line were harvested by centrifugation at 1,500 rpm, washed in 3xPBS and whole cell extracts were prepared. The AOA1 and WT whole cell extracts were then assayed for their ability to repair an abortive ligation intermediate by incubating 6.25μg of extract with 25nM of the abortive ligation intermediate described in Figure 3.2 & 3.3 and depicted again in Figure 3.5. Reaction products were fractionated by denaturing PAGE and detected by phosphorimaging (Figure 3. 5).

Removal of the AMP from the 5'-terminus of the SSB was indicated by an increase in the electrophoretic mobility of the AMP-^{32}P-25mer, due to loss of the AMP moiety. In the lanes containing the products of reactions containing wild-type extract the AMP-^{32}P-25mer was rapidly converted to ^{32}P-25mer (Figure 3.5 lanes 4-7). One limitation of reactions involving whole cell extracts is the presence of non-specific nucleases that result in degradation of the substrate. Whilst the impact of such nucleases was suppressed by inclusion of a 1000x fold molar excess of a single-stranded competitor oligonucleotide, some non-specific nucleolytic products were still evident (Figure 3.5 asterisk). Notably, however, whilst non-specific

nucleolytic products were also produced in reactions containing AOA1 LCL extracts, formation of the ^{32}P-25mer product of APTX activity was not evident in such reactions, and there was no detectable loss of AMP-^{32}P-25mer, during the 60min incubation (Figure 3.5. lanes 9-12). Indeed the difference in size between the non-specific bands present in lanes containing WT and AOA1 extracts is due to the persistence of the 5'AMP in the latter. This suggests that APTX is the major, if not only, AMP-DNA hydrolyse activity present in human lymphoblastoid cells.

Direct processing of the 3' termini of the SSB (i.e. on the 17-mer) could not be visualised due to the location of the ^{32}P radiolabel on the 25mer oligonucleotide. However the presence of a fully repaired ligation product of 43bp requires both 3' phosphatase and gap filling activities and is therefore an indirect measure of 3' processing. Wild-type whole cell extracts proved able to repair the abortive ligation intermediate and ligation was evident from 10min onwards (Figure 3.5 lanes 4-7). There was very little if any ligation product detectable in reactions containing AOA1 whole cell extract, at any time point examined (Figure 3.5 lanes 9-12). Whole cell extract prepared from AOA1 cells, lacking 5'AMP-DNA deadenylase activity, were unable to support short-patch SSBR of an abortive ligation intermediate *in vitro*.

3.2.4 AOA1 cell free extracts are proficient in the short-patch SSBR of a non-adenylated oxidative SSB

To confirm that the short-patch repair defect in reactions containing AOA1 extracts was caused by loss of aprataxin, I first compared the presence of levels of core SSBR proteins involved in the repair of oxidative SSBs (Figure 3.6). The repair of a common oxidative SSB consisting of a 1 nucleotide gap and 3'-P is thought to require the activities of PNK, Polβ and LigIIIα. XRCC1 has also been reported to stimulate the activities of SSBR end-processing enzymes *in vitro* and is required for the stability of LigIIIα and a defect in this protein could result in less efficient repair of SSBs *in vitro* (Caldecott et al., 1995, Whitehouse et al., 2001). 10µg of wild-type and AOA1 whole cell extracts were immunoblotted for the SSBR proteins APTX, PNK, Polβ, LigIIIα and XRCC1 (Figure 3.6). The extracts were also probed for β-tubulin and actin as loading controls. AOA1 whole cell extracts had levels of protein similar to the wild-type control, with the exception of APTX which was undetectable in the AOA1 extracts (Figure 3.6). This supports

the hypothesis that AOA1 extracts are defective in the short-patch repair of abortive ligation intermediates due to the loss of APTX and not other core SSBR factors.

To confirm directly that the short-patch repair defect in reactions containing AOA1 extracts was caused by loss of aprataxin, I attempted to complement reactions containing AOA1 whole cell extracts with recombinant His-APTX and (Figure 3.7). A titration of wild-type and AOA1 whole cell extracts (5µg, 1µg, 0.1µg) was incubated with 25nM of the adenylated SSB in the presence or absence of 100nM His-APTX at 30°C for 60min. In the absence of recombinant His-APTX, 5'AMP deadenylase activity was detectable in reactions containing as little as 0.1µg of wild-type whole cell extract (Figure 3.7 lane 5). This activity was greater in reactions containing 1µg and 5µg of wild type whole cell extract and ligation product was also detected at these concentrations (Figure 3.7 lanes 3&4). In contrast, as observed in Figure 3.4, AOA1 whole cell extracts were unable to repair the abortive ligation intermediate and the 5'AMP termini persisted at all concentrations of extract employed (Figure 3.7 lanes 6-8). Notably, complementation of AOA1 whole cell extracts was observed by the inclusion of 100nM His-APTX, which completely rescued repair of the abortive ligation intermediate (Figure 3.7 compare lanes 12-14 to lanes 3-5). In contrast, there was no increase in the repair of abortive ligation intermediate in wild type extracts supplemented with His-APTX (Figure 3.7 compare lanes 3-5 and 9-11) indicating that APTX activity is not rate limiting in the wild-type lymphoblastoid extracts. These data confirm that short-patch SSBR of an abortive ligation intermediate fails in reactions containing AOA1 whole cell extract *in vitro* due to the absence of APTX.

It has been reported in one study that APTX possesses 3' phosphatase activity (Takahashi et al., 2007a). The loss of 3' phosphatase activity in AOA1 whole cell extracts might contribute to defective short-patch SSBR because the persistence of an unrepaired 3'-P terminus would inhibit gap-filling. To determine if the APTX dependant SSBR defect was due to loss of 5'AMP deadenylase activity and/or 3' phosphatase activity, the ability of AOA1 whole cell extracts to repair a non-adenylated SSB was examined (Figure 3.8). 5µg of AOA1 and WT whole cell extract were incubated at 30°C for 60min with 25nM of a mock-adenylated or adenylated SSB, containing a 1 nucleotide gap and a 3'-phosphate terminus. As observed in the previous

experiments, AOA1 whole cell extracts could not repair the adenylated oxidative SSB (lane 5). Importantly, however, AOA1 cell extracts were proficient in the repair of a non-adenylated SSB (compare lanes 3 and 5) and showed levels of repair comparable to wild-type (compare lanes 3 and 4). This shows that AOA1 whole cell extracts are proficient in the repair of a non-adenylated SSB containing a 3'-phosphate terminus and thus that the repair of an abortive ligation intermediate stalls in AOA1 whole cell extracts due to the presence of a 5'-AMP terminus, and not a 3'-phosphate terminus.

3.2.5 Short Patch SSBR reaction requires 1nt gap filling

Due to the location of the ^{32}P radiolabel on the 5' termini of the SSB, repair of the 3' terminus cannot be directly visualised, and so 3' end processing and gap-filling events are measured indirectly by the appearance of DNA ligation product. Whilst the appearance of ligation product requires processing of the 3'-terminus I considered the possibility that the repair reaction could occur in the absence of 1nt gap filling by ligation across the 1nt gap. Such ligation has been reported by T4 DNA ligase (Nilsson and Magnusson, 1982). Because I wished to ensure the repair reaction faithfully recapitulated short patch SSBR it was important to confirm that the repair reaction was dependent upon gap filling. To test this, 5µg of wild type and AOA1 whole cell extract was incubated with 25nM of an abortive ligation intermediate in the presence or absence of 100µM dNTPs (Figure 3.9). The absence of dNTPs from the reaction mix impaired the full repair of the abortive ligation intermediate in wild-type extracts. Repair of the 5'-AMP terminus was still complete upon incubation with 5µg of wild-type extract but ligation product was not detectable (compare lanes 1 and 5), suggesting that repair of abortive ligation intermediates was dependent on gap-filling. This experiment confirms that short-patch SSBR proceeds through a gap-filling event. This also suggests that since repair of a non-adenylated 3'-phosphate substrate was normal in AOA1 then 1nt gap filling is also most likely to be normal.

As controls I also included in the above experiments reactions lacking ATP or $MgCl_2$ (Figure 3.9). Since PNK, Polβ and LigIIIα activities all require a metal divalent metal cofactor the repair reaction was, as expected, dependent on Mg^{2+} (lanes 7 and 8). However, wild type extracts

removed AMP from the 5'-termini of the SSB, consistent with the metal independence of APTX activity (Parks et al., 2004, Seidle et al., 2005, Ahel et al., 2006) (compare lanes 1 to 7). It is also noteworthy that the non-specific nucleolytic degradation of the substrate is also dependent on the presence of $MgCl_2$ (compare lanes 1 and 2 to 7 and 8). Interestingly, the absence of ATP from the reaction mix had no effect on the repair of an abortive ligation intermediate and there was only a small reduction in the levels of ligation (compare lanes 1 and 3). Although the reaction mechanism of mammalian ligases is ATP-dependent, ligases exist in both pre-adenylated form and non-adenylated state, enabling one round of ligation even in the absence of exogenous ATP (Figure 1.11) (Little et al., 1967, Weiss et al., 1968a, Gumport and Lehman, 1971). Alternatively, it is possible that there is ATP present in the whole cell extracts.

3.3 Discussion

The data presented in this chapter reveal that whole cell extracts prepared from a human AOA1 disease cell line are defective in the short-patch SSBR of an abortive ligation intermediate *in vitro*. This defect is caused by the loss of APTX 5'-AMP DNA deadenylase activity because AOA1 cell extracts are proficient in the repair of a non-adenylated SSB. This suggests that it is the persistence of the unrepaired 5'AMP that blocks subsequent repair events in the AOA1 whole cell extracts, rather than processing of 3'-phosphate termini, gap filling, or DNA ligation. This is consistent with data previously seen in *APTX*$^{-/-}$ DT40 cells and *APTX*$^{-/-}$ primary mouse cortical astrocytes (Ahel et al., 2006). Having established an assay to measure the short-patch repair of a SSB *in vitro*, I employed the assay in the following chapters to further investigate the nature for the repair defect in AOA1.

CHAPTER FOUR

Defective DNA ligation of Adenylated Nicks in AOA1 cell extracts

4.1 Introduction

The data presented in the previous chapter showed that whole cell extracts prepared from an AOA1 lymphoblastoid cell line are unable to support short-patch SSBR of an abortive ligation intermediate *in vitro*. This repair defect is a consequence of APTX loss as repair of an abortive ligation intermediate was rescued to WT levels when AOA1 extracts were supplemented with recombinant His-APTX. Importantly AOA1 extracts were also proficient in the repair of a non-adenylated SSB indicating that the repair defect resulted from the loss of 5-'AMP DNA deadenylase activity.

The SSB substrate employed in the *in vitro* repair assays in the previous chapter was an oligonucleotide duplex containing a SSB designed to model an abortive ligation of a common oxidative DNA lesion. The substrate harboured a 1 nucleotide gap with 3'-P and 5'-AMP termini and in WT extracts the repair of this substrate would be expected to involve processing of the 5'-terminus by APTX, processing of the 3'-terminus by PNK, gap-filling by Polβ, and finally ligation for complete repair (Figure 4.1A). Whilst the previous chapter demonstrated that persistence of 5'-AMP blocked repair, this observation is puzzling because should processing of the 3'-terminus proceed normally via end processing by PNK and gap filling by Polβ, then the resulting adenylated nick should simply be ligated by non-adenylated DNA ligase IIIα (Figure 4.1B). Since this didn't occur, it was hypothesised that either end processing by PNK or gap filling by Polβ could be blocked by the presence of the 5'-AMP (Figure 4.1B). This possibility was tested in this chapter.

4.1.2 Aims of this chapter

The aim of this chapter was to determine at which stage the repair of an SSB with a 5'-AMP terminus fails in AOA1 whole cell extracts. The effect of the presence of the 5'AMP on 3' end-processing by PNK, gap-filling by the short-patch polymerase Polβ, and finally ligation by DNA ligase III was thus measured using a combination of recombinant SSBR proteins and AOA1 and wild-type whole cell extracts.

4.2 Results

To directly measure repair of the 3'-phosphate by PNK and gap-filling by Polβ, an abortive ligation intermediate was prepared containing a 5' ^{32}P radiolabelled 17mer oligonucleotide with either a 3'-P or 3'-OH terminus annealed to a ^{32}P-25mer and an unlabelled 43mer. This substrate was then adenylated or mock-adenylated with T4 DNA ligase as previously described. The fully annealed dual ^{32}P radiolabelled substrate was purified from partially annealed species by native PAGE gel extraction. The final purified substrates consisted of an oligonucleotide duplex with a SSB consisting of a 1 nucleotide gap, a 3'-phosphate or 3'-hydroxyl terminus and a 5'-AMP terminus (Figure 4.2).

4.2.1 Overexpression and purification of recombinant His-tagged PNK from *E.coli*

To obtain recombinant His-PNK for these experiments I first optimised the expression conditions of the recombinant human protein in *E.coli*. Optimal expression conditions for His-PNK in *E.coli* were determined by setting up six small scale cultures with different induction conditions (Figure 4.3). Three growth temperatures of 15°C, 20°C and 25°C and two induction times of 90min and 180min were tested and aliquots of the soluble and insoluble fractions were analysed by 10% SDS-PAGE. As both incubation time and temperature increased, the total level of His-PNK expressed in bacterial cells increased (Figure 4.3 A), but the amount of soluble protein compared to insoluble protein decreased (Figure 4.3 B). An incubation temperature of 20°C for 90min was considered optimal because this produced a high ratio of soluble to insoluble His-PNK without sacrificing high levels of total protein expression.

Clarified extract containing soluble His-PNK was prepared as previously described for His-APTX in chapter 3 and purified by immobilised metal affinity chromatography (IMAC) on a Ni-NTA agarose column (Figure 4.4 A). His-PNK eluted from the column over six fractions, with a large peak occurring in the second fraction (Figure 4.4 A). His-PNK co-eluted with a large number of contaminating bands necessitating a further purification step. PNK has a predicted PI of 8.73 and is a basic protein at neutral pH. Peak elution fractions (2 & 3) were pooled and His-PNK was further purified by cation exchange chromatography (Figure 4.4 B). The peak elution fractions from cation exchange (16 & 17) contained a single major band that corresponded to

His-PNK, as measured by coomassie blue staining, with some evidence of a smaller contaminating species in fraction 16. Elution fraction 17 was chosen for use in experiments and was dialysed into appropriate buffer.

4.2.2 The presence of a 5'-AMP does not block the 3' phosphatase activity of PNK

The ability of His- PNK to convert a 3'-P to a 3-OH in the presence and absence of a 5'-AMP terminus was compared *in vitro.* Reactions containing various amounts of recombinant His-PNK (250nM, 100nM, 50nM and 25nM) and 25nM of either an adenylated or mock-adenylated SSB substrate containing a 3'-P terminus were incubated for 1hr at 30°C (Figure 4.5). The reaction products were then fractionated by 15% denaturing PAGE and visualised by phosphorimaging. PNK-dependent conversion of the 3'-P terminus to a 3-OH terminus was indicated by decreased mobility of oligonucleotide containing the latter, due to the loss of negative charge. Comparable levels of conversion of 3'-P termini to 3'-OH termini by His-PNK were observed with the adenylated and mock-adenylated substrates. These data reveal that the presence of a 5'-AMP terminus does not prevent processing of a 3-'P terminus by His-PNK suggesting that the short-patch SSBR repair defect observed in reactions driven by AOA1 whole cell extracts in the last chapter was not due to reduced 3'-end processing by PNK.

4.2.3 Overexpression and purification of recombinant Polβ from *E.coli*

As the presence of a 5'-AMP terminus at a SSB does not inhibit the 3' phosphatase of recombinant PNK the next stage of repair that could fail in the presence of a 5'-AMP is gap-filling by Polβ. To test this, recombinant human Polβ was purified to by ion exchange chromatography employing anion and cation exchange as described previously (Sobol et al 1996). Aliquots of the column load, flow through and representative elution fractions were analysed by 10% SDS PAGE (Figure 4.6). The peak elution fraction (14) of Polβ contained very little contaminating protein as measured by coomassie blue staining and following dialysis into an appropriate buffer was employed for the experiments described below.

4.2.4 The presence of a 5'-AMP terminus does not block gap-filling by Polβ

The ability of recombinant human to insert a single nucleotide into a SSB containing a 5'-AMP was tested. To test this, a titration of Polβ (100nM, 30nM, 15nM and 5nM) was incubated with 25nM of an adenylated or mock-adenylated SSB substrate with a 1 nucleotide gap, a 3'OH terminus, and either a 5'-AMP or a 5'-P terminus for 1hr at 30°C (Figure 4.7). The reaction products were fractionated by 15% denaturing PAGE and visualised by phosphorimaging. Gap-filling was indicated by conversion of the ^{32}P-17mer-OH to a ^{32}P-18mer-OH, which consequently exhibited reduced electrophoretic mobility indicating that a single nucleotide had been inserted into the gap. Similar levels of single nucleotide incorporation was visualised on both adenylated and mock-adenylated substrates revealing that the presence of a 5'-AMP terminus did not prevent recombinant Polβ. This suggests that that the short-patch SSBR defect observed in reactions containing AOA1 extract in the last chapter was not due to reduced Polβ activity.

4.2.5 Short-patch SSBR stalls at the final stage of DNA ligation in AOA1 whole cell extracts

The previous data suggests that short-patch SSBR repair of an abortive ligation intermediate by AOA1 extract does not stall during PNK dependent end-processing or Polβ mediated gap-filling. This suggests that short patch SSBR in such extracts stalls at the stage of DNA ligation, thereby accumulating adenylated nicks. This is surprising because adenylated nicks arise as a normal intermediate of DNA ligation as very transient repair intermediate that are rapidly converted into an intact phosphodiester bond by non-adenylated ligase, which catalyses nucleophilic attack of the 5'-AMP terminus by the 3'-OH terminus releasing the AMP and reforming the phosphpodiester bond (Olivera et al., 1968, Harvey et al., 1971, Weiss et al., 1968b, Gumport and Lehman, 1971, Lehmann, 1978) (a more detailed description of the ligase mechanism is found in section 1.3.4.1 and in Figure 1.11).

To confirm that short patch SSBR reactions fail in AOA1 extracts due to failed DNA ligation, the ability of AOA1 and WT whole cell extracts to ligate an adenylated nick was compared directly *in vitro*. 6.25µg of whole cell extracts prepared from WT and AOA1 LCLs were incubated at

30°C for the indicated times with 25nM of an adenylated nick (Figure 4.8). In contrast to the substrates used in the previous experiments in this chapter, the substrate used for this experiment contained a single ^{32}P radiolabel on the 5' terminus of the 25mer oligonucleotide (^{32}P-25mer). The reaction products were fractionated by 15% denaturing PAGE and detected by phosphorimaging. As seen previously the 5'-AMP was rapidly removed in WT extracts and the resulting non-adenylated nick was ligated (lanes 4-7). However in contrast, not only did the AOA1 extract fail to remove the 5'-AMP, as expected, but also failed to reseal the adenylated nick (lanes 9-12). This experiment confirmed that short-patch repair of SSBs containing 5'-AMP termini fail in the absence of aprataxin at the very step of DNA ligation.

4.3 Discussion

The data presented in this chapter reveal that the presence of a 5'-AMP at a SSB does not inhibit the activities of either recombinant PNK or Polβ *in vitro*. Rather AOA1 extracts fail to repair such SSBs due to an inability to conduct the final step of ligating the adenylated nick. This in turn suggested that adenylated nicks could potentially accumulate in the absence of APTX. This was surprising because adenylated nicks arise as normal intermediates of DNA ligation reactions and are normally rapidly resealed by non-adenylated DNA ligase. Why then does non-adenylated DNA ligase not reseal these nicks in AOA1 extracts? One possibility is that lower levels of active DNA ligase are present in AOA1 extracts compared to wild-type extracts. This can be discounted, however, as AOA1 extracts were normal for the repair of a non-adenylated SSB (Figure 3.8).

Another possibility is that there are very low levels of non-adenylated ligase in AOA1 extracts. This could be a specific deficit in AOA1 extracts, if APTX can also deadenylate DNA ligases. APTX is a member of the Hint branch of the HIT superfamily of nucleotide hydrolases and transferases which exhibit AMP-lysine hydrolase activity (Brenner, 2002, Brenner et al., 1999, Bieganowski et al., 2002b, Krakowiak et al., 2004b). Indeed it has been shown that APTX possesses weak AMP-lysine hydrolase activity (Seidle et al., 2005). Alternatively, however, it is not necessary to invoke a specific reduction in levels of non adenylated ligase in AOA1, since the presence of relatively high levels of ATP in cells and in the reactions described here ensure

that most DNA ligases are present predominantly in their adenylated form. The addition of an excess of pyrophosphate to the reaction could be used to investigate this. Pyrophosphate is generated when the ATP molecule is cleaved and the AMP moiety is transferred to the active site lysine during ligase adenylation (Olivera et al., 1968, Harvey et al., 1971, Weiss et al., 1968b, Gumport and Lehman, 1971, Lehmann, 1978). The presence of excess pyrophosphate should alter the equilibrium of this reaction in favour of the deadenylated ligase which could be used to rescue the defec t in the AOA1 extracts.

The hypothesis that limiting levels of non-adenylated ligase is cause for the failure of AOA1 whole cells extracts to ligate a pre-adenylated nick raises specific predictions that can be tested. In particular, if the lack of APTX-independent short patch repair results from insufficient non adenylated DNA ligase then the repair of an abortive ligation intermediate should be rescued in AOA1 extracts by addition of excess recombinant DNA ligase in the absence of ATP (to minimise adenylation of the recombinant ligase). This possibility was tested in the next chapter.

CHAPTER FIVE

Short-patch SSBR of an abortive ligation intermediate fails in AOA1 cells *in vitro* due to insufficient levels of non-adenylated ligase

5.1 Introduction

The data presented in previous chapters demonstrated that short-patch repair of a single-stranded gap with 5'-AMP termini failed in AOA1 whole cell extracts *in vitro*. The persistence of the 5'-AMP at the SSB in the absence of APTX did not block either PNK-mediated end-processing or Polβ-mediated gap-filling. Rather, it was observed that repair failed at the final stage of ligating the residual adenylated nick. This was surprising because adenylated nicks arise as a normal intermediate of every DNA ligation reaction, and require only non-adenylated DNA ligase for ligation to be completed. The inability of AOA1 extracts to ligate adenylated nicks was not due to a general defect in DNA ligation because AOA1 whole cell extracts were proficient in the short-patch repair of a non-adenylated break.

DNA ligases are nucleotidyltransferases (NTases) that utilise a high energy cofactor to catalyse phosphodiseter bond formation in a universal three-step reaction mechanism and all eukaryotic ligases use ATP as a cofactor (Figure 5.1). In the first step of DNA ligation, the ligase reacts with ATP to form a ligase-adenylate intermediate in which AMP is covalently linked to the active-site lysine via a phosphoamide bond (Olivera et al., 1968, Harvey et al., 1971, Weiss et al., 1968b, Gumport and Lehman, 1971, Lehmann, 1978). The formation of this ligase-adenylate intermediate is energetically favourable at cellular concentrations of ATP and the adenylated form of the ligase is stable in the absence of DNA breaks. Consequently, although DNA ligases exist in two forms it is likely that the adenylated form is the predominant one present in cells.

Once adenylated DNA ligase encounters a DNA break the second step of ligation is the activation of the 5'P by adenylation of the DNA (Sekiguchi and Shuman, 1997, Sriskanda and Shuman, 1998a, Odell et al., 2000, Odell et al., 2003, Tomkinson et al., 2006, Nair et al., 2007b). During this step the oxygen of the 5'P attacks the phosphorus of the AMP, dispelling the lysine and transferring the adenylate group onto the 5'P, forming an AMP-DNA intermediate (Odell et al., 2003, Nair et al., 2007a). The final step of ligation is the reformation of the phosphodiester backbone (Lehmann, 1978). During this step the non-adenylated ligase catalyses the nucleophilic attack of the 5'AMP by the 3'OH, displacing the AMP and joining the

two polynucleotides by formation of a phosphodiester bond (Odell et al., 2000, Sriskanda and Shuman, 2002b, Sriskanda and Shuman, 2002a, Nair et al., 2007a, Crut et al., 2008). This step is very rapid, and the rate of phosphodiester resynthesis is much faster than the adenylation of the DNA (Crut et al., 2008). Normally these two steps are coupled such that the adenylated nick is rapidly sealed by the deadenylated ligase (Figure 5.1).

However, if step 2 and 3 are 'uncoupled', due to abortive ligation events at breaks with blocked 3'-termini, the non-adenylated ligase will be rapidly readenylated. Consequently, it is possibile that the cellular level of non-adenylated DNA ligase is insufficient to complete ligation of pre-adenylated nicks. This may not be a problem in WT extracts because the presence of APTX restores the nick to a non-adenylated state (Figure 5.2A.) However, in AOA1 extracts, repair is now dependent on the pre-existing level of non-adenylated ligase, which we hypothesize, may be too low to facilitate step 3 of the ligase reaction (Figure 5.2B).

5.1.2 Aims of this chapter

The hypothesis that limiting levels of non-adenylated ligase account for the failure of AOA1 whole cells extracts to ligate adenylated nicks invokes the testable predictions that the repair of an adenylated gap or nick can be restored in AOA1 extracts by supplementing repair reactions with recombinant de-adenylated DNA ligase, in an ATP-sensitive manner. This is because omitting ATP will increase the relative level of recombinant DNA ligase that is non-adenylated, which the above hypothesis predicts will promote complementation, whereas including ATP will reduce the presence of adenylated DNA ligase, which the above hypothesis predicts will inhibit complementation. Also, as this model requires the addition of deadenylated ligase, T4 DNA ligase was initially used instead of human ligase, as commercial preparations of T4 DNA ligase are largely deadenylated. Additionally the hypothesis also predicts that repair of an adenylated gap or nick can be reconstituted with purified recombinant proteins *in vitro* in the absence of aprataxin, if the reactions are conducted in the absence of ATP. These predictions were tested in the current chapter.

5.2 Results

5.2.1 *Short-patch repair of SSBs with 5'-AMP termini is rescued in AOA1 cell extracts by addition of recombinant DNA ligase*

To test whether the failure of AOA1 whole cell extracts to repair a pre-adenylated nick was due to limiting levels of non-adenylated DNA ligase, AOA1 whole cell extracts were complemented with T4 DNA ligase (Roche) in the presence or absence of ATP (Figure 5.3). T4 DNA ligase was used as commercial preparations are not pre-adenylated. 5μg of WT and AOA1 whole cell extracts were incubated at 30°C for 1 hour with an a 1nt gap harbouring 3'-P and a 5'-AMP termini in the presence or absence of 1mM ATP and 1U T4 DNA ligase (Roche). The reaction products were fractionated by 15% denaturing PAGE and detected by phosphorimaging. 1000x fold molar excess of a single-stranded competitor oligonucleotide was added to the reactions to reduce the impact of the non-specific nucleolytic degradation of the substrate (Figure 5.3 asterisk).

As observed previously, AOA1 whole cell extracts were unable to repair the adenylated 1nt gap (lanes 4 and 6). Strikingly, addition of T4 DNA ligase in the absence of ATP rescued short-patch SSBR in AOA1 whole cell extracts to levels similar to WT (compare lanes 5 and 6 to lanes 9 and 10). Importantly, this APTX-independent repair was strongly inhibited by the presence of 1mM ATP (compare lanes 8 and 10), consistent with the non-adenylated sub-fraction of T4 ligase being responsible for restoration of repair in AOA1 whole cell extracts. It is also important to note that the addition of T4 DNA ligase did not significantly increase levels of repair in WT extracts either in the presence or absence of ATP (compare lanes 3 and 4 to lanes 7 and 8).

5.2.2 *APTX-independent repair of an adenylated 1nt gap occurs by short patch SSBR*

It has been previously been shown that T4 DNA ligase can ligate single-strand gaps where several nucleotides are missing, by ligation across the gap (Nilsson and Magnusson, 1982). It was considered possible that the complementation by T4 ligase observed above was not occurring by bona fide short patch repair but rather by this route. To test this, dideoxythymidine triphosphate (ddTTP) was added to the reactions. Dideoxynucleotides lack a

3'OH and so are unable to form a phosphodiester bond with another nucleotide, thereby terminating further DNA ligation following their insertion in a 1nt gap (Figure 5.3). Since the nucleotide putatively inserted in the 1nt gap was thymidine, the dNTP reaction mix was prepared with ddTTP instead of dTTP. If the repair of the abortive ligation intermediate was proceeding through a gap-filling event then the ddTTP would be inserted into the gap, and due to the absence of the 3'OH on the ddTTP, the resulting nick would be un-ligatable. Thus repair would be inhibited by the presence of ddTTP in the reaction. However if the addition of T4 DNA ligase to the reaction was biasing repair towards an 'across-the-gap' ligation event then the full repair product would be resistant to addition of the ddTTP.

The adenylated 1nt gap (see cartoon in Figure 5.4) was incubated at 30°C for 1 hour with 5µg of WT or AOA1 whole cell extract in the presence or absence of 1mM ATP, 1U of T4 DNA ligase and 100µM dNTPs containing either dTTP or ddTTP (Figure 5.4). The reaction products were then fractionated by 15% denaturing PAGE and detected by phosphorimaging. As observed previously, complementation of the AOA1 whole cell extracts with T4 DNA ligase completely rescued the repair of an abortive ligation intermediate *in vitro*, in the absence of ATP (compare lanes 6 and 8). Importantly the presence of ddTTP in the reaction mix completely inhibited the short-patch repair conducted by either WT or AOA1 extracts, both in the presence and absence of T4 DNA ligase (lanes 9 – 16). This result demonstrates that the SSBR reactions in my experiments required DNA gap-filling, as expected for bona fide short patch SSBR reactions.

5.2.3 *Short-patch repair of SSBs with 5'-AMP termini is rescued in extracts prepared from quiescent* APTX$^{-/-}$ *mouse neural extracts by addition of recombinant DNA ligase*

Since it was confirmed that the ligase complementation was occurring via a bona fide short-patch repair mechanism, I next wished to repeat these experiments using a neuronal cell type as neurodegeneration is the primary presentation of AOA1. I thus employed cell extracts prepared from quiescent neural astrocytes recovered from *APTX*$^{+/+}$ and *APTX*$^{-/-}$ mice (Figure 5.5) (Reynolds et al., 2009). As seen with the AOA1 cell extracts, the addition of 1 U T4 DNA

ligase to *APTX*$^{-/-}$ neural cell extracts restored the repair of adenylated 1nt gaps to WT levels in the absence of ATP (compare lanes 5 and 6 to lanes 9 and 10). Once again, the addition of ATP to the reaction strongly inhibited the ability of T4 DNA ligase to complement the repair defect in *APTX*$^{-/-}$ extracts (compare lanes 8 and 10).

5.2.4 *Restoration of short-patch repair of an adenylated 1nt gap in AOA1 whole cell extracts by recombinant human LigIIIα*

The ability of human LigIIIα to complement the AOA1 short-patch repair defect of an abortive ligation intermediate was tested. Numerous studies have suggested that LigIIIα is responsible for the majority of short-patch repair events and it was therefore important to determine if the ability of T4 DNA ligase to complement AOA1 extracts was unique or also applicable to human ligases. Recombinant His-LigIIIα was expressed and purified essentially as described previously (Caldecott et al., 1995) and in materials and methods. Aliquots of the recombinant protein prior to and following purification by IMAC and cation exchange chromatography are shown in Figure 5.6.

The adenylated 1nt gapped substrate (see cartoon in Figure 5.7) was incubated with 5µg of WT or AOA1 whole cell extract as indicated and 8nM-72nM His-LigIIIα in the presence or absence of 1mM ATP at 30°C for 1 hour (Figure 5.7). As observed with recombinant T4 DNA ligase, the addition of His-LigIIIα to AOA1 whole cell extracts in the absence of ATP increased repair of the adenylated 1nt gap (compare lanes 15-17 to lane 2). However, in contrast to T4 DNA ligase, which restored repair to WT levels, His-LigIIIα only partially rescued the repair defect in AOA1 cell extracts (Figure 5.3). Once again, the addition of ATP to the reaction inhibited the ability of the DNA ligase to restore repair of the gapped substrate in AOA1 extracts (compare lanes 6-8 to lanes 15-17). Additionally no repair was evident when His-LigIIIα was incubated alone with the substrate showing that repair of the abortive ligation intermediate required processing of the 3' terminus. A possible explanation for this difference between T4 DNA ligase and His-LigIIIα could be that while commercial T4 DNA ligase is largely non-adenylated, His-LigIIIα purified from *E.coli* is likely to be predominantly pre-adenylated as the ligase adenylation reaction is very rapid in cellular concentrations of ATP.

5.2.5 Reconstitution of *APTX-independent SSBR of adenylated SSBs by purified recombinant human proteins*

So far the data presented here has shown that short-patch SSBR of an adenylated 1nt gap can be rescued in AOA1 whole cell extracts by increasing the level of DNA ligase, in the absence of ATP, indicating that APTX-independent repair of adenylated SSBs is possible. I next examined whether APTX-independent SSBR could be reconstituted *in vitro* using purified recombinant human short-patch repair proteins. 60nM of adenylated 1 nt gapped substrate was incubated at 30°C for 1 hour with 250nM His-PNK, 100nM Polβ and 80nM His-LigIIIα in the presence or absence of 100nM His-APTX and 1mM ATP (Figure 5.8). As expected, in the presence of ATP, repair of the adenylated 1nt gap was dependent on His-APTX (compare lanes 1 and 2). However, in the absence of ATP, short-patch SSBR of the abortive ligation intermediate was independent of His-APTX (compare lanes 3 and 4). I noted that the absence of ATP only mildly reduced repair of the adenylated nick in the presence of APTX (compare lanes 1 and 3), suggesting that the preparation of His-LigIIIα contained significant levels of pre-adenylated DNA ligase. This also supports the explanation that the partial complementation of AOA1 extracts with His-LigIIIα compared to T4 DNA ligase was indeed due to high levels of pre-adenylated His-LigIIIα (Figure 5.7). I also noted that, as expected, and in contrast to APTX-dependent SSBR, APTX-independent SSBR proceeded without removal of AMP from the 5'-terminus (compare the amount of AMP-32P-25mer present in lanes 3 & 4).

5.2.6 *Complementation of the AOA1 repair defect independently of ATP with a non-adenylatable ligase mutant*

The data described above confirmed the prediction that repair of adenylated SSBs can be repaired in an APTX-independent manner, by supplementing reactions with recombinant DNA ligase in an ATP sensitive fashion. This in turn supports the hypothesis that short patch SSBR reactions fail in the absence of APTX due to insufficient levels of non-adenylated DNA ligase. To test this hypothesis directly, I next employed recombinant preparations of a mutant DNA ligase. The three catalytic steps of DNA ligation are relatively separate reactions and mutant derivatives of DNA ligases have been created that disrupt each of the individual steps. A direct

prediction of the above hypothesis is that a mutation that prevents or reduces the adenylation of a DNA ligase (step 1 in Figure 5.1), but which still allows catalysis of ligation in the presence of adenylated nicked substrate (i.e. still allows step 3; Figure 5.1) should support APTX-independent short patch SSBR, even in the presence of ATP. The most well characterised DNA ligase is the *Chlorella* Virus PBCV-1 (CV DNA Ligase) (Ho et al., 1997). CV DNA ligase is the simplest known eukaryotic ATP-dependent DNA ligase and although it consists of only the catalytic core it can almost fully compensate the loss of both *S.cerevisiae* DNA ligases, Cdc9p and Lig4p, *in vivo* making it ideal to use in biochemical assays requiring a functional ligase (Sriskanda et al., 1999).

A mutant CV DNA ligase has been characterised that lacks the five most C-terminal amino acids of the enzyme and which prevents formation of the ligase-AMP complex and, strikingly, a exhibits a 16x increased rate of ligation of pre-adenylated nick (Sriskanda and Shuman, 1998b). All ATP dependent ligases contain 6 short highly conserved NTase motifs (I, III, IIIa, IV, V and VI) each arranged in the same order and with similar spacing (Shuman and Schwer, 1995). Different motifs have been shown to have critical roles in each of the three stages of DNA ligation. In chlorella virus DNA ligase, Motif VI consists of the six most C-terminal amino acids and is critical for the first step of ligase adenylation. It has been postulated that a closed conformation in the ligase brings motif VI into contact with the β- and γ- phosphates of ATP, allowing it to reorientate the α- phosphate for nucleophilic attack from the active site lysine in motif I (Sriskanda and Shuman, 1998b). Once this happens the ligase-AMP adopts a more open conformation facilitates nick-sensing. Therefore a non-adenylated wild-type ligase would naturally be in the closed conformation which is thought to be rate-limiting in the ligation of a pre-adenylated nick. Loss of the five most C-terminal amino acids of the enzyme is thought to open up the ligase, preventing it from interacting with ATP, but adopting a conformation that is more amenable to the ligation of a pre-adenylated nick (Sriskanda and Shuman, 1998b). Thus, due to the simplicity of the CV DNA ligase, along with the well characterised nature of both the WT protein and the C-terminal deletion mutation, this mutant would be an ideal ligase to complement the AOA1 short-patch SSBR defect.

Wild-type and mutant chlorella virus (CV) DNA ligase were expressed in *E.coli* and purified as described previously (Sriskanda and Shuman, 1998b) and in materials and methods. Aliquots of the two CV ligases before and after purification by IMAC are shown in Figure 5.9. The ability of the two chlorella virus DNA ligases to auto-adenylate was tested by incubating 100ng of each DNA ligase with α-^{32}P ATP at 30°C for 5min and analyzing the reaction products by SDS-PAGE and autoradiography (Figure 5.10 A). During ligase adenylation, the α-phosphate of ATP is transferred to the active site lysine of the protein and in the process the ligase will become ^{32}P-radiolabelled. There was a very strong ^{32}P signal in the lane containing reaction products from the WT CV ligase adenylation reaction which ran at the expected size for WT CV ligase. However in the lane containing reaction products from the CΔ5 CV ligase adenylation there was no detectable signal confirming, as reported (Sriskanda and Shuman, 1998b) that the ligase mutant was unable to efficiently adenylate itself.

The ability of WT and mutant CΔ5 chlorella virus DNA ligase to complement the short-patch SSBR defect in AOA1 cell extracts was next tested (Figure 5.9 B). As observed for T4 and human LigIIIα DNA ligases, WT chlorella virus DNA ligase supported the repair of adenylated 1nt gapped substrates by AOA1 extracts, and the presence of ATP inhibited this rescue (compare lanes 6 and 8). Importantly, CΔ5 chlorella virus DNA ligase also supported repair in AOA1 whole cell extracts, and this rescue was not inhibited by ATP (compare lanes 2 and 4).

APTX-independent SSBR was next reconstituted *in vitro* using the two chlorella DNA ligases and recombinant SSBR proteins (Figure 5.11). In agreement with previous data WT CV ligase rescued APTX-independent short-patch repair in the absence of ATP and this rescue was inhibited by the addition of ATP (compare lanes 2 & 4). TheCΔ5 mutant CV ligase also supported APTX-independent repair and, importantly, this rescue was not inhibited by the presence of ATP in (compare lanes 6 and 8).

5.3 Discussion

The previous chapters have demonstrated that short-patch SSBR of an abortive ligation intermediate fails in AOA1 whole cell extracts *in vitro*. This does not reflect a general defect in SSBR as short-patch repair is rescued to WT levels in AOA1 extracts when complemented with recombinant his-APTX (Figure 3.7) and importantly AOA1 extracts are proficient in the repair of a non-adenylated oxidative SSB (Figure 3.8). Additionally, levels of core SSBR proteins in AOA1 LCLs are largely comparable to WT when analysed by western blot (Figure 3.6). In this study I have also presented data showing that the repair defect lies within the ligation step. PNK-mediated end-processing (Figure 4.4) or Polβ-mediated gap-filling (Figure 4.6) were both unaffected by the presence of a 5'AMP and finally it was shown that AOA1 extracts were unable to ligate an adenylated nick *in vitro* (Figure 4.7). As adenylated nicks arise as normal intermediates of DNA ligation this was unexpected. The first step of ligation, the formation of the ligase-adenylate intermediate is very energetically favourable at cellular concentrations of ATP and this adenylated form of the ligase is stable in the absence of DNA. Consequently, although ligases can exist in two forms in the cell it is likely that the adenylated ligase is the predominant form in the cell. Therefore in the unique situation where APTX is not present in the cell and unrepaired adenylated nicks persist, it is likely that the level of non-adenylated ligase present in the cell is too low to support ligation of adenlyated nicks.

Although adenylated nicks do arise as normal intermediates during the second step of DNA ligation, this is usually tightly coupled with the third step of phosphodiester bond formation. In fact, this final step is very rapid, and the rate of phosphodiester synthesis is much faster than adenylation of the DNA and probably the only time the second and third steps of ligation would become uncoupled is in the event of a ligase attempting to prematurely ligate a nick with an incompatible 3' terminus (Crut et al., 2008). If this occurs in a WT cell then APTX would be present to remove the 5'-AMP and the abortive ligation would be effectively reset. Therefore in a WT situation it is unlikely that a DNA ligase would ever encounter a persisting adenylated nick and the need to directly ligate an adenylated nick would only arise in the absence of APTX.

The hypothesis that insufficient levels of non-adenylated ligase are the cause of the AOA1 short-patch repair defect was tested by making two predictions; firstly that the complementation of AOA1 extracts with non-adenylated DNA ligase would rescue the short-patch repair defect of an adenylated 1nt gapped substrate, typical of those likely arising during 'abortive' ligation by adenylation of 1nt gaps with 'blocked' 3'-termini, and secondly that this repair would be strongly inhibited by the presence of ATP. In the case of the first prediction it was shown that the AOA1 short-patch repair defect could be rescued by the addition of recombinant human LigIIIα, T4 DNA ligase or CV Ligase in the absence of ATP (Figure 5.3, 5.7 and 5.10). The second prediction was also proved correct and the presence of ATP in the reaction buffers prevented the recombinant ligases from rescuing repair in an AOA1 extract. Finally complementation of AOA1 extracts with a ligase mutant defective in the first step of enzyme adenylation restored repair in an AOA1 extract both in the presence and absence of ATP to equal levels, further supporting the hypothesis that the AOA1 repair defect is the result of limiting levels of non-adenylated ligase (Figure 5.10 and 5.11).

It was noted when comparing the ligase complementation with the human LigIIIα to T4 DNA ligase or CV Ligase that His-LigIIIα only partially rescued the repair defect in AOA1 cell extracts (Figure 5.7) compared to complementation with T4 DNA ligase or CV Ligase (Figure 5.3 and 5.10). This could be explained by either by differences in the relative level of pre-adenylated DNA ligase in the recombinant preparations and/or the possibility that the amount of LigIIIα used in the experiments was less active than the amount of T4 DNA ligase used. As commercial T4 DNA ligase is largely non-adenylated, while His-LigIIIα purified from *E.coli* is likely to be predominantly pre-adenylated, as the ligase adenylation reaction is very rapid in cellular concentrations of ATP, differences in the adenylation states of the ligases is the most probable explanation. This could be addressed using an adenylation assay in which His-LigIIIα is adenylated with [α^{32}P] ATP. A comparison of samples which have been deadenylated with pyrophosphate or mock deadenylation could be used to evaluate the levels of preadenylation in the Hi-LigIIIα preparation. However the partial rescue nonetheless still supports to the hypothesis that the failure of AOA1 whole cell extracts to repair an abortive ligation intermediate is due to limiting levels of non-adenylated ligase in the extracts.

Importantly, APTX-independent short-patch repair of an abortive ligation intermediate could also be reconstituted *in vitro* in the absence of ATP using recombinant SSBR proteins (Figure 5.8 and 5.11). As expected, in the presence of ATP, repair of the abortive ligation intermediate was dependent on APTX (Figure 5.8 compare lanes 1 and 2) and, in the absence of ATP, short-patch SSBR of the abortive ligation intermediate was independent of APTX (Figure 5.8 compare lanes 3 and 4). I noted that the absence of ATP only mildly reduced repair of the adenylated nick in the presence of APTX (Figure 5.8 compare lanes 1 and 3), suggesting that the preparation of LigIIIα contained sufficient levels of pre-adenylated DNA ligase to drive ligation of non-adenylated nicks.

The data presented here provides evidence that adenylated nicks persist during short-patch repair in AOA1 extracts *in vitro*, due to insufficient levels of non-adenylated ligase. Although it has yet to be determined that these lesions actually arise in cells, this is still an intriguing observation as it could provide an explanation for why AOA1 cell lines do not exhibit a consistent cellular repair defect. As end-processing and gap-filling can proceed as normal in AOA1 extracts and the adenylated nicks that could potentially accumulate during short-patch repair should possess a conventional 3'-OH, these lesions could act as potential substrates for long-patch repair. Therefore, in living cells, the existence of a short-patch repair defect in AOA1 cells could be masked by the action of long-patch repair. This hypothesis could be tested by blocking long-patch SSBR in AOA1 cells. If long-patch repair was compensating for a short-patch repair defect in AOA1 cells then blocking long-patch repair would uncover an APTX-dependent cellular SSBR defect.

This could also have important implications in understanding the pathology of the disease and provide a potential explanation for why the brain is so sensitive to loss of APTX. Many long-patch repair factors are also replicative factors, and are known to be down regulated in post-mitotic neurones (Cam et al., 2004). Additionally post-mitotic neurones in G0 would lack alternate repair pathways associated with S-phase or G2 phase, such as homologous recombination or replication coupled SSBR and would therefore be more dependent on short-patch repair. In the case of defective short-patch repair, unrepaired SSBs could accumulate leading to blocked transcription forks and eventual cell death. The observation that a ligase

mutant that is defective in the adenylation of a DNA ligase, but which can still catalyse the ligation of an adenylated nicked substrate supported APTX-independent short patch SSBR even in the presence of ATP could have implications in the treatment of the disease. As the catalytic steps of DNA ligation are relatively separate reactions, it is possible that a compound could be developed that mimics the CV CΔ5 DNA ligase mutant by inhibiting ligase adenylation but leaving the third step intact. Indeed a number of ligase inhibitors which have different specificities for DNA LigI, LigIIIα and LigIV have been discovered (Zhong et al., 2008, Chen et al., 2008). Interestingly these inhibitors prevented DNA-adenylation and ligation, but have no detectable effect on ligase-adenylation, showing that the individual stages of DNA ligation can be individually targeted for inhibition, raising the intriguing possibility that other inhibitors could potentially be found to target ligase-adenylation while leaving nick ligation unaffected. If administered to patients it may be possible to temporarily reset the ligase present in the cell and allow it to repair any persisting adenylated breaks.

This is entirely speculative, however, and there are numerous obstacles to overcome. The first is how to administer any inhibitors to the target tissue. The brain is surrounded by a barrier, called the blood-brain barrier, which is composed of high density cells that restrict the passage of substances between the bloodstream and the brain (Alavijeh et al., 2005). This is a limitation common to many agents designed to target the brain. Another more important issue is that the affected tissue in AOA1 is post-mitotic and non-regenerative. Thus any treatment of the disorder could only hope to prevent the progression of the disease at the onset rather than cure it.

A question that still needs to be address is whether this is specific to AOA1 extracts or whether it is true for wild-type extracts as well. It is possible that APTX plays a role in deadenylating DNA ligases. APTX is a member of the Hint branch of the HIT superfamily of nucleotide hydrolases and transferases which exhibit AMP-lysine hydrolase activity (Brenner, 2002, Bieganowski et al., 2002a, Krakowiak et al., 2004a, Seidle et al., 2005, Kijas et al., 2006). Indeed it has been shown that mutations in APTX that are associated with AOA1 inactivate AMP-lysine hydrolase activity (Seidle et al., 2005). In AOA1 extracts this would lead to a decrease in the levels of non-adenylated ligase. To answer this, one strategy would be to

determine levels of LigIIIα adenylation in AOA1 and wild-type cells by immunoprecipitating the XRCC1-LigIIIα complex from cells and incubating with [α^{32}P] ATP. Co-immunoprecipitating LigIIIα via its interaction with XRCC1 would avoid the potential issue that the α-LigIIIα antibody could inactivate the ligase by blocking the active site (Caldecott et al., 1994, Caldecott et al., 1995).

There is precedence for the regulation of ligase adenylation levels being regulated by a component of a DNA repair pathway in the proposed role of LigIV readenylation by XLF following DNA ligation (Riballo et al., 2009). Unlike other DNA ligases, the adenylation reaction of DNA LigIV proceeds very slowly and is the rate limiting step *in vitro* (Wang et al., 2007). XLF can enhance this reaction *in vitro* and it has been proposed that XLF stimulates NHEJ by readenylating LigIV (Riballo et al., 2009). Thus it is possible that APTX fulfils an opposing role to XLF by deadenylating DNA ligases following premature adenylation of a non-ligatable nick. This would effectively reset the ligase and allow it to repair any persisting adenylating nicks.

CHAPTER SIX

Investigating the role of APTX in DNA repair in living cells

6.1 Introduction

The data presented in the previous three chapters have demonstrated that short-patch SSBR of an abortive ligation intermediate fails in AOA1 whole cell extracts *in vitro* at the final stage of ligating an adenylated nick. This defect was due to loss of APTX because short-patch SSBR was rescued to levels comparable to WT in AOA1 whole cell extracts when complemented with recombinant His-APTX (Figure 3.7). It was also specific for adenylated nicks, because AOA1 extracts were proficient in the repair of a non-adenylated SSB (Figure 3.8).

While the evidence for the existence of defective short-patch SSBR in AOA1 extracts *in vitro* is compelling, the evidence for the existence of a cellular repair defect in living cells is conflicting. While some studies report that APTX defective cells exhibit defective DNA repair (Hirano et al., 2007, Mosesso et al., 2005), this is contradicted by other studies (Reynolds et al., 2009, El-Khamisy et al., 2009). It has also been reported that APTX defective cells are mildly sensitive to DNA damaging agents (Gueven et al., 2004, Clements et al., 2004). However, the finding that short–patch repair of abortive ligation intermediates stall at the stage of ligating an adenylated nick offers a potential explanation for the discrepancy between the *in vitro* and cellular data. Since neither PNK mediated end-processing or Polβ mediated gap-filling are disrupted the unrepaired adenylated nicks that accumulate in AOA1 cells would potentially possess a 3'-hydroxyl terminus, and might thus be channelled into long-patch SSBR.

The hypothesis that long-patch repair can compensate for the loss of APTX in a cellular context has been tested using quiescent neural astrocytes from WT and *APTX*$^{-/-}$ littermate mice (Reynolds et al., 2009). As the pathology of the disease is restricted to the brain, mouse astrocytes are more likely to mimic the affected cell types in AOA1 individuals than fibroblast or lymphoblastoid cell lines. Aphidicolin (APH) is a selective inhibitor of the B family polymerases α, δ and ε and is traditionally used to block DNA replication (Oguro et al., 1979, Ikegami et al., 1979, Wist and Prydz, 1979, Byrnes, 1984, Wright et al., 1994). As Pol δ/ε are also involved with PCNA dependent long-patch SSBR, APH can be employed to inhibit this process, rendering SSBR dependent on short-patch DNA polymerases.

In the absence of APH, quiescent WT and *APTX*$^{-/-}$ mouse astrocytes exhibit similar rates of SSBR after induction of oxidative DNA damage (Reynolds et al., 2009) (Figure 6.1; reproduced with permission from Sherif El-Khamisy). The rate of repair in the WT astrocytes was also unaffected by the presence of APH, demonstrating that APH – resistant polymerases can support the repair of oxidative damage in quiescent mouse astrocytes. In contrast, quiescent *APTX*$^{-/-}$ mouse astrocytes showed reduced rates of repair in the presence of APH, suggesting that in the absence of APTX an alternate repair pathway involving APH-sensitive polymerases (most likely Pol δ/ε) can repair oxidative DNA strand breaks. In the presence of APH this repair pathway is significantly delayed. It is also noteworthy that SSBR was delayed rather than prevented, implying the presence of an additional, albeit slower, APTX – independent repair process involving one or more APH-resistant DNA polymerases (Figure.6.1).

Quiescent *APTX*$^{-/-}$ mouse astrocytes were also found to be defective in the repair of MMS induced alkylation DNA damage in the presence of APH (Reynolds et al., 2009). The data from these experiments are presented in Figure 6.2 with permission of Sherif El-Khamisy. Quiescent WT and *APTX*$^{-/-}$ mouse astrocytes were incubated with a titration of MMS in the presence or absence of APH and rates of repair measured by alkaline comet assay. Repair of MMS induced alkylation DNA damage is measured in a different way to ROS induced oxidative damage. MMS introduces base damage which has to be recognised and cleaved before it can be seen as a DNA break in the alkaline comet assay. The rate of repair of these damaged bases is measured indirectly by quantifying the total level of DNA breaks present in a cell after incubation with an alkylating agent at 37°C for a specified time period. The total level of DNA breaks measured in this way will represent the net difference between damage induction and damage removal, and is an efficient way to measure defects in SSBR. Consistent with these data, deletion of *HNT3* (the APTX homologue) in budding yeast in a *rad27Δ* (FEN1 homolog) background resulted in synergistic sensitivity to H_2O_2 and MMS (Daley et al., 2010).

6.1.2 Aims of this chapter

The aim of this chapter is to investigate the role of alternate APTX independent mechanisms in the repair of abortive ligation intermediates in AOA1 cells. The existence of redundancy in the

repair of an adenylated SSB would explain why AOA1 cells do not exhibit a consistent cellular SSBR defect. One hypothesis is that unrepaired adenylated nicks can be channelled into long-patch SSBR in the absence of APTX-dependent short-patch repair in AOA1 cells. This hypothesis is supported by the existence of an APH – dependent repair defect in quiescent *APTX*$^{-/-}$ mouse astrocytes and observation that *hnt3Δ*/*rad27Δ* double mutant is more sensitive to DNA damage than the single mutants. However confirmation is required that long–patch repair can compensate for defective short–patch repair in human AOA1 cells.

6.2 Results

6.2.1 *Repair of γ-irradiation induced SSBs in human fibroblasts utilises B family polymerases*

It has been shown that APTX has a role in the repair of oxidative and alkylating DNA damage in mouse astrocytes. A SSBR defect was uncovered in quiescent *APTX*$^{-/-}$ mouse astrocytes upon incubation with APH, suggesting that long–patch SSBR can compensate for the loss of APTX (Reynolds et al., 2009). However whether or not long-patch repair can substitute for APTX-dependent repair in human AOA1 cell lines remained to be determined. To test this, hTERT immortalised AOA1 fibroblasts (FD105 hTERT) that were either mock-complemented (FD105 M20 hTERT cells (AOA1)) or complemented by stable retroviral expression of human APTX (FD105 M21 hTERT (Corrected)) were employed. A western blot comparing the total level of APTX protein expressed in these cell lines and also in a WT hTERT fibroblast cell harbouring the empty expression vector (1BR M20 hTERT) is shown (Figure 6.3A).

It was decided in these experiments to employ γ-irradiation to induce oxidative DNA strand breaks in AOA1 fibroblasts, rather than hydrogen peroxide for technical reasons. Whilst both agents are sources of ROS and generate DNA breaks with termini of similar chemistry, the level of DNA breaks induced by γ-irradiation is more uniform between individual cells than hydrogen peroxide which displays large variations in DNA break induction between cells. The dose of γ-irradiation chosen for my experiments (30 Gy) was established using a dose response curve generated with the hTERT cell lines FD105 M20 and FD105 M21, with DNA strand breaks quantified by alkaline comet assays (Figure 6.3B). This dose was chosen because it induced a high level of DNA strand breaks (~30,000 SSBs & ~1,000 DSBs) and was still in the linear region of the dose response curve.

To render human hTERT fibroblasts quiescent I employed by contact inhibition followed by serum starvation for 7 days (Coller et al., 2006). In initial experiments I employed pulse-labeling with [^{3}H] thymidine, as described in materials and methods, to verify that this approach resulted in non-replicating populations fibroblasts (Figure 6.4). Cycling and quiescent

cells were also mock-treated (using DMSO) or treated with 50μM APH for 1hr prior to pulse labelling with [^{3}H] thymidine, to confirm that replication was also inhibited by this inhibitor under the conditions employed (Figure 6.4B). [^{3}H] incorporation was evident in both APTX complemented and AOA1 cycling hTERT fibroblasts, albeit to a lesser extent in the latter. While maintaining the cell line it was noticed that the AOA1 cycling hTERT fibroblasts grew at a slower rate than the corrected line, which was consistent with the observed rates of [^{3}H] incorporation. Incubation with 50μM APH decreased the level of [^{3}H] signal to low levels in cycling populations of both APTX complemented and AOA1 fibroblasts, suggesting that that the concentration of APH employed was sufficient to block DNA synthesis (Figure 6.4B). Notably, [^{3}H] incorporation was greatly reduced in populations of both APTX complemented and AOA1 fibroblasts following confluence and serum starvation and this level was not reduced further by incubation with APH, confirming that these cells were not replicating.

Surprisingly, I failed to detect a significant difference between the rate of repair of γ-ray induced DNA strand breaks in APTX-corrected FD105 M21 hTERT cells, compared to FD105 M20 hTERT cells (harbouring empty vector), irrespective of whether or not cells were incubated with APH (compare grey and green bars in Figure 6.5). Moreover, APH largely or completely blocked SSBR in both APTX complemented and AOA1 cell lines, with little detectable reduction in the quantity of DNA breaks present after a 60 min repair period (Figure 6.5). This result contrasts with data from experiments employing quiescent mouse astrocytes, in which APH-sensitive repair was evident only if APTX-dependent repair was absent. This result was unexpected because APH-sensitive DNA polymerases such as Polδ/ε are believed to operate during long–patch SSBR, which is normally suppressed in non- cycling cells due to down-regulation of the essential long–patch DNA repair factors PCNA and FEN1 (Takasaki et al., 1981, Otterlei et al., 1999, Warbrick et al., 1998, Iatropoulos and Williams, 1996). Indeed, immunoblotting confirmed that both PCNA and FEN-1 levels were greatly reduced in quiescent cell population employed for my experiments (Figure 6.6). Together these data suggest that, in contrast to quiescent mouse neural astrocytes, most if not all SSBR in quiescent immortalised human fibroblasts following γ-irradiation is dependent on aphidicolin-sensitive DNA polymerases typically associated with long-patch repair.

Because the hTERT fibroblasts employed above were immortilised by hTERT expression I repeated the experiments using primary WT (1BR) and AOA1 (FD105) human fibroblasts (Figure 6.7). However, the observed results were similar to those described above, with SSBR rates largely or entirely determined by APH-sensitive repair and unaffected by loss of APTX.

To examine whether the results described above reflected the quiescent status of the cell lines, I repeated the experiments using cycling fibroblasts (Figure 6.8 and 6.9). However, once again, repair was largely APH sensitive, and was unaffected by loss of APTX, irrespective of whether or not the cells were primary (Figure 6.9) or were immortalised with hTERT (Figure 6.8). It was noticeable however, that repair did occur in the presence of APH, albeit very slowly and independently of APTX, suggesting that whilst cycling human fibroblasts are also highly dependent on the APH – sensitive repair some APH–resistant repair does occur.

6.2.2 *Short-patch repair in WT whole cell extracts is APH resistant* in vitro

The experiments described above strongly suggest that SSBR in human fibroblasts is conducted largely if not entirely by the aphidicolin-sensitive polymerases Polδ and/or Polε. This contrasts with the widely held view that most SSBR following oxidative stress is conducted by the short patch DNA polymerase Polβ, in non-cycling cells at least. I was thus concerned that the concentration of APH employed here, whilst within the range used in previous literature (Reynolds et al 2009) might inhibit Polβ. To address this possibility I examined the impact of 50μM APH on the polymerisation activity of purified recombinant human Polβ (Figure 6.10). Notably, this concentration of APH failed to inhibit Polβ, suggesting that the aphidicolin sensitivity of SSBR in human fibroblasts γ-irradiation was not due to an 'off-target' impact of this inhibitor on Polβ (Wist and Prydz, 1979).

6.3 Discussion

The data presented in Chapter 3 showed that short-patch SSBR of an abortive ligation intermediate fails in AOA1 whole cell extracts *in vitro*. This short-patch repair defect reflects a

failure to ligate an adenylated nick in the absence of APTX, due to insufficient levels of non-adenylated ligase, resulting in an inability to ligate a pre-adenylated nick (see chapters 4 & 5). These observations can provide a possible explanation for the lack of a detectable chromosomal SSBR defect in APTX defective cell lines. Because end-processing and gap-filling occurs normally in AOA1 extracts, the adenylated nicks that accumulate during short-patch repair could be channelled into long-patch repair. Consistent with this idea, quiescent *APTX*$^{-/-}$ mouse astrocytes that were pre-treated with APH to inhibit the long-patch repair polymerases Polδ/ε exhibited significantly reduced rates of chromosomal SSBR, compared to similarly treated WT cells (Reynolds et al., 2009). Similar results were observed with mouse granule cells, a bona fide type of post-mitotic cortical neuron (Caldecott and S.F. El-Khamisy et al, unpublished observations).

To investigate the presence of redundant APTX-independent repair pathways in human cells, I employed human fibroblasts that were mock-complemented or complemented by stable expression of human APTX. Interestingly, [^{3}H] thymidine incorporation in aprataxin-defective AOA1 fibroblasts was significantly less than in complemented AOA1 cells (Figure 6.4). This may reflect a requirement for APTX during S phase, or an impact of loss of APTX on cell cycle progression. However if this was a consistent phenotype of APTX-defective cells then it might be expected that AOA1 individuals would exhibit pronounced developmental defects, which they not appear to do. Moreover, differences in growth rate have not been reported for other cell types in response to loss of APTX, including chicken DT40 cells (Caldecott, unpublished observations). Alternatively, although the two cell lines were created from the same parental cell line it is possible that there has been significant genetic drift. To resolve this question will require the creation and analysis of additional matching WT and APTX-defective cell lines.

In contrast to mouse neural cells, both AOA1 and WT human fibroblasts exhibited a striking SSBR defect upon incubation with APH, irrespective of whether such cells were primary or immortalised, and to a large extent independent of proliferation status. These data suggest that all repair events occurring in the quiescent human fibroblasts following induction of oxidative damage by γ-irradiation are aphidicolin-sensitive, and can be conducted independently of APTX.

There are number of possible explanations for the different results observed with mouse neural cells versus human fibroblasts. First, astrocytes and fibroblasts are different cell types and it is possible that they employ different DNA polymerases during SSBR. Second, it is possible that there are major differences between mouse and man in terms of DNA polymerase selection during DNA repair. Differences between human and mouse in terms of the response to DNA damage is most evident from the fact that *APTX*$^{-/-}$ mice do not recapitulate the neurodegenerative pathology evident in AOA1 individuals (unpublished observations). This means that the *APTX*$^{-/-}$ mice are perhaps not the ideal model system to study APTX dependent repair in the context of the AOA1 disorder. Perhaps a better model cell system for future studies of this type would be to differentiate human stem cells or SH-SY5Y neuroblastoma cells before or after depletion of APTX by siRNA.

Third, whereas the experiments employing mouse neural cells used hydrogen peroxide to induce oxidative DNA breaks, my experiments employed γ-irradiation. γ-irradiation was chosen for technical reasons as, whilst both agents induce oxidative damage via attack of deoxyribose and DNA bases by reactive oxygen species, resulting in DNA strand breaks with termini of similar chemistry, the level of DNA breaks induced by γ-irradiation is more uniform between individual cells than hydrogen peroxide. Individual cells treated with hydrogen peroxide display large variations in the levels of damage induction. However H_2O_2 induces ~2000 SSBs for every DSB, whereas IR induces ~20-40 SSBs for every DSB (Ward, 1998, Ward et al., 1987). Therefore it is possible that different cellular responses/SSBR repair pathways are elicited in response to the two agents, with different DNA polymerase requirements. Finally another possibility is that Polδ/ε, and/or some other APH sensitive DNA polymerase, are essential for SSBR in response to very high levels of oxidative damage while Polβ and other APH – resistant polymerases are involved in the repair of lower, more physiological, doses of DNA damage. It has been suggested that the fraction of repair carried out by either APH-sensitive or APH-resistant polymerases can change according to the dose of damaging agent used (Dresler and Lieberman, 1983a, Dresler and Lieberman, 1983b). It would be prudent to repeat the experiments with dose response of γ-irradiation to determine if APH-resistant SSBR operates at lower doses of DNA damage.

6.3.1 *The roles of the different families of polymerases in SSBR in human fibroblasts*

The unexpected observation that emerged from the experiments utilising human fibroblasts was that APH sensitive polymerases were essential for repair of γIR induced DNA damage in human fibroblasts, irrespective of proliferative status. It would be important in future studies to determine if this was common to other human cell lines, or whether this is a characteristic of the specific fibroblast cell lines employed here.

Numerous biochemical studies with recombinant protein and whole cell extracts have implicated the APH-resistant DNA polymerase, Polβ, as fulfilling the primary role in gap filling during short-patch SSBR, as well as participating during long-patch repair. Quiescent *Polβ*$^{-/-}$ MEFs exhibit sensitivity to γ-irradiation, although this sensitivity is not evident in cycling *Polβ*$^{-/-}$ MEFs, and whole cell extracts prepared from Polβ defective mouse cell lines show a reduced capacity for BER *in vitro* (Vermeulen et al., 2007b, Vermeulen et al., 2008, Parlanti et al., 2004). This is reduced further, but not absent, when the extracts are treated with APH. Polλ a DNA polymerases from the same family as Polβ, and Polι, have also been implicated in APH-resistant repair *in vitro* (Braithwaite et al., 2005a, Braithwaite et al., 2010, Braithwaite et al., 2005b, Petta et al., 2008, Shimazaki et al., 2002b, Vens et al., 2007).

Given the evidence for a role for Polβ and other APH – resistant polymerases in SSBR, it was surprising that the human fibroblasts employed in my experiments were largely unable to repair γ-irradiation induced DNA damage in the presence of APH. These data suggest that Polδ and/or Polε, and/or some other APH sensitive DNA polymerase, are essential for SSBR in response to oxidative stress in human fibroblasts. Whilst these data could represent the activity of an APH-sensitive polymerase during short patch repair, it seems more likely that the APH-sensitive SSBR detected in these experiments reflects a long patch process. Indeed, the latter would be compatible with the apparent absence of requirement for APTX during SSBR in human fibroblasts, since the latter is likely of utility only during short patch repair.

Notably, however, total levels of PCNA and FEN1 protein were greatly reduced in the quiescent fibroblasts compared to the cycling fibroblasts. Such a reduction has been observed previously and is consistent with the primary role of PCNA and FEN1 being during S phase (Li et al., 1995b, Takasaki et al., 1981, Levin et al., 1997, Levin et al., 2000, Iatropoulos and Williams, 1996). This would imply that long patch repair is attenuated in quiescent human fibroblasts, rather than being the dominant source of SSBR. However, it is still possible that the residual level of PCNA and FEN1 present in the quiescent human fibroblasts employed here is sufficient for SSBR. Alternatively, the APH sensitive repair detected in these experiments may reflect a long patch repair pathway that employs PCNA and FEN-1 independent mechanism for gap filling and removal of the 5' DNA flap. In terms of the endonuclease involved, Mre11/Rad50/Nbs1 complex (MRN) is a candidate, since it can process 5'-termini during DNA resection and during the removal of 5'-termini harbouring covalently linked protein (Nicolette et al., 2010b, Paull, 2010a, You et al., 2009a, Mimitou and Symington, 2009, Moreau et al., 1999, Milman et al., 2009, Hartsuiker et al., 2009, Rass et al., 2009, Xie et al., 2009).

Additionally, mutation of the MRX complex in *S.cerevisiae* results in hypersensitivity to alkylating agent MMS and significantly reduced ability to repair base damage *in vitro* (Steininger et al., 2010). Intriguingly there was no further decrease in efficient of repair of the uracil containing substrate when the *xrs2* mutant extracts were incubated with APH, placing the MRX complex in the same pathway as the APH – sensitive polymerases. When investigated further it was revealed that the MRX complex was required for efficient strand elongation during gap filling *in vitro*. As the MRX complex is required for the processing of the 5' termini of DSBs, it can be imagined that it may also function to remove a 5' DNA flap created during long-patch repair. This hypothesis could be tested using human fibroblast cell lines derived from patients with Ataxia Telangtiectasia - Like Disorder (ATLD), a disorder in which Mre11 is mutated (Stewart et al., 1999).

The aim of this chapter was to investigate the role of alternate APTX independent mechanisms in the repair of abortive ligation intermediates in AOA1 cells. The presence of redundant repair mechanisms can explain why AOA1 cells do not exhibit a cellular SSBR defect. In

contrast to mouse neural cells however, which can employ an APH-resistant repair process if APTX is missing, quiescent and proliferating human fibroblasts are largely or entirely dependent on APH-dependent repair, such that APTX is completely dispensable. It will now be important to examine if this is also the case in other cell types, including human neural cell types obtained by differentiation of human stem cells or neuroblastoma cell lines.

CHAPTER SEVEN

Discussion

7.1 Discussion

AOA1 is an autosomal recessive ataxia that clinically presents with early onset ataxia, oculomotor apraxia, cerebellar atrophy, and axonal motor neuropathy caused by mutations in the gene *APTX* a member of the Hint-like histidine triad (HIT) superfamily, which consist of adenosine 5'-monophosphoramide hydrolyases (Date et al., 2001, Barbot et al., 2001, Brenner, 2002, Bieganowski et al., 2002a, Krakowiak et al., 2004a, Seidle et al., 2005, Kijas et al., 2006). APTX is a nuclear protein (Sano et al., 2004) that possess a divergent zinc finger motif (ZnF) and an amino-terminal fork-head associated (FHA) domain that has homology with the amino-terminus of PNK (Barbot et al., 2001). APTX interacts with CK2 phosphorylated XRCC1 and XRCC4 via the N-terminal FHA domain and co-immunoprecipitates in complexes containing SSBR and DSBR machinery (Luo et al., 2004, Sano et al., 2004, Clements et al., 2004, Date et al., 2004, Gueven et al., 2004).

APTX catalyses the release of adenylate groups covalently linked to 5' phosphate termini of a DNA SSB or DSB (Ahel et al., 2006, Rass et al., 2007b, Rass et al., 2008) and cell-free extracts prepared from *APTX*$^{-/-}$ mouse cortical astrocytes are defective in assays that measure short patch SSBR of an adenylated SSB *in vitro* (Ahel et al., 2006). Adenylated nicks are produced as a normal intermediate during ligation by an ATP-dependant DNA ligase, and a stable abortive ligation intermediate can arise if a ligase has prematurely adenylated a SSB with a 3' terminus other than a 3'OH (Figure 1.11). Thus, APTX has been proposed to play a role in SSBR in the rapid resetting of abortive ligations as they arise.

7.1.1 Short-patch repair of abortive ligation intermediates fails in the absence of Aprataxin due to insufficient levels of non-adenylated DNA ligase

To date, data on the role of APTX in repairing abortive ligation intermediates has emerged from *in vitro* repair assays employing recombinant proteins and cell free extracts from *APTX*$^{-/-}$ avian DT40 cells or mouse *APTX*$^{-/-}$ cortical astrocytes (Ahel et al., 2006, Rass et al., 2007b, Rass et al., 2008). It was therefore important to determine if whole cell extracts prepared from human AOA1 disease cells lines are similarly defective in the short-patch SSBR of abortive ligation intermediates and indeed lymphoblastoid cell lines (LCL) derived from an AOA1

individual homozygous for a whole genome deletion of *APTX* were found to be defective in the short-patch SSBR of an abortive ligation intermediate *in vitro* (Figure 3.5).

This defect was caused by the loss of APTX 5'-AMP DNA deadenylase activity because complementation of AOA1 extracts with recombinant human His-APTX completely rescued this defect (Figure 3.7) and AOA1 cell extracts were proficient in the repair of a non-adenylated SSB substrate (Figure 3.8). This suggested that it is the persistence of the unrepaired 5'AMP that blocks one or more subsequent repair events in AOA1 extracts *in vitro*, rather than defective processing of 3'-phosphate termini, gap filling, or DNA ligation per se and consistent with this, it was found that an inability to ligate an adenylated nick was responsible for the short-patch repair defect in AOA1 extracts (Figure 4.8). This was not due to lower levels of active DNA ligase per se in AOA1 extracts compared to wild-type extracts, as AOA1 extracts were competent for repair of a non-adenylated SSB. Notably, the presence of a 5'-AMP at a SSB did not inhibit the activities of either recombinant PNK or Polβ *in vitro*.

Alternatively, it was considered possible that WT and/or AOA1 cells possess levels of non-adenylated ligase that are insufficient to catalyse efficient ligation of non adenylated nicks. Such a defect might be specific to AOA1, if APTX has a role in deadenylating DNA ligases in addition to deadenyating DNA. Consistent with this idea, APTX is a member of the Hint branch of the HIT superfamily of nucleotide hydrolases/transferases that possess AMP-lysine hydrolase activity (Brenner, 2002, Bieganowski et al., 2002a, Krakowiak et al., 2004a, Seidle et al., 2005, Kijas et al., 2006). Although preliminary experiments failed to reveal any activity of APTX on adenylated LigIIIa, the activity of APTX on LigI was not tested (Caldecott, unpublished observations). As DNA LigI was recently implicated in two studies to be the main DNA ligase involved in XRCC1 dependent SSBR, it cannot yet be discounted that APTX has a role in deadenylating DNA LigI instead of LigIIIα (Simsek et al., 2011, Katyal and McKinnon, 2011, Gao et al., 2011).

There is precedence for the role of a DNA repair factor in the regulation of adenylation levels of a DNA ligase. Unlike other DNA ligases, DNA ligation events catalysed by DNA LigIV proceed

slowly *in vitro* due to a rate limiting enzyme-adenylation reaction (Wang et al., 2007). Consistent with this, LigIV ligation events are not stimulated by the presence of ATP (Riballo et al., 2001). Recently it has been shown that XLF promotes LigIV-dependent ligation events by stimulating adenylation of the ligase (Riballo et al., 2009). Thus XLF has been proposed to perform an important, though non-essential, role as a NHEJ stimulatory factor by promoting the readenylation of LigIV following ligation events. Although it is possible that there are also active mechanisms to stimulate the adenylation of DNA LigIIIα or DNA LigI, both ligases are stimulated by the addition of ATP and show no evidence of a slow ligase-adenylation reaction, so it is unlikely that they would require a recharging step in the same manner as LigIV (Ellenberger and Tomkinson, 2008b).

Alternatively, another explanation is that both WT and AOA1 extracts possess levels of non-adenylated DNA ligase too low to support the ligation of non-adenylated nicks that accumulate in the absence of APTX. The majority of DNA ligases, including DNA LigI and LigIIIα, are rapidly adenylated in the presence of ATP, forming a ligase-adenylate intermediate in which AMP is covalently linked to the active-site lysine via a phosphoamide bond and consequently, although DNA ligases exist in equilibrium between adenylated and non adenylated state, the adenylated form predominates in cells. (Olivera et al., 1968, Harvey et al., 1971, Weiss et al., 1968b, Gumport and Lehman, 1971, Lehmann, 1978). Once an adenylated DNA ligase encounters a DNA break the second step of ligation results in formation of an AMP-DNA intermediate (Olivera et al., 1968, Harvey et al., 1971, Odell et al., 2003, Nair et al., 2007a). In the final step of ligation the DNA phosphodiester bond is reformed (Lehmann, 1978) when the newly de-adenylated ligase catalyses nucleophilic attack of the 5'AMP by the free 3'OH terminus, (Odell et al., 2000, Sriskanda and Shuman, 2002b, Sriskanda and Shuman, 2002a, Nair et al., 2007a, Crut et al., 2008). Normally the formation of deadenylated ligase during step 2 and the completion of step 3 are coupled, such that the adenylated nick is rapidly sealed by the deadenylated ligase. However, if step 2 and 3 become 'uncoupled' (e.g. due to the presence of blocked 3'-termini) the non-adenylated ligase will likely be rapidly readenylated by cellular ATP (Olivera et al., 1968, Harvey et al., 1971, Weiss et al., 1968b, Gumport and Lehman, 1971, Lehmann, 1978). This will not be a problem in WT extracts because the presence of APTX restores the nick to a non-adenylated state. However, in AOA1 extracts,

repair is now dependent on the pre-existing level of non-adenylated ligase, which we hypothesized, may be too low to facilitate step 3 of the ligase reaction.

The hypothesis that insufficient levels of non-adenylated ligase are the cause of the AOA1 short-patch repair defect was tested by making two predictions; firstly that the complementation of AOA1 extracts with non-adenylated DNA ligase would rescue the short-patch repair defect of an adenylated 1nt gapped substrate, typical of those likely arising during 'abortive' ligation by adenylation of 1nt gaps with 'blocked' 3'-termini, and secondly that this repair would be strongly inhibited by the presence of ATP. Indeed both of these predictions proved to be true using not only human LigIIIα but also with two unrelated DNA ligases, T4 DNA ligase and Chlorella ligase, suggesting that this is an inherent limitation of ATP-dependent DNA ligases rather than a feature of a specific ligase. In addition, complementation of AOA1 extracts with a mutant Chlorella ligase defective in the first step of enzyme adenylation restored repair in an AOA1 extract both in the presence and absence of ATP, further supporting the hypothesis that the AOA1 repair defect is the result of limiting levels of non-adenylated ligase (Figure 5.10 and 5.11). Importantly, APTX-independent short-patch repair of an abortive ligation intermediate was reconstituted *in vitro* in the absence of ATP using recombinant human SSBR proteins, and was also reconstituted in the presence of ATP by employing the Chlorella mutant DNA ligase.

These data support a hypothesis that adenylated nicks accumulate during short-patch repair in AOA1 extracts *in vitro* due to insufficient levels of non-adenylated ligase. However one critical piece of the puzzle is still missing as it has yet to be shown that adenylated SSBs are a physiologically relevant lesion in living cells. Until 5'AMP-DNA lesions are observed to be present in living cells, the role for APTX in the repair of abortive ligation intermediates can only be hypothesised. However, detecting the presence of 5'AMP lesions in living cells has proved to be difficult. Attempts to show that genomic DNA extracted from AOA1 cells possessed higher levels of AMP than wild-type cells by mass-spec analysis has proved largely unsuccessful due to a high level of background and the high sensitivity of the assay (Caldecott and El-Khamisy, unpublished observations). An alternative strategy would be to generate a lesion specific antibody that recognised the adenylate groups in the context of DNA, such as the well

characterised antibody that recognises the oxidative base lesion, 8-oxo-G (Bespalov et al., 1999).

Another strategy would be to attempt to increase the amount of abortive ligations in AOA1 cells to detectable levels. The depletion or inhibition of PNK in AOA1 cells could serve to increase the amount of abortive ligations due to the increased levels of un-ligatable SSBs possessing 3'-P termini (Bernstein et al., 2008, Freschauf et al., 2010, Freschauf et al., 2009). There is precedence for this in the synergistic decrease in SSBR rates observed in a *APTX*$^{-/-}$ *TDP1*$^{-/-}$ double knockout mice compared to either single mutant (El-Khamisy et al., 2009). Alternatively, abortive ligations could be directly increased through the use of a 'toxic' ligase that harbours a mutation that allows adenylation of the ligase and DNA but blocks the final step of ligating an adenylated nick. One such mutation has been found in chlorella virus DNA ligase within NTase motif V (K188A) (Sriskanda and Shuman, 2002a). Overexpression of this 'toxic' ligase in AOA1 cells might be sufficient to overload the capacity of any redundant APTX-independent repair pathways, and unrepaired SSBs may be visualised in AOA1 cell lines. Indeed this strategy has already proved useful in investigating the role of TDP1 in *S.cerevisiae* by showing that induction of a 'toxic' topoisomerase 1 mutant in a *tdp1Δ* background sensitises the cells (Pouliot et al., 2001).

7.1.3 Pathway redundancy during the repair of adenylated SSBs in human cells

While the evidence for a SSBR defect in AOA1 extracts *in vitro* is convincing, the existence of a cellular repair defect is less so. Several studies have shown that APTX defective cell lines exhibit normal rates of SSBR upon treatment with H_2O_2 or MMS when measured by comet assay or NAD(P)H depletion assay (Gueven et al., 2004, Reynolds et al., 2009, El-Khamisy et al., 2009) while other studies have reported that APTX defective cells possess a SSBR defect upon treatment with CPT as measured by alkaline comet assay, or following UV irradiation in cells in which these lesions are channelled into SSBR (Mosesso et al., 2005, Hirano et al., 2007).

The hypothesis that adenylated nicks accumulate during short-patch repair in AOA1 provides a possible explanation for the absence of a major or consistent cellular repair defect in these cells. This is because adenylated nicks are potential substrates for long-patch repair, which in a cellular context might compensate for the absence of APTX-dependent short patch repair. This could also have important implications in understanding the pathology of the disease and provide a potential explanation for why the brain is sensitive to loss of APTX. Many long-patch repair factors are also replicative factors, and are known to be down regulated in post-mitotic neurones (Cam et al., 2004). Additionally post-mitotic neurones in G0 would lack alternate repair pathways associated with S-phase or G2 phase, such as replication coupled SSBR, is hypothesis to predominantly involve long-patch repair factors, and would therefore be more dependent on short-patch repair (Caldecott, 2008, Caldecott, 2001, Caldecott, 2003b). Unrepaired SSBs might thus lead to blocked transcription in post-mitotic neurones, and eventual cell death. The hypothesis that long-patch repair might compensate for the loss of APTX in some cellular contexts was addressed using quiescent neural astrocytes from WT and *APTX*$^{-/-}$ littermate mice, and using Aphidicolin (APH) to inhibit 'classical' long patch repair polymerases Polδ and Polε (Reynolds et al., 2009).

Notably, WT and *APTX*$^{-/-}$ mouse astrocytes exhibit similar rates of SSBR following either oxidative DNA damage or treatment with the base damaging agent, MMS (Reynolds et al., 2009), and the rate of repair in WT astrocytes was unaffected by the presence of APH. However, quiescent *APTX*$^{-/-}$ mouse astrocytes showed reduced rates of repair in the presence of APH, suggesting that in the absence of APTX an alternate repair pathway involving APH-sensitive polymerases (most likely Pol δ/ε) can indeed repair SSBs. Similar results were observed with mouse granule cells, a bona fide type of post-mitotic cortical neurone (Caldecott and S.F. El-Khamisy et al, unpublished observations). It is also noteworthy that SSBR was delayed rather than prevented, implying the presence of an additional, albeit slower, APTX – independent repair process involving one or more APH-resistant DNA polymerases (Figure 6.1). Together, the results obtained with mouse neural cells support the hypothesis that, in the absence of APTX, adenylated SSBs can be channelled into long-patch repair. However, different results were observed if human fibroblasts were employed. In contrast to mouse neural cells, both AOA1 and WT human fibroblasts exhibited a striking SSBR defect upon incubation with APH, irrespective of whether such cells were primary or immortalised, and to a

large extent independent of proliferation status. These data suggest that all repair events occurring in the quiescent human fibroblasts following induction of oxidative damage by γ-irradiation are aphidicolin-sensitive, and can be conducted independently of APTX.

There are several possible explanations for the different results observed with mouse neural cells versus human fibroblasts. First, astrocytes and fibroblasts are different cell types and may employ different DNA polymerases during SSBR. Differences between human and mouse in terms of the response to DNA damage is most evident from the fact that *APTX*$^{-/-}$ mice do not recapitulate the neurodegenerative pathology evident in AOA1 individuals (unpublished observations). Perhaps a better model cell system for future studies of this type would be to differentiate human stem cells or SH-SY5Y neuroblastoma cells before or after depletion of APTX by siRNA. The SH-SY5Y cell line possesses many biochemical and functional properties of neurons and can be differentiated into a functionally mature neuronal cell type in the presence of various agents, making it a popular model system for the study of neurotoxicity and neurodegeneration and has been used to model the neuropathology seen in Parkinson's disease (Xie et al., 2010). Thus SH-SY5Ys could also prove to be a useful tool for investigating the impact of DNA repair defects on the survival of functionally mature neurons.

Second, whereas the experiments employing mouse neural cells used hydrogen peroxide to induce oxidative DNA breaks my experiments employed γ-irradiation. Both agents induce oxidative damage via attack of deoxyribose and DNA bases by reactive oxygen species, resulting in DNA strand breaks with termini of similar chemistry. γ-irradiation was originally chosen as a source of oxidative DNA damage as, unlike hydrogen peroxide which exhibits large variations in damage induction between individual cells, γ-IR induces a more uniform level of DNA breaks between samples. However H_2O_2 induces ~2000 SSBs for every DSB, whereas IR induces ~20-40 SSBs for every DSB (Ward, 1998, Ward et al., 1987). Therefore it is possible that different cellular responses/SSBR repair pathways are elicited in response to the two agents, with different DNA polymerase requirements.

A final possibility is that Polδ/ε, and/or some other APH sensitive DNA polymerase, are involved in the response to very high levels of oxidative DNA damage while Polβ and other APH – resistant polymerases are involved in the repair of lower, more physiological, doses of DNA damage. Previous studies have shown that the fraction of repair carried out by either APH-sensitive or APH-resistant polymerases can change according to the dose of DNA damaging agent used, and indeed the higher the level of DNA damage, the higher the dependence on APH-sensitive polymerases (Dresler and Lieberman, 1983a, Dresler and Lieberman, 1983b). To test this hypothesis, the experiments could be repeated with lower doses of γ-irradiation to determine if APH-resistant SSBR operates at lower doses of DNA damage.

As these experiments were unable to demonstrate the existence of APTX-dependent repair following oxidative DNA damage in living cells, it is necessary to attempt different approaches to investigate the role of APTX in DNA repair in living cells. To investigate whether long-patch SSBR could function to repair adenylated SSBs in the absence of APTX, the *APTX*$^{-/-}$ mouse could be crossed with a mouse strain possessing deletions in one or more long-patch repair factors. FEN1 is a core component of long-patch repair and an *APTX*$^{-/-}$*FEN1*$^{-/-}$ double knockout mouse would be an ideal tool to test the redundancy between APTX and long-patch SSBR. Although germline deletion of FEN1 is embryonically lethal due to the essential role of FEN1 in the maturation of Okazaki fragments during DNA replication, FEN1 could be conditionally disrupted in the central nervous system, a strategy previously used to overcome the lethality of a whole body knockout of XRCC1 in mice (Larsen et al., 2003, Zheng et al., 2007, Lee et al., 2009). Rates of chromosomal SSBR could then be compared using astrocytes obtained from *APTX*$^{-/-}$*FEN1*$^{-/-}$, *APTX*$^{-/-}$, and *FEN1*$^{-/-}$ mice to determine if there was a synergistic reduction in repair rates in the double mutant compared to either single mutant, which would be predicted if there was redundancy between APTX and long-patch dependent repair of abortive ligation intermediates.

Another advantage of an *APTX*$^{-/-}$*FEN1*$^{-/-}$ double knockout mouse is that this could potentially lead to an increase in the levels of unrepaired adenylated SSBs in the nervous system. A potential explanation for the lack of neurodegenerative pathology in *APTX*$^{-/-}$ mice is that adenylated SSBs do not accumulate in sufficient numbers in the adult mice due to their

comparatively short life spans. The age of onset of AOA1 is between early childhood and adolescence and which is considerably longer than the lifespan of a mouse and the co-disruption of long-patch repair and APTX in mouse could increase levels of adenylated SSBs to a level sufficient to impact on the survival of post-mitotic neurons.

This strategy of crossing *APTX*$^{-/-}$ mice with DNA repair defective strains of mice strains could also be used to investigate the role of other DNA repair pathways in the APTX-independent repair of adenylated SSBs. It has been considered possible that components of HDR and SSBR function together as a back-up mechanism to ensure that SSBs do not become permanent blocks to replication in RC-SSBR, which raises the possibility that nucleases involved in the processing of DSBs, such as MRN, could also function to process adenlyated SSBs in the absence of APTX (Nicolette et al., 2010b, Paull, 2010a, You et al., 2009a, Mimitou and Symington, 2009, Moreau et al., 1999, Milman et al., 2009, Hartsuiker et al., 2009, Rass et al., 2009, Xie et al., 2009). Such a hypothesis could also be tested by crossing *APTX*$^{-/-}$ with a mouse strain possessing a neural specific disruption of Mre11 (Stracker and Petrini, 2011). Depletion APTX in ATLD cell lines or Mre11 in AOA1 cell lines by siRNA could also be performed in parallel to lend support to this hypothesis.

7.1.4 *The roles of different DNA polymerases during SSBR*

As discussed in the previous chapter, the surprising observation that arose from the experiments employing human fibroblasts was that SSBR following oxidative damage was driven almost exclusively by one or more APH sensitive DNA polymerases. This contradicts numerous biochemical and cellular studies have implicated the APH resistant polymerases β, λ and ι as having a significant role in both short-patch and long-patch SSBR (Braithwaite et al., 2005a, Braithwaite et al., 2010, Braithwaite et al., 2005b, Petta et al., 2008, Vermeulen et al., 2007a, Vermeulen et al., 2008, Vens et al., 2007, Parlanti et al., 2004). However, as most of the cellular studies have employed MEFs, whereas my experiments have employed human fibroblasts. It is possible that this reflects differences in the contributions of polymerases in SSBR between human and mouse, with the APH-sensitive polymerases perform a much larger role in human fibroblasts than MEFS.

It would be interesting to extend my experiments to other human cell lines, and particularly other primary cells, to determine if the dependence of APH-sensitive polymerases for the repair of oxidative DNA damage is a feature of fibroblast cell lines or whether it is common to other human cell lines. Lymphoblastoid cell lines, MRC5, which is an embryonic lung fibroblast cell line and 293T, which is a cell line derived from embryonic kidney cells, are three commonly used non-malignant human cell lines which could be used to test the roles of APH-sensitive polymerases in SSBR in different cell types. Alternatively, another strategy would be to use siRNA mediated depletion of different combinations of polymerases in human cells to test their contributions to SSBR.

However, what is not clear from my experiments is whether the APH-sensitive repair seen in human fibroblasts is a long patch repair mechanism. Total levels of the classical long patch repair factors PCNA and FEN1 protein were reduced in the quiescent fibroblasts, yet SSBR following oxidative stress was still largely APH-dependent. It is possible that the level of PCNA and FEN1 was sufficient for Pol δ/ε mediated long patch repair, or that another APH-sensitive polymerase and/or nuclease mediates this process in these cells. Finally, the repair event could reflect a short patch mechanism, mediated either by an as yet unidentified APH-sensitive polymerase or by Polδ/ε. Another possibility is that the APH sensitive repair could reflect Polδ/ε–dependent short – patch repair. Polδ/ε have been shown to be capable of inserting a single nucleotide into a SSB, albeit less efficiently than Polβ is more efficient at this.

7.1.5 Conclusions and future perspectives

The major finding of this study is that short-patch repair of an abortive ligation intermediate fails in AOA1 due to limiting levels of non-adenylated ligase, supporting the hypothesis that adenylated nicks accumulate in the absence of APTX. This finding has implications for the pathology of AOA1 as the accumulation of unrepaired SSBs could result in an increase in the levels of collapsed transcription forks in post-mitotic neurons, ultimately leading to a higher occurrence of neuronal cell death in AOA1 individuals. This has also been proposed to be the underlying cause of the neurodegeneration seen in SCAN1individuals. Indeed it has been

demonstrated that a significant portion of the abortive Top1-SSBs seen in SCAN1 cells following CPT treatment by alkaline comet assay are dependent on the presence of active transcription and it has been known for a while that collision with transcription machinery converts Top1 cleave complexes into abortive Top1-SSB (Kroeger and Rowe, 1989, Bendixen et al., 1990, Wu and Liu, 1997, Miao et al., 2006, El-Khamisy et al., 2005).

Another factor which could be significant in the pathology of AOA1 is that post-mitotic neurons are highly active cells and exhibit high levels of mitochondrial respiration but have a reduced capacity to neutralise reactive oxygen species, which would lead to a higher level of oxidative stress in the central nervous system compared to other tissue types (Weissman et al., 2007, Barzilai, 2007). This high level of oxidative damage would result in higher levels of SSBs with blocked 3' termini which could lead to an increase in the levels of abortive ligations. Thus, in combination with absence of redundant DNA repair pathways that operate in S-phase and G2 and the proposed attenuation of long-patch repair, post-mitotic neurons could be more heavily reliant on APTX-dependent repair pathways that other tissue types.

The findings in this study could also have implications for possible future clinical interventions. For example, the observation that the short-patch repair in AOA1 extracts is rescued *in vitro* with the addition of non-adenylated DNA ligase, may provide a possible route for clinical intervention. The three steps of DNA ligation are relatively separate reactions that can be independently disrupted with individual point mutations and a recent study presented data on three compounds, with different specificities for the three human DNA ligases, that selectively inhibited the last two steps of DNA ligation while leaving the ligase-adenylation reaction unaffected (Chen et al., 2008, Zhong et al., 2008). This raises the possibility that an inhibitor could be designed that selectively inhibits ligase re-adenylation but allows the ligation of an adenylated nick. It can be speculated that the use of such an inhibitor in AOA1 cells might increase the level of non-adenylated DNA ligase, transiently at least, and thereby cleanse the genome of accumulated adenylated nicks.

This is, however, at present entirely speculative and there are a number of issues to be addressed. The first is that, as mentioned previously, it has yet to be proved that that adenylated SSBs are a physiologically relevant lesion in living cells, and it cannot be ruled out that APTX can act on other DNA substrates (Takahashi et al., 2007a). Such an inhibitor would only work if the disease pathology in AOA1 was due to the accumulation of unrepaired adenylated SSBs, and not another type of lesion. Secondly, a limitation of any compound that is targeted to the brain is the existence of the blood-brain barrier that completely separates the brain from the bloodstream and prevents the transmission of most small molecules between the two (Alavijeh et al., 2005). Indeed, due to this and other complications inherent with targeting drugs to the brain, it takes significantly longer for a therapeutic drug targeted to the central nervous system to get to market compared to other drugs (Alavijeh et al., 2005). Another issue with this approach, and possibly the most significant issue for the patients suffering from this disorder, is that due to the low regenerative capacity of the brain, it would not be possible to reverse the neurodegeneration seen in AOA1. The most that can be hoped for is that regular treatments with a drug could halt the progression of the disease once it has been diagnosed.

While it is very unlikely that any pharmaceutical companies would invest the huge amount of time and money required for drug development in a drug specifically designed to treat AOA1, a very rare disorder when compared to the incidence of major diseases such as cancer, the potential use of DNA ligase inhibitors as novel chemotherapeutic agents has already been proposed. The success of PARP inhibitors in the treatment of BRCA1 and BRCA2 defective tumours has demonstrated the potency of inhibiting SSBR in homologous recombination defective cells and fuelled the search for novel chemotherapeutic drug targets (Farmer et al., 2005, Bryant et al., 2005, Guo et al., 2011). Indeed, along with DNA ligase inhibitors, PNK inhibitors have also been proposed as a strategy to increase the cytotoxicity of either radiotherapy or CPT treatment (Bernstein et al., 2008, Freschauf et al., 2010, Freschauf et al., 2009).

There are some important questions about APTX and the disease that need to be addressed. It is currently not clear whether the neuropathology of the disease is due to unrepaired SSBs or

DSBs. Although a role for APTX in DSBR has not been discussed in this study, APTX is found in a constitutive interaction with CK2 phosphorylated XRCC4 and thus could have a role in the processing of DNA ends during NHEJ (Clements et al., 2004). Although it has been proposed that an accumulation of unrepaired adenylated nicks in AOA1 neurones could lead to blocked transcription and eventual cell death, resulting in the pathology of the disease, it could also be the result of accumulating DSBs. However as was the case with the previously conflicting evidence for the existence of a chromosomal SSBR defect in AOA1 cells, a convincing DSBR defect has not been found in APTX-defective cells.

Another critical question is what are the affected cerebellar cell types in AOA1? Because the *Aptx*$^{-/-}$ mice do not exhibit neurodegeneration it has not been possible to pinpoint which neural populations are the affected. It has been shown that severe purkinje cell loss is associated with AOA1 (Sugawara et al., 2008). This could reflect a direct impact of unrepaired breaks on purkinje cell viability an indirect result of cell death in cells that maintain neuronal homeostasis, such as neuroglia cells.

Additionally AOA1 lacks any extra-neurological symptoms that are commonly associated with DNA repair defective disorders, in particular cancer predisposition. This is a feature with is shared by AOA1, SCAN1 (caused by mutations in *TDP1*) and MCSZ (caused by mutations in *PNK*) despite the different neuropathologies of AOA1 and SCAN1 compared to MCSZ. As mentioned earlier, one explanation for this is that cycling cells possess redundant DNA repair pathways that operate solely during S-phase or G2 that can deal with any unrepaired SSBs, such as the replication-coupled SSBR or HR (Caldecott, 2008, Caldecott, 2001, Caldecott, 2003b). It is likely that RC-SSBR would predominantly involve long-patch repair due to its association with the replication machinery, which as discussed earlier is a potential mechanism for repairing adenylated nicks in the absence of APTX. The nucleases involved in resection of DNA ends during HR, such as MRN, could also function as redundant mechanisms for the processing of SSBs with blocked 3' or 5' DNA ends in the absence of APTX, PNK or TDP1. Additionally, as HR is an error-free repair pathway, this would prevent the mis-repair of any persisting SSBs and DSBs by more error prone pathways, such as NHEJ, which has been implicated in carcinogenesis (Schlissel et al., 2006).

Finally, although the clinical presentations of AOA1 and SCAN1 are similar and probably have similar underlying causes, the neuropathology of MCSZ is very different. While both AOA1 and SCAN1 are neurodegenerative disorders that are associated with progressive degeneration and atrophy of the cerebellum after birth, MCSZ presents with severe microcephaly from birth, but exhibits no evidence of subsequent degeneration (Shen et al., 2010, Date et al., 2001, Moreira et al., 2001, Takashima et al., 2002). The underlying cause of microcephaly is a reduction in total brain volume caused by defects occurring during brain development (O'Driscoll and Jeggo, 2008). Therefore the different presentations potentially reflects that the loss of APTX and TDP1 primarily effect post-mitotic neurones while mutations in PNKP have a greater impact upon the developing brain.

The absence of microcephaly in AOA1 and SCAN1 could reflect the potential rarity of the DNA lesions that APTX and TDP1 repair. It is possible that these rare lesions would not accumulate in enough numbers to impact upon the neuronal progenitors in the VZ and SVZ of the developing brain, whereas PNKP substrates would be amongst the most commonly arising DNA lesions due to the highly metabolic status of the developing brain (Bayer et al., 1991, Barnes et al., 1998, Gao et al., 1998, Hoshino and Kameyama, 1988, Hoshino et al., 1991, Narasimhaiah et al., 2005).

References

ADACHI, N., SUZUKI, H., IIIZUMI, S. & KOYAMA, H. 2003. Hypersensitivity of nonhomologous DNA end-joining mutants to VP-16 and ICRF-193: implications for the repair of topoisomerase II-mediated DNA damage. *The Journal of biological chemistry,* 278**,** 35897-902.

AHEL, I., RASS, U., EL-KHAMISY, S. F., KATYAL, S., CLEMENTS, P. M., MCKINNON, P. J., CALDECOTT, K. W. & WEST, S. C. 2006. The neurodegenerative disease protein aprataxin resolves abortive DNA ligation intermediates. *Nature,* 443**,** 713-6.

AHNESORG, P., SMITH, P. & JACKSON, S. P. 2006. XLF interacts with the XRCC4-DNA ligase IV complex to promote DNA nonhomologous end-joining. *Cell,* 124**,** 301-13.

AICARDI, J., BARBOSA, C., ANDERMANN, E., ANDERMANN, F., MORCOS, R., GHANEM, Q., FUKUYAMA, Y., AWAYA, Y. & MOE, P. 1988. Ataxia-ocular motor apraxia: a syndrome mimicking ataxia-telangiectasia. *Ann Neurol,* 24**,** 497-502.

AKBARI, M. & KROKAN, H. E. 2008. Cytotoxicity and mutagenicity of endogenous DNA base lesions as potential cause of human aging. *Mech Ageing Dev,* 129**,** 353-65.

AL-ZOUGHOOL, M. & KREWSKI, D. 2009. Health effects of radon: a review of the literature. *International journal of radiation biology,* 85**,** 57-69.

ALAVIJEH, M. S., CHISHTY, M., QAISER, M. Z. & PALMER, A. M. 2005. Drug metabolism and pharmacokinetics, the blood-brain barrier, and central nervous system drug discovery. *NeuroRx : the journal of the American Society for Experimental NeuroTherapeutics,* 2**,** 554-71.

AMOURI, R., MOREIRA, M. C., ZOUARI, M., EL EUCH, G., BARHOUMI, C., KEFI, M., BELAL, S., KOENIG, M. & HENTATI, F. 2004. Aprataxin gene mutations in Tunisian families. *Neurology,* 63**,** 928-9.

ANHEIM, M., FLEURY, M., MONGA, B., LAUGEL, V., CHAIGNE, D., RODIER, G., GINGLINGER, E., BOULAY, C., COURTOIS, S., DROUOT, N., FRITSCH, M., DELAUNOY, J. P., STOPPA-LYONNET, D., TRANCHANT, C. & KOENIG, M. 2010. Epidemiological, clinical, paraclinical and molecular study of a cohort of 102 patients affected with autosomal recessive progressive cerebellar ataxia from Alsace, Eastern France: implications for clinical management. *Neurogenetics,* 11**,** 1-12.

ARAKI, M., MASUTANI, C., TAKEMURA, M., UCHIDA, A., SUGASAWA, K., KONDOH, J., OHKUMA, Y. & HANAOKA, F. 2001. Centrosome protein centrin 2/caltractin 1 is part of the xeroderma pigmentosum group C complex that initiates global genome nucleotide excision repair. *The Journal of biological chemistry,* 276**,** 18665-72.

ARAUJO, S. J., NIGG, E. A. & WOOD, R. D. 2001. Strong functional interactions of TFIIH with XPC and XPG in human DNA nucleotide excision repair, without a preassembled repairosome. *Molecular and cellular biology,* 21**,** 2281-91.

BABA, Y., UITTI, R. J., BOYLAN, K. B., UEHARA, Y., YAMADA, T., FARRER, M. J., COUCHON, E., BATISH, S. D. & WSZOLEK, Z. K. 2007. Aprataxin (APTX) gene mutations resembling multiple system atrophy. *Parkinsonism Relat Disord,* 13**,** 139-42.

BALAKRISHNAN, L., BRANDT, P. D., LINDSEY-BOLTZ, L. A., SANCAR, A. & BAMBARA, R. A. 2009. Long patch base excision repair proceeds via coordinated stimulation of the multienzyme DNA repair complex. *J Biol Chem,* 284**,** 15158-72.

BANERJEE, D., MANDAL, S. M., DAS, A., HEGDE, M. L., DAS, S., BHAKAT, K. K., BOLDOGH, I., SARKAR, P. S., MITRA, S. & HAZRA, T. K. 2011. Preferential repair of oxidized base damage in the transcribed genes of mammalian cells. *The Journal of biological chemistry,* 286**,** 6006-16.

BARBOT, C., COUTINHO, P., CHORAO, R., FERREIRA, C., BARROS, J., FINEZA, I., DIAS, K., MONTEIRO, J., GUIMARAES, A., MENDONCA, P., DO CEU MOREIRA, M. & SEQUEIROS,

J. 2001. Recessive ataxia with ocular apraxia: review of 22 Portuguese patients. *Arch Neurol,* 58**,** 201-5.

BARNES, D. E. & LINDAHL, T. 2004. Repair and genetic consequences of endogenous DNA base damage in mammalian cells. *Annu Rev Genet,* 38**,** 445-76.

BARNES, D. E., STAMP, G., ROSEWELL, I., DENZEL, A. & LINDAHL, T. 1998. Targeted disruption of the gene encoding DNA ligase IV leads to lethality in embryonic mice. *Current biology : CB,* 8**,** 1395-8.

BARNES, D. E., TOMKINSON, A. E., LEHMANN, A. R., WEBSTER, A. D. & LINDAHL, T. 1992. Mutations in the DNA ligase I gene of an individual with immunodeficiencies and cellular hypersensitivity to DNA-damaging agents. *Cell,* 69**,** 495-503.

BARROWS, L. R. & MAGEE, P. N. 1982. Nonenzymatic methylation of DNA by S-adenosylmethionine in vitro. *Carcinogenesis,* 3**,** 349-51.

BARZILAI, A. 2007. The contribution of the DNA damage response to neuronal viability. *Antioxidants & redox signaling,* 9**,** 211-8.

BAYER, S. A., ALTMAN, J., DAI, X. F. & HUMPHREYS, L. 1991. Planar differences in nuclear area and orientation in the subventricular and intermediate zones of the rat embryonic neocortex. *The Journal of comparative neurology,* 307**,** 487-98.

BEARD, W. A. & WILSON, S. H. 2000. Structural design of a eukaryotic DNA repair polymerase: DNA polymerase beta. *Mutat Res,* 460**,** 231-44.

BEBENEK, K., TISSIER, A., FRANK, E. G., MCDONALD, J. P., PRASAD, R., WILSON, S. H., WOODGATE, R. & KUNKEL, T. A. 2001. 5'-Deoxyribose phosphate lyase activity of human DNA polymerase iota in vitro. *Science,* 291**,** 2156-9.

BECKMAN, K. B. & AMES, B. N. 1997. Oxidative decay of DNA. *J Biol Chem,* 272**,** 19633-6.

BEKKER-JENSEN, S., RENDTLEW DANIELSEN, J., FUGGER, K., GROMOVA, I., NERSTEDT, A., LUKAS, C., BARTEK, J., LUKAS, J. & MAILAND, N. 2010. HERC2 coordinates ubiquitin-dependent assembly of DNA repair factors on damaged chromosomes. *Nature cell biology,* 12**,** 80-6; sup pp 1-12.

BENDIXEN, C., THOMSEN, B., ALSNER, J. & WESTERGAARD, O. 1990. Camptothecin-stabilized topoisomerase I-DNA adducts cause premature termination of transcription. *Biochemistry,* 29**,** 5613-9.

BENJAMIN, R. C. & GILL, D. M. 1980. Poly(ADP-ribose) synthesis in vitro programmed by damaged DNA. A comparison of DNA molecules containing different types of strand breaks. *J Biol Chem,* 255**,** 10502-8.

BERNSTEIN, N. K., KARIMI-BUSHERI, F., RASOULI-NIA, A., MANI, R., DIANOV, G., GLOVER, J. N. & WEINFELD, M. 2008. Polynucleotide kinase as a potential target for enhancing cytotoxicity by ionizing radiation and topoisomerase I inhibitors. *Anti-cancer agents in medicinal chemistry,* 8**,** 358-67.

BERNSTEIN, N. K., WILLIAMS, R. S., RAKOVSZKY, M. L., CUI, D., GREEN, R., KARIMI-BUSHERI, F., MANI, R. S., GALICIA, S., KOCH, C. A., CASS, C. E., DUROCHER, D., WEINFELD, M. & GLOVER, J. N. 2005a. The molecular architecture of the mammalian DNA repair enzyme, polynucleotide kinase. *Molecular cell,* 17**,** 657-70.

BERNSTEIN, N. K., WILLIAMS, R. S., RAKOVSZKY, M. L., CUI, D., GREEN, R., KARIMI-BUSHERI, F., MANI, R. S., GALICIA, S., KOCH, C. A., CASS, C. E., DUROCHER, D., WEINFELD, M. & GLOVER, J. N. 2005b. The molecular architecture of the mammalian DNA repair enzyme, polynucleotide kinase. *Mol Cell,* 17**,** 657-70.

BESPALOV, I. A., BOND, J. P., PURMAL, A. A., WALLACE, S. S. & MELAMEDE, R. J. 1999. Fabs specific for 8-oxoguanine: control of DNA binding. *Journal of molecular biology,* 293**,** 1085-95.

BIEGANOWSKI, P., GARRISON, P. N., HODAWADEKAR, S. C., FAYE, G., BARNES, L. D. & BRENNER, C. 2002a. Adenosine monophosphoramidase activity of Hint and Hnt1 supports function of Kin28, Ccl1, and Tfb3. *J Biol Chem,* 277**,** 10852-60.

BIEGANOWSKI, P., GARRISON, P. N., HODAWADEKAR, S. C., FAYE, G., BARNES, L. D. & BRENNER, C. 2002b. Adenosine monophosphoramidase activity of Hint and Hnt1 supports function of Kin28, Ccl1, and Tfb3. *The Journal of biological chemistry,* 277**,** 10852-60.

BISSETT, R. J. & MCLAUGHLIN, J. R. 2010. Radon. *Chronic diseases in Canada,* 29 Suppl 1**,** 38-50.

BJELLAND, S. & SEEBERG, E. 2003. Mutagenicity, toxicity and repair of DNA base damage induced by oxidation. *Mutat Res,* 531**,** 37-80.

BODER, E. & SEDGWICK, R. P. 1958. Ataxia-telangiectasia; a familial syndrome of progressive cerebellar ataxia, oculocutaneous telangiectasia and frequent pulmonary infection. *Pediatrics,* 21**,** 526-54.

BOHGAKI, T., BOHGAKI, M., CARDOSO, R., PANIER, S., ZEEGERS, D., LI, L., STEWART, G. S., SANCHEZ, O., HANDE, M. P., DUROCHER, D., HAKEM, A. & HAKEM, R. 2011. Genomic instability, defective spermatogenesis, immunodeficiency, and cancer in a mouse model of the RIDDLE syndrome. *PLoS genetics,* 7**,** e1001381.

BRAITHWAITE, E. K., KEDAR, P. S., LAN, L., POLOSINA, Y. Y., ASAGOSHI, K., POLTORATSKY, V. P., HORTON, J. K., MILLER, H., TEEBOR, G. W., YASUI, A. & WILSON, S. H. 2005a. DNA polymerase lambda protects mouse fibroblasts against oxidative DNA damage and is recruited to sites of DNA damage/repair. *J Biol Chem,* 280**,** 31641-7.

BRAITHWAITE, E. K., KEDAR, P. S., STUMPO, D. J., BERTOCCI, B., FREEDMAN, J. H., SAMSON, L. D. & WILSON, S. H. 2010. DNA polymerases beta and lambda mediate overlapping and independent roles in base excision repair in mouse embryonic fibroblasts. *PLoS One,* 5**,** e12229.

BRAITHWAITE, E. K., PRASAD, R., SHOCK, D. D., HOU, E. W., BEARD, W. A. & WILSON, S. H. 2005b. DNA polymerase lambda mediates a back-up base excision repair activity in extracts of mouse embryonic fibroblasts. *J Biol Chem,* 280**,** 18469-75.

BRAMSON, J., PREVOST, J., MALAPETSA, A., NOE, A. J., POIRIER, G. G., DESNOYERS, S., ALAOUI-JAMALI, M. & PANASCI, L. 1993. Poly(ADP-ribose) polymerase can bind melphalan damaged DNA. *Cancer Res,* 53**,** 5370-3.

BRENNER, C. 2002. Hint, Fhit, and GalT: function, structure, evolution, and mechanism of three branches of the histidine triad superfamily of nucleotide hydrolases and transferases. *Biochemistry,* 41**,** 9003-14.

BRENNER, C., BIEGANOWSKI, P., PACE, H. C. & HUEBNER, K. 1999. The histidine triad superfamily of nucleotide-binding proteins. *Journal of cellular physiology,* 181**,** 179-87.

BRESLIN, C. & CALDECOTT, K. W. 2009. DNA 3'-phosphatase activity is critical for rapid global rates of single-strand break repair following oxidative stress. *Mol Cell Biol,* 29**,** 4653-62.

BROOKMAN, K. W., TEBBS, R. S., ALLEN, S. A., TUCKER, J. D., SWIGER, R. R., LAMERDIN, J. E., CARRANO, A. V. & THOMPSON, L. H. 1994. Isolation and characterization of mouse Xrcc-1, a DNA repair gene affecting ligation. *Genomics,* 22**,** 180-8.

BROWN, J. A., PACK, L. R., SANMAN, L. E. & SUO, Z. 2011. Efficiency and fidelity of human DNA polymerases lambda and beta during gap-filling DNA synthesis. *DNA Repair (Amst),* 10**,** 24-33.

BRYANT, H. E., SCHULTZ, N., THOMAS, H. D., PARKER, K. M., FLOWER, D., LOPEZ, E., KYLE, S., MEUTH, M., CURTIN, N. J. & HELLEDAY, T. 2005. Specific killing of BRCA2-deficient tumours with inhibitors of poly(ADP-ribose) polymerase. *Nature,* 434**,** 913-7.

BUCK, D., MALIVERT, L., DE CHASSEVAL, R., BARRAUD, A., FONDANECHE, M. C., SANAL, O., PLEBANI, A., STEPHAN, J. L., HUFNAGEL, M., LE DEIST, F., FISCHER, A., DURANDY, A., DE

VILLARTAY, J. P. & REVY, P. 2006a. Cernunnos, a novel nonhomologous end-joining factor, is mutated in human immunodeficiency with microcephaly. *Cell,* 124**,** 287-99.

BUCK, D., MOSHOUS, D., DE CHASSEVAL, R., MA, Y., LE DEIST, F., CAVAZZANA-CALVO, M., FISCHER, A., CASANOVA, J. L., LIEBER, M. R. & DE VILLARTAY, J. P. 2006b. Severe combined immunodeficiency and microcephaly in siblings with hypomorphic mutations in DNA ligase IV. *European journal of immunology,* 36**,** 224-35.

BURMA, S., CHEN, B. P., MURPHY, M., KURIMASA, A. & CHEN, D. J. 2001. ATM phosphorylates histone H2AX in response to DNA double-strand breaks. *The Journal of biological chemistry,* 276**,** 42462-7.

BYRNES, J. J. 1984. Structural and functional properties of DNA polymerase delta from rabbit bone marrow. *Mol Cell Biochem,* 62**,** 13-24.

CADET, J., DOUKI, T., GASPARUTTO, D. & RAVANAT, J. L. 2003. Oxidative damage to DNA: formation, measurement and biochemical features. *Mutat Res,* 531**,** 5-23.

CADET, J., SAGE, E. & DOUKI, T. 2005a. Ultraviolet radiation-mediated damage to cellular DNA. *Mutation research,* 571**,** 3-17.

CADET, J., SAGE, E. & DOUKI, T. 2005b. Ultraviolet radiation-mediated damage to cellular DNA. *Mutat Res,* 571**,** 3-17.

CALDECOTT, K. W. 2001. Mammalian DNA single-strand break repair: an X-ra(y)ted affair. *Bioessays,* 23**,** 447-55.

CALDECOTT, K. W. 2003a. Protein-protein interactions during mammalian DNA single-strand break repair. *Biochem Soc Trans,* 31**,** 247-51.

CALDECOTT, K. W. 2003b. XRCC1 and DNA strand break repair. *DNA Repair (Amst),* 2**,** 955-69.

CALDECOTT, K. W. 2008. Single-strand break repair and genetic disease. *Nat Rev Genet,* 9**,** 619-31.

CALDECOTT, K. W., AOUFOUCHI, S., JOHNSON, P. & SHALL, S. 1996. XRCC1 polypeptide interacts with DNA polymerase beta and possibly poly (ADP-ribose) polymerase, and DNA ligase III is a novel molecular 'nick-sensor' in vitro. *Nucleic Acids Res,* 24**,** 4387-94.

CALDECOTT, K. W., MCKEOWN, C. K., TUCKER, J. D., LJUNGQUIST, S. & THOMPSON, L. H. 1994. An interaction between the mammalian DNA repair protein XRCC1 and DNA ligase III. *Mol Cell Biol,* 14**,** 68-76.

CALDECOTT, K. W., TUCKER, J. D., STANKER, L. H. & THOMPSON, L. H. 1995. Characterization of the XRCC1-DNA ligase III complex in vitro and its absence from mutant hamster cells. *Nucleic Acids Res,* 23**,** 4836-43.

CAM, H., BALCIUNAITE, E., BLAIS, A., SPEKTOR, A., SCARPULLA, R. C., YOUNG, R., KLUGER, Y. & DYNLACHT, B. D. 2004. A common set of gene regulatory networks links metabolism and growth inhibition. *Mol Cell,* 16**,** 399-411.

CAMPALANS, A., MARSIN, S., NAKABEPPU, Y., O'CONNOR T, R., BOITEUX, S. & RADICELLA, J. P. 2005. XRCC1 interactions with multiple DNA glycosylases: a model for its recruitment to base excision repair. *DNA Repair (Amst),* 4**,** 826-35.

CAPPELLI, E., TAYLOR, R., CEVASCO, M., ABBONDANDOLO, A., CALDECOTT, K. & FROSINA, G. 1997. Involvement of XRCC1 and DNA ligase III gene products in DNA base excision repair. *J Biol Chem,* 272**,** 23970-5.

CARMICHAEL, J. & WOODS, C. 2006. Genetic defects of human brain development. *Current neurology and neuroscience reports,* 6**,** 437-46.

CEJKA, P., CANNAVO, E., POLACZEK, P., MASUDA-SASA, T., POKHAREL, S., CAMPBELL, J. L. & KOWALCZYKOWSKI, S. C. 2010. DNA end resection by Dna2-Sgs1-RPA and its stimulation by Top3-Rmi1 and Mre11-Rad50-Xrs2. *Nature,* 467**,** 112-6.

CELESTE, A., PETERSEN, S., ROMANIENKO, P. J., FERNANDEZ-CAPETILLO, O., CHEN, H. T., SEDELNIKOVA, O. A., REINA-SAN-MARTIN, B., COPPOLA, V., MEFFRE, E.,

DIFILIPPANTONIO, M. J., REDON, C., PILCH, D. R., OLARU, A., ECKHAUS, M., CAMERINI-OTERO, R. D., TESSAROLLO, L., LIVAK, F., MANOVA, K., BONNER, W. M., NUSSENZWEIG, M. C. & NUSSENZWEIG, A. 2002. Genomic instability in mice lacking histone H2AX. *Science,* 296**,** 922-7.

CHAN, W. Y., LORKE, D. E., TIU, S. C. & YEW, D. T. 2002. Proliferation and apoptosis in the developing human neocortex. *The Anatomical record,* 267**,** 261-76.

CHAPPELL, C., HANAKAHI, L. A., KARIMI-BUSHERI, F., WEINFELD, M. & WEST, S. C. 2002. Involvement of human polynucleotide kinase in double-strand break repair by non-homologous end joining. *The EMBO journal,* 21**,** 2827-32.

CHEN, D. S., HERMAN, T. & DEMPLE, B. 1991. Two distinct human DNA diesterases that hydrolyze 3'-blocking deoxyribose fragments from oxidized DNA. *Nucleic Acids Res,* 19**,** 5907-14.

CHEN, X., ZHONG, S., ZHU, X., DZIEGIELEWSKA, B., ELLENBERGER, T., WILSON, G. M., MACKERELL, A. D., JR. & TOMKINSON, A. E. 2008. Rational design of human DNA ligase inhibitors that target cellular DNA replication and repair. *Cancer research,* 68**,** 3169-77.

CHEN, X. B., MELCHIONNA, R., DENIS, C. M., GAILLARD, P. H., BLASINA, A., VAN DE WEYER, I., BODDY, M. N., RUSSELL, P., VIALARD, J. & MCGOWAN, C. H. 2001. Human Mus81-associated endonuclease cleaves Holliday junctions in vitro. *Molecular cell,* 8**,** 1117-27.

CHUN, H. H. & GATTI, R. A. 2004. Ataxia-telangiectasia, an evolving phenotype. *DNA repair,* 3**,** 1187-96.

CLEMENTS, P. M., BRESLIN, C., DEEKS, E. D., BYRD, P. J., JU, L., BIEGANOWSKI, P., BRENNER, C., MOREIRA, M. C., TAYLOR, A. M. & CALDECOTT, K. W. 2004. The ataxia-oculomotor apraxia 1 gene product has a role distinct from ATM and interacts with the DNA strand break repair proteins XRCC1 and XRCC4. *DNA Repair (Amst),* 3**,** 1493-502.

COLEMAN, K. A. & GREENBERG, R. A. 2011. The BRCA1-RAP80 complex regulates DNA repair mechanism utilization by restricting end resection. *The Journal of biological chemistry,* 286**,** 13669-80.

COLLER, H. A., SANG, L. & ROBERTS, J. M. 2006. A new description of cellular quiescence. *PLoS Biol,* 4**,** e83.

COOKE, M. S., EVANS, M. D., DIZDAROGLU, M. & LUNEC, J. 2003. Oxidative DNA damage: mechanisms, mutation, and disease. *FASEB J,* 17**,** 1195-214.

CORTES LEDESMA, F., EL KHAMISY, S. F., ZUMA, M. C., OSBORN, K. & CALDECOTT, K. W. 2009. A human 5'-tyrosyl DNA phosphodiesterase that repairs topoisomerase-mediated DNA damage. *Nature,* 461**,** 674-8.

CORTES, U., TONG, W. M., COYLE, D. L., MEYER-FICCA, M. L., MEYER, R. G., PETRILLI, V., HERCEG, Z., JACOBSON, E. L., JACOBSON, M. K. & WANG, Z. Q. 2004. Depletion of the 110-kilodalton isoform of poly(ADP-ribose) glycohydrolase increases sensitivity to genotoxic and endotoxic stress in mice. *Mol Cell Biol,* 24**,** 7163-78.

COSTANTINI, S., WOODBINE, L., ANDREOLI, L., JEGGO, P. A. & VINDIGNI, A. 2007. Interaction of the Ku heterodimer with the DNA ligase IV/Xrcc4 complex and its regulation by DNA-PK. *DNA repair,* 6**,** 712-22.

COTNER-GOHARA, E., KIM, I. K., TOMKINSON, A. E. & ELLENBERGER, T. 2008. Two DNA-binding and nick recognition modules in human DNA ligase III. *J Biol Chem,* 283**,** 10764-72.

COVERLEY, D., KENNY, M. K., LANE, D. P. & WOOD, R. D. 1992. A role for the human single-stranded DNA binding protein HSSB/RPA in an early stage of nucleotide excision repair. *Nucleic acids research,* 20**,** 3873-80.

CRISCUOLO, C., MANCINI, P., MENCHISE, V., SACCA, F., DE MICHELE, G., BANFI, S. & FILLA, A. 2005. Very late onset in ataxia oculomotor apraxia type I. *Ann Neurol,* 57**,** 777.

CRISCUOLO, C., MANCINI, P., SACCA, F., DE MICHELE, G., MONTICELLI, A., SANTORO, L., SCARANO, V., BANFI, S. & FILLA, A. 2004. Ataxia with oculomotor apraxia type 1 in Southern Italy: late onset and variable phenotype. *Neurology,* 63**,** 2173-5.

CRITCHLOW, S. E., BOWATER, R. P. & JACKSON, S. P. 1997. Mammalian DNA double-strand break repair protein XRCC4 interacts with DNA ligase IV. *Current biology : CB,* 7**,** 588-98.

CRUT, A., NAIR, P. A., KOSTER, D. A., SHUMAN, S. & DEKKER, N. H. 2008. Dynamics of phosphodiester synthesis by DNA ligase. *Proc Natl Acad Sci U S A,* 105**,** 6894-9.

D'AMOURS, D., DESNOYERS, S., D'SILVA, I. & POIRIER, G. G. 1999. Poly(ADP-ribosyl)ation reactions in the regulation of nuclear functions. *Biochem J,* 342 (Pt 2)**,** 249-68.

D'ARRIGO, S., RIVA, D., BULGHERONI, S., CHIAPPARINI, L., CASTELLOTTI, B., GELLERA, C. & PANTALEONI, C. 2008. Ataxia with oculomotor apraxia type 1 (AOA1): clinical and neuropsychological features in 2 new patients and differential diagnosis. *J Child Neurol,* 23**,** 895-900.

DALEY, J. M., WILSON, T. E. & RAMOTAR, D. 2010. Genetic interactions between HNT3/Aprataxin and RAD27/FEN1 suggest parallel pathways for 5' end processing during base excision repair. *DNA Repair (Amst),* 9**,** 690-9.

DAS, A., WIEDERHOLD, L., LEPPARD, J. B., KEDAR, P., PRASAD, R., WANG, H., BOLDOGH, I., KARIMI-BUSHERI, F., WEINFELD, M., TOMKINSON, A. E., WILSON, S. H., MITRA, S. & HAZRA, T. K. 2006. NEIL2-initiated, APE-independent repair of oxidized bases in DNA: Evidence for a repair complex in human cells. *DNA Repair (Amst),* 5**,** 1439-48.

DATE, H., IGARASHI, S., SANO, Y., TAKAHASHI, T., TAKANO, H., TSUJI, S., NISHIZAWA, M. & ONODERA, O. 2004. The FHA domain of aprataxin interacts with the C-terminal region of XRCC1. *Biochem Biophys Res Commun,* 325**,** 1279-85.

DATE, H., ONODERA, O., TANAKA, H., IWABUCHI, K., UEKAWA, K., IGARASHI, S., KOIKE, R., HIROI, T., YUASA, T., AWAYA, Y., SAKAI, T., TAKAHASHI, T., NAGATOMO, H., SEKIJIMA, Y., KAWACHI, I., TAKIYAMA, Y., NISHIZAWA, M., FUKUHARA, N., SAITO, K., SUGANO, S. & TSUJI, S. 2001. Early-onset ataxia with ocular motor apraxia and hypoalbuminemia is caused by mutations in a new HIT superfamily gene. *Nat Genet,* 29**,** 184-8.

DEANS, A. J. & WEST, S. C. 2011. DNA interstrand crosslink repair and cancer. *Nature reviews. Cancer,* 11**,** 467-80.

DECKBAR, D., BIRRAUX, J., KREMPLER, A., TCHOUANDONG, L., BEUCHER, A., WALKER, S., STIFF, T., JEGGO, P. & LOBRICH, M. 2007. Chromosome breakage after G2 checkpoint release. *J Cell Biol,* 176**,** 749-55.

DEFAZIO, L. G., STANSEL, R. M., GRIFFITH, J. D. & CHU, G. 2002. Synapsis of DNA ends by DNA-dependent protein kinase. *The EMBO journal,* 21**,** 3192-200.

DELACOTE, F. & LOPEZ, B. S. 2008. Importance of the cell cycle phase for the choice of the appropriate DSB repair pathway, for genome stability maintenance: the trans-S double-strand break repair model. *Cell cycle,* 7**,** 33-8.

DEMPLE, B. & DEMOTT, M. S. 2002. Dynamics and diversions in base excision DNA repair of oxidized abasic lesions. *Oncogene,* 21**,** 8926-34.

DEMPLE, B. & HARRISON, L. 1994. Repair of oxidative damage to DNA: enzymology and biology. *Annu Rev Biochem,* 63**,** 915-48.

DEMPLE, B., HERMAN, T. & CHEN, D. S. 1991. Cloning and expression of APE, the cDNA encoding the major human apurinic endonuclease: definition of a family of DNA repair enzymes. *Proc Natl Acad Sci U S A,* 88**,** 11450-4.

DIANOV, G., PRICE, A. & LINDAHL, T. 1992. Generation of single-nucleotide repair patches following excision of uracil residues from DNA. *Mol Cell Biol,* 12**,** 1605-12.

DIANOV, G. L., PRASAD, R., WILSON, S. H. & BOHR, V. A. 1999. Role of DNA polymerase beta in the excision step of long patch mammalian base excision repair. *J Biol Chem,* 274**,** 13741-3.

DIANOV, G. L., SOUZA-PINTO, N., NYAGA, S. G., THYBO, T., STEVNSNER, T. & BOHR, V. A. 2001. Base excision repair in nuclear and mitochondrial DNA. *Prog Nucleic Acid Res Mol Biol,* 68**,** 285-97.

DIANOVA, II, SLEETH, K. M., ALLINSON, S. L., PARSONS, J. L., BRESLIN, C., CALDECOTT, K. W. & DIANOV, G. L. 2004. XRCC1-DNA polymerase beta interaction is required for efficient base excision repair. *Nucleic Acids Res,* 32**,** 2550-5.

DIGIUSEPPE, J. A. & DRESLER, S. L. 1989. Bleomycin-induced DNA repair synthesis in permeable human fibroblasts: mediation of long-patch and short-patch repair by distinct DNA polymerases. *Biochemistry,* 28**,** 9515-20.

DOBSON, C. J. & ALLINSON, S. L. 2006. The phosphatase activity of mammalian polynucleotide kinase takes precedence over its kinase activity in repair of single strand breaks. *Nucleic Acids Res,* 34**,** 2230-7.

DOGLIOTTI, E., FORTINI, P., PASCUCCI, B. & PARLANTI, E. 2001. The mechanism of switching among multiple BER pathways. *Prog Nucleic Acid Res Mol Biol,* 68**,** 3-27.

DOIL, C., MAILAND, N., BEKKER-JENSEN, S., MENARD, P., LARSEN, D. H., PEPPERKOK, R., ELLENBERG, J., PANIER, S., DUROCHER, D., BARTEK, J., LUKAS, J. & LUKAS, C. 2009. RNF168 binds and amplifies ubiquitin conjugates on damaged chromosomes to allow accumulation of repair proteins. *Cell,* 136**,** 435-46.

DOUKI, T. & CADET, J. 2001. Individual determination of the yield of the main UV-induced dimeric pyrimidine photoproducts in DNA suggests a high mutagenicity of CC photolesions. *Biochemistry,* 40**,** 2495-501.

DRAPKIN, R., REARDON, J. T., ANSARI, A., HUANG, J. C., ZAWEL, L., AHN, K., SANCAR, A. & REINBERG, D. 1994. Dual role of TFIIH in DNA excision repair and in transcription by RNA polymerase II. *Nature,* 368**,** 769-72.

DRESLER, S. L. & LIEBERMAN, M. W. 1983a. DNA polymerase function in repair synthesis in human fibroblasts. *Princess Takamatsu Symp,* 13**,** 253-65.

DRESLER, S. L. & LIEBERMAN, M. W. 1983b. Identification of DNA polymerases involved in DNA excision repair in diploid human fibroblasts. *J Biol Chem,* 258**,** 9990-4.

DUDLEY, D. D., CHAUDHURI, J., BASSING, C. H. & ALT, F. W. 2005. Mechanism and control of V(D)J recombination versus class switch recombination: similarities and differences. *Advances in immunology,* 86**,** 43-112.

DULIC, A., BATES, P. A., ZHANG, X., MARTIN, S. R., FREEMONT, P. S., LINDAHL, T. & BARNES, D. E. 2001. BRCT domain interactions in the heterodimeric DNA repair protein XRCC1-DNA ligase III. *Biochemistry,* 40**,** 5906-13.

DUQUETTE, A., RODDIER, K., MCNABB-BALTAR, J., GOSSELIN, I., ST-DENIS, A., DICAIRE, M. J., LOISEL, L., LABUDA, D., MARCHAND, L., MATHIEU, J., BOUCHARD, J. P. & BRAIS, B. 2005. Mutations in senataxin responsible for Quebec cluster of ataxia with neuropathy. *Ann Neurol,* 57**,** 408-14.

DURKACZ, B. W., OMIDIJI, O., GRAY, D. A. & SHALL, S. 1980. (ADP-ribose)n participates in DNA excision repair. *Nature,* 283**,** 593-6.

EL-KHAMISY, S. F. & CALDECOTT, K. W. 2006. TDP1-dependent DNA single-strand break repair and neurodegeneration. *Mutagenesis,* 21**,** 219-24.

EL-KHAMISY, S. F., HARTSUIKER, E. & CALDECOTT, K. W. 2007. TDP1 facilitates repair of ionizing radiation-induced DNA single-strand breaks. *DNA Repair (Amst),* 6**,** 1485-95.

EL-KHAMISY, S. F., KATYAL, S., PATEL, P., JU, L., MCKINNON, P. J. & CALDECOTT, K. W. 2009. Synergistic decrease of DNA single-strand break repair rates in mouse neural cells lacking both Tdp1 and aprataxin. *DNA Repair (Amst),* 8**,** 760-6.

EL-KHAMISY, S. F., MASUTANI, M., SUZUKI, H. & CALDECOTT, K. W. 2003. A requirement for PARP-1 for the assembly or stability of XRCC1 nuclear foci at sites of oxidative DNA damage. *Nucleic Acids Res,* 31**,** 5526-33.

EL-KHAMISY, S. F., SAIFI, G. M., WEINFELD, M., JOHANSSON, F., HELLEDAY, T., LUPSKI, J. R. & CALDECOTT, K. W. 2005. Defective DNA single-strand break repair in spinocerebellar ataxia with axonal neuropathy-1. *Nature,* 434**,** 108-13.

ELLENBERGER, T. & TOMKINSON, A. E. 2008a. Eukaryotic DNA ligases: structural and functional insights. *Annu Rev Biochem,* 77**,** 313-38.

ELLENBERGER, T. & TOMKINSON, A. E. 2008b. Eukaryotic DNA ligases: structural and functional insights. *Annual review of biochemistry,* 77**,** 313-38.

EVANS, M. D., GRIFFITHS, H. R., LUNEC, J. 1997. Reactive oxygen species and their cytotoxic mechanisms. *In:* CHIPMAN, J. K. (ed.) *Mechanisms of Cell Toxicity.* London: JAI Press Inc.

FAN, J., OTTERLEI, M., WONG, H. K., TOMKINSON, A. E. & WILSON, D. M., 3RD 2004. XRCC1 co-localizes and physically interacts with PCNA. *Nucleic Acids Res,* 32**,** 2193-201.

FARMER, H., MCCABE, N., LORD, C. J., TUTT, A. N., JOHNSON, D. A., RICHARDSON, T. B., SANTAROSA, M., DILLON, K. J., HICKSON, I., KNIGHTS, C., MARTIN, N. M., JACKSON, S. P., SMITH, G. C. & ASHWORTH, A. 2005. Targeting the DNA repair defect in BRCA mutant cells as a therapeutic strategy. *Nature,* 434**,** 917-21.

FERRARINI, M., SQUINTANI, G., CAVALLARO, T., FERRARI, S., RIZZUTO, N. & FABRIZI, G. M. 2007. A novel mutation of aprataxin associated with ataxia ocular apraxia type 1: phenotypical and genotypical characterization. *J Neurol Sci,* 260**,** 219-24.

FERRO, A. M. & OLIVERA, B. M. 1982. Poly(ADP-ribosylation) in vitro. Reaction parameters and enzyme mechanism. *J Biol Chem,* 257**,** 7808-13.

FISHER, A. E., HOCHEGGER, H., TAKEDA, S. & CALDECOTT, K. W. 2007. Poly(ADP-ribose) polymerase 1 accelerates single-strand break repair in concert with poly(ADP-ribose) glycohydrolase. *Mol Cell Biol,* 27**,** 5597-605.

FLANGAS, A. L. & BOWMAN, R. E. 1970. Differential metabolism of RNA in neuronal-enriched and glial-enriched fractions of rat cerebrum. *J Neurochem,* 17**,** 1237-45.

FORTINI, P., PARLANTI, E., SIDORKINA, O. M., LAVAL, J. & DOGLIOTTI, E. 1999. The type of DNA glycosylase determines the base excision repair pathway in mammalian cells. *J Biol Chem,* 274**,** 15230-6.

FORTINI, P., PASCUCCI, B., PARLANTI, E., SOBOL, R. W., WILSON, S. H. & DOGLIOTTI, E. 1998. Different DNA polymerases are involved in the short- and long-patch base excision repair in mammalian cells. *Biochemistry,* 37**,** 3575-80.

FRESCHAUF, G. K., KARIMI-BUSHERI, F., ULACZYK-LESANKO, A., MERENIUK, T. R., AHRENS, A., KOSHY, J. M., RASOULI-NIA, A., PASARJ, P., HOLMES, C. F., RININSLAND, F., HALL, D. G. & WEINFELD, M. 2009. Identification of a small molecule inhibitor of the human DNA repair enzyme polynucleotide kinase/phosphatase. *Cancer research,* 69**,** 7739-46.

FRESCHAUF, G. K., MANI, R. S., MERENIUK, T. R., FANTA, M., VIRGEN, C. A., DIANOV, G. L., GRASSOT, J. M., HALL, D. G. & WEINFELD, M. 2010. Mechanism of action of an imidopiperidine inhibitor of human polynucleotide kinase/phosphatase. *The Journal of biological chemistry,* 285**,** 2351-60.

FRIEDBERG EC, WALKER GC, SIEDE W, WOOD RD, SCHULTZ RA & T., E. 2006. *DNA Repair and Mutagenesis,* Washington, DC, ASM Press.

FRIEDBERG, E. C., WALKER, G. C., SIEDE, W., WOOD, R. D., SCHULTZ, R. A. & ELLENBERGER, T. 2006. *DNA Repair and Mutagenesis, 2nd Edition,* Washington, ASM Press.

FROSINA, G., FORTINI, P., ROSSI, O., CARROZZINO, F., RASPAGLIO, G., COX, L. S., LANE, D. P., ABBONDANDOLO, A. & DOGLIOTTI, E. 1996. Two pathways for base excision repair in mammalian cells. *J Biol Chem,* 271**,** 9573-8.

GAO, Y., KATYAL, S., LEE, Y., ZHAO, J., REHG, J. E., RUSSELL, H. R. & MCKINNON, P. J. 2011. DNA ligase III is critical for mtDNA integrity but not Xrcc1-mediated nuclear DNA repair. *Nature,* 471**,** 240-4.

GAO, Y., SUN, Y., FRANK, K. M., DIKKES, P., FUJIWARA, Y., SEIDL, K. J., SEKIGUCHI, J. M., RATHBUN, G. A., SWAT, W., WANG, J., BRONSON, R. T., MALYNN, B. A., BRYANS, M., ZHU, C., CHAUDHURI, J., DAVIDSON, L., FERRINI, R., STAMATO, T., ORKIN, S. H., GREENBERG, M. E. & ALT, F. W. 1998. A critical role for DNA end-joining proteins in both lymphogenesis and neurogenesis. *Cell,* 95**,** 891-902.

GARCIA-DIAZ, M., BEBENEK, K., KUNKEL, T. A. & BLANCO, L. 2001. Identification of an intrinsic 5'-deoxyribose-5-phosphate lyase activity in human DNA polymerase lambda: a possible role in base excision repair. *J Biol Chem,* 276**,** 34659-63.

GARCIA-DIAZ, M., BEBENEK, K., SABARIEGOS, R., DOMINGUEZ, O., RODRIGUEZ, J., KIRCHHOFF, T., GARCIA-PALOMERO, E., PICHER, A. J., JUAREZ, R., RUIZ, J. F., KUNKEL, T. A. & BLANCO, L. 2002. DNA polymerase lambda, a novel DNA repair enzyme in human cells. *J Biol Chem,* 277**,** 13184-91.

GARCIA-DIAZ, M., DOMINGUEZ, O., LOPEZ-FERNANDEZ, L. A., DE LERA, L. T., SANIGER, M. L., RUIZ, J. F., PARRAGA, M., GARCIA-ORTIZ, M. J., KIRCHHOFF, T., DEL MAZO, J., BERNAD, A. & BLANCO, L. 2000. DNA polymerase lambda (Pol lambda), a novel eukaryotic DNA polymerase with a potential role in meiosis. *J Mol Biol,* 301**,** 851-67.

GASCON, G. G., ABDO, N., SIGUT, D., HEMIDAN, A. & HANNAN, M. A. 1995. Ataxia-oculomotor apraxia syndrome. *J Child Neurol,* 10**,** 118-22.

GATZ, S. A., JU, L., GRUBER, R., HOFFMANN, E., CARR, A. M., WANG, Z. Q., LIU, C. & JEGGO, P. A. 2011. Requirement for DNA ligase IV during embryonic neuronal development. *The Journal of neuroscience : the official journal of the Society for Neuroscience,* 31**,** 10088-100.

GENSCHEL, J., BAZEMORE, L. R. & MODRICH, P. 2002. Human exonuclease I is required for 5' and 3' mismatch repair. *The Journal of biological chemistry,* 277**,** 13302-11.

GILLET, L. C. & SCHARER, O. D. 2006. Molecular mechanisms of mammalian global genome nucleotide excision repair. *Chemical reviews,* 106**,** 253-76.

GODON, C., CORDELIERES, F. P., BIARD, D., GIOCANTI, N., MEGNIN-CHANET, F., HALL, J. & FAVAUDON, V. 2008. PARP inhibition versus PARP-1 silencing: different outcomes in terms of single-strand break repair and radiation susceptibility. *Nucleic Acids Res,* 36**,** 4454-64.

GRAWUNDER, U., WILM, M., WU, X., KULESZA, P., WILSON, T. E., MANN, M. & LIEBER, M. R. 1997. Activity of DNA ligase IV stimulated by complex formation with XRCC4 protein in mammalian cells. *Nature,* 388**,** 492-5.

GRAWUNDER, U., ZIMMER, D., FUGMANN, S., SCHWARZ, K. & LIEBER, M. R. 1998a. DNA ligase IV is essential for V(D)J recombination and DNA double-strand break repair in human precursor lymphocytes. *Molecular cell,* 2**,** 477-84.

GRAWUNDER, U., ZIMMER, D. & LEIBER, M. R. 1998b. DNA ligase IV binds to XRCC4 via a motif located between rather than within its BRCT domains. *Current biology : CB,* 8**,** 873-6.

GU, J., LU, H., TSAI, A. G., SCHWARZ, K. & LIEBER, M. R. 2007. Single-stranded DNA ligation and XLF-stimulated incompatible DNA end ligation by the XRCC4-DNA ligase IV complex: influence of terminal DNA sequence. *Nucleic acids research,* 35**,** 5755-62.

GU, Y., JIN, S., GAO, Y., WEAVER, D. T. & ALT, F. W. 1997. Ku70-deficient embryonic stem cells have increased ionizing radiosensitivity, defective DNA end-binding activity, and inability to support V(D)J recombination. *Proceedings of the National Academy of Sciences of the United States of America,* 94**,** 8076-81.

GUEVEN, N., BECHEREL, O. J., KIJAS, A. W., CHEN, P., HOWE, O., RUDOLPH, J. H., GATTI, R., DATE, H., ONODERA, O., TAUCHER-SCHOLZ, G. & LAVIN, M. F. 2004. Aprataxin, a novel protein that protects against genotoxic stress. *Hum Mol Genet,* 13**,** 1081-93.

GUEVEN, N., CHEN, P., NAKAMURA, J., BECHEREL, O. J., KIJAS, A. W., GRATTAN-SMITH, P. & LAVIN, M. F. 2007. A subgroup of spinocerebellar ataxias defective in DNA damage responses. *Neuroscience,* 145**,** 1418-25.

GUMPORT, R. I. & LEHMAN, I. R. 1971. Structure of the DNA ligase-adenylate intermediate: lysine (epsilon-amino)-linked adenosine monophosphoramidate. *Proc Natl Acad Sci U S A,* 68**,** 2559-63.

GUO, G. S., ZHANG, F. M., GAO, R. J., DELSITE, R., FENG, Z. H. & POWELL, S. N. 2011. DNA repair and synthetic lethality. *International journal of oral science,* 3**,** 176-9.

GUZDER, S. N., HABRAKEN, Y., SUNG, P., PRAKASH, L. & PRAKASH, S. 1995. Reconstitution of yeast nucleotide excision repair with purified Rad proteins, replication protein A, and transcription factor TFIIH. *The Journal of biological chemistry,* 270**,** 12973-6.

HABECK, M., ZUHLKE, C., BENTELE, K. H., UNKELBACH, S., KRESS, W., BURK, K., SCHWINGER, E. & HELLENBROICH, Y. 2004. Aprataxin mutations are a rare cause of early onset ataxia in Germany. *J Neurol,* 251**,** 591-4.

HAMMEL, M., REY, M., YU, Y., MANI, R. S., CLASSEN, S., LIU, M., PIQUE, M. E., FANG, S., MAHANEY, B., WEINFELD, M., SCHRIEMER, D. C., LEES-MILLER, S. P. & TAINER, J. A. 2011. XRCC4 interactions with XRCC4-like factor (XLF) create an extended grooved scaffold for DNA ligation and double-strand break repair. *The Journal of biological chemistry*.

HARPER, J. W. & ELLEDGE, S. J. 2007. The DNA damage response: ten years after. *Molecular cell,* 28**,** 739-45.

HARRIS, J. L., JAKOB, B., TAUCHER-SCHOLZ, G., DIANOV, G. L., BECHEREL, O. J. & LAVIN, M. F. 2009. Aprataxin, poly-ADP ribose polymerase 1 (PARP-1) and apurinic endonuclease 1 (APE1) function together to protect the genome against oxidative damage. *Hum Mol Genet,* 18**,** 4102-17.

HARTLERODE, A. J. & SCULLY, R. 2009. Mechanisms of double-strand break repair in somatic mammalian cells. *The Biochemical journal,* 423**,** 157-68.

HARTSUIKER, E., NEALE, M. J. & CARR, A. M. 2009. Distinct requirements for the Rad32(Mre11) nuclease and Ctp1(CtIP) in the removal of covalently bound topoisomerase I and II from DNA. *Mol Cell,* 33**,** 117-23.

HARVEY, C. L., GABRIEL, T. F., WILT, E. M. & RICHARDSON, C. C. 1971. Enzymatic breakage and joining of deoxyribonucleic acid. IX. Synthesis and properties of the deoxyribonucleic acid adenylate in the phage T4 ligase reaction. *J Biol Chem,* 246**,** 4523-30.

HEGDE, M. L., HAZRA, T. K. & MITRA, S. 2008. Early steps in the DNA base excision/single-strand interruption repair pathway in mammalian cells. *Cell Res,* 18**,** 27-47.

HENDERSON, L. M., ARLETT, C. F., HARCOURT, S. A., LEHMANN, A. R. & BROUGHTON, B. C. 1985. Cells from an immunodeficient patient (46BR) with a defect in DNA ligation are hypomutable but hypersensitive to the induction of sister chromatid exchanges. *Proceedings of the National Academy of Sciences of the United States of America,* 82**,** 2044-8.

HERMANSON-MILLER, I. L. & TURCHI, J. J. 2002. Strand-specific binding of RPA and XPA to damaged duplex DNA. *Biochemistry,* 41**,** 2402-8.

HIRANO, M., YAMAMOTO, A., MORI, T., LAN, L., IWAMOTO, T. A., AOKI, M., SHIMADA, K., FURIYA, Y., KARIYA, S., ASAI, H., YASUI, A., NISHIWAKI, T., IMOTO, K., KOBAYASHI, N., KIRIYAMA, T., NAGATA, T., KONISHI, N., ITOYAMA, Y. & UENO, S. 2007. DNA single-strand break repair is impaired in aprataxin-related ataxia. *Ann Neurol,* 61**,** 162-74.

HO, C. K., VAN ETTEN, J. L. & SHUMAN, S. 1997. Characterization of an ATP-dependent DNA ligase encoded by Chlorella virus PBCV-1. *J Virol,* 71**,** 1931-7.

HOEIJMAKERS, J. H. 2001. Genome maintenance mechanisms for preventing cancer. *Nature,* 411**,** 366-74.

HOEIJMAKERS, J. H. 2007. Genome maintenance mechanisms are critical for preventing cancer as well as other aging-associated diseases. *Mechanisms of ageing and development,* 128**,** 460-2.

HOPFNER, K. P., CRAIG, L., MONCALIAN, G., ZINKEL, R. A., USUI, T., OWEN, B. A., KARCHER, A., HENDERSON, B., BODMER, J. L., MCMURRAY, C. T., CARNEY, J. P., PETRINI, J. H. & TAINER, J. A. 2002. The Rad50 zinc-hook is a structure joining Mre11 complexes in DNA recombination and repair. *Nature,* 418**,** 562-6.

HOSHINO, K. & KAMEYAMA, Y. 1988. Developmental-stage-dependent radiosensitivity of neural cells in the ventricular zone of telencephalon in mouse and rat fetuses. *Teratology,* 37**,** 257-62.

HOSHINO, K., KAMEYAMA, Y. & INOUYE, M. 1991. Split-dose effect of X-irradiation on the induction of cell death in the fetal mouse brain. *Journal of radiation research,* 32**,** 23-7.

HSIEH, P. & YAMANE, K. 2008. DNA mismatch repair: molecular mechanism, cancer, and ageing. *Mechanisms of ageing and development,* 129**,** 391-407.

HUEN, M. S., GRANT, R., MANKE, I., MINN, K., YU, X., YAFFE, M. B. & CHEN, J. 2007. RNF8 transduces the DNA-damage signal via histone ubiquitylation and checkpoint protein assembly. *Cell,* 131**,** 901-14.

HUERTAS, P. & JACKSON, S. P. 2009. Human CtIP mediates cell cycle control of DNA end resection and double strand break repair. *The Journal of biological chemistry,* 284**,** 9558-65.

IATROPOULOS, M. J. & WILLIAMS, G. M. 1996. Proliferation markers. *Exp Toxicol Pathol,* 48**,** 175-81.

IKEGAMI, S., AMEMIYA, S., OGURO, M., NAGANO, H. & MANO, Y. 1979. Inhibition by aphidicolin of cell cycle progression and DNA replication in sea urchin embryos. *J Cell Physiol,* 100**,** 439-44.

ILES, N., RULTEN, S., EL-KHAMISY, S. F. & CALDECOTT, K. W. 2007. APLF (C2orf13) is a novel human protein involved in the cellular response to chromosomal DNA strand breaks. *Molecular and cellular biology,* 27**,** 3793-803.

INAMDAR, K. V., POULIOT, J. J., ZHOU, T., LEES-MILLER, S. P., RASOULI-NIA, A. & POVIRK, L. F. 2002. Conversion of phosphoglycolate to phosphate termini on 3' overhangs of DNA double strand breaks by the human tyrosyl-DNA phosphodiesterase hTdp1. *J Biol Chem,* 277**,** 27162-8.

INTERTHAL, H., CHEN, H. J., KEHL-FIE, T. E., ZOTZMANN, J., LEPPARD, J. B. & CHAMPOUX, J. J. 2005. SCAN1 mutant Tdp1 accumulates the enzyme--DNA intermediate and causes camptothecin hypersensitivity. *Embo J,* 24**,** 2224-33.

INTERTHAL, H., POULIOT, J. J. & CHAMPOUX, J. J. 2001. The tyrosyl-DNA phosphodiesterase Tdp1 is a member of the phospholipase D superfamily. *Proc Natl Acad Sci U S A,* 98**,** 12009-14.

ITO, A., YAMAGATA, T., MORI, M. & MOMOI, M. Y. 2005. Early-onset ataxia with oculomotor apraxia with a novel APTX mutation. *Pediatr Neurol,* 33**,** 53-6.

IZUMI, T., BROWN, D. B., NAIDU, C. V., BHAKAT, K. K., MACINNES, M. A., SAITO, H., CHEN, D. J. & MITRA, S. 2005. Two essential but distinct functions of the mammalian abasic endonuclease. *Proc Natl Acad Sci U S A,* 102**,** 5739-43.

IZUMI, T., HAZRA, T. K., BOLDOGH, I., TOMKINSON, A. E., PARK, M. S., IKEDA, S. & MITRA, S. 2000. Requirement for human AP endonuclease 1 for repair of 3'-blocking damage at DNA single-strand breaks induced by reactive oxygen species. *Carcinogenesis,* 21**,** 1329-34.

JACKSON, S. P. & BARTEK, J. 2009. The DNA-damage response in human biology and disease. *Nature,* 461**,** 1071-8.

JAKOB, B., RUDOLPH, J. H., GUEVEN, N., LAVIN, M. F. & TAUCHER-SCHOLZ, G. 2005. Live cell imaging of heavy-ion-induced radiation responses by beamline microscopy. *Radiat Res,* 163**,** 681-90.

JASPERS, N. G., RAAMS, A., SILENGO, M. C., WIJGERS, N., NIEDERNHOFER, L. J., ROBINSON, A. R., GIGLIA-MARI, G., HOOGSTRATEN, D., KLEIJER, W. J., HOEIJMAKERS, J. H. & VERMEULEN, W. 2007. First reported patient with human ERCC1 deficiency has cerebro-oculo-facio-skeletal syndrome with a mild defect in nucleotide excision repair and severe developmental failure. *American journal of human genetics,* 80**,** 457-66.

JILANI, A., RAMOTAR, D., SLACK, C., ONG, C., YANG, X. M., SCHERER, S. W. & LASKO, D. D. 1999. Molecular cloning of the human gene, PNKP, encoding a polynucleotide kinase 3'-phosphatase and evidence for its role in repair of DNA strand breaks caused by oxidative damage. *J Biol Chem,* 274**,** 24176-86.

JIN, S., KHARBANDA, S., MAYER, B., KUFE, D. & WEAVER, D. T. 1997. Binding of Ku and c-Abl at the kinase homology region of DNA-dependent protein kinase catalytic subunit. *The Journal of biological chemistry,* 272**,** 24763-6.

JIRICNY, J. 2006. The multifaceted mismatch-repair system. *Nature reviews. Molecular cell biology,* 7**,** 335-46.

KARIMI-BUSHERI, F., LEE, J., TOMKINSON, A. E. & WEINFELD, M. 1998. Repair of DNA strand gaps and nicks containing 3'-phosphate and 5'-hydroxyl termini by purified mammalian enzymes. *Nucleic Acids Res,* 26**,** 4395-400.

KARIMI-BUSHERI, F., RASOULI-NIA, A., ALLALUNIS-TURNER, J. & WEINFELD, M. 2007. Human polynucleotide kinase participates in repair of DNA double-strand breaks by nonhomologous end joining but not homologous recombination. *Cancer research,* 67**,** 6619-25.

KASAI, H., TANOOKA, H. & NISHIMURA, S. 1984. Formation of 8-hydroxyguanine residues in DNA by X-irradiation. *Gann,* 75**,** 1037-9.

KASTAN, M. B. & BARTEK, J. 2004. Cell-cycle checkpoints and cancer. *Nature,* 432**,** 316-23.

KASTAN, M. B. & LIM, D. S. 2000. The many substrates and functions of ATM. *Nature reviews. Molecular cell biology,* 1**,** 179-86.

KATYAL, S., EL-KHAMISY, S. F., RUSSELL, H. R., LI, Y., JU, L., CALDECOTT, K. W. & MCKINNON, P. J. 2007. TDP1 facilitates chromosomal single-strand break repair in neurons and is neuroprotective in vivo. *Embo J,* 26**,** 4720-31.

KATYAL, S. & MCKINNON, P. J. 2011. Disconnecting XRCC1 and DNA ligase III. *Cell cycle,* 10**,** 2269-75.

KIJAS, A. W., HARRIS, J. L., HARRIS, J. M. & LAVIN, M. F. 2006. Aprataxin forms a discrete branch in the HIT (histidine triad) superfamily of proteins with both DNA/RNA binding and nucleotide hydrolase activities. *J Biol Chem,* 281**,** 13939-48.

KIM, J. K., PATEL, D. & CHOI, B. S. 1995. Contrasting structural impacts induced by cis-syn cyclobutane dimer and (6-4) adduct in DNA duplex decamers: implication in mutagenesis and repair activity. *Photochemistry and photobiology,* 62**,** 44-50.

KIM, K., BIADE, S. & MATSUMOTO, Y. 1998. Involvement of flap endonuclease 1 in base excision DNA repair. *J Biol Chem,* 273**,** 8842-8.

KIM, M. Y., ZHANG, T. & KRAUS, W. L. 2005. Poly(ADP-ribosyl)ation by PARP-1: 'PAR-laying' NAD+ into a nuclear signal. *Genes Dev,* 19**,** 1951-67.

KLUNGLAND, A. & LINDAHL, T. 1997. Second pathway for completion of human DNA base excision-repair: reconstitution with purified proteins and requirement for DNase IV (FEN1). *EMBO J,* 16**,** 3341-8.

KOCH, C. A., AGYEI, R., GALICIA, S., METALNIKOV, P., O'DONNELL, P., STAROSTINE, A., WEINFELD, M. & DUROCHER, D. 2004. Xrcc4 physically links DNA end processing by polynucleotide kinase to DNA ligation by DNA ligase IV. *The EMBO journal,* 23**,** 3874-85.

KOLAS, N. K., CHAPMAN, J. R., NAKADA, S., YLANKO, J., CHAHWAN, R., SWEENEY, F. D., PANIER, S., MENDEZ, M., WILDENHAIN, J., THOMSON, T. M., PELLETIER, L., JACKSON, S. P. & DUROCHER, D. 2007. Orchestration of the DNA-damage response by the RNF8 ubiquitin ligase. *Science,* 318**,** 1637-40.

KOUZMINOVA, E. A. & KUZMINOV, A. 2006. Fragmentation of replicating chromosomes triggered by uracil in DNA. *J Mol Biol,* 355**,** 20-33.

KRAKOWIAK, A., PACE, H. C., BLACKBURN, G. M., ADAMS, M., MEKHALFIA, A., KACZMAREK, R., BARANIAK, J., STEC, W. J. & BRENNER, C. 2004a. Biochemical, crystallographic, and mutagenic characterization of hint, the AMP-lysine hydrolase, with novel substrates and inhibitors. *J Biol Chem,* 279**,** 18711-6.

KRAKOWIAK, A., PACE, H. C., BLACKBURN, G. M., ADAMS, M., MEKHALFIA, A., KACZMAREK, R., BARANIAK, J., STEC, W. J. & BRENNER, C. 2004b. Biochemical, crystallographic, and mutagenic characterization of hint, the AMP-lysine hydrolase, with novel substrates and inhibitors. *The Journal of biological chemistry,* 279**,** 18711-6.

KROEGER, P. E. & ROWE, T. C. 1989. Interaction of topoisomerase 1 with the transcribed region of the Drosophila HSP 70 heat shock gene. *Nucleic acids research,* 17**,** 8495-509.

KROKAN, H. E., DRABLOS, F. & SLUPPHAUG, G. 2002. Uracil in DNA--occurrence, consequences and repair. *Oncogene,* 21**,** 8935-48.

KUBOTA, Y., NASH, R. A., KLUNGLAND, A., SCHAR, P., BARNES, D. E. & LINDAHL, T. 1996. Reconstitution of DNA base excision-repair with purified human proteins: interaction between DNA polymerase beta and the XRCC1 protein. *EMBO J,* 15**,** 6662-70.

KUNKEL, T. A. & ERIE, D. A. 2005. DNA mismatch repair. *Annual review of biochemistry,* 74**,** 681-710.

KUNZ, C., SAITO, Y. & SCHAR, P. 2009. DNA Repair in mammalian cells: Mismatched repair: variations on a theme. *Cellular and molecular life sciences : CMLS,* 66**,** 1021-38.

KUSUMOTO, R., MASUTANI, C., SUGASAWA, K., IWAI, S., ARAKI, M., UCHIDA, A., MIZUKOSHI, T. & HANAOKA, F. 2001. Diversity of the damage recognition step in the global genomic nucleotide excision repair in vitro. *Mutation research,* 485**,** 219-27.

KUZMINOV, A. 2001. Single-strand interruptions in replicating chromosomes cause double-strand breaks. *Proc Natl Acad Sci U S A,* 98**,** 8241-6.

LAGERWERF, S., VROUWE, M. G., OVERMEER, R. M., FOUSTERI, M. I. & MULLENDERS, L. H. 2011. DNA damage response and transcription. *DNA repair,* 10**,** 743-50.

LAKSHMIPATHY, U. & CAMPBELL, C. 1999. The human DNA ligase III gene encodes nuclear and mitochondrial proteins. *Mol Cell Biol,* 19**,** 3869-76.

LARSEN, E., GRAN, C., SAETHER, B. E., SEEBERG, E. & KLUNGLAND, A. 2003. Proliferation failure and gamma radiation sensitivity of Fen1 null mutant mice at the blastocyst stage. *Molecular and cellular biology,* 23**,** 5346-53.

LAVIN, M. F. 2007. ATM and the Mre11 complex combine to recognize and signal DNA double-strand breaks. *Oncogene,* 26**,** 7749-58.

LAVIN, M. F. 2008. Ataxia-telangiectasia: from a rare disorder to a paradigm for cell signalling and cancer. *Nature reviews. Molecular cell biology,* 9**,** 759-69.

LE BER, I., MOREIRA, M. C., RIVAUD-PECHOUX, S., CHAMAYOU, C., OCHSNER, F., KUNTZER, T., TARDIEU, M., SAID, G., HABERT, M. O., DEMARQUAY, G., TANNIER, C., BEIS, J. M., BRICE, A., KOENIG, M. & DURR, A. 2003. Cerebellar ataxia with oculomotor apraxia type 1: clinical and genetic studies. *Brain,* 126**,** 2761-72.

LE PAGE, F., SCHREIBER, V., DHERIN, C., DE MURCIA, G. & BOITEUX, S. 2003. Poly(ADP-ribose) polymerase-1 (PARP-1) is required in murine cell lines for base excision repair of oxidative DNA damage in the absence of DNA polymerase beta. *J Biol Chem,* 278**,** 18471-7.

LEE, Y., BARNES, D. E., LINDAHL, T. & MCKINNON, P. J. 2000. Defective neurogenesis resulting from DNA ligase IV deficiency requires Atm. *Genes & development,* 14**,** 2576-80.

LEE, Y., KATYAL, S., LI, Y., EL-KHAMISY, S. F., RUSSELL, H. R., CALDECOTT, K. W. & MCKINNON, P. J. 2009. The genesis of cerebellar interneurons and the prevention of neural DNA damage require XRCC1. *Nat Neurosci,* 12**,** 973-80.

LEHMANN, A. R. 1978. Repair processes for radiation-induced DNA damage. *Mol Biol Biochem Biophys,* 27**,** 312-34.

LEHMANN, A. R. 2003. DNA repair-deficient diseases, xeroderma pigmentosum, Cockayne syndrome and trichothiodystrophy. *Biochimie,* 85**,** 1101-11.

LEHMANN, A. R., WILLIS, A. E., BROUGHTON, B. C., JAMES, M. R., STEINGRIMSDOTTIR, H., HARCOURT, S. A., ARLETT, C. F. & LINDAHL, T. 1988. Relation between the human fibroblast strain 46BR and cell lines representative of Bloom's syndrome. *Cancer research,* 48**,** 6343-7.

LEVIN, D. S., BAI, W., YAO, N., O'DONNELL, M. & TOMKINSON, A. E. 1997. An interaction between DNA ligase I and proliferating cell nuclear antigen: implications for Okazaki fragment synthesis and joining. *Proc Natl Acad Sci U S A,* 94**,** 12863-8.

LEVIN, D. S., MCKENNA, A. E., MOTYCKA, T. A., MATSUMOTO, Y. & TOMKINSON, A. E. 2000. Interaction between PCNA and DNA ligase I is critical for joining of Okazaki fragments and long-patch base-excision repair. *Curr Biol,* 10**,** 919-22.

LI, G. M. 2008. Mechanisms and functions of DNA mismatch repair. *Cell research,* 18**,** 85-98.

LI, L., ELLEDGE, S. J., PETERSON, C. A., BALES, E. S. & LEGERSKI, R. J. 1994. Specific association between the human DNA repair proteins XPA and ERCC1. *Proceedings of the National Academy of Sciences of the United States of America,* 91**,** 5012-6.

LI, L., PETERSON, C. A., LU, X. & LEGERSKI, R. J. 1995a. Mutations in XPA that prevent association with ERCC1 are defective in nucleotide excision repair. *Molecular and cellular biology,* 15**,** 1993-8.

LI, X., LI, J., HARRINGTON, J., LIEBER, M. R. & BURGERS, P. M. 1995b. Lagging strand DNA synthesis at the eukaryotic replication fork involves binding and stimulation of FEN-1 by proliferating cell nuclear antigen. *J Biol Chem,* 270**,** 22109-12.

LIEBER, M. R. 2010. The mechanism of double-strand DNA break repair by the nonhomologous DNA end-joining pathway. *Annual review of biochemistry,* 79**,** 181-211.

LIEBER, M. R. & KARANJAWALA, Z. E. 2004. Ageing, repetitive genomes and DNA damage. *Nature reviews. Molecular cell biology,* 5**,** 69-75.

LIEBER, M. R., MA, Y., PANNICKE, U. & SCHWARZ, K. 2003. Mechanism and regulation of human non-homologous DNA end-joining. *Nature reviews. Molecular cell biology,* 4**,** 712-20.

LINDAHL, T. 1974. An N-glycosidase from Escherichia coli that releases free uracil from DNA containing deaminated cytosine residues. *Proc Natl Acad Sci U S A,* 71**,** 3649-53.

LINDAHL, T. 1993. Instability and decay of the primary structure of DNA. *Nature,* 362**,** 709-15.

LINDAHL, T. & NYBERG, B. 1972. Rate of depurination of native deoxyribonucleic acid. *Biochemistry,* 11**,** 3610-8.

LITTLE, J. W., ZIMMERMAN, S. B., OSHINSKY, C. K. & GELLERT, M. 1967. Enzymatic joining of DNA strands, II. An enzyme-adenylate intermediate in the dpn-dependent DNA ligase reaction. *Proc Natl Acad Sci U S A,* 58**,** 2004-11.

LIU, W. & NARAYANAN, V. 2008. Ataxia with oculomotor apraxia. *Semin Pediatr Neurol,* 15**,** 216-20.

LIU, Y., BEARD, W. A., SHOCK, D. D., PRASAD, R., HOU, E. W. & WILSON, S. H. 2005. DNA polymerase beta and flap endonuclease 1 enzymatic specificities sustain DNA synthesis for long patch base excision repair. *J Biol Chem,* 280**,** 3665-74.

LJUNGMAN, M. & LANE, D. P. 2004. Transcription - guarding the genome by sensing DNA damage. *Nature reviews. Cancer,* 4**,** 727-37.

LOIZOU, J. I., EL-KHAMISY, S. F., ZLATANOU, A., MOORE, D. J., CHAN, D. W., QIN, J., SARNO, S., MEGGIO, F., PINNA, L. A. & CALDECOTT, K. W. 2004. The protein kinase CK2 facilitates repair of chromosomal DNA single-strand breaks. *Cell,* 117**,** 17-28.

LONN, U., LONN, S., NYLEN, U. & WINBLAD, G. 1989. Altered formation of DNA replication intermediates in human 46 BR fibroblast cells hypersensitive to 3-aminobenzamide. *Carcinogenesis,* 10**,** 981-5.

LOU, Z., MINTER-DYKHOUSE, K., FRANCO, S., GOSTISSA, M., RIVERA, M. A., CELESTE, A., MANIS, J. P., VAN DEURSEN, J., NUSSENZWEIG, A., PAULL, T. T., ALT, F. W. & CHEN, J. 2006. MDC1 maintains genomic stability by participating in the amplification of ATM-dependent DNA damage signals. *Molecular cell,* 21**,** 187-200.

LU, H., PANNICKE, U., SCHWARZ, K. & LIEBER, M. R. 2007. Length-dependent binding of human XLF to DNA and stimulation of XRCC4.DNA ligase IV activity. *The Journal of biological chemistry,* 282**,** 11155-62.

LU, M., MANI, R. S., KARIMI-BUSHERI, F., FANTA, M., WANG, H., LITCHFELD, D. W. & WEINFELD, M. 2010. Independent mechanisms of stimulation of polynucleotide kinase/phosphatase by phosphorylated and non-phosphorylated XRCC1. *Nucleic Acids Res,* 38**,** 510-21.

LUKAS, C., MELANDER, F., STUCKI, M., FALCK, J., BEKKER-JENSEN, S., GOLDBERG, M., LERENTHAL, Y., JACKSON, S. P., BARTEK, J. & LUKAS, J. 2004. Mdc1 couples DNA double-strand break recognition by Nbs1 with its H2AX-dependent chromatin retention. *The EMBO journal,* 23**,** 2674-83.

LUO, H., CHAN, D. W., YANG, T., RODRIGUEZ, M., CHEN, B. P., LENG, M., MU, J. J., CHEN, D., SONGYANG, Z., WANG, Y. & QIN, J. 2004. A new XRCC1-containing complex and its role in cellular survival of methyl methanesulfonate treatment. *Mol Cell Biol,* 24**,** 8356-65.

MA, Y., PANNICKE, U., SCHWARZ, K. & LIEBER, M. R. 2002. Hairpin opening and overhang processing by an Artemis/DNA-dependent protein kinase complex in nonhomologous end joining and V(D)J recombination. *Cell,* 108**,** 781-94.

MA, Y., SCHWARZ, K. & LIEBER, M. R. 2005. The Artemis:DNA-PKcs endonuclease cleaves DNA loops, flaps, and gaps. *DNA repair,* 4**,** 845-51.

MACKEY, Z. B., NIEDERGANG, C., MURCIA, J. M., LEPPARD, J., AU, K., CHEN, J., DE MURCIA, G. & TOMKINSON, A. E. 1999. DNA ligase III is recruited to DNA strand breaks by a zinc finger motif homologous to that of poly(ADP-ribose) polymerase. Identification of two functionally distinct DNA binding regions within DNA ligase III. *J Biol Chem,* 274**,** 21679-87.

MACKEY, Z. B., RAMOS, W., LEVIN, D. S., WALTER, C. A., MCCARREY, J. R. & TOMKINSON, A. E. 1997. An alternative splicing event which occurs in mouse pachytene spermatocytes generates a form of DNA ligase III with distinct biochemical properties that may function in meiotic recombination. *Mol Cell Biol,* 17**,** 989-98.

MACRAE, C. J., MCCULLOCH, R. D., YLANKO, J., DUROCHER, D. & KOCH, C. A. 2008. APLF (C2orf13) facilitates nonhomologous end-joining and undergoes ATM-dependent hyperphosphorylation following ionizing radiation. *DNA repair,* 7**,** 292-302.

MAHAJNAH, M., BASEL-VANAGAITE, L., INBAR, D., KORNREICH, L., WEITZ, R. & STRAUSSBERG, R. 2005. Familial cognitive impairment with ataxia with oculomotor apraxia. *J Child Neurol,* 20**,** 523-5.

MAHANEY, B. L., MEEK, K. & LEES-MILLER, S. P. 2009. Repair of ionizing radiation-induced DNA double-strand breaks by non-homologous end-joining. *The Biochemical journal,* 417**,** 639-50.

MAILAND, N., BEKKER-JENSEN, S., FAUSTRUP, H., MELANDER, F., BARTEK, J., LUKAS, C. & LUKAS, J. 2007. RNF8 ubiquitylates histones at DNA double-strand breaks and promotes assembly of repair proteins. *Cell,* 131**,** 887-900.

MANI, R. S., FANTA, M., KARIMI-BUSHERI, F., SILVER, E., VIRGEN, C. A., CALDECOTT, K. W., CASS, C. E. & WEINFELD, M. 2007. XRCC1 stimulates polynucleotide kinase by enhancing its damage discrimination and displacement from DNA repair intermediates. *J Biol Chem,* 282**,** 28004-13.

MANI, R. S., YU, Y., FANG, S., LU, M., FANTA, M., ZOLNER, A. E., TAHBAZ, N., RAMSDEN, D. A., LITCHFIELD, D. W., LEES-MILLER, S. P. & WEINFELD, M. 2010. Dual modes of interaction between XRCC4 and polynucleotide kinase/phosphatase: implications for nonhomologous end joining. *The Journal of biological chemistry,* 285**,** 37619-29.

MARI, P. O., FLOREA, B. I., PERSENGIEV, S. P., VERKAIK, N. S., BRUGGENWIRTH, H. T., MODESTI, M., GIGLIA-MARI, G., BEZSTAROSTI, K., DEMMERS, J. A., LUIDER, T. M., HOUTSMULLER, A. B. & VAN GENT, D. C. 2006. Dynamic assembly of end-joining complexes requires interaction between Ku70/80 and XRCC4. *Proceedings of the National Academy of Sciences of the United States of America,* 103**,** 18597-602.

MARINTCHEV, A., ROBERTSON, A., DIMITRIADIS, E. K., PRASAD, R., WILSON, S. H. & MULLEN, G. P. 2000. Domain specific interaction in the XRCC1-DNA polymerase beta complex. *Nucleic Acids Res,* 28**,** 2049-59.

MARSIN, S., VIDAL, A. E., SOSSOU, M., MENISSIER-DE MURCIA, J., LE PAGE, F., BOITEUX, S., DE MURCIA, G. & RADICELLA, J. P. 2003. Role of XRCC1 in the coordination and stimulation of oxidative DNA damage repair initiated by the DNA glycosylase hOGG1. *J Biol Chem,* 278**,** 44068-74.

MARTIN, G. M., SMITH, A. C., KETTERER, D. J., OGBURN, C. E. & DISTECHE, C. M. 1985. Increased chromosomal aberrations in first metaphases of cells isolated from the kidneys of aged mice. *Israel journal of medical sciences,* 21**,** 296-301.

MASSON, M., NIEDERGANG, C., SCHREIBER, V., MULLER, S., MENISSIER-DE MURCIA, J. & DE MURCIA, G. 1998. XRCC1 is specifically associated with poly(ADP-ribose) polymerase and negatively regulates its activity following DNA damage. *Mol Cell Biol,* 18**,** 3563-71.

MATSUMOTO, Y. & KIM, K. 1995. Excision of deoxyribose phosphate residues by DNA polymerase beta during DNA repair. *Science,* 269**,** 699-702.

MATSUMOTO, Y., KIM, K. & BOGENHAGEN, D. F. 1994. Proliferating cell nuclear antigen-dependent abasic site repair in Xenopus laevis oocytes: an alternative pathway of base excision DNA repair. *Mol Cell Biol,* 14**,** 6187-97.

MATSUMOTO, Y., KIM, K., HURWITZ, J., GARY, R., LEVIN, D. S., TOMKINSON, A. E. & PARK, M. S. 1999. Reconstitution of proliferating cell nuclear antigen-dependent repair of apurinic/apyrimidinic sites with purified human proteins. *J Biol Chem,* 274**,** 33703-8.

MATSUNAGA, T., MU, D., PARK, C. H., REARDON, J. T. & SANCAR, A. 1995. Human DNA repair excision nuclease. Analysis of the roles of the subunits involved in dual incisions by using anti-XPG and anti-ERCC1 antibodies. *The Journal of biological chemistry,* 270**,** 20862-9.

MCCULLOUGH, A. K., DODSON, M. L. & LLOYD, R. S. 1999. Initiation of base excision repair: glycosylase mechanisms and structures. *Annual review of biochemistry,* 68**,** 255-85.

MCKINNON, P. J. 2009. DNA repair deficiency and neurological disease. *Nat Rev Neurosci,* 10**,** 100-12.

MCKINNON, P. J. & CALDECOTT, K. W. 2007. DNA strand break repair and human genetic disease. *Annual review of genomics and human genetics,* 8**,** 37-55.

MEEK, K., DOUGLAS, P., CUI, X., DING, Q. & LEES-MILLER, S. P. 2007. trans Autophosphorylation at DNA-dependent protein kinase's two major autophosphorylation site clusters facilitates end processing but not end joining. *Molecular and cellular biology,* 27**,** 3881-90.

MEHROTRA, P. V., AHEL, D., RYAN, D. P., WESTON, R., WIECHENS, N., KRAEHENBUEHL, R., OWEN-HUGHES, T. & AHEL, I. 2011. DNA repair factor APLF is a histone chaperone. *Molecular cell,* 41**,** 46-55.

MIAO, Z. H., AGAMA, K., SORDET, O., POVIRK, L., KOHN, K. W. & POMMIER, Y. 2006. Hereditary ataxia SCAN1 cells are defective for the repair of transcription-dependent topoisomerase I cleavage complexes. *DNA repair,* 5**,** 1489-94.

MILLER, M. R. & CHINAULT, D. N. 1982a. Evidence that DNA polymerases alpha and beta participate differentially in DNA repair synthesis induced by different agents. *J Biol Chem,* 257**,** 46-9.

MILLER, M. R. & CHINAULT, D. N. 1982b. The roles of DNA polymerases alpha, beta, and gamma in DNA repair synthesis induced in hamster and human cells by different DNA damaging agents. *J Biol Chem,* 257**,** 10204-9.

MILMAN, N., HIGUCHI, E. & SMITH, G. R. 2009. Meiotic DNA double-strand break repair requires two nucleases, MRN and Ctp1, to produce a single size class of Rec12 (Spo11)-oligonucleotide complexes. *Mol Cell Biol,* 29**,** 5998-6005.

MIMAKI, T., ITOH, N., ABE, J., TAGAWA, T., SATO, K., YABUUCHI, H. & TAKEBE, H. 1986. Neurological manifestations in xeroderma pigmentosum. *Annals of neurology,* 20**,** 70-5.

MIMITOU, E. P. & SYMINGTON, L. S. 2008. Sae2, Exo1 and Sgs1 collaborate in DNA double-strand break processing. *Nature,* 455**,** 770-4.

MIMITOU, E. P. & SYMINGTON, L. S. 2009. DNA end resection: many nucleases make light work. *DNA Repair (Amst),* 8**,** 983-95.

MITRA, S., IZUMI, T., BOLDOGH, I., BHAKAT, K. K., CHATTOPADHYAY, R. & SZCZESNY, B. 2007. Intracellular trafficking and regulation of mammalian AP-endonuclease 1 (APE1), an essential DNA repair protein. *DNA Repair (Amst),* 6**,** 461-9.

MOREAU, S., FERGUSON, J. R. & SYMINGTON, L. S. 1999. The nuclease activity of Mre11 is required for meiosis but not for mating type switching, end joining, or telomere maintenance. *Mol Cell Biol,* 19**,** 556-66.

MOREIRA, M. C., BARBOT, C., TACHI, N., KOZUKA, N., UCHIDA, E., GIBSON, T., MENDONCA, P., COSTA, M., BARROS, J., YANAGISAWA, T., WATANABE, M., IKEDA, Y., AOKI, M., NAGATA, T., COUTINHO, P., SEQUEIROS, J. & KOENIG, M. 2001. The gene mutated in

ataxia-ocular apraxia 1 encodes the new HIT/Zn-finger protein aprataxin. *Nat Genet,* 29**,** 189-93.

MOSBAUGH, D. W. & LINN, S. 1983. Excision repair and DNA synthesis with a combination of HeLa DNA polymerase beta and DNase V. *J Biol Chem,* 258**,** 108-18.

MOSER, J., KOOL, H., GIAKZIDIS, I., CALDECOTT, K., MULLENDERS, L. H. & FOUSTERI, M. I. 2007. Sealing of chromosomal DNA nicks during nucleotide excision repair requires XRCC1 and DNA ligase III alpha in a cell-cycle-specific manner. *Molecular cell,* 27**,** 311-23.

MOSESSO, P., PIANE, M., PALITTI, F., PEPE, G., PENNA, S. & CHESSA, L. 2005. The novel human gene aprataxin is directly involved in DNA single-strand-break repair. *Cell Mol Life Sci,* 62**,** 485-91.

MOSHOUS, D., CALLEBAUT, I., DE CHASSEVAL, R., CORNEO, B., CAVAZZANA-CALVO, M., LE DEIST, F., TEZCAN, I., SANAL, O., BERTRAND, Y., PHILIPPE, N., FISCHER, A. & DE VILLARTAY, J. P. 2001. Artemis, a novel DNA double-strand break repair/V(D)J recombination protein, is mutated in human severe combined immune deficiency. *Cell,* 105**,** 177-86.

MU, D., PARK, C. H., MATSUNAGA, T., HSU, D. S., REARDON, J. T. & SANCAR, A. 1995. Reconstitution of human DNA repair excision nuclease in a highly defined system. *The Journal of biological chemistry,* 270**,** 2415-8.

MUELLER, G. A., MOON, A. F., DEROSE, E. F., HAVENER, J. M., RAMSDEN, D. A., PEDERSEN, L. C. & LONDON, R. E. 2008. A comparison of BRCT domains involved in nonhomologous end-joining: introducing the solution structure of the BRCT domain of polymerase lambda. *DNA repair,* 7**,** 1340-51.

NAGAI, A., SAIJO, M., KURAOKA, I., MATSUDA, T., KODO, N., NAKATSU, Y., MIMAKI, T., MINO, M., BIGGERSTAFF, M., WOOD, R. D. & ET AL. 1995. Enhancement of damage-specific DNA binding of XPA by interaction with the ERCC1 DNA repair protein. *Biochemical and biophysical research communications,* 211**,** 960-6.

NAGASAWA, K., KITAMURA, K., YASUI, A., NIMURA, Y., IKEDA, K., HIRAI, M., MATSUKAGE, A. & NAKANISHI, M. 2000. Identification and characterization of human DNA polymerase beta 2, a DNA polymerase beta -related enzyme. *J Biol Chem,* 275**,** 31233-8.

NAIR, P. A., NANDAKUMAR, J., SMITH, P., ODELL, M., LIMA, C. D. & SHUMAN, S. 2007a. Structural basis for nick recognition by a minimal pluripotent DNA ligase. *Nat Struct Mol Biol*.

NAIR, P. A., NANDAKUMAR, J., SMITH, P., ODELL, M., LIMA, C. D. & SHUMAN, S. 2007b. Structural basis for nick recognition by a minimal pluripotent DNA ligase. *Nat Struct Mol Biol,* 14**,** 770-8.

NARASIMHAIAH, R., TUCHMAN, A., LIN, S. L. & NAEGELE, J. R. 2005. Oxidative damage and defective DNA repair is linked to apoptosis of migrating neurons and progenitors during cerebral cortex development in Ku70-deficient mice. *Cerebral cortex,* 15**,** 696-707.

NASH, R. A., CALDECOTT, K. W., BARNES, D. E. & LINDAHL, T. 1997. XRCC1 protein interacts with one of two distinct forms of DNA ligase III. *Biochemistry,* 36**,** 5207-11.

NEALON, K., NICHOLL, I. D. & KENNY, M. K. 1996. Characterization of the DNA polymerase requirement of human base excision repair. *Nucleic Acids Res,* 24**,** 3763-70.

NEGRINI, S., GORGOULIS, V. G. & HALAZONETIS, T. D. 2010. Genomic instability--an evolving hallmark of cancer. *Nature reviews. Molecular cell biology,* 11**,** 220-8.

NICK MCELHINNY, S. A. & RAMSDEN, D. A. 2004. Sibling rivalry: competition between Pol X family members in V(D)J recombination and general double strand break repair. *Immunological reviews,* 200**,** 156-64.

NICK MCELHINNY, S. A., SNOWDEN, C. M., MCCARVILLE, J. & RAMSDEN, D. A. 2000. Ku recruits the XRCC4-ligase IV complex to DNA ends. *Molecular and cellular biology,* 20**,** 2996-3003.

NICOLETTE, M. L., LEE, K., GUO, Z., RANI, M., CHOW, J. M., LEE, S. E. & PAULL, T. T. 2010a. Mre11-Rad50-Xrs2 and Sae2 promote 5' strand resection of DNA double-strand breaks. *Nature structural & molecular biology,* 17**,** 1478-85.

NICOLETTE, M. L., LEE, K., GUO, Z., RANI, M., CHOW, J. M., LEE, S. E. & PAULL, T. T. 2010b. Mre11-Rad50-Xrs2 and Sae2 promote 5' strand resection of DNA double-strand breaks. *Nat Struct Mol Biol,* 17**,** 1478-85.

NILSSON, S. V. & MAGNUSSON, G. 1982. Sealing of gaps in duplex DNA by T4 DNA ligase. *Nucleic Acids Res,* 10**,** 1425-37.

NIMONKAR, A. V., GENSCHEL, J., KINOSHITA, E., POLACZEK, P., CAMPBELL, J. L., WYMAN, C., MODRICH, P. & KOWALCZYKOWSKI, S. C. 2011. BLM-DNA2-RPA-MRN and EXO1-BLM-RPA-MRN constitute two DNA end resection machineries for human DNA break repair. *Genes & development,* 25**,** 350-62.

NITISS, J. L. 2009a. DNA topoisomerase II and its growing repertoire of biological functions. *Nature reviews. Cancer,* 9**,** 327-37.

NITISS, J. L. 2009b. Targeting DNA topoisomerase II in cancer chemotherapy. *Nature reviews. Cancer,* 9**,** 338-50.

NOUSPIKEL, T. 2009. DNA repair in mammalian cells : Nucleotide excision repair: variations on versatility. *Cellular and molecular life sciences : CMLS,* 66**,** 994-1009.

O'CONNOR, T. R. & LAVAL, J. 1989. Physical association of the 2,6-diamino-4-hydroxy-5N-formamidopyrimidine-DNA glycosylase of Escherichia coli and an activity nicking DNA at apurinic/apyrimidinic sites. *Proc Natl Acad Sci U S A,* 86**,** 5222-6.

O'DONOVAN, A., DAVIES, A. A., MOGGS, J. G., WEST, S. C. & WOOD, R. D. 1994. XPG endonuclease makes the 3' incision in human DNA nucleotide excision repair. *Nature,* 371**,** 432-5.

O'DRISCOLL, M., CEROSALETTI, K. M., GIRARD, P. M., DAI, Y., STUMM, M., KYSELA, B., HIRSCH, B., GENNERY, A., PALMER, S. E., SEIDEL, J., GATTI, R. A., VARON, R., OETTINGER, M. A., NEITZEL, H., JEGGO, P. A. & CONCANNON, P. 2001. DNA ligase IV mutations identified in patients exhibiting developmental delay and immunodeficiency. *Molecular cell,* 8**,** 1175-85.

O'DRISCOLL, M. & JEGGO, P. A. 2008. The role of the DNA damage response pathways in brain development and microcephaly: insight from human disorders. *DNA repair,* 7**,** 1039-50.

ODELL, M., MALININA, L., SRISKANDA, V., TEPLOVA, M. & SHUMAN, S. 2003. Analysis of the DNA joining repertoire of Chlorella virus DNA ligase and a new crystal structure of the ligase-adenylate intermediate. *Nucleic Acids Res,* 31**,** 5090-100.

ODELL, M., SRISKANDA, V., SHUMAN, S. & NIKOLOV, D. B. 2000. Crystal structure of eukaryotic DNA ligase-adenylate illuminates the mechanism of nick sensing and strand joining. *Mol Cell,* 6**,** 1183-93.

OGURO, M., SUZUKI-HORI, C., NAGANO, H., MANO, Y. & IKEGAMI, S. 1979. The mode of inhibitory action by aphidicolin on eukaryotic DNA polymerase alpha. *Eur J Biochem,* 97**,** 603-7.

OLIVERA, B. M., HALL, Z. W., ANRAKU, Y., CHIEN, J. R. & LEHMAN, I. R. 1968. On the mechanism of the polynucleotide joining reaction. *Cold Spring Harb Symp Quant Biol,* 33**,** 27-34.

OTTERLEI, M., WARBRICK, E., NAGELHUS, T. A., HAUG, T., SLUPPHAUG, G., AKBARI, M., AAS, P. A., STEINSBEKK, K., BAKKE, O. & KROKAN, H. E. 1999. Post-replicative base excision repair in replication foci. *Embo J,* 18**,** 3834-44.

PALAU, F. & ESPINOS, C. 2006. Autosomal recessive cerebellar ataxias. *Orphanet J Rare Dis,* 1**,** 47.

PAQUES, F. & HABER, J. E. 1999. Multiple pathways of recombination induced by double-strand breaks in Saccharomyces cerevisiae. *Microbiology and molecular biology reviews : MMBR,* 63**,** 349-404.

PARK, C. H., BESSHO, T., MATSUNAGA, T. & SANCAR, A. 1995. Purification and characterization of the XPF-ERCC1 complex of human DNA repair excision nuclease. *The Journal of biological chemistry,* 270**,** 22657-60.

PARK, C. H. & SANCAR, A. 1994. Formation of a ternary complex by human XPA, ERCC1, and ERCC4(XPF) excision repair proteins. *Proceedings of the National Academy of Sciences of the United States of America,* 91**,** 5017-21.

PARK, C. J. & CHOI, B. S. 2006. The protein shuffle. Sequential interactions among components of the human nucleotide excision repair pathway. *The FEBS journal,* 273**,** 1600-8.

PARKS, K. P., SEIDLE, H., WRIGHT, N., SPERRY, J. B., BIEGANOWSKI, P., HOWITZ, K., WRIGHT, D. L. & BRENNER, C. 2004. Altered specificity of Hint-W123Q supports a role for Hint inhibition by ASW in avian sex determination. *Physiol Genomics,* 20**,** 12-4.

PARLANTI, E., LOCATELLI, G., MAGA, G. & DOGLIOTTI, E. 2007. Human base excision repair complex is physically associated to DNA replication and cell cycle regulatory proteins. *Nucleic Acids Res,* 35**,** 1569-77.

PARLANTI, E., PASCUCCI, B., TERRADOS, G., BLANCO, L. & DOGLIOTTI, E. 2004. Aphidicolin-resistant and -sensitive base excision repair in wild-type and DNA polymerase beta-defective mouse cells. *DNA Repair (Amst),* 3**,** 703-10.

PARSONS, J. L., PRESTON, B. D., O'CONNOR, T. R. & DIANOV, G. L. 2007. DNA polymerase delta-dependent repair of DNA single strand breaks containing 3'-end proximal lesions. *Nucleic Acids Res,* 35**,** 1054-63.

PASCAL, J. M., O'BRIEN, P. J., TOMKINSON, A. E. & ELLENBERGER, T. 2004. Human DNA ligase I completely encircles and partially unwinds nicked DNA. *Nature,* 432**,** 473-8.

PASCUCCI, B., MAGA, G., HUBSCHER, U., BJORAS, M., SEEBERG, E., HICKSON, I. D., VILLANI, G., GIORDANO, C., CELLAI, L. & DOGLIOTTI, E. 2002. Reconstitution of the base excision repair pathway for 7,8-dihydro-8-oxoguanine with purified human proteins. *Nucleic Acids Res,* 30**,** 2124-30.

PASCUCCI, B., STUCKI, M., JONSSON, Z. O., DOGLIOTTI, E. & HUBSCHER, U. 1999. Long patch base excision repair with purified human proteins. DNA ligase I as patch size mediator for DNA polymerases delta and epsilon. *J Biol Chem,* 274**,** 33696-702.

PAULL, T. T. 2010a. Making the best of the loose ends: Mre11/Rad50 complexes and Sae2 promote DNA double-strand break resection. *DNA Repair (Amst),* 9**,** 1283-91.

PAULL, T. T. 2010b. Making the best of the loose ends: Mre11/Rad50 complexes and Sae2 promote DNA double-strand break resection. *DNA repair,* 9**,** 1283-91.

PAYNE, A. & CHU, G. 1994. Xeroderma pigmentosum group E binding factor recognizes a broad spectrum of DNA damage. *Mutation research,* 310**,** 89-102.

PELLEGRINI, L., YU, D. S., LO, T., ANAND, S., LEE, M., BLUNDELL, T. L. & VENKITARAMAN, A. R. 2002. Insights into DNA recombination from the structure of a RAD51-BRCA2 complex. *Nature,* 420**,** 287-93.

PERERA, F., TANG, D., WHYATT, R., LEDERMAN, S. A. & JEDRYCHOWSKI, W. 2005. DNA damage from polycyclic aromatic hydrocarbons measured by benzo[a]pyrene-DNA adducts in mothers and newborns from Northern Manhattan, the World Trade Center Area, Poland, and China. *Cancer epidemiology, biomarkers & prevention : a publication of the American Association for Cancer Research, cosponsored by the American Society of Preventive Oncology,* 14**,** 709-14.

PEREZ-JANNOTTI, R. M., KLEIN, S. M. & BOGENHAGEN, D. F. 2001. Two forms of mitochondrial DNA ligase III are produced in Xenopus laevis oocytes. *J Biol Chem,* 276**,** 48978-87.

PETERMANN, E., KEIL, C. & OEI, S. L. 2006. Roles of DNA ligase III and XRCC1 in regulating the switch between short patch and long patch BER. *DNA Repair (Amst),* 5**,** 544-55.

PETERMANN, E., ZIEGLER, M. & OEI, S. L. 2003. ATP-dependent selection between single nucleotide and long patch base excision repair. *DNA Repair (Amst),* 2**,** 1101-14.

PETTA, T. B., NAKAJIMA, S., ZLATANOU, A., DESPRAS, E., COUVE-PRIVAT, S., ISHCHENKO, A., SARASIN, A., YASUI, A. & KANNOUCHE, P. 2008. Human DNA polymerase iota protects cells against oxidative stress. *EMBO J,* 27**,** 2883-95.

PIERSEN, C. E., PRASAD, R., WILSON, S. H. & LLOYD, R. S. 1996. Evidence for an imino intermediate in the DNA polymerase beta deoxyribose phosphate excision reaction. *J Biol Chem,* 271**,** 17811-5.

PODLUTSKY, A. J., DIANOVA, II, PODUST, V. N., BOHR, V. A. & DIANOV, G. L. 2001a. Human DNA polymerase beta initiates DNA synthesis during long-patch repair of reduced AP sites in DNA. *EMBO J,* 20**,** 1477-82.

PODLUTSKY, A. J., DIANOVA, II, WILSON, S. H., BOHR, V. A. & DIANOV, G. L. 2001b. DNA synthesis and dRPase activities of polymerase beta are both essential for single-nucleotide patch base excision repair in mammalian cell extracts. *Biochemistry,* 40**,** 809-13.

POMMIER, Y., REDON, C., RAO, V. A., SEILER, J. A., SORDET, O., TAKEMURA, H., ANTONY, S., MENG, L., LIAO, Z., KOHLHAGEN, G., ZHANG, H. & KOHN, K. W. 2003. Repair of and checkpoint response to topoisomerase I-mediated DNA damage. *Mutat Res,* 532**,** 173-203.

POPANDA, O. & THIELMANN, H. W. 1992. The function of DNA topoisomerases in UV-induced DNA excision repair: studies with specific inhibitors in permeabilized human fibroblasts. *Carcinogenesis,* 13**,** 2321-8.

PORATH, J., CARLSSON, J., OLSSON, I. & BELFRAGE, G. 1975. Metal chelate affinity chromatography, a new approach to protein fractionation. *Nature,* 258**,** 598-9.

POULIOT, J. J., ROBERTSON, C. A. & NASH, H. A. 2001. Pathways for repair of topoisomerase I covalent complexes in Saccharomyces cerevisiae. *Genes Cells,* 6**,** 677-87.

POURQUIER, P., PILON, A. A., KOHLHAGEN, G., MAZUMDER, A., SHARMA, A. & POMMIER, Y. 1997. Trapping of mammalian topoisomerase I and recombinations induced by damaged DNA containing nicks or gaps. Importance of DNA end phosphorylation and camptothecin effects. *J Biol Chem,* 272**,** 26441-7.

POVIRK, L. F., ZHOU, T., ZHOU, R., COWAN, M. J. & YANNONE, S. M. 2007. Processing of 3'-phosphoglycolate-terminated DNA double strand breaks by Artemis nuclease. *The Journal of biological chemistry,* 282**,** 3547-58.

PRAKASH, S., JOHNSON, R. E. & PRAKASH, L. 2005. Eukaryotic translesion synthesis DNA polymerases: specificity of structure and function. *Annu Rev Biochem,* 74**,** 317-53.

PRASAD, R., BEBENEK, K., HOU, E., SHOCK, D. D., BEARD, W. A., WOODGATE, R., KUNKEL, T. A. & WILSON, S. H. 2003. Localization of the deoxyribose phosphate lyase active site in human DNA polymerase iota by controlled proteolysis. *J Biol Chem,* 278**,** 29649-54.

PRASAD, R., DIANOV, G. L., BOHR, V. A. & WILSON, S. H. 2000. FEN1 stimulation of DNA polymerase beta mediates an excision step in mammalian long patch base excision repair. *J Biol Chem,* 275**,** 4460-6.

PRASAD, R., LAVRIK, O. I., KIM, S. J., KEDAR, P., YANG, X. P., VANDE BERG, B. J. & WILSON, S. H. 2001. DNA polymerase beta -mediated long patch base excision repair. Poly(ADP-ribose)polymerase-1 stimulates strand displacement DNA synthesis. *J Biol Chem,* 276**,** 32411-4.

PRASAD, R., SINGHAL, R. K., SRIVASTAVA, D. K., MOLINA, J. T., TOMKINSON, A. E. & WILSON, S. H. 1996. Specific interaction of DNA polymerase beta and DNA ligase I in a multiprotein base excision repair complex from bovine testis. *J Biol Chem,* 271**,** 16000-7.

QUINZII, C. M., KATTAH, A. G., NAINI, A., AKMAN, H. O., MOOTHA, V. K., DIMAURO, S. & HIRANO, M. 2005. Coenzyme Q deficiency and cerebellar ataxia associated with an aprataxin mutation. *Neurology,* 64**,** 539-41.

RASOULI-NIA, A., KARIMI-BUSHERI, F. & WEINFELD, M. 2004. Stable down-regulation of human polynucleotide kinase enhances spontaneous mutation frequency and sensitizes cells to genotoxic agents. *Proc Natl Acad Sci U S A,* 101**,** 6905-10.

RASS, E., GRABARZ, A., PLO, I., GAUTIER, J., BERTRAND, P. & LOPEZ, B. S. 2009. Role of Mre11 in chromosomal nonhomologous end joining in mammalian cells. *Nat Struct Mol Biol,* 16**,** 819-24.

RASS, U., AHEL, I. & WEST, S. C. 2007a. Actions of aprataxin in multiple DNA repair pathways. *J Biol Chem*.

RASS, U., AHEL, I. & WEST, S. C. 2007b. Defective DNA repair and neurodegenerative disease. *Cell,* 130**,** 991-1004.

RASS, U., AHEL, I. & WEST, S. C. 2008. Molecular mechanism of DNA deadenylation by the neurological disease protein aprataxin. *J Biol Chem,* 283**,** 33994-4001.

RASS, U., COMPTON, S. A., MATOS, J., SINGLETON, M. R., IP, S. C., BLANCO, M. G., GRIFFITH, J. D. & WEST, S. C. 2010. Mechanism of Holliday junction resolution by the human GEN1 protein. *Genes & development,* 24**,** 1559-69.

REED, W. B., MARY, S. B. & NICKEL, W. R. 1965. Xeroderma Pigmentosum with Neurological Complications: The De Sanctis-Cacchione Syndrome. *Archives of dermatology,* 91**,** 224-6.

REYNOLDS, J. J., EL-KHAMISY, S. F., KATYAL, S., CLEMENTS, P., MCKINNON, P. J. & CALDECOTT, K. W. 2009. Defective DNA ligation during short-patch single-strand break repair in ataxia oculomotor apraxia 1. *Mol Cell Biol,* 29**,** 1354-62.

RIBALLO, E., DOHERTY, A. J., DAI, Y., STIFF, T., OETTINGER, M. A., JEGGO, P. A. & KYSELA, B. 2001. Cellular and biochemical impact of a mutation in DNA ligase IV conferring clinical radiosensitivity. *The Journal of biological chemistry,* 276**,** 31124-32.

RIBALLO, E., WOODBINE, L., STIFF, T., WALKER, S. A., GOODARZI, A. A. & JEGGO, P. A. 2009. XLF-Cernunnos promotes DNA ligase IV-XRCC4 re-adenylation following ligation. *Nucleic acids research,* 37**,** 482-92.

RICH, T., ALLEN, R. L. & WYLLIE, A. H. 2000. Defying death after DNA damage. *Nature,* 407**,** 777-83.

ROBERTS, S. A., STRANDE, N., BURKHALTER, M. D., STROM, C., HAVENER, J. M., HASTY, P. & RAMSDEN, D. A. 2010. Ku is a 5'-dRP/AP lyase that excises nucleotide damage near broken ends. *Nature,* 464**,** 1214-7.

ROBERTSON, A. B., KLUNGLAND, A., ROGNES, T. & LEIROS, I. 2009. DNA repair in mammalian cells: Base excision repair: the long and short of it. *Cell Mol Life Sci,* 66**,** 981-93.

ROCA, J. 1995. The mechanisms of DNA topoisomerases. *Trends Biochem Sci,* 20**,** 156-60.

RULTEN, S. L., CORTES-LEDESMA, F., GUO, L., ILES, N. J. & CALDECOTT, K. W. 2008. APLF (C2orf13) is a novel component of poly(ADP-ribose) signaling in mammalian cells. *Molecular and cellular biology,* 28**,** 4620-8.

RULTEN, S. L., FISHER, A. E., ROBERT, I., ZUMA, M. C., ROULEAU, M., JU, L., POIRIER, G., REINA-SAN-MARTIN, B. & CALDECOTT, K. W. 2011. PARP-3 and APLF function together to accelerate nonhomologous end-joining. *Molecular cell,* 41**,** 33-45.

RYDBERG, B. & LINDAHL, T. 1982. Nonenzymatic methylation of DNA by the intracellular methyl group donor S-adenosyl-L-methionine is a potentially mutagenic reaction. *EMBO J,* 1**,** 211-6.

SAIJO, M., KURAOKA, I., MASUTANI, C., HANAOKA, F. & TANAKA, K. 1996. Sequential binding of DNA repair proteins RPA and ERCC1 to XPA in vitro. *Nucleic acids research,* 24**,** 4719-24.

SALVATORE, E., VARRONE, A., CRISCUOLO, C., MANCINI, P., SANSONE, V., STRISCIUGLIO, C., CICALA, D., SCARANO, V., SALVATORE, M., PAPPATA, S., DE MICHELE, G. & FILLA, A. 2008. Nigrostriatal involvement in ataxia with oculomotor apraxia type 1. *J Neurol,* 255**,** 45-8.

SAMBROOK, J. & RUSSELL, D. W. 2001. *Molecular Cloning: A Laboratory Manual,* New York, Cold Sping Harbour Laboratory Press.

SAN FILIPPO, J., CHI, P., SEHORN, M. G., ETCHIN, J., KREJCI, L. & SUNG, P. 2006. Recombination mediator and Rad51 targeting activities of a human BRCA2 polypeptide. *The Journal of biological chemistry,* 281**,** 11649-57.

SANDER, M., CADET, J., CASCIANO, D. A., GALLOWAY, S. M., MARNETT, L. J., NOVAK, R. F., PETTIT, S. D., PRESTON, R. J., SKARE, J. A., WILLIAMS, G. M., VAN HOUTEN, B. & GOLLAPUDI, B. B. 2005. Proceedings of a workshop on DNA adducts: biological significance and applications to risk assessment Washington, DC, April 13-14, 2004. *Toxicol Appl Pharmacol,* 208**,** 1-20.

SANO, Y., DATE, H., IGARASHI, S., ONODERA, O., OYAKE, M., TAKAHASHI, T., HAYASHI, S., MORIMATSU, M., TAKAHASHI, H., MAKIFUCHI, T., FUKUHARA, N. & TSUJI, S. 2004. Aprataxin, the causative protein for EAOH is a nuclear protein with a potential role as a DNA repair protein. *Ann Neurol,* 55**,** 241-9.

SARKANDER, H. I. & UTHOFF, C. G. 1976. Comparison of the number of RNA initiation sites in rat brain fractions enriched in neuronal or glial nuclei. *FEBS Lett,* 72**,** 53-6.

SARTORI, A. A., LUKAS, C., COATES, J., MISTRIK, M., FU, S., BARTEK, J., BAER, R., LUKAS, J. & JACKSON, S. P. 2007. Human CtIP promotes DNA end resection. *Nature,* 450**,** 509-14.

SAVITSKY, K., SFEZ, S., TAGLE, D. A., ZIV, Y., SARTIEL, A., COLLINS, F. S., SHILOH, Y. & ROTMAN, G. 1995. The complete sequence of the coding region of the ATM gene reveals similarity to cell cycle regulators in different species. *Human molecular genetics,* 4**,** 2025-32.

SAXOWSKY, T. T. & DOETSCH, P. W. 2006. RNA polymerase encounters with DNA damage: transcription-coupled repair or transcriptional mutagenesis? *Chemical reviews,* 106**,** 474-88.

SCHLISSEL, M. S., KAFFER, C. R. & CURRY, J. D. 2006. Leukemia and lymphoma: a cost of doing business for adaptive immunity. *Genes & development,* 20**,** 1539-44.

SEDGWICK, B., ROBINS, P. & LINDAHL, T. 2006. Direct removal of alkylation damage from DNA by AlkB and related DNA dioxygenases. *Methods Enzymol,* 408**,** 108-20.

SEGAL-RAZ, H., MASS, G., BARANES-BACHAR, K., LERENTHAL, Y., WANG, S. Y., CHUNG, Y. M., ZIV-LEHRMAN, S., STROM, C. E., HELLEDAY, T., HU, M. C., CHEN, D. J. & SHILOH, Y. 2011. ATM-mediated phosphorylation of polynucleotide kinase/phosphatase is required for effective DNA double-strand break repair. *EMBO reports,* 12**,** 713-9.

SEIDLE, H. F., BIEGANOWSKI, P. & BRENNER, C. 2005. Disease-associated mutations inactivate AMP-lysine hydrolase activity of Aprataxin. *J Biol Chem,* 280**,** 20927-31.

SEKIGUCHI, J., FERGUSON, D. O., CHEN, H. T., YANG, E. M., EARLE, J., FRANK, K., WHITLOW, S., GU, Y., XU, Y., NUSSENZWEIG, A. & ALT, F. W. 2001. Genetic interactions between ATM and the nonhomologous end-joining factors in genomic stability and development.

Proceedings of the National Academy of Sciences of the United States of America, 98**,** 3243-8.

SEKIGUCHI, J. & SHUMAN, S. 1997. Nick sensing by vaccinia virus DNA ligase requires a 5' phosphate at the nick and occupancy of the adenylate binding site on the enzyme. *J Virol,* 71**,** 9679-84.

SEKIJIMA, Y., HASHIMOTO, T., ONODERA, O., DATE, H., OKANO, T., NAITO, K., TSUJI, S. & IKEDA, S. 2003. Severe generalized dystonia as a presentation of a patient with aprataxin gene mutation. *Mov Disord,* 18**,** 1198-200.

SHAHWAN, A., BYRD, P. J., TAYLOR, A. M., NESTOR, T., RYAN, S. & KING, M. D. 2006. Atypical presentation of ataxia-oculomotor apraxia type 1. *Dev Med Child Neurol,* 48**,** 529-32.

SHEN, J., GILMORE, E. C., MARSHALL, C. A., HADDADIN, M., REYNOLDS, J. J., EYAID, W., BODELL, A., BARRY, B., GLEASON, D., ALLEN, K., GANESH, V. S., CHANG, B. S., GRIX, A., HILL, R. S., TOPCU, M., CALDECOTT, K. W., BARKOVICH, A. J. & WALSH, C. A. 2010. Mutations in PNKP cause microcephaly, seizures and defects in DNA repair. *Nat Genet,* 42**,** 245-9.

SHIBUTANI, S., TAKESHITA, M. & GROLLMAN, A. P. 1991. Insertion of specific bases during DNA synthesis past the oxidation-damaged base 8-oxodG. *Nature,* 349**,** 431-4.

SHIMAZAKI, H., TAKIYAMA, Y., SAKOE, K., IKEGUCHI, K., NIIJIMA, K., KANEKO, J., NAMEKAWA, M., OGAWA, T., DATE, H., TSUJI, S., NAKANO, I. & NISHIZAWA, M. 2002a. Early-onset ataxia with ocular motor apraxia and hypoalbuminemia: the aprataxin gene mutations. *Neurology,* 59**,** 590-5.

SHIMAZAKI, N., YOSHIDA, K., KOBAYASHI, T., TOJI, S., TAMAI, K. & KOIWAI, O. 2002b. Over-expression of human DNA polymerase lambda in E. coli and characterization of the recombinant enzyme. *Genes Cells,* 7**,** 639-51.

SHIVJI, K. K., KENNY, M. K. & WOOD, R. D. 1992. Proliferating cell nuclear antigen is required for DNA excision repair. *Cell,* 69**,** 367-74.

SHUMAN, S. 1995. Vaccinia virus DNA ligase: specificity, fidelity, and inhibition. *Biochemistry,* 34**,** 16138-47.

SHUMAN, S. & SCHWER, B. 1995. RNA capping enzyme and DNA ligase: a superfamily of covalent nucleotidyl transferases. *Mol Microbiol,* 17**,** 405-10.

SIBANDA, B. L., CRITCHLOW, S. E., BEGUN, J., PEI, X. Y., JACKSON, S. P., BLUNDELL, T. L. & PELLEGRINI, L. 2001. Crystal structure of an Xrcc4-DNA ligase IV complex. *Nature structural biology,* 8**,** 1015-9.

SIJBERS, A. M., DE LAAT, W. L., ARIZA, R. R., BIGGERSTAFF, M., WEI, Y. F., MOGGS, J. G., CARTER, K. C., SHELL, B. K., EVANS, E., DE JONG, M. C., RADEMAKERS, S., DE ROOIJ, J., JASPERS, N. G., HOEIJMAKERS, J. H. & WOOD, R. D. 1996. Xeroderma pigmentosum group F caused by a defect in a structure-specific DNA repair endonuclease. *Cell,* 86**,** 811-22.

SIMMONDS, H. A., WEBSTER, D. R., WILSON, J. & LINGHAM, S. 1982. An X-linked syndrome characterised by hyperuricaemia, deafness, and neurodevelopmental abnormalities. *Lancet,* 2**,** 68-70.

SIMSEK, D., FURDA, A., GAO, Y., ARTUS, J., BRUNET, E., HADJANTONAKIS, A. K., VAN HOUTEN, B., SHUMAN, S., MCKINNON, P. J. & JASIN, M. 2011. Crucial role for DNA ligase III in mitochondria but not in Xrcc1-dependent repair. *Nature,* 471**,** 245-8.

SINGHAL, R. K., PRASAD, R. & WILSON, S. H. 1995. DNA polymerase beta conducts the gap-filling step in uracil-initiated base excision repair in a bovine testis nuclear extract. *J Biol Chem,* 270**,** 949-57.

SLEETH, K. M., ROBSON, R. L. & DIANOV, G. L. 2004. Exchangeability of mammalian DNA ligases between base excision repair pathways. *Biochemistry,* 43**,** 12924-30.

SOBOL, R. W., HORTON, J. K., KUHN, R., GU, H., SINGHAL, R. K., PRASAD, R., RAJEWSKY, K. & WILSON, S. H. 1996. Requirement of mammalian DNA polymerase-beta in base-excision repair. *Nature,* 379**,** 183-6.

SOBOL, R. W., PRASAD, R., EVENSKI, A., BAKER, A., YANG, X. P., HORTON, J. K. & WILSON, S. H. 2000. The lyase activity of the DNA repair protein beta-polymerase protects from DNA-damage-induced cytotoxicity. *Nature,* 405**,** 807-10.

SONODA, E., HOCHEGGER, H., SABERI, A., TANIGUCHI, Y. & TAKEDA, S. 2006. Differential usage of non-homologous end-joining and homologous recombination in double strand break repair. *DNA repair,* 5**,** 1021-9.

SQUIRES, S. & JOHNSON, R. T. 1983. U.v. induces long-lived DNA breaks in Cockayne's syndrome and cells from an immunodeficient individual (46BR): defects and disturbance in post incision steps of excision repair. *Carcinogenesis,* 4**,** 565-72.

SRISKANDA, V., SCHWER, B., HO, C. K. & SHUMAN, S. 1999. Mutational analysis of Escherichia coli DNA ligase identifies amino acids required for nick-ligation in vitro and for in vivo complementation of the growth of yeast cells deleted for CDC9 and LIG4. *Nucleic Acids Res,* 27**,** 3953-63.

SRISKANDA, V. & SHUMAN, S. 1998a. Chlorella virus DNA ligase: nick recognition and mutational analysis. *Nucleic Acids Res,* 26**,** 525-31.

SRISKANDA, V. & SHUMAN, S. 1998b. Mutational analysis of Chlorella virus DNA ligase: catalytic roles of domain I and motif VI. *Nucleic Acids Res,* 26**,** 4618-25.

SRISKANDA, V. & SHUMAN, S. 1998c. Specificity and fidelity of strand joining by Chlorella virus DNA ligase. *Nucleic Acids Res,* 26**,** 3536-41.

SRISKANDA, V. & SHUMAN, S. 2002a. Role of nucleotidyl transferase motif V in strand joining by chlorella virus DNA ligase. *J Biol Chem,* 277**,** 9661-7.

SRISKANDA, V. & SHUMAN, S. 2002b. Role of nucleotidyltransferase motifs I, III and IV in the catalysis of phosphodiester bond formation by Chlorella virus DNA ligase. *Nucleic Acids Res,* 30**,** 903-11.

STEININGER, S., AHNE, F., WINKLER, K., KLEINSCHMIDT, A., ECKARDT-SCHUPP, F. & MOERTL, S. 2010. A novel function for the Mre11-Rad50-Xrs2 complex in base excision repair. *Nucleic Acids Res,* 38**,** 1853-65.

STEWART, G. S., MASER, R. S., STANKOVIC, T., BRESSAN, D. A., KAPLAN, M. I., JASPERS, N. G., RAAMS, A., BYRD, P. J., PETRINI, J. H. & TAYLOR, A. M. 1999. The DNA double-strand break repair gene hMRE11 is mutated in individuals with an ataxia-telangiectasia-like disorder. *Cell,* 99**,** 577-87.

STEWART, G. S., PANIER, S., TOWNSEND, K., AL-HAKIM, A. K., KOLAS, N. K., MILLER, E. S., NAKADA, S., YLANKO, J., OLIVARIUS, S., MENDEZ, M., OLDREIVE, C., WILDENHAIN, J., TAGLIAFERRO, A., PELLETIER, L., TAUBENHEIM, N., DURANDY, A., BYRD, P. J., STANKOVIC, T., TAYLOR, A. M. & DUROCHER, D. 2009. The RIDDLE syndrome protein mediates a ubiquitin-dependent signaling cascade at sites of DNA damage. *Cell,* 136**,** 420-34.

STEWART, G. S., STANKOVIC, T., BYRD, P. J., WECHSLER, T., MILLER, E. S., HUISSOON, A., DRAYSON, M. T., WEST, S. C., ELLEDGE, S. J. & TAYLOR, A. M. 2007. RIDDLE immunodeficiency syndrome is linked to defects in 53BP1-mediated DNA damage signaling. *Proceedings of the National Academy of Sciences of the United States of America,* 104**,** 16910-5.

STIFF, T., REIS, C., ALDERTON, G. K., WOODBINE, L., O'DRISCOLL, M. & JEGGO, P. A. 2005. Nbs1 is required for ATR-dependent phosphorylation events. *The EMBO journal,* 24**,** 199-208.

STOLER, D. L., CHEN, N., BASIK, M., KAHLENBERG, M. S., RODRIGUEZ-BIGAS, M. A., PETRELLI, N. J. & ANDERSON, G. R. 1999. The onset and extent of genomic instability in sporadic colorectal tumor progression. *Proceedings of the National Academy of Sciences of the United States of America,* 96**,** 15121-6.

STRACKER, T. H. & PETRINI, J. H. 2011. The MRE11 complex: starting from the ends. *Nature reviews. Molecular cell biology,* 12**,** 90-103.

STRATTON, M. R., CAMPBELL, P. J. & FUTREAL, P. A. 2009. The cancer genome. *Nature,* 458**,** 719-24.

STUCKI, M. & JACKSON, S. P. 2004. MDC1/NFBD1: a key regulator of the DNA damage response in higher eukaryotes. *DNA repair,* 3**,** 953-7.

STUCKI, M., PASCUCCI, B., PARLANTI, E., FORTINI, P., WILSON, S. H., HUBSCHER, U. & DOGLIOTTI, E. 1998. Mammalian base excision repair by DNA polymerases delta and epsilon. *Oncogene,* 17**,** 835-43.

SUGASAWA, K., NG, J. M., MASUTANI, C., IWAI, S., VAN DER SPEK, P. J., EKER, A. P., HANAOKA, F., BOOTSMA, D. & HOEIJMAKERS, J. H. 1998. Xeroderma pigmentosum group C protein complex is the initiator of global genome nucleotide excision repair. *Molecular cell,* 2**,** 223-32.

SUGASAWA, K., OKAMOTO, T., SHIMIZU, Y., MASUTANI, C., IWAI, S. & HANAOKA, F. 2001. A multistep damage recognition mechanism for global genomic nucleotide excision repair. *Genes & development,* 15**,** 507-21.

SUGAWARA, M., WADA, C., OKAWA, S., KOBAYASHI, M., SAGESHIMA, M., IMOTA, T. & TOYOSHIMA, I. 2008. Purkinje cell loss in the cerebellar flocculus in patients with ataxia with ocular motor apraxia type 1/early-onset ataxia with ocular motor apraxia and hypoalbuminemia. *Eur Neurol,* 59**,** 18-23.

SUNG, P. & KLEIN, H. 2006. Mechanism of homologous recombination: mediators and helicases take on regulatory functions. *Nature reviews. Molecular cell biology,* 7**,** 739-50.

SUWA, A., HIRAKATA, M., TAKEDA, Y., JESCH, S. A., MIMORI, T. & HARDIN, J. A. 1994. DNA-dependent protein kinase (Ku protein-p350 complex) assembles on double-stranded DNA. *Proceedings of the National Academy of Sciences of the United States of America,* 91**,** 6904-8.

SVENDSEN, J. M. & HARPER, J. W. 2010. GEN1/Yen1 and the SLX4 complex: Solutions to the problem of Holliday junction resolution. *Genes & development,* 24**,** 521-36.

SY, S. M., HUEN, M. S. & CHEN, J. 2009. PALB2 is an integral component of the BRCA complex required for homologous recombination repair. *Proceedings of the National Academy of Sciences of the United States of America,* 106**,** 7155-60.

TACHI, N., KOZUKA, N., OHYA, K., CHIBA, S. & SASAKI, K. 2000. Hereditary cerebellar ataxia with peripheral neuropathy and mental retardation. *Eur Neurol,* 43**,** 82-7.

TADA, M., YOKOSEKI, A., SATO, T., MAKIFUCHI, T. & ONODERA, O. 2010. Early-onset ataxia with ocular motor apraxia and hypoalbuminemia/ataxia with oculomotor apraxia 1. *Adv Exp Med Biol,* 685**,** 21-33.

TAKAHASHI, T., TADA, M., IGARASHI, S., KOYAMA, A., DATE, H., YOKOSEKI, A., SHIGA, A., YOSHIDA, Y., TSUJI, S., NISHIZAWA, M. & ONODERA, O. 2007a. Aprataxin, causative gene product for EAOH/AOA1, repairs DNA single-strand breaks with damaged 3'-phosphate and 3'-phosphoglycolate ends. *Nucleic Acids Res*.

TAKAHASHI, T., TADA, M., IGARASHI, S., KOYAMA, A., DATE, H., YOKOSEKI, A., SHIGA, A., YOSHIDA, Y., TSUJI, S., NISHIZAWA, M. & ONODERA, O. 2007b. Aprataxin, causative gene product for EAOH/AOA1, repairs DNA single-strand breaks with damaged 3'-phosphate and 3'-phosphoglycolate ends. *Nucleic Acids Res,* 35**,** 3797-809.

TAKASAKI, Y., DENG, J. S. & TAN, E. M. 1981. A nuclear antigen associated with cell proliferation and blast transformation. *J Exp Med,* 154**,** 1899-909.

TAKASHIMA, H., BOERKOEL, C. F., JOHN, J., SAIFI, G. M., SALIH, M. A., ARMSTRONG, D., MAO, Y., QUIOCHO, F. A., ROA, B. B., NAKAGAWA, M., STOCKTON, D. W. & LUPSKI, J. R. 2002. Mutation of TDP1, encoding a topoisomerase I-dependent DNA damage repair enzyme, in spinocerebellar ataxia with axonal neuropathy. *Nat Genet,* 32**,** 267-72.

TAKATA, M., SASAKI, M. S., SONODA, E., MORRISON, C., HASHIMOTO, M., UTSUMI, H., YAMAGUCHI-IWAI, Y., SHINOHARA, A. & TAKEDA, S. 1998. Homologous recombination and non-homologous end-joining pathways of DNA double-strand break repair have overlapping roles in the maintenance of chromosomal integrity in vertebrate cells. *The EMBO journal,* 17**,** 5497-508.

TANAKA, K., MIURA, N., SATOKATA, I., MIYAMOTO, I., YOSHIDA, M. C., SATOH, Y., KONDO, S., YASUI, A., OKAYAMA, H. & OKADA, Y. 1990. Analysis of a human DNA excision repair gene involved in group A xeroderma pigmentosum and containing a zinc-finger domain. *Nature,* 348**,** 73-6.

TANTIN, D. 1998. RNA polymerase II elongation complexes containing the Cockayne syndrome group B protein interact with a molecular complex containing the transcription factor IIH components xeroderma pigmentosum B and p62. *The Journal of biological chemistry,* 273**,** 27794-9.

TAPIAS, A., AURIOL, J., FORGET, D., ENZLIN, J. H., SCHARER, O. D., COIN, F., COULOMBE, B. & EGLY, J. M. 2004. Ordered conformational changes in damaged DNA induced by nucleotide excision repair factors. *The Journal of biological chemistry,* 279**,** 19074-83.

TAVANI, F., ZIMMERMAN, R. A., BERRY, G. T., SULLIVAN, K., GATTI, R. & BINGHAM, P. 2003. Ataxia-telangiectasia: the pattern of cerebellar atrophy on MRI. *Neuroradiology,* 45**,** 315-9.

TAYLOR, A. M., GROOM, A. & BYRD, P. J. 2004. Ataxia-telangiectasia-like disorder (ATLD)-its clinical presentation and molecular basis. *DNA repair,* 3**,** 1219-25.

TAYLOR, R. M., MOORE, D. J., WHITEHOUSE, J., JOHNSON, P. & CALDECOTT, K. W. 2000a. A cell cycle-specific requirement for the XRCC1 BRCT II domain during mammalian DNA strand break repair. *Mol Cell Biol,* 20**,** 735-40.

TAYLOR, R. M., WHITEHOUSE, C. J. & CALDECOTT, K. W. 2000b. The DNA ligase III zinc finger stimulates binding to DNA secondary structure and promotes end joining. *Nucleic Acids Res,* 28**,** 3558-63.

TAYLOR, R. M., WICKSTEAD, B., CRONIN, S. & CALDECOTT, K. W. 1998. Role of a BRCT domain in the interaction of DNA ligase III-alpha with the DNA repair protein XRCC1. *Curr Biol,* 8**,** 877-80.

TEBBS, R. S., FLANNERY, M. L., MENESES, J. J., HARTMANN, A., TUCKER, J. D., THOMPSON, L. H., CLEAVER, J. E. & PEDERSEN, R. A. 1999. Requirement for the Xrcc1 DNA base excision repair gene during early mouse development. *Dev Biol,* 208**,** 513-29.

TEBBS, R. S., THOMPSON, L. H. & CLEAVER, J. E. 2003. Rescue of Xrcc1 knockout mouse embryo lethality by transgene-complementation. *DNA Repair (Amst),* 2**,** 1405-17.

TEO, I. A., ARLETT, C. F., HARCOURT, S. A., PRIESTLEY, A. & BROUGHTON, B. C. 1983a. Multiple hypersensitivity to mutagens in a cell strain (46BR) derived from a patient with immuno-deficiencies. *Mutation research,* 107**,** 371-86.

TEO, I. A., BROUGHTON, B. C., DAY, R. S., JAMES, M. R., KARRAN, P., MAYNE, L. V. & LEHMANN, A. R. 1983b. A biochemical defect in the repair of alkylated DNA in cells from an immunodeficient patient (46BR). *Carcinogenesis,* 4**,** 559-64.

TIJSTERMAN, M., VERHAGE, R. A., VAN DE PUTTE, P., TASSERON-DE JONG, J. G. & BROUWER, J. 1997. Transitions in the coupling of transcription and nucleotide excision repair within

RNA polymerase II-transcribed genes of Saccharomyces cerevisiae. *Proceedings of the National Academy of Sciences of the United States of America,* 94**,** 8027-32.

TOMKINSON, A. E., VIJAYAKUMAR, S., PASCAL, J. M. & ELLENBERGER, T. 2006. DNA ligases: structure, reaction mechanism, and function. *Chem Rev,* 106**,** 687-99.

TORNALETTI, S. 2009. DNA repair in mammalian cells: Transcription-coupled DNA repair: directing your effort where it's most needed. *Cellular and molecular life sciences : CMLS,* 66**,** 1010-20.

TRANCHANT, C., FLEURY, M., MOREIRA, M. C., KOENIG, M. & WARTER, J. M. 2003. Phenotypic variability of aprataxin gene mutations. *Neurology,* 60**,** 868-70.

TSAI, C. J., KIM, S. A. & CHU, G. 2007. Cernunnos/XLF promotes the ligation of mismatched and noncohesive DNA ends. *Proceedings of the National Academy of Sciences of the United States of America,* 104**,** 7851-6.

TSAO, C. Y. & PAULSON, G. 2005. Type 1 ataxia with oculomotor apraxia with aprataxin gene mutations in two American children. *J Child Neurol,* 20**,** 619-20.

TU, Y., BATES, S. & PFEIFER, G. P. 1997. Sequence-specific and domain-specific DNA repair in xeroderma pigmentosum and Cockayne syndrome cells. *The Journal of biological chemistry,* 272**,** 20747-55.

TU, Y., BATES, S. & PFEIFER, G. P. 1998. The transcription-repair coupling factor CSA is required for efficient repair only during the elongation stages of RNA polymerase II transcription. *Mutation research,* 400**,** 143-51.

UEMATSU, N., WETERINGS, E., YANO, K., MOROTOMI-YANO, K., JAKOB, B., TAUCHER-SCHOLZ, G., MARI, P. O., VAN GENT, D. C., CHEN, B. P. & CHEN, D. J. 2007. Autophosphorylation of DNA-PKCS regulates its dynamics at DNA double-strand breaks. *The Journal of cell biology,* 177**,** 219-29.

UZIEL, T., LERENTHAL, Y., MOYAL, L., ANDEGEKO, Y., MITTELMAN, L. & SHILOH, Y. 2003. Requirement of the MRN complex for ATM activation by DNA damage. *The EMBO journal,* 22**,** 5612-21.

VARON, R., VISSINGA, C., PLATZER, M., CEROSALETTI, K. M., CHRZANOWSKA, K. H., SAAR, K., BECKMANN, G., SEEMANOVA, E., COOPER, P. R., NOWAK, N. J., STUMM, M., WEEMAES, C. M., GATTI, R. A., WILSON, R. K., DIGWEED, M., ROSENTHAL, A., SPERLING, K., CONCANNON, P. & REIS, A. 1998. Nibrin, a novel DNA double-strand break repair protein, is mutated in Nijmegen breakage syndrome. *Cell,* 93**,** 467-76.

VENKITARAMAN, A. R. 2002. Cancer susceptibility and the functions of BRCA1 and BRCA2. *Cell,* 108**,** 171-82.

VENS, C., HOFLAND, I. & BEGG, A. C. 2007. Involvement of DNA polymerase beta in repair of ionizing radiation damage as measured by in vitro plasmid assays. *Radiat Res,* 168**,** 281-91.

VERMEULEN, C., BERTOCCI, B., BEGG, A. C. & VENS, C. 2007a. Ionizing radiation sensitivity of DNA polymerase lambda-deficient cells. *Radiat Res,* 168**,** 683-8.

VERMEULEN, C., VERWIJS-JANSSEN, M., BEGG, A. C. & VENS, C. 2008. Cell cycle phase dependent role of DNA polymerase beta in DNA repair and survival after ionizing radiation. *Radiother Oncol,* 86**,** 391-8.

VERMEULEN, C., VERWIJS-JANSSEN, M., CRAMERS, P., BEGG, A. C. & VENS, C. 2007b. Role for DNA polymerase beta in response to ionizing radiation. *DNA Repair (Amst),* 6**,** 202-12.

VIDAL, A. E., BOITEUX, S., HICKSON, I. D. & RADICELLA, J. P. 2001. XRCC1 coordinates the initial and late stages of DNA abasic site repair through protein-protein interactions. *EMBO J,* 20**,** 6530-9.

VOLKER, M., MONE, M. J., KARMAKAR, P., VAN HOFFEN, A., SCHUL, W., VERMEULEN, W., HOEIJMAKERS, J. H., VAN DRIEL, R., VAN ZEELAND, A. A. & MULLENDERS, L. H. 2001.

Sequential assembly of the nucleotide excision repair factors in vivo. *Molecular cell,* 8**,** 213-24.

VON SONNTAG, C. 1987. *The Chemical Basis of Radiation Biology,* London, Taylor and Francis.

WAGA, S. & STILLMAN, B. 1998. The DNA replication fork in eukaryotic cells. *Annu Rev Biochem,* 67**,** 721-51.

WALKER, J. R., CORPINA, R. A. & GOLDBERG, J. 2001. Structure of the Ku heterodimer bound to DNA and its implications for double-strand break repair. *Nature,* 412**,** 607-14.

WALTON, C., INTERTHAL, H., HIRANO, R., SALIH, M. A., TAKASHIMA, H. & BOERKOEL, C. F. 2010. Spinocerebellar ataxia with axonal neuropathy. *Adv Exp Med Biol,* 685**,** 75-83.

WANG, J. C. 2002. Cellular roles of DNA topoisomerases: a molecular perspective. *Nat Rev Mol Cell Biol,* 3**,** 430-40.

WANG, Y., LAMARCHE, B. J. & TSAI, M. D. 2007. Human DNA ligase IV and the ligase IV/XRCC4 complex: analysis of nick ligation fidelity. *Biochemistry,* 46**,** 4962-76.

WARBRICK, E., COATES, P. J. & HALL, P. A. 1998. Fen1 expression: a novel marker for cell proliferation. *J Pathol,* 186**,** 319-24.

WARD, J. 1998. Nature of lesions formed by ionising radiation. *In:* JA, N. (ed.) *DNA Damage and Repair Vol2: DNA Repair in Higher Eukaryotes.* Totowa NJ: Human Press Inc.

WARD, J. F. 1975. Radiation-induced strand breakage in DNA. *Basic Life Sci,* 5B**,** 471-2.

WARD, J. F., EVANS, J. W., LIMOLI, C. L. & CALABRO-JONES, P. M. 1987. Radiation and hydrogen peroxide induced free radical damage to DNA. *Br J Cancer Suppl,* 8**,** 105-12.

WATSON, J. D. & HAYES, W. 1953. Genetic Exchange in Escherichia Coli K(12): Evidence for Three Linkage Groups. *Proceedings of the National Academy of Sciences of the United States of America,* 39**,** 416-26.

WEINFELD, M., CHAUDHRY, M. A., D'AMOURS, D., PELLETIER, J. D., POIRIER, G. G., POVIRK, L. F. & LEES-MILLER, S. P. 1997. Interaction of DNA-dependent protein kinase and poly(ADP-ribose) polymerase with radiation-induced DNA strand breaks. *Radiat Res,* 148**,** 22-8.

WEISS, B., JACQUEMIN-SABLON, A., LIVE, T. R., FAREED, G. C. & RICHARDSON, C. C. 1968a. Enzymatic breakage and joining of deoxyribonucleic acid. VI. Further purification and properties of polynucleotide ligase from Escherichia coli infected with bacteriophage T4. *J Biol Chem,* 243**,** 4543-55.

WEISS, B., THOMPSON, A. & RICHARDSON, C. C. 1968b. Ezymatic breakage and joining of deoxyribonucleic acid. VII. Properties of the enzyme-adenylate intermediate in the polynucleotide ligase reaction. *J Biol Chem,* 243**,** 4556-63.

WEISSMAN, L., DE SOUZA-PINTO, N. C., STEVNSNER, T. & BOHR, V. A. 2007. DNA repair, mitochondria, and neurodegeneration. *Neuroscience,* 145**,** 1318-29.

WEST, S. C. 2003. Molecular views of recombination proteins and their control. *Nature reviews. Molecular cell biology,* 4**,** 435-45.

WHITEHOUSE, C. J., TAYLOR, R. M., THISTLETHWAITE, A., ZHANG, H., KARIMI-BUSHERI, F., LASKO, D. D., WEINFELD, M. & CALDECOTT, K. W. 2001. XRCC1 stimulates human polynucleotide kinase activity at damaged DNA termini and accelerates DNA single-strand break repair. *Cell,* 104**,** 107-17.

WILLIAMS, R. S., MONCALIAN, G., WILLIAMS, J. S., YAMADA, Y., LIMBO, O., SHIN, D. S., GROOCOCK, L. M., CAHILL, D., HITOMI, C., GUENTHER, G., MOIANI, D., CARNEY, J. P., RUSSELL, P. & TAINER, J. A. 2008. Mre11 dimers coordinate DNA end bridging and nuclease processing in double-strand-break repair. *Cell,* 135**,** 97-109.

WILLIAMS, R. S., WILLIAMS, J. S. & TAINER, J. A. 2007. Mre11-Rad50-Nbs1 is a keystone complex connecting DNA repair machinery, double-strand break signaling, and the chromatin template. *Biochemistry and cell biology = Biochimie et biologie cellulaire,* 85**,** 509-20.

WINTERS, T. A., HENNER, W. D., RUSSELL, P. S., MCCULLOUGH, A. & JORGENSEN, T. J. 1994. Removal of 3'-phosphoglycolate from DNA strand-break damage in an oligonucleotide substrate by recombinant human apurinic/apyrimidinic endonuclease 1. *Nucleic Acids Res,* 22**,** 1866-73.

WINTERS, T. A., RUSSELL, P. S., KOHLI, M., DAR, M. E., NEUMANN, R. D. & JORGENSEN, T. J. 1999. Determination of human DNA polymerase utilization for the repair of a model ionizing radiation-induced DNA strand break lesion in a defined vector substrate. *Nucleic Acids Res,* 27**,** 2423-33.

WINTERS, T. A., WEINFELD, M. & JORGENSEN, T. J. 1992. Human HeLa cell enzymes that remove phosphoglycolate 3'-end groups from DNA. *Nucleic Acids Res,* 20**,** 2573-80.

WIST, E. & PRYDZ, H. 1979. The effect of aphidicolin on DNA synthesis in isolated HeLa cell nuclei. *Nucleic Acids Res,* 6**,** 1583-90.

WONG, A. K., PERO, R., ORMONDE, P. A., TAVTIGIAN, S. V. & BARTEL, P. L. 1997. RAD51 interacts with the evolutionarily conserved BRC motifs in the human breast cancer susceptibility gene brca2. *The Journal of biological chemistry,* 272**,** 31941-4.

WRIGHT, G. E., HUBSCHER, U., KHAN, N. N., FOCHER, F. & VERRI, A. 1994. Inhibitor analysis of calf thymus DNA polymerases alpha, delta and epsilon. *FEBS Lett,* 341**,** 128-30.

WU, J. & LIU, L. F. 1997. Processing of topoisomerase I cleavable complexes into DNA damage by transcription. *Nucleic acids research,* 25**,** 4181-6.

WU, L. & HICKSON, I. D. 2003. The Bloom's syndrome helicase suppresses crossing over during homologous recombination. *Nature,* 426**,** 870-4.

WU, P. Y., FRIT, P., MALIVERT, L., REVY, P., BIARD, D., SALLES, B. & CALSOU, P. 2007. Interplay between Cernunnos-XLF and nonhomologous end-joining proteins at DNA ends in the cell. *The Journal of biological chemistry,* 282**,** 31937-43.

XANTHOUDAKIS, S., SMEYNE, R. J., WALLACE, J. D. & CURRAN, T. 1996. The redox/DNA repair protein, Ref-1, is essential for early embryonic development in mice. *Proc Natl Acad Sci U S A,* 93**,** 8919-23.

XIE, A., KWOK, A. & SCULLY, R. 2009. Role of mammalian Mre11 in classical and alternative nonhomologous end joining. *Nat Struct Mol Biol,* 16**,** 814-8.

XIE, H. R., HU, L. S. & LI, G. Y. 2010. SH-SY5Y human neuroblastoma cell line: in vitro cell model of dopaminergic neurons in Parkinson's disease. *Chinese medical journal,* 123**,** 1086-92.

YANG, S. W., BURGIN, A. B., JR., HUIZENGA, B. N., ROBERTSON, C. A., YAO, K. C. & NASH, H. A. 1996. A eukaryotic enzyme that can disjoin dead-end covalent complexes between DNA and type I topoisomerases. *Proc Natl Acad Sci U S A,* 93**,** 11534-9.

YANO, K., MOROTOMI-YANO, K., WANG, S. Y., UEMATSU, N., LEE, K. J., ASAITHAMBY, A., WETERINGS, E. & CHEN, D. J. 2008. Ku recruits XLF to DNA double-strand breaks. *EMBO reports,* 9**,** 91-6.

YOO, S. & DYNAN, W. S. 1999. Geometry of a complex formed by double strand break repair proteins at a single DNA end: recruitment of DNA-PKcs induces inward translocation of Ku protein. *Nucleic acids research,* 27**,** 4679-86.

YOON, G., WESTMACOTT, R., MACMILLAN, L., QUERCIA, N., KOUTSOU, P., GEORGHIOU, A., CHRISTODOULOU, K. & BANWELL, B. 2008. Complete deletion of the aprataxin gene: ataxia with oculomotor apraxia type 1 with severe phenotype and cognitive deficit. *J Neurol Neurosurg Psychiatry,* 79**,** 234-6.

YOU, Z., SHI, L. Z., ZHU, Q., WU, P., ZHANG, Y. W., BASILIO, A., TONNU, N., VERMA, I. M., BERNS, M. W. & HUNTER, T. 2009a. CtIP links DNA double-strand break sensing to resection. *Mol Cell,* 36**,** 954-69.

YOU, Z., SHI, L. Z., ZHU, Q., WU, P., ZHANG, Y. W., BASILIO, A., TONNU, N., VERMA, I. M., BERNS, M. W. & HUNTER, T. 2009b. CtIP links DNA double-strand break sensing to resection. *Molecular cell,* 36**,** 954-69.

ZAHRADKA, P. & EBISUZAKI, K. 1982. A shuttle mechanism for DNA-protein interactions. The regulation of poly(ADP-ribose) polymerase. *Eur J Biochem,* 127**,** 579-85.

ZENG, Z., CORTES-LEDESMA, F., EL KHAMISY, S. F. & CALDECOTT, K. W. 2011. TDP2/TTRAP is the major 5'-tyrosyl DNA phosphodiesterase activity in vertebrate cells and is critical for cellular resistance to topoisomerase II-induced DNA damage. *The Journal of biological chemistry,* 286**,** 403-9.

ZHANG, F., MA, J., WU, J., YE, L., CAI, H., XIA, B. & YU, X. 2009. PALB2 links BRCA1 and BRCA2 in the DNA-damage response. *Current biology : CB,* 19**,** 524-9.

ZHANG, Y., YUAN, F., PRESNELL, S. R., TIAN, K., GAO, Y., TOMKINSON, A. E., GU, L. & LI, G. M. 2005. Reconstitution of 5'-directed human mismatch repair in a purified system. *Cell,* 122**,** 693-705.

ZHENG, L., DAI, H., ZHOU, M., LI, M., SINGH, P., QIU, J., TSARK, W., HUANG, Q., KERNSTINE, K., ZHANG, X., LIN, D. & SHEN, B. 2007. Fen1 mutations result in autoimmunity, chronic inflammation and cancers. *Nature medicine,* 13**,** 812-9.

ZHONG, S., CHEN, X., ZHU, X., DZIEGIELEWSKA, B., BACHMAN, K. E., ELLENBERGER, T., BALLIN, J. D., WILSON, G. M., TOMKINSON, A. E. & MACKERELL, A. D., JR. 2008. Identification and validation of human DNA ligase inhibitors using computer-aided drug design. *Journal of medicinal chemistry,* 51**,** 4553-62.

ZHOU, T., LEE, J. W., TATAVARTHI, H., LUPSKI, J. R., VALERIE, K. & POVIRK, L. F. 2005. Deficiency in 3'-phosphoglycolate processing in human cells with a hereditary mutation in tyrosyl-DNA phosphodiesterase (TDP1). *Nucleic Acids Res,* 33**,** 289-97.

ZHOU, W. & DOETSCH, P. W. 1994. Transcription bypass or blockage at single-strand breaks on the DNA template strand: effect of different 3' and 5' flanking groups on the T7 RNA polymerase elongation complex. *Biochemistry,* 33**,** 14926-34.

ZHU, C., BOGUE, M. A., LIM, D. S., HASTY, P. & ROTH, D. B. 1996. Ku86-deficient mice exhibit severe combined immunodeficiency and defective processing of V(D)J recombination intermediates. *Cell,* 86**,** 379-89.

ZHU, Z., CHUNG, W. H., SHIM, E. Y., LEE, S. E. & IRA, G. 2008. Sgs1 helicase and two nucleases Dna2 and Exo1 resect DNA double-strand break ends. *Cell,* 134**,** 981-94.

ZUHLKE, C., BERNARD, V. & GILLESSEN-KAESBACH, G. 2007. Investigation of recessive ataxia loci in patients with young age of onset. *Neuropediatrics,* 38**,** 207-9.

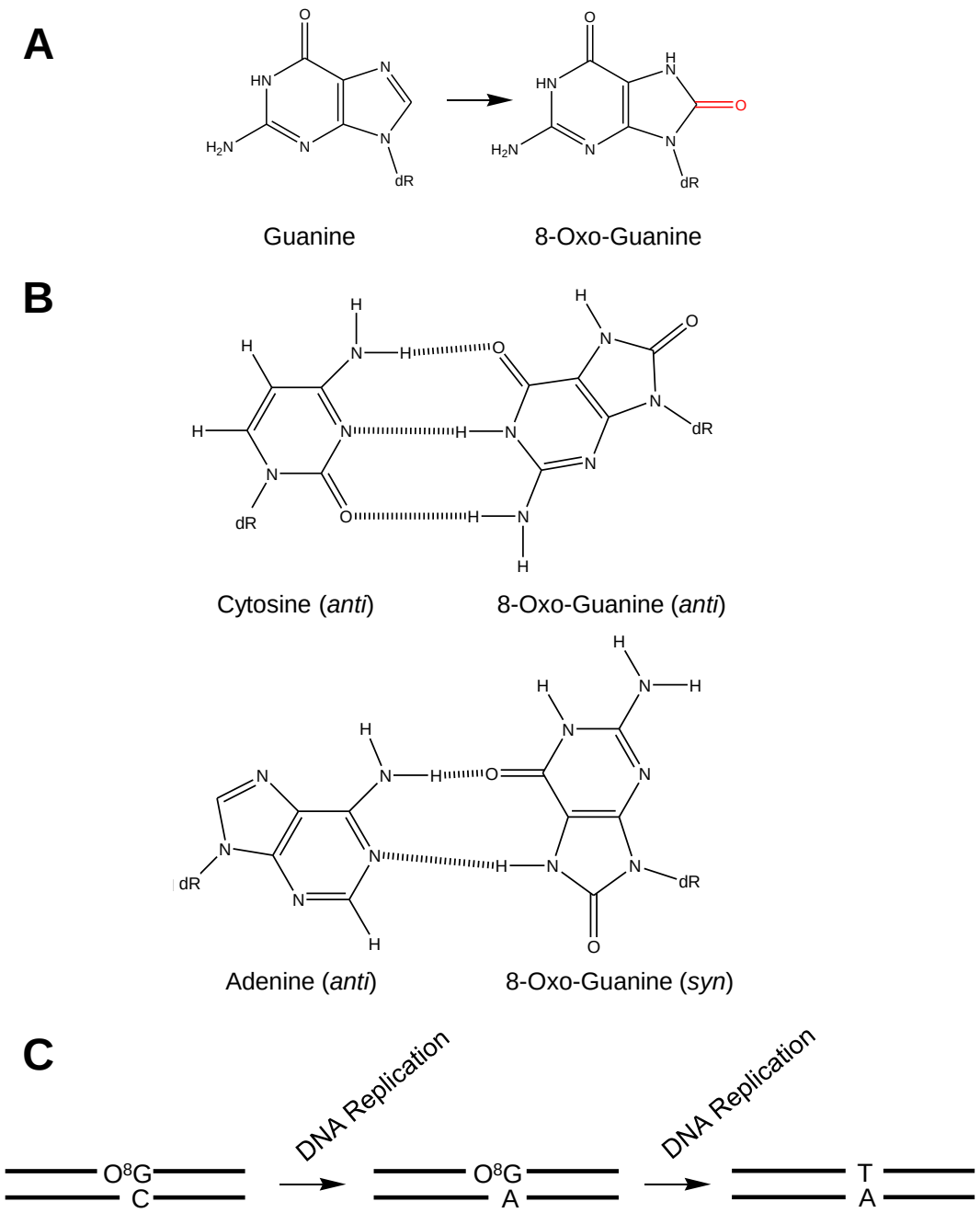

Figure 1.1 - The mutagenic potential of the common oxidative lesion 8-oxo-guanine

Oxidative base adducts are an abundant type of DNA damage that can be caused by reactive oxygen species generated as by-products of cellular metabolism. Oxidation of guanine can lead to the formation of 8-oxo-guanine (8-oxo-G) (**A**)**.** 8-oxo-G is the probably one of the most abundant oxidative DNA lesions. 8-oxo-G is has the potential to be mutagenic as it can form base pairs with both cytosine and adenine (**B**). The mis-incorporation of adenine opposite the oxidative lesion can lead to a G→T conversion following two rounds of DNA replication (**C**).

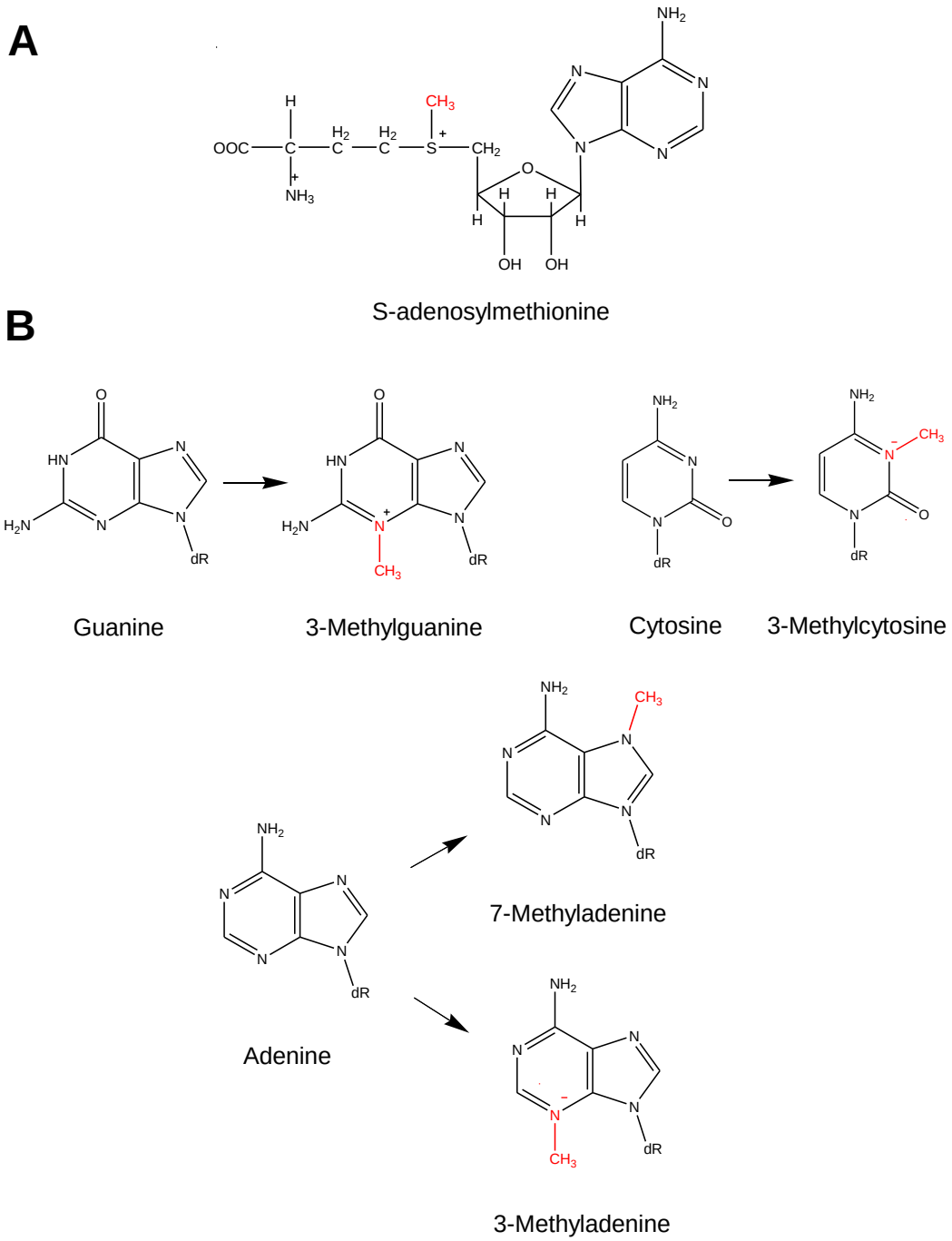

Figure 1.2 - ***Alkylation base damage in DNA***

Alkylating agents from exogenous and endogenous sources can cause a variety of alkylation base adducts in DNA.
A S-adenosylmethionine (SAM) is an intermediate in the synthesis of the amino acid methionine and functions as a methyl donor in enzyme-catalysed reactions during a number of cellular metabolic processes. It has been shown *in vitro* that SAM can also catalyse the non-enzymatic transfer of its methyl group (high-lighted in red) to DNA and has been implicated as an endogenous source of alkylation damage in cells.
B Some common alkylation base adducts that can arise in DNA.

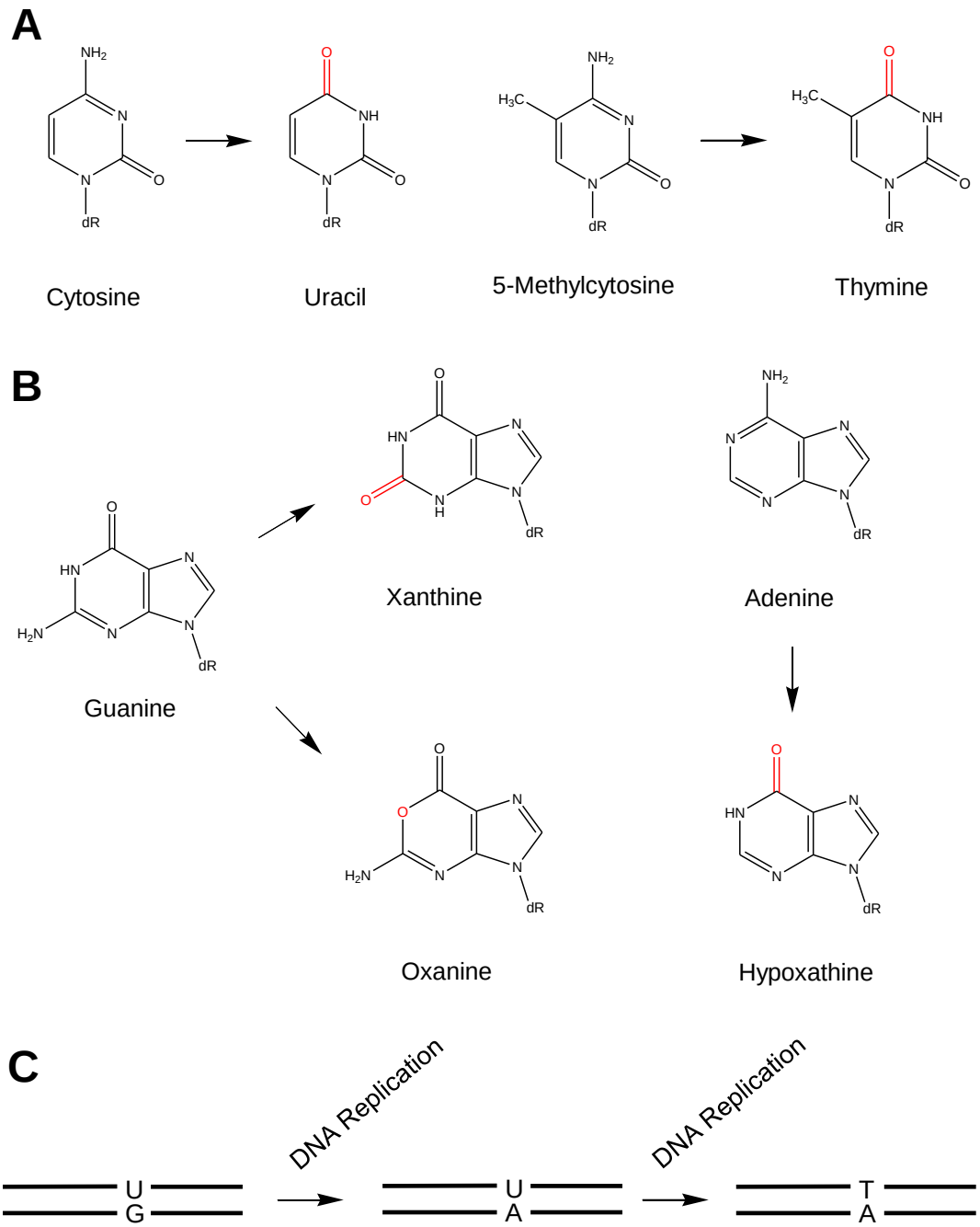

Figure 1.3 - *Spontaneous deamination of bases in DNA*

DNA base residues are susceptible to spontaneous hydrolytic deamination. **A** Cytosine and it's methylated form, 5-methlycytosine, are the most susceptible bases to spontaneous deamination and can be converted to uracil and thymine respectively. **B** Although the rate of hydrolytic deamination of purine bases is much slower than that of pyramidine bases, guanine can also be converted to xanthine and oxanine and adenine can be converted to hypoxathine,. **C** Deamination of cytosine to uracil results in mutagenic U:G mis-pairs and can lead to a C→T conversion following two rounds of DNA replication. C→T conversions can also result from the deamination of 5-methylcytosine and are the most common single site mutation found in mammalian cells.

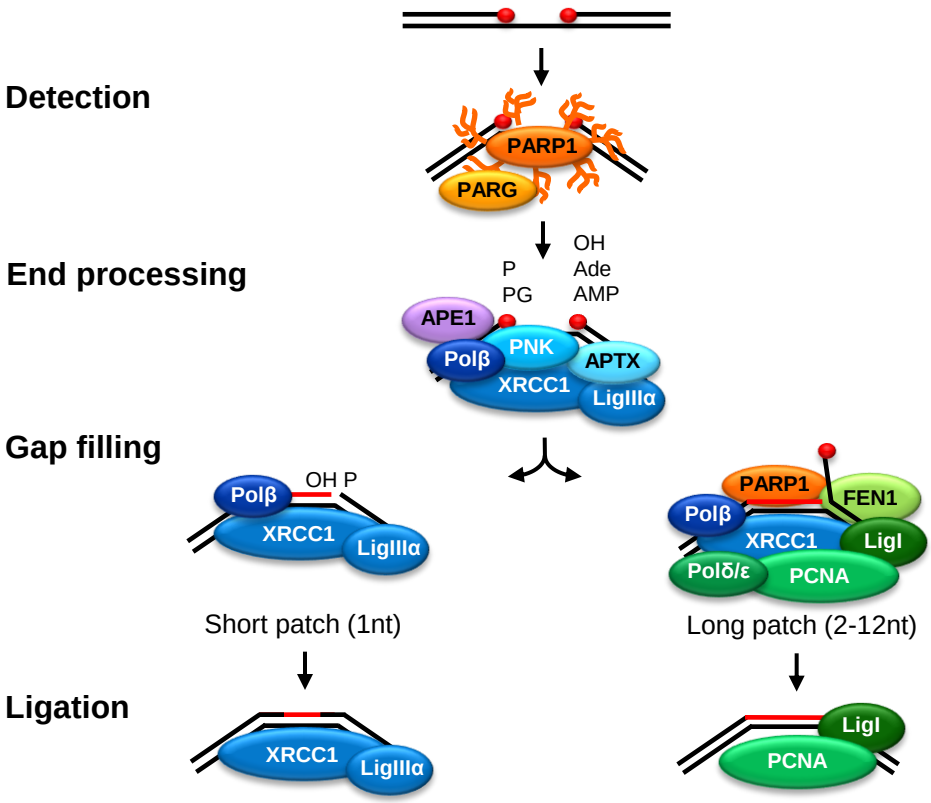

Figure 1.4 - ***Model of direct single strand break repair***
Direct DNA single-strand breaks (SSB) induced by reactive oxygen species (ROS) are typically associated with a 1 nucleotide gap and "damaged" termini (represented by red circles) and are repaired in rapid repair pathways collectively termed single-strand break repair (SSBR).

Detection: Direct SSBs are detected by poly(ADP-ribose) polymerase 1 (PARP1), which binds to the break and auto-ribosylates itself, promoting the rapid accumulation of the scaffold protein XRCC1 and other downstream SSBR factors. Once auto-modified, PARP1 disassociates from the SSB and Poly(ADP-ribose) glycohydrolase (PARG) rapidly degrades the PAR chains, recycling the PARP1 molecule for another round of SSB detection.

End processing: During end processing the damaged termini (red circles) are restored to the conventional 3'-OH and 5'-P chemistries. Direct SSBs are processed by polynucleotide kinase 3′-phosphatase (PNK), AP endonuclease I (APE1) and aprataxin (APTX) (Table 1.).

Gap-filling: Two sub-pathways operate during SSBR; short-patch repair, during which polymerase β (Polβ) inserts a single nucleotide to fill the gap, and long-patch repair, which involves extension of 2-12 nucleotides by either Pol β or the processive polymerases Pol δ or Pol ε (Pol δ/ε). During this step, a 5' DNA flap is produced which is cleaved by the enzyme, Flap endonuclease 1 (FEN1).

DNA ligation: Two DNA ligases are thought to operate in SSBR. DNA ligase IIIα (LigIIIα) is traditionally associated with short-patch repair events while DNA ligase I (LigI) is associated with long-patch repair. (Adapted from Caldecott 2009)

Ade, aldehyde; AMP, 5′-AMP; OH, 5′-hydroxyl; P, 3′-phosphate; PG, 3′-phosphoglycolate

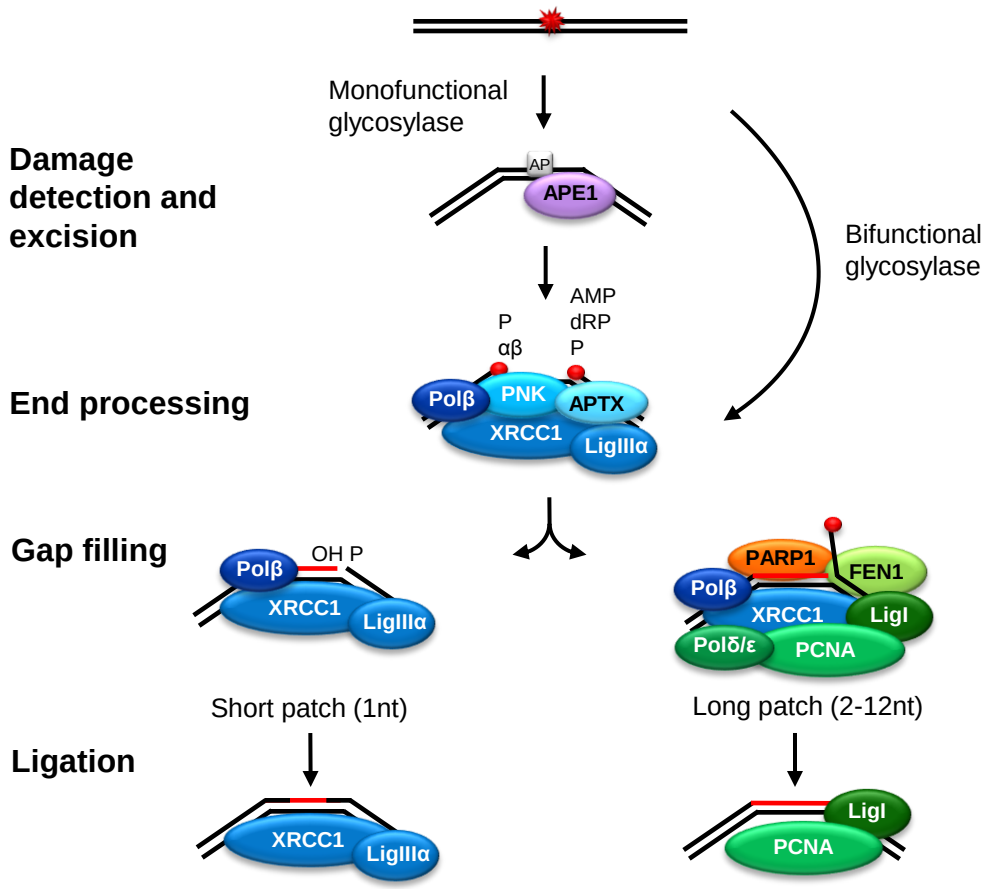

Figure 1.5 - ***Model of mammalian base excision repair***
Base excision repair (BER) is a repair pathway that is responsible for the repair of damaged bases (red star) and is a major source of indirect SSBs. Base damage can arise from either oxidative or alkylating DNA damage.

Recognition and excision of base damagde is carried out by DNA glycosylases. There are two types of DNA glycosylase. Mono-functional DNA glycosylases excise only the damaged base, leaving an intact apurinic/apyramidinic (AP), site which is processed by APE1. Bi-functional DNA glycosylases contain an additional AP lyase activity after excision of the damaged base, it cleaves the AP site, via either a β or βδ elimination reaction mechanism. The indirect SSBs produced during these steps are then repaired in the single-strand break repair pathway (SSBR).

Indirect SSBs produced during BER have “damaged” termini (red circles) and require end processing by Pol β, APTX and/or PNK to restore the conventional 3’-OH and 5’-P chemistries. Following end-processing, the gap is filled by the action of either short-patch or long-patch SSBR. During short-patch repair, Polβ inserts a single nucleotide to fill the gap. In contrast, long-patch repair involves extension of 2-12 nucleotides by either Pol β or the processive polymerases Pol δ or Pol ε (Pol δ/ε), during which a 5’ DNA flap is displaced and removed by the enzyme Flap endonuclease 1 (FEN1). The final stage in the repair of indirect SSBs is DNA ligation. Like the repair of direct SSBs, two DNA ligases are thought to operate in SSBR. LigIIIα is mainly associated with short-patch repair events while LigI is associated with long-patch repair (Adapted from Caldecott 2009)

(α,β, 3′-α,β unsaturated aldehyde; P, 3′-phosphate; PG, 3′-phosphoglycolate; AMP, 5′-AMP; OH, 5′-hydroxyl; dRP, 5′-deoxyribose phosphate.)

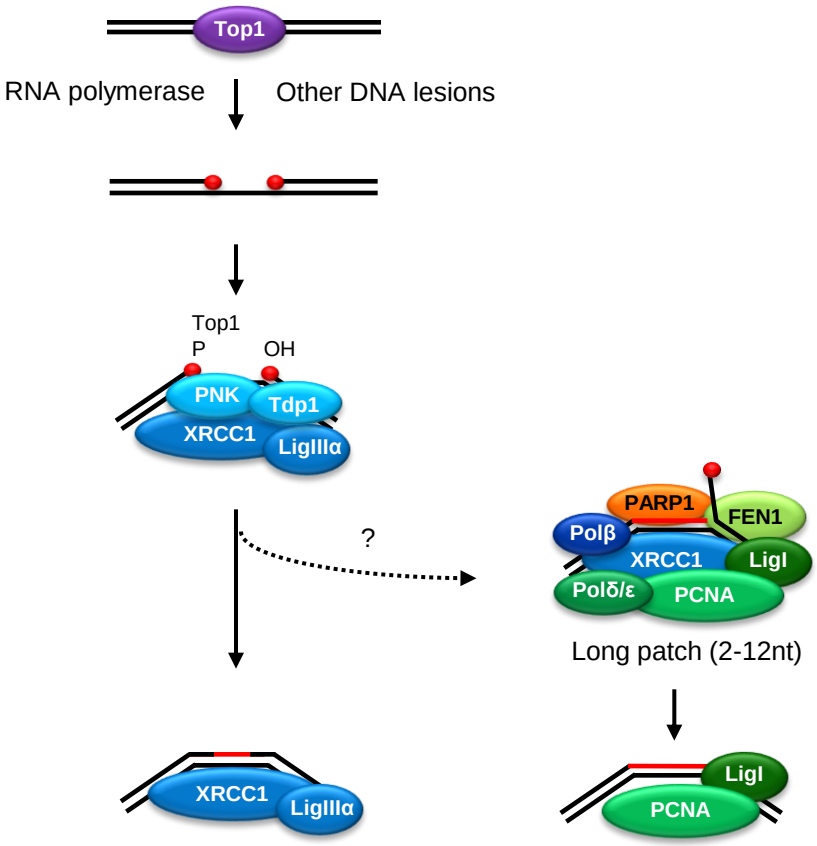

Figure 1.6 - *Model of the repair of topoisomerase 1 induced SSBs*

Another source of SSBs is the abortive activity of DNA topoisomerase 1 (Top1). Top1 relaxes supercoiled duplex DNA during transcription and DNA replication by nicking one strand of the DNA double helix and allowing the DNA to unwind. These cleavage complexes can become trapped, however, upon collision with either a transcription or replication fork or if the cleavage complex occurs in close proximity to other DNA lesions.

These Top1-linked SSBs are repaired by the end-processing enzyme Tyrosyl-DNA phosphodiesterase 1 (Tdp1), which leaves a 3'-P and 5'-OH, and PNK, which restores the conventional DNA termini. Processing of the Top1-SSB leaves a conventional nick which can then be re-ligated. As Tdp1 interacts with LigIIIα it is likely that Top1-SSBs will be quickly ligated following end-processing. However it is possible that under some circumstances, a gap-filling step could be involved.

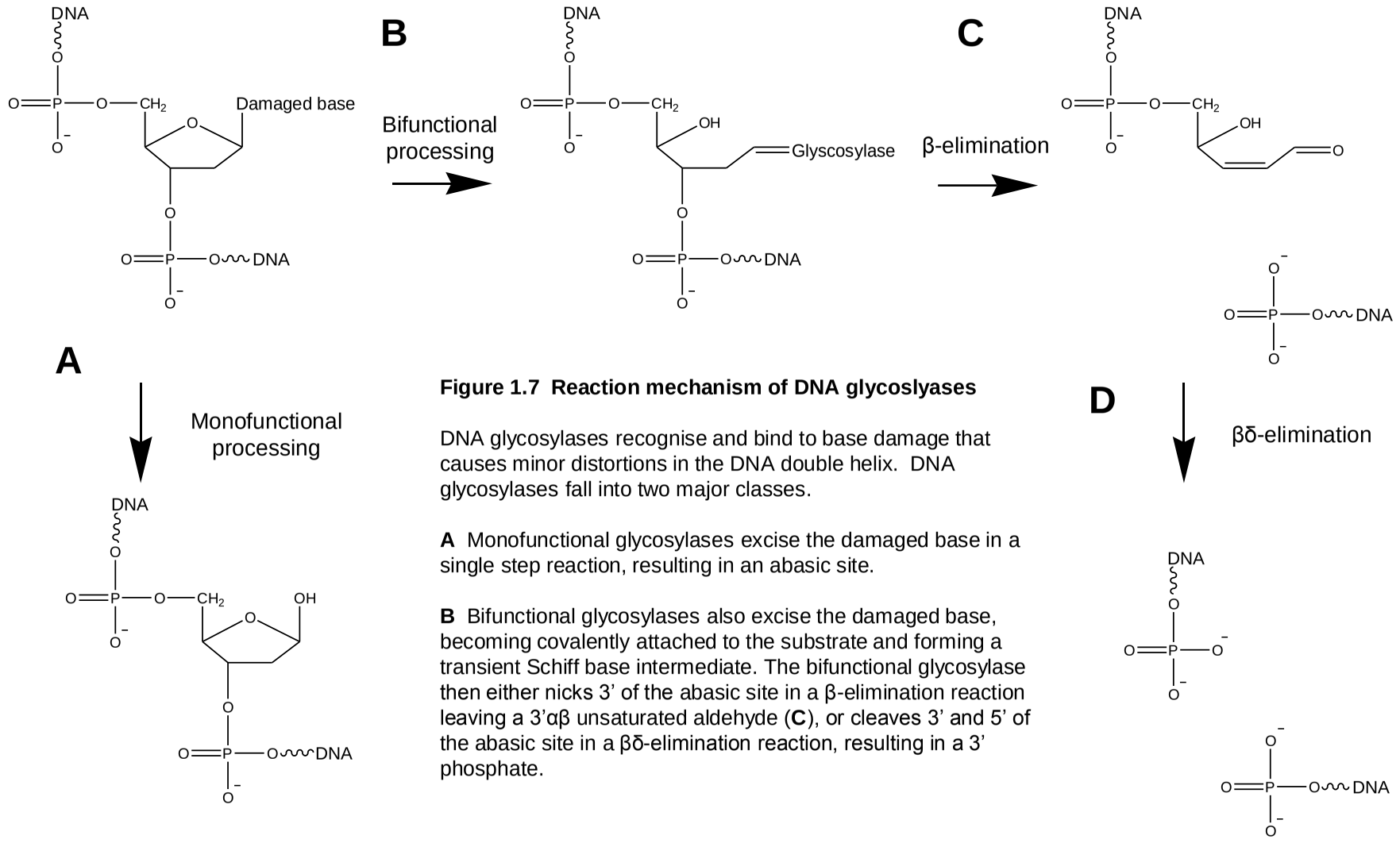

Figure 1.7 Reaction mechanism of DNA glycoslyases

DNA glycosylases recognise and bind to base damage that causes minor distortions in the DNA double helix. DNA glycosylases fall into two major classes.

A Monofunctional glycosylases excise the damaged base in a single step reaction, resulting in an abasic site.

B Bifunctional glycosylases also excise the damaged base, becoming covalently attached to the substrate and forming a transient Schiff base intermediate. The bifunctional glycosylase then either nicks 3' of the abasic site in a β-elimination reaction leaving a 3'αβ unsaturated aldehyde (**C**), or cleaves 3' and 5' of the abasic site in a βδ-elimination reaction, resulting in a 3' phosphate.

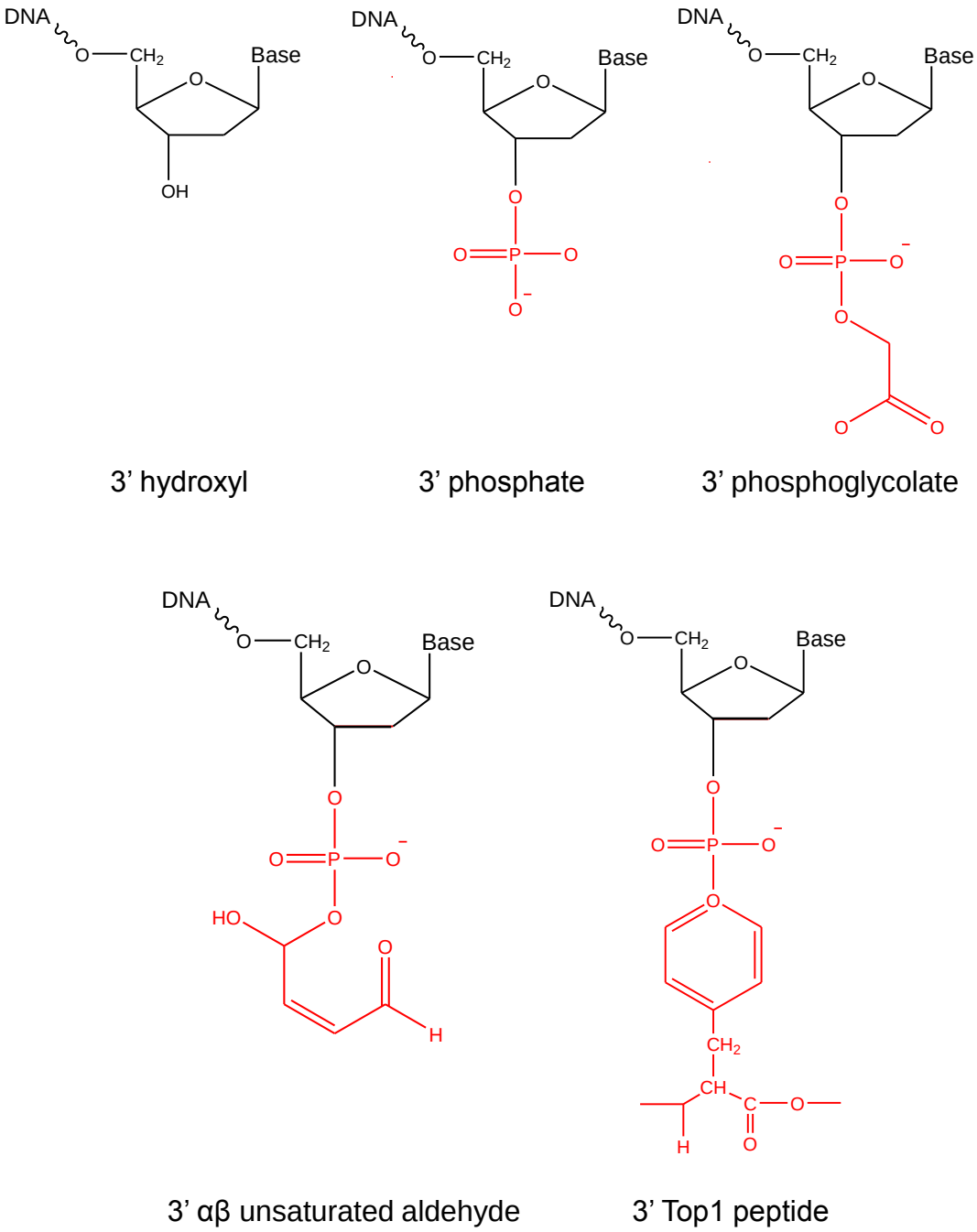

Figure 1.8 - Structures of the types of damaged 3’ termini that can arise at DNA single-strand breaks

Types of damaged termini that arise at the 3’ of a DNA single strand break include a 3’ phosphate (3’P), 3’ phosphoglycolate (3’PG), 3’ αβ unsaturated aldehyde (3’PUA) and a 3’ Top1-linked SSB (3’ Top1). The altered chemistries of the DNA termini are highlighted in red.

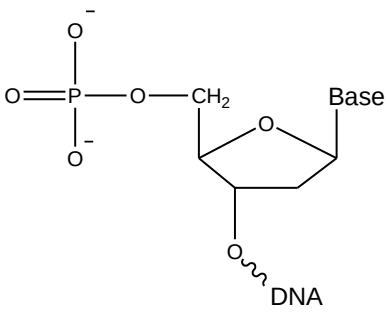

5’ phosphate

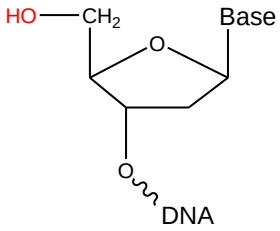

5’ hydroxyl

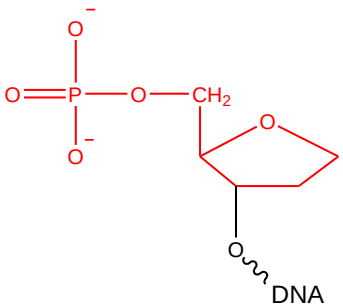

5’ deoxyribose phosphate

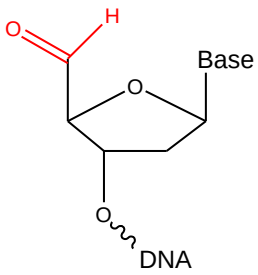

5’ aldehyde

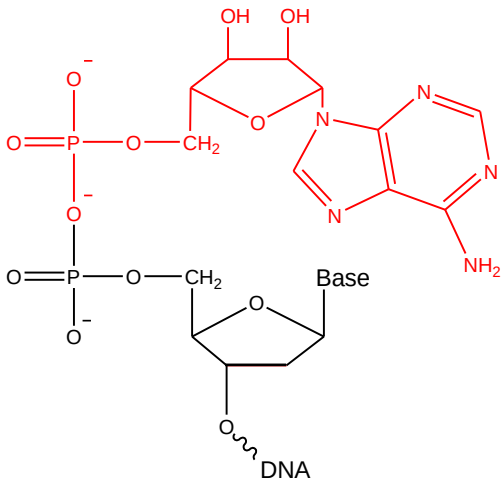

5’ adenosine monophosphate

Figure 1.9 - Structures of the types of damaged 5’ termini that can arise at DNA single-strand breaks

Types of damaged termini that can arise at the 5’ of a DNA single strand break include a 5’ hydroxyl (5’OH), 5’ deoxyribose phosphate (5’dRP), 5’ aldehyde (3’PG), and a 5’ adenosine monophosphate (5’AMP). The altered chemistries of the DNA termini are highlighted in red.

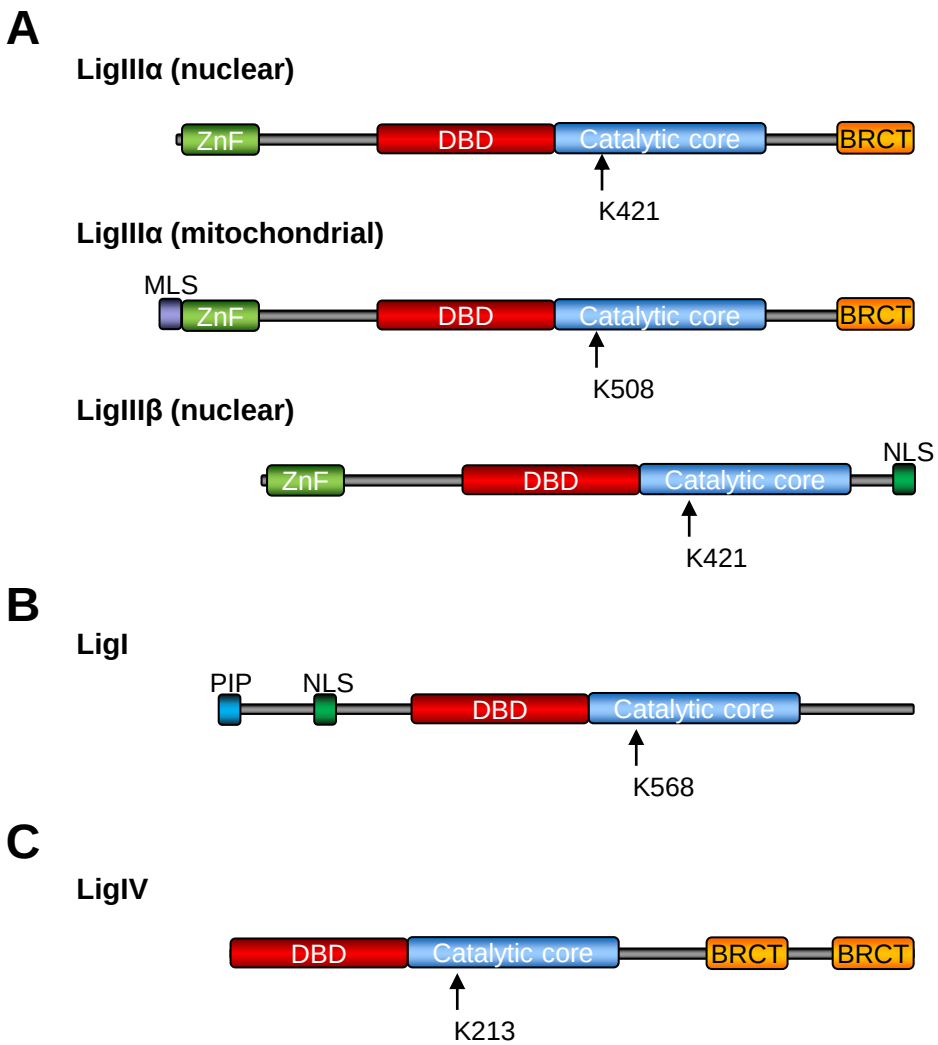

Figure 1.10 – Domain structure of mammalian ligases

There are 3 DNA ligases that are present in mammalian cells. All mammalian ligases contain a DNA binding domain (DBD) and a catalytic core which contains the active site lysine that becomes adenylated during the ligation mechanism.

A The mammalian *LIG3* gene encodes three distinct DNA Ligase III polypeptides. LigIIIα is ubiquitously expressed in all tissue types and an alternate translation initiation mechanism allows for the encoding of nuclear and mitochondrial versions. Additionally a germ-line specific alternative splicing mechanism, in which the terminal 3'-coding exon of LigIIIα is replaced by a different exon, generates LigIIIβ, which also includes a nuclear and mitochondrial version. All three polypeptides contain an N-terminal zinc-finger domain (ZnF) which gives LigIIIα and LigIIIβ a nick sensing ability. LigIIIα also interacts with XRCC1 through its C-terminal BRCT domain.

B Mammalian cells only contain one LigI polypeptide which contains only the core DNA binding and catalytic domains. The N-terminal region of LigI contains a PIP box through which it interacts with PCNA.

C In addition to the core catalytic domains LigIV contains two tandem C-terminal BRCT domains which mediate its interaction with XRCC4.

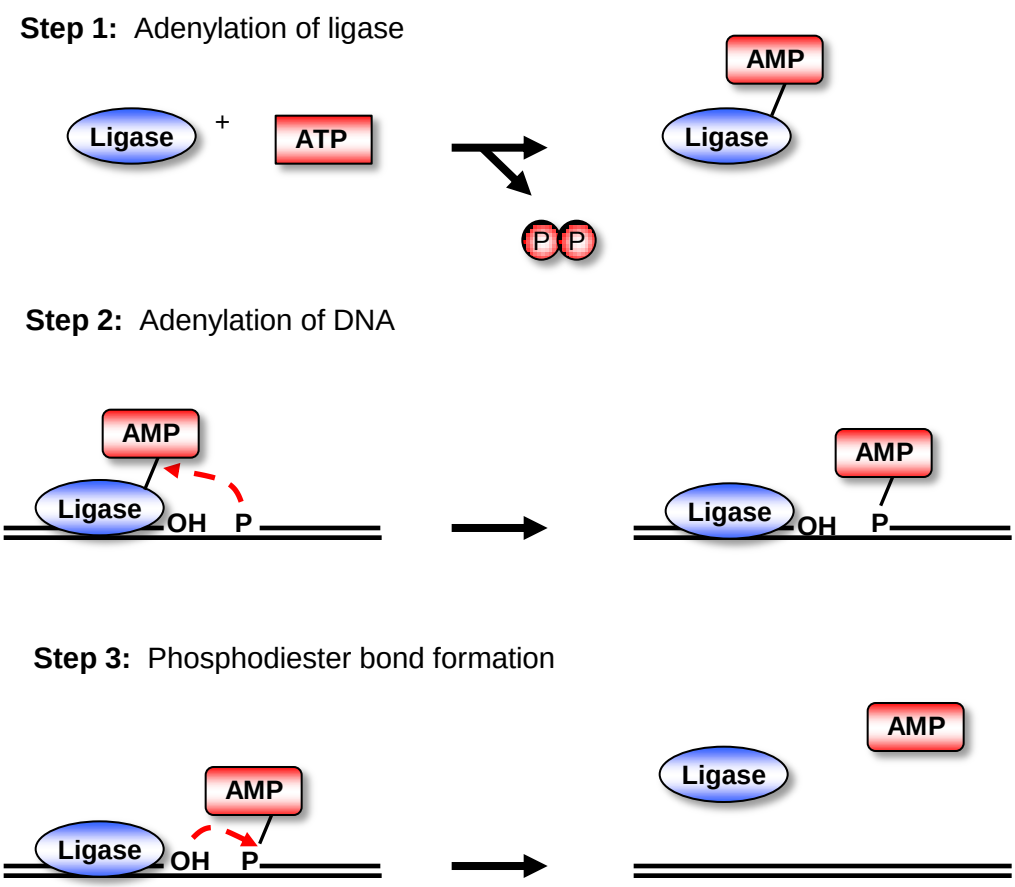

Figure 1.11 – *Reaction mechanism of mammalian ligases*

DNA ligases are nucleotidyltransferases (NTases) that utilise a high energy cofactor to catalyse phosphodiseter bond formation in a universal three-step reaction mechanism.

Step 1: In the first step of DNA ligation reacts with ATP to form a ligase-adenylate intermediate in which AMP is covalently linked to the active-site lysine. This reaction is very energetically favourable and the ligase-adenylate intermediate is stable in the absence of a DNA substrate. Therefore this reaction can be seen as essentially irreversible, meaning that the majority of ligase in the cell is likely to be in the adenylated form.

Step 2: The second step of ligation is the activation of the 5'P by adenylation of the DNA. During this step the oxygen of the 5'P attacks the phosphorus of the AMP, dispelling the lysine and transferring the adenylate group onto the 5'P, forming an AMP-DNA intermediate.

Step 3: The final step of ligation is the reformation of the phosphodiester backbone. During this step the non-adenylated ligase catalyses the nucleophilic attack of the 5'AMP by the 3'OH, displacing the AMP and joining the two polynucleotides by formation of a phosphodiester bond

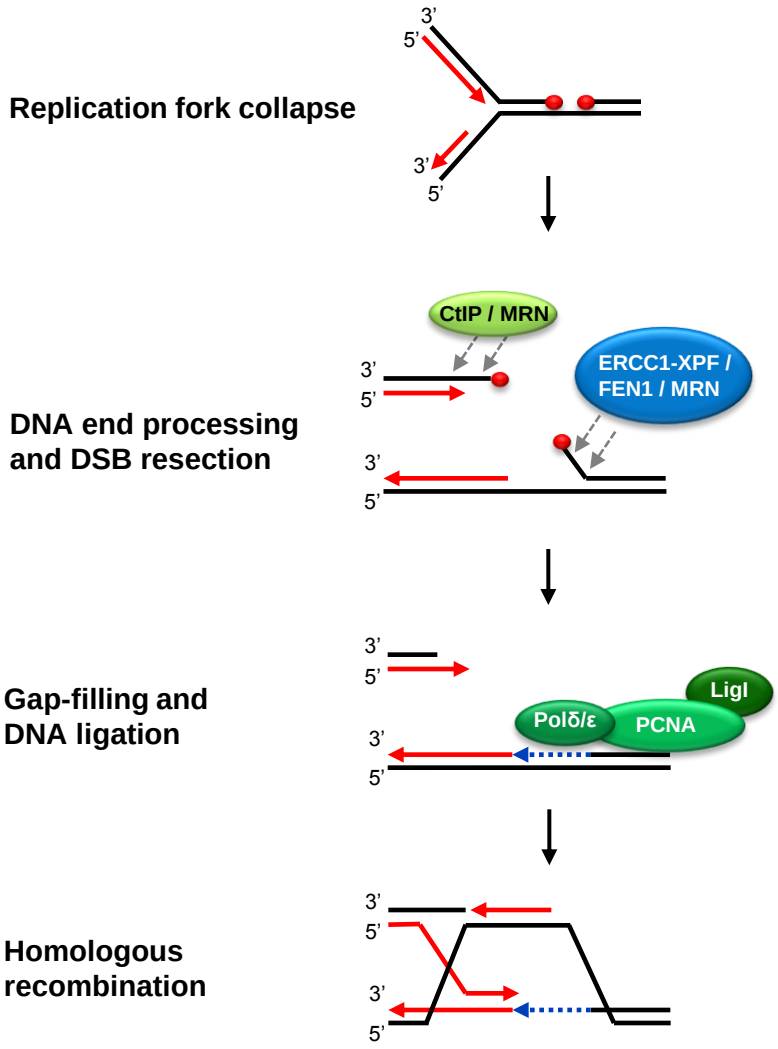

Figure 1.12 - *Model of replication-coupled single strand break repair*
The collision of a replication fork with a SSB creates a one-ended DSB and a residual SSB. Red circles denoted damaged termini.

End processing: The 5'-terminus of the DSB is processed and resected by CtIP and the MRN complex in anticipation of strand invasion and replication fork restart. End processing of the SSB is carried out by either global SSBR factors or alternatively by structure specific nucleases such as ERCC1-XPF, MRN or FEN1.

Gap-filling and DNA ligation: Gap-filling and DNA ligation is carried out by Polδ/ε and LigI respectively.

Homologous recombination: The replication fork is reformed by formation of a Rad51 nucleofilament and template switching.

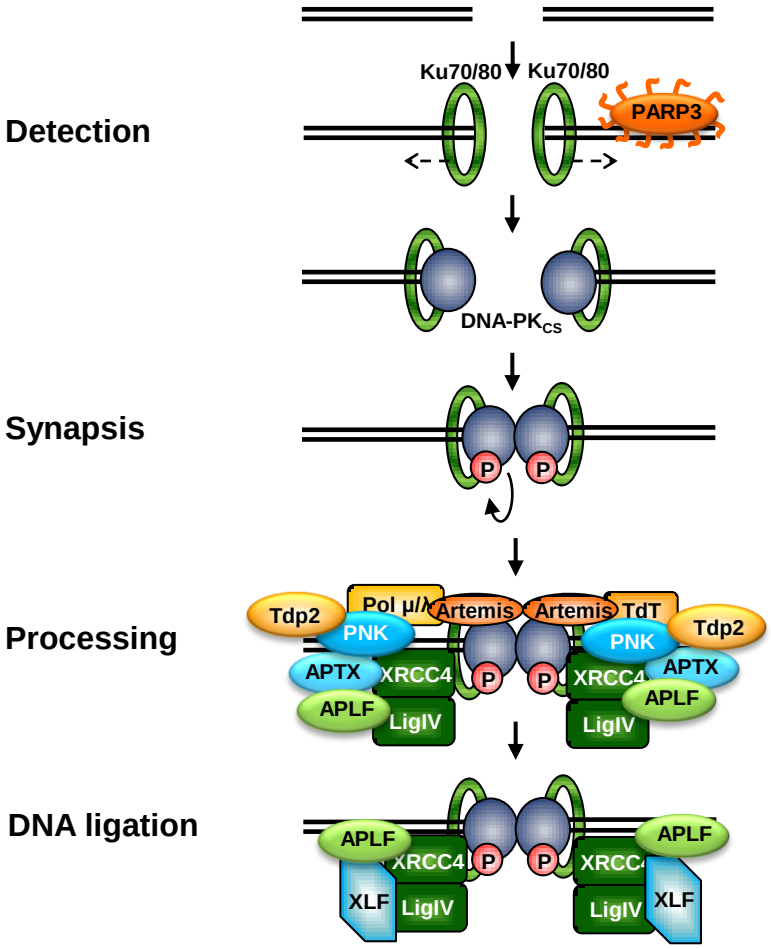

Figure 1.13 Mechanism of non-homologous end-joining in mammalian cells
Non-homologous end-joining (NHEJ) is a double-strand break repair (DSBR) pathway that is in operation throughout the cell cycle and is the predominant pathway of choice during G1.

Detection: DNA double-strand breaks (DSB) are rapidly bound by the Ku70/80 heterodimer which forms a ring-like structure around the DNA. This leads to the activation of the catalytic subunit of the DNA-PK protein complex, DNA-PK_{cs}, which catalyses the inward translocation of Ku70/80. This reveals the ends of the break allowing two DNA PK_{cs} molecules to load onto the DNA. Another aspect of DSB signalling is the activation of PARP3 at the site of the break.

Synapsis: DNA-PK_{cs} plays a critical role in non-homologous end-joining (NHEJ), preventing end resection through a series of phosphorylation events and also stabilising the break by interacting with each other to form a synapse, tethering the ends of the break together. The loading of DNA-PK_{cs} onto the DNA ends also leads to the recruitment of XRCC4/LigIV.

End-processing: As many DNA DSBs contain 'damaged' unligatable DNA termini, a variety of end-processing factors, including Artemis, Tdp2, PNKP and APTX, are required to restore the ends of the DNA to the conventional 3'OH and 5'P before DNA ligation is possible.

DNA ligation: Once the DNA ends are processed the break is ligated by XRCC4/LigIV with the aid of the stimulatory factor XLF and the poly (ADP-ribose) binding protein APLF.

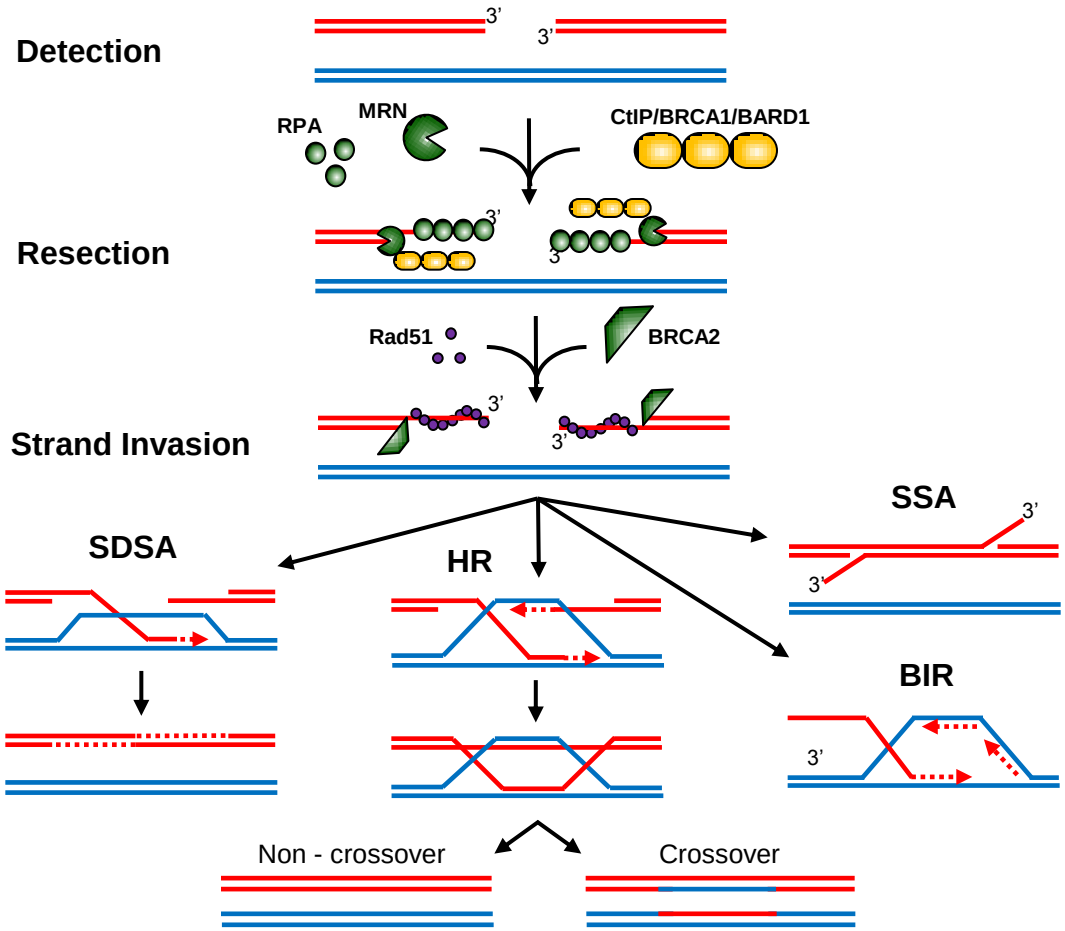

Figure 1.14 Model of homology directed DSBR in mammalian cells
Homologous recombination (HR) is a double-strand break repair pathway (DSBR) that operates preferentially in late S and G2 phases of the cell cycle. HR uses an undamaged homologous sequence as a repair template. During HR, a DSB is recognised by the MRN complex, which tethers the DNA ends and in cooperation with the CtIP/BRCA1/BARD1 complex initiates 5' → 3' end resection to generate 3' single-stranded DNA (ssDNA) overhangs. RPA coats the ssDNA to prevent the formation of DNA secondary structures, allowing the loading of Rad51 by BRCA1 onto the DNA. Strand invasion and homology searching of the intact DNA strand is catalysed by the Rad51 filament.

Synthesis dependent strand annealing: During SDSA, a single DNA end is captured by a migrating D-Loop and DNA synthesis occurs from the captured strand. Following DNA extension, the invading strand is displaced, anneals to the resected second end and is ligated.

Homologous recombination: In the HR model, the second DNA end is captured by annealing to the extended D-Loop, forming two Holiday Junctions (HJ). The double HJ structure is then resolved to form either crossover or non-crossover products depending on the orientation of resolution.

Single-strand annealing: During SSA, resection reveals two homologous sequences within complementary strands on either side of the break which anneal to each other.

Break induced recombination: BIR occurs when a one-ended DSB invades the intact template, resulting in the formation of a replication fork. (Adapted from Hartlerode and Scully, 2009).

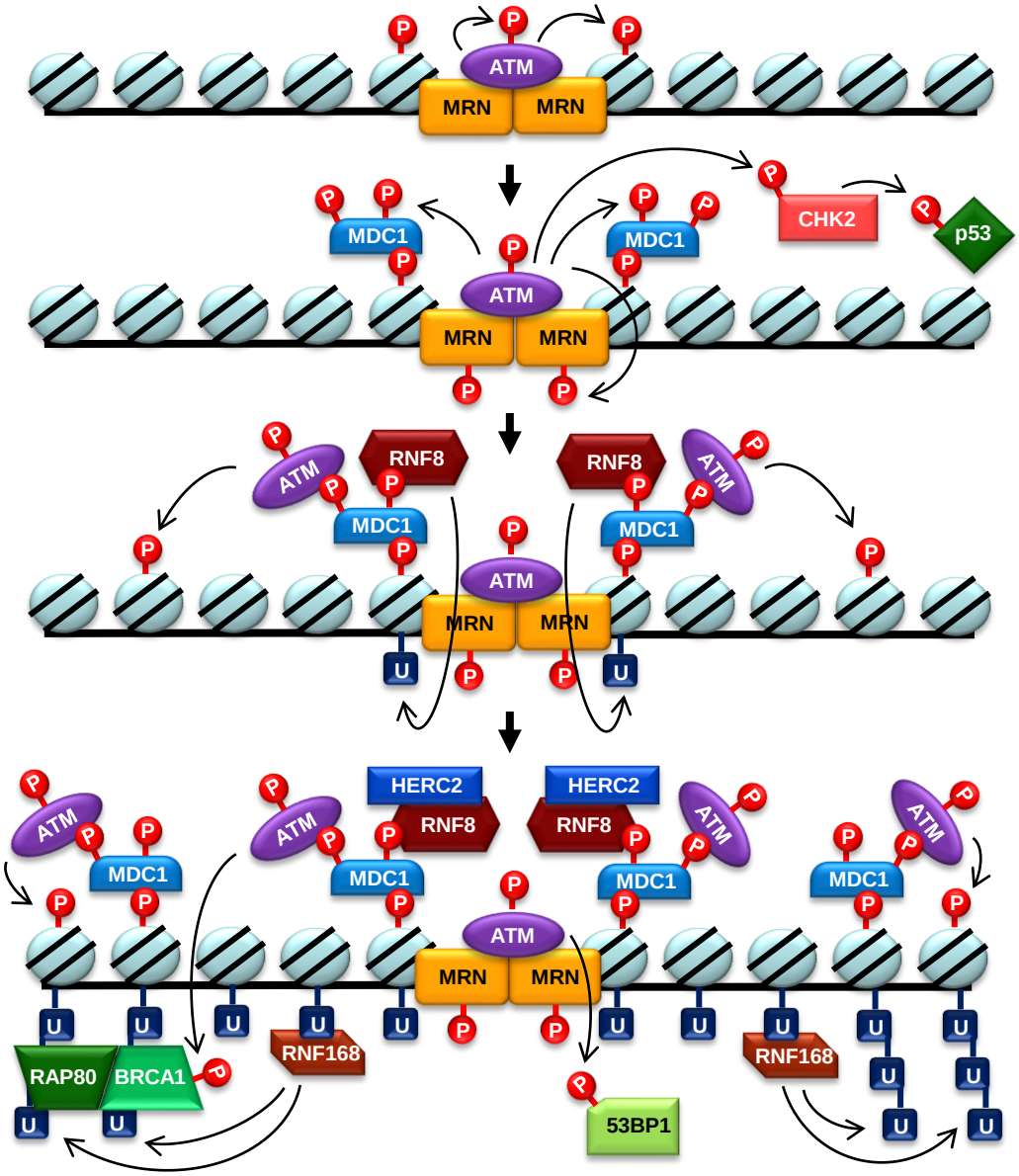

Figure 1.15 - Model for the ATM signalling cascade in the DNA damage response
ATM is a member of phosphatidylinositol 3-kinase-related kinases (PIKK) family of serine/threonine protein kinase and has a critical role in the DNA damage response (DDR). Upon induction of a DSB, MRN rapidly binds to the break and recruits and activates ATM which undergoes auto-phosphorylation at S1981. Upon activation ATM immediately phosphorylates the histone variant H2AX on S139, producing γH2AX, and the checkpoint protein, CHK2, leading to the phosphorylation of p53. The mediator protein, MDC1, is recruited by γH2AX and becomes phosphorylated by ATM, which then aids in the propagation of the γH2AX signal by recruiting more ATM to the break. MDC1 also recruits the ubiquitin ligase RNF8, which ubiquitinates H2A and γH2AX and begins a ubiquitin signalling cascade. Two more ubiquitin ligases, RNF168 which binds to the ubiquinated histones, and HERC2, which interacts with RNF8, stimulate spreading of the ubiquitin signal. The BRCA1 complex, itself an E3 ubiquitin ligase, is then recruited to the polyubiquitin chains. The mediator protein 53BP1 is also recruited to the site of the break in a manner that is dependent on the presence of γH2AX, MDC1 and RNF8. This intricate ATM dependent signalling cascade serves to stimulate DNA repair as well as to initiate check point arrest, preventing cell cycle progression if unrepaired DNA DSBs persist.

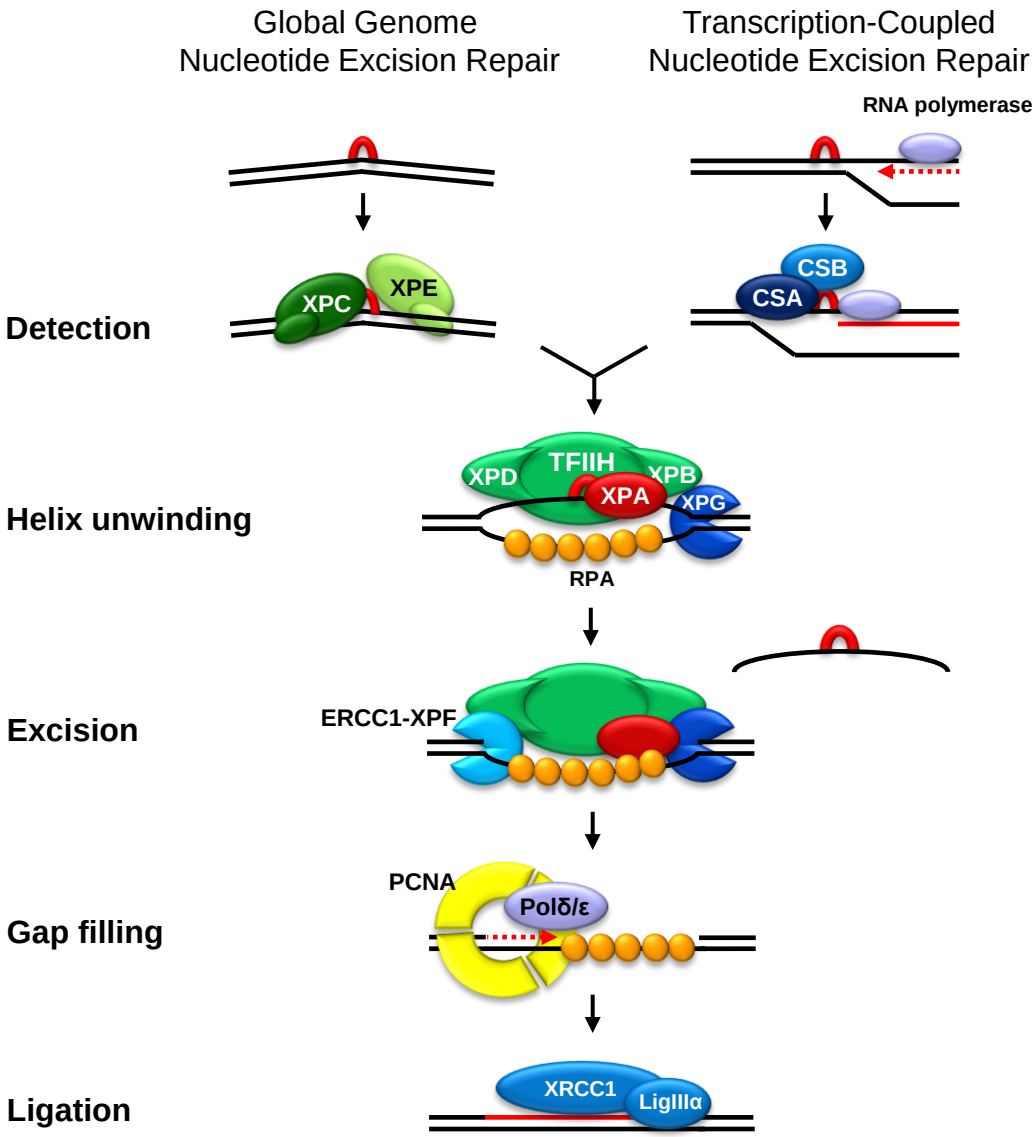

Figure 1.16 - ***Model for nucleotide excision repair***
Nucleotide excision repair (NER) is a DNA repair pathway that detects and repairs bulky, helix-distorting DNA lesions. Two sub-pathways exist within NER that differ in the initial stages of detecting the lesion. During global-genome NER helix-distorting DNA damage that arises anywhere in the genome, such as 6-4 photoproducts, is recognised and stabilised by XPC and XPE which recruits the large protein complex THIIF. Transcription-coupled NER (TCR) operates on lesions in the transcribed strands of expressed genes, such as cyclobutane pyrimidine dimers (CPD). The CSA and CSB proteins are involved in this process in recruiting TFIIH to the sites of blocked RNA polymerases.

XPD and XPB are subunits of the THIIH complex that contain ATP dependent 5' → 3' and 3' → 5' DNA helicase activities that unction to open up an bubble surrounding the lesion. RPA is loaded onto the undamaged strand as soon as the ssDNA is revealed. Excision of the damaged strand is then achieved by dual incision of the bubble at the 5' and 3' by the structure specific nucleases ERCC1-XPF and XPG. In the final stages of NER, Polδ/ε and PCNA catalyse gap-filling and XRCC1/LigIII ligates the resulting nick.

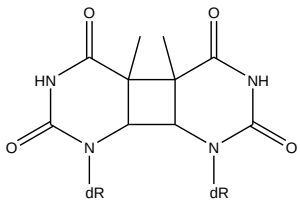

Cyclobutane pyrimidines

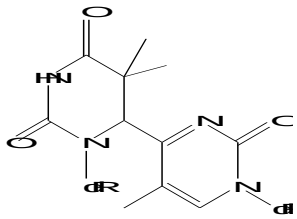

(6-4) photoproduct

Figure 1.17 - Structures of the most common types of UV induced photodamage

Cyclobutane pyrimidines (CPD) and (6-4) photoproducts are the two most common types of UVB induced photodamage. These bulky DNA adducts cause distortions in the DNA double helix which are recognised and repaired by the nucleotide excision repair pathway.

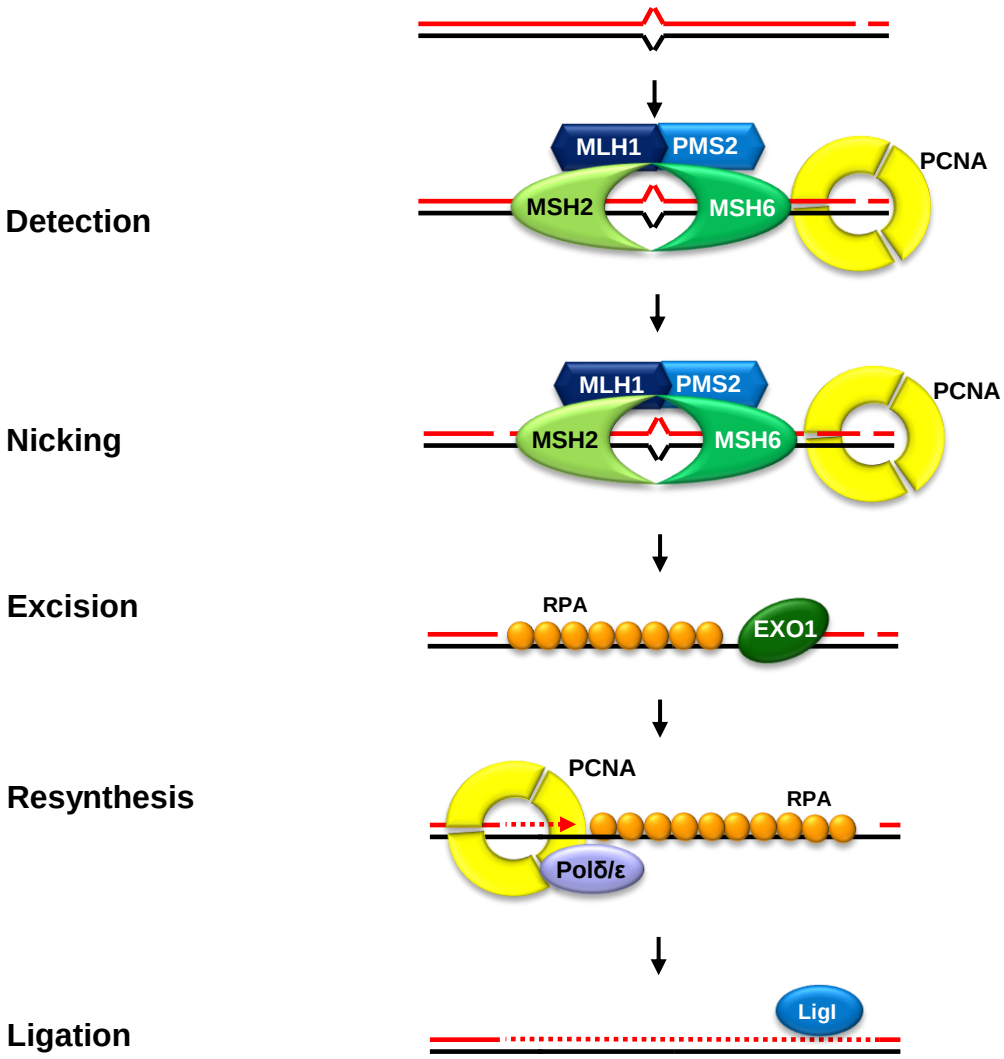

Figure 1.18 Mechanism of DNA mismatch repair in mammalian cells

DNA mismatches are recognised by the heterodimers MSH2/MSH6 or MSH2/MSH3 (not shown) which recruits the MLH1/PMS2 heterodimer. The protein complex then undergoes a conformational shift allowing it to slide away from the mismatch. The PMS2 subunit then introduces nicks in the discontinuous strand (red) in a process that requires PCNA and ATP. The nicked strand is then degraded by EXO1, generating a single-stranded gap which is immediately coated by RPA. Gap-filling is carried out by Polδ/ε in with PCNA and DNA ligase I ligates the remaining nick.

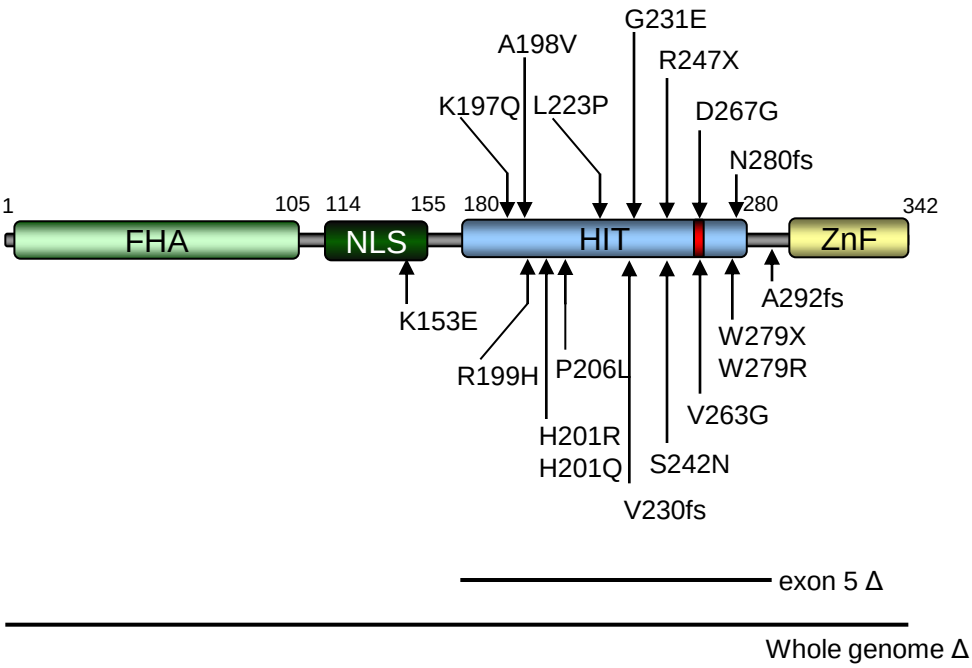

Figure 1.19 - ***APTX mutations found in individuals with ataxia oculomotor apraxia 1***

Ataxia oculomotor apraxia 1 is an autosomal recessive ataxia caused by mutations in the gene *APTX* (Date et al 2001; Moreira et al 2001). APTX is a member of the Hint-like histidine triad (HIT) superfamily and is involved in the repair of abortive ligation intermediates by removing the AMP moiety from the 5' of SSBs and DSBs (Ahel et al 2006). *APTX* also contains a HIT domain (blue), a divergent zinc finger motif (ZnF) (yellow), an amino-terminal fork-head associated (FHA) domain (light green) and an NLS (dark green). APTX interacts with CK2 phosphorylated XRCC1 and XRCC4 via the FHA domain (Clements et al 2004). The red box denotes the location of the H-φ-H-φ-H-φ-φ HIT motif. "fs" denotes a frameshift mutation and "Δ" denotes a deletion. (Adapted from Caldecott 2009)

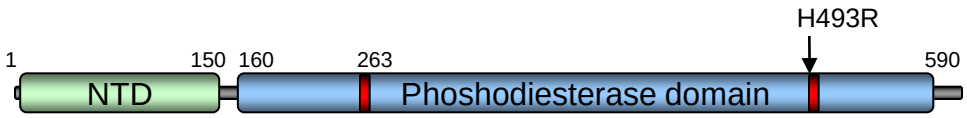

Figure 1.20 - ***Mutation in Tdp1 found in individuals with spinocerebellar ataxia with axonal neuropathy 1***

Spinocerebellar ataxia with axonal neuropathy 1 is an autosomal recessive ataxia that is caused by mutations in *TDP1* (Takashima et al 2002). Tdp1 contains a phoshodiesterase domain (blue) and is involved in the repair of abortive topoisomerase 1 (Top1) cleavage complexes by removing a 3'-Top1 peptide (Interthal et al 2001). The red boxes indicate the locations of critical HKD active sites (Interthal et al 2001). Tdp1 has been shown to interact with LigIIIα via the N-terminal domain (NTD) (green) (Chiang et al 2010). So far only one mutation (H493R) has been found in individuals suffering from SCAN1. (Adapted from Caldecott 2009).

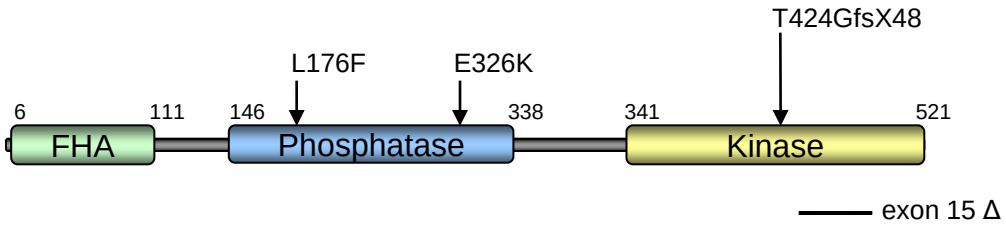

Figure 1.21 - *PNK mutations found in individuals with microcephaly, early-onset, intractable seizures and developmental delay*
Microcephaly, early-onset, intractable seizures and developmental delay is an autosomal recessive disorder caused by mutations in the gene *PNK* (Shen et al 2010). *PNK* has an amino-terminal fork-head associated domain (FHA) (green) and phosphatase (blue) and kinase (yellow) active site domains. *PNK* interacts with CK2 phosphorylated XRCC1 and XRCC4 via the FHA domain. Two point mutations have been discovered in the phosphatase domain (L176F and E326K). A frameshift mutation associated with a premature stop codon (T424GfsX48) and a splice mutation resulting in deletion of exon 15 (exon 15 Δ) have been discovered in the kinase domain.

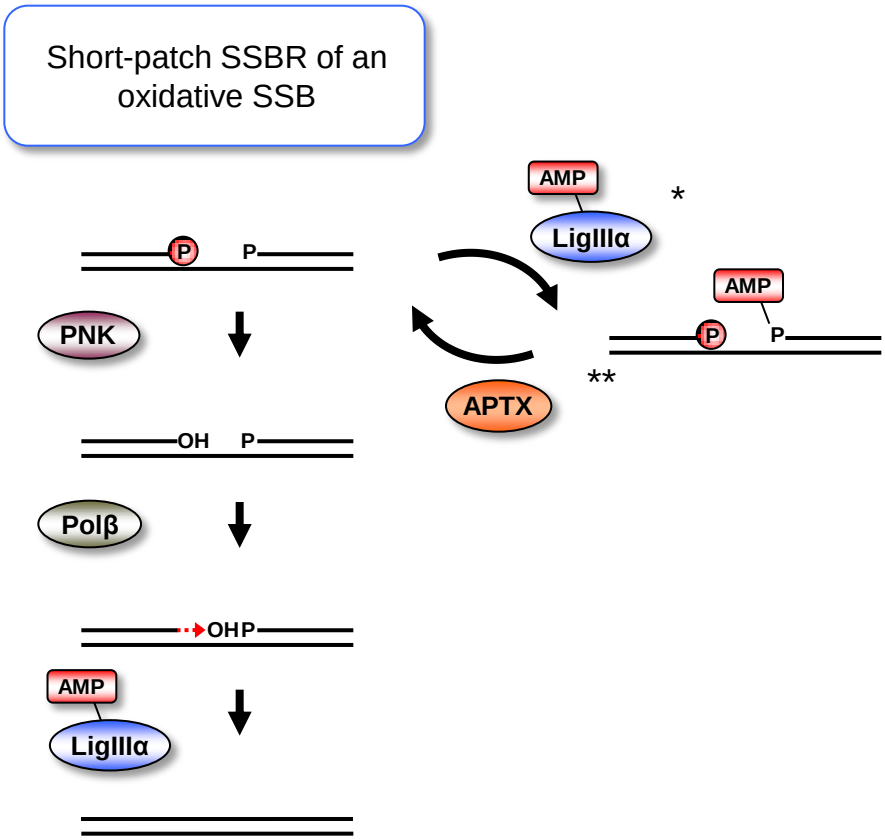

Figure 3.1 – *Model for the role of APTX in resetting abortive ligation intermediates during short-patch SSBR*

Direct SSBs, primarily arising as the result of exposure to ionising radiation or reactive oxygen species, occur thousands of times in each cell per day and are typically associated with base and it has been estimated that ~70% of these breaks possess a 3'- phosphate (Caldecott 2001). During short-patch SSBR of these oxidative breaks, 3' end processing by PNK and gap-filling by Polβ would be required to restore a ligatable nick.

However if a ligase attempts to prematurely ligate the oxidative SSB before the action of PNK or Polβ then the ligation reaction will stall and a stable abortive ligation intermediate will be produced (*). APTX is a nuclear DNA repair protein that catalyses the release of adenylate groups covalently linked to 5' phosphate termini of a DNA SSBs and it has been proposed that APTX acts to rapidly reset abortive ligations that arise during SSBR (**) (Ahel et al 2006; Rass et al 2007; Rass et al 2008).

It has been shown that APTX defective cell extracts lack AMP-DNA hydrolase activity and are unable to perform short-patch SSBR on an *in vitro* substrate modelling an abortive ligation of an oxidative SSB (Ahel et al, 2006). In AOA1 cells, abortive ligation intermediates that arise would not be resolved by APTX and could accumulate in the absence of redundant repair mechanisms

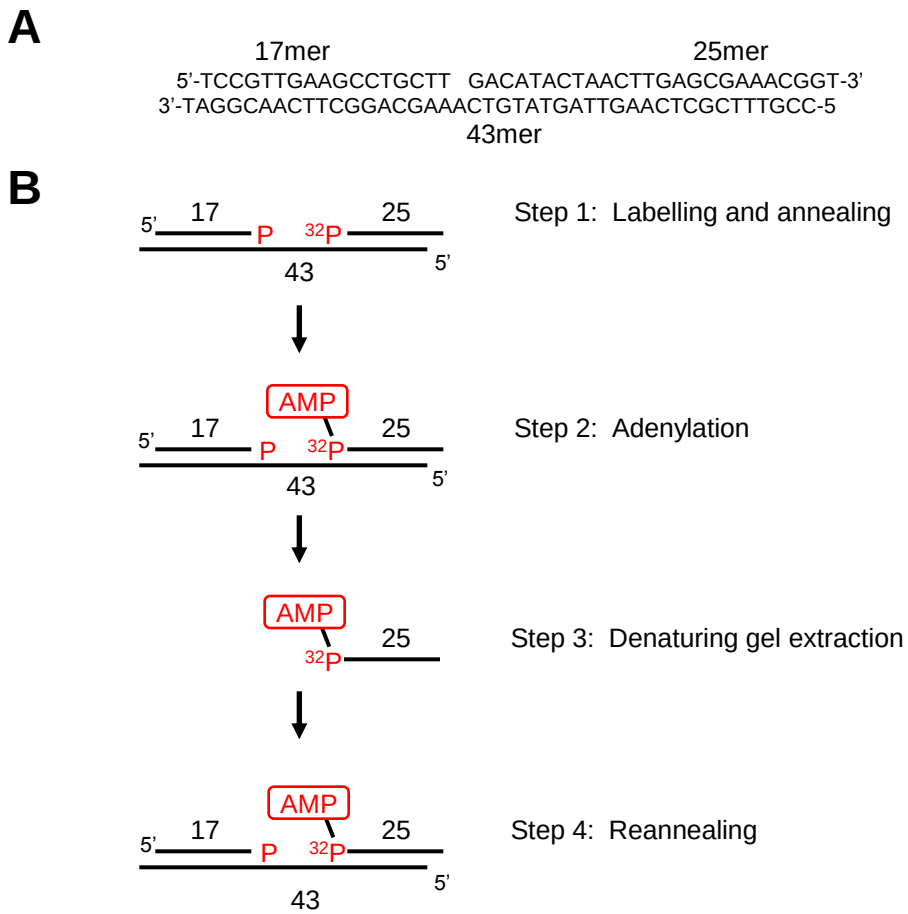

Figure 3.2 – *A schematic detailing the preparation of an aborted ligation intermediate* in vitro

Schematic detailing the preparation of the aborted ligation intermediate. The final annealed oligonucleotide substrate has a 1 nucleotide gap and 1bp non-complementary 3' overhangs. A SSB with a nick can be made by replacing the 17mer with an 18mer. The sequences of the oligonucleotides used to prepare the substrate are shown in **A**.
B The 5'-AMP substrate is prepared as follows.

Step 1: The 25mer is ^{32}P radiolabelled on the 5' termini by incubation with T4 PNK and γ^{32}P ATP at 30°C for 1hr. The ^{32}P-25mer is annealed to a 2x fold excess of unlabelled 17mer possessing a 3'P (17mer-P) and unlabelled 43mer backbone oligonucleotide.

Step 2: The 5' termini of the ^{32}P-25mer is then adenylated or mock adenylated by incubation with T4 ligase (Roche) or T4 storage buffer for 1 hour at 30°C.

Step 3: The reaction is stopped by addition of 3x formamide loading buffer and then fractionated by denaturing PAGE. The adenylated ^{32}P-25mer is gel extracted and ethanol precipitated. The mock adenylated ^{32}P-25mer is purified in parallel.

Step 4: The purified AMP-^{32}P-25mer and mock adenylated ^{32}P-25mer are reannealed to a 2x fold excess of unlabelled 17mer-P and 43mer. The final substrate contains a 1 nucleotide gap possessing a 3'P and a 5'AMP.

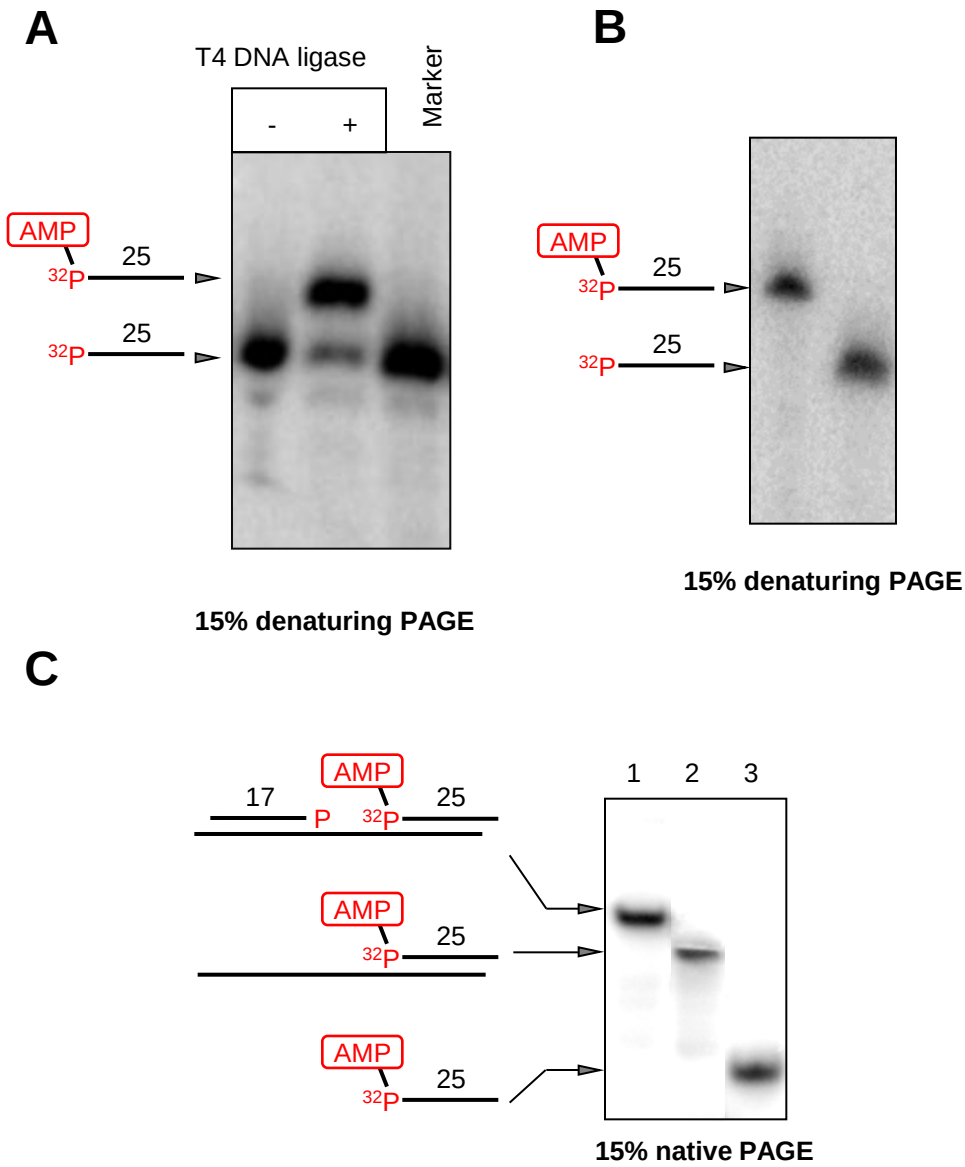

Figure 3.3 – *Preparation of an aborted ligation intermediate* in vitro

A Adenylated AMP-^{32}P-25mer and mock-adenylated ^{32}P-25 oligonucleotide separated by 15% denaturing PAGE. Note that the adenylation reaction was not 100% efficient and non-adenylated ^{32}P-25mer was still present.

B Gel extracted AMP-^{32} P-25mer and ^{32}P-25mer separated by 15% denaturing PAGE.

C The annealed adenylated duplex (1) can be separated on a 15% native PAGE from a partially annealed duplex lacking the 17mer oligonucleotide (2) and the purified AMP-^{32}P-25 oligonucleotide (3) by 15% native PAGE.

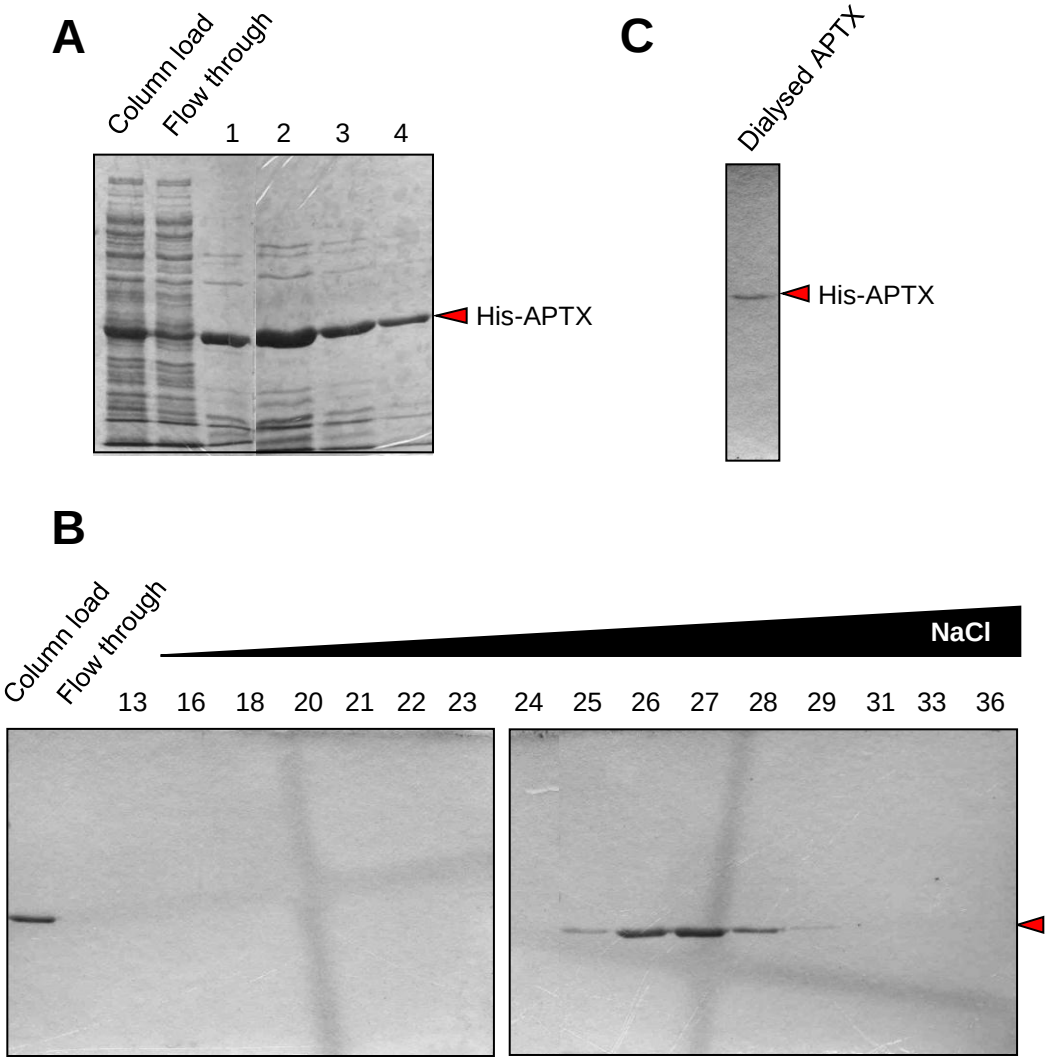

Figure 3.4 – *Overexpression and purification of recombinant His-tagged human APTX*

A 20ml clarified *E.coli* extract containing His-APTX was loaded onto a 0.5ml Ni-NTA agarose column. His-APTX was eluted with sonication buffer containing 250mM imidazole and aliquots of the column load, flow through and elution fractions (numbered) of the purification were analysed by 10% SDS PAGE. His-APTX runs above the 37kDa marker at approximately 40kDa (red arrow). His-APTX protein eluted in the first 4 fractions.

B Peak His-APTX fractions from IMAC were (1 & 2) were pooled and were purified to homogeneity by cation exchange chromatography. His-APTX was eluted from the column by increasing the salt concentration from 0.1M to 1M and the elution fractions (numbered) were analysed by 10% SDS PAGE. His-APTX eluted in a sharp peak at approximately 300-400mM NaCl.

C The purity of the final dialysed preparation of His-APTX was determined by analysing 500ng of protein by 15% SDS-PAGE.

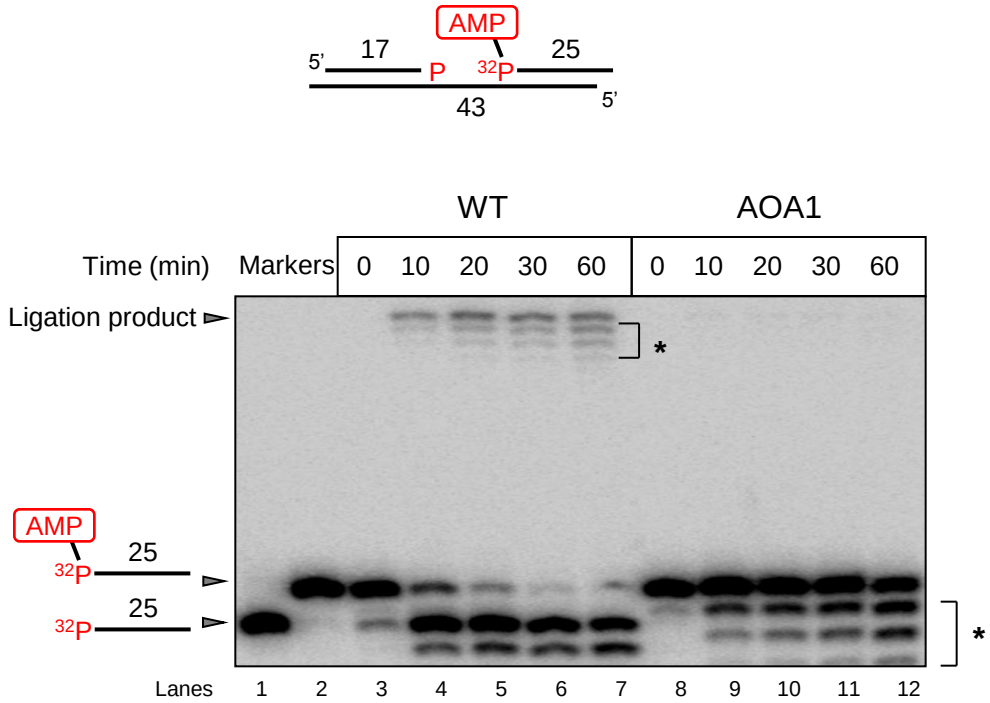

Figure 3.5 - *AOA1 cell-free extracts are defective in the short-patch SSBR of an abortive ligation intermediate* in vitro

6.25µg of whole cell extracts prepared from WT and AOA1 LCLs were incubated at 30°C for the indicated times with 25nM of an abortive ligation intermediate containing a 1 nucleotide gap and a 3'P and a 5'AMP. The substrate was ^{32}P radiolabelled on the 5' of the 25mer oligonucleotide (^{32}P-25mer). A cartoon of the substrate is displayed (top). The reaction products were fractionated by 15% denaturing PAGE and detected by phosphorimaging. Gel extracted AMP-^{32}P-25mer and ^{32}P-25mer were included as markers (Lanes 1 and 2).

Repair of the 5'AMP and restoration of a 5'P in the SSB is measured by a decrease in size of the AMP-^{32}P-25mer to the ^{32}P-25mer. Full repair of the SSB is indicated by the appearance of a ligation product and requires processing of the 3'-P and filling of the 1 nucleotide gap. Cell-extracts from lymphoblastoid cell lines have high levels of non-specific nuclease activity (*) which was supressed by addition of an 1000x fold molar excess of competitor oligonucleotide.

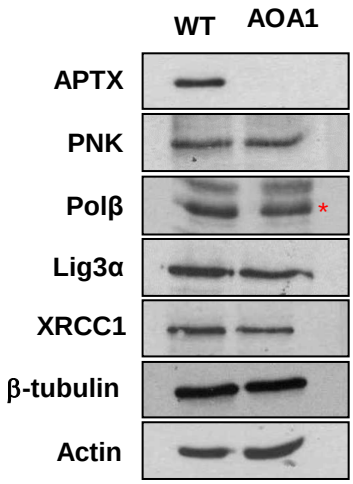

Figure 3.6 – *Levels of short patch SSBR proteins are normal in AOA1 whole cell extracts*

10μg of AOA1 and WT whole cell extract were immunoblotted for the core SSBR proteins APTX, PNK, Polβ, LigIIIα and XRCC1. β–tubulin and actin were used as loading controls. AOA1 whole cell extracts had undetectable levels of APTX but levels of PNK, Polβ, LigIIIα and XRCC1 were largely comparable to WT.

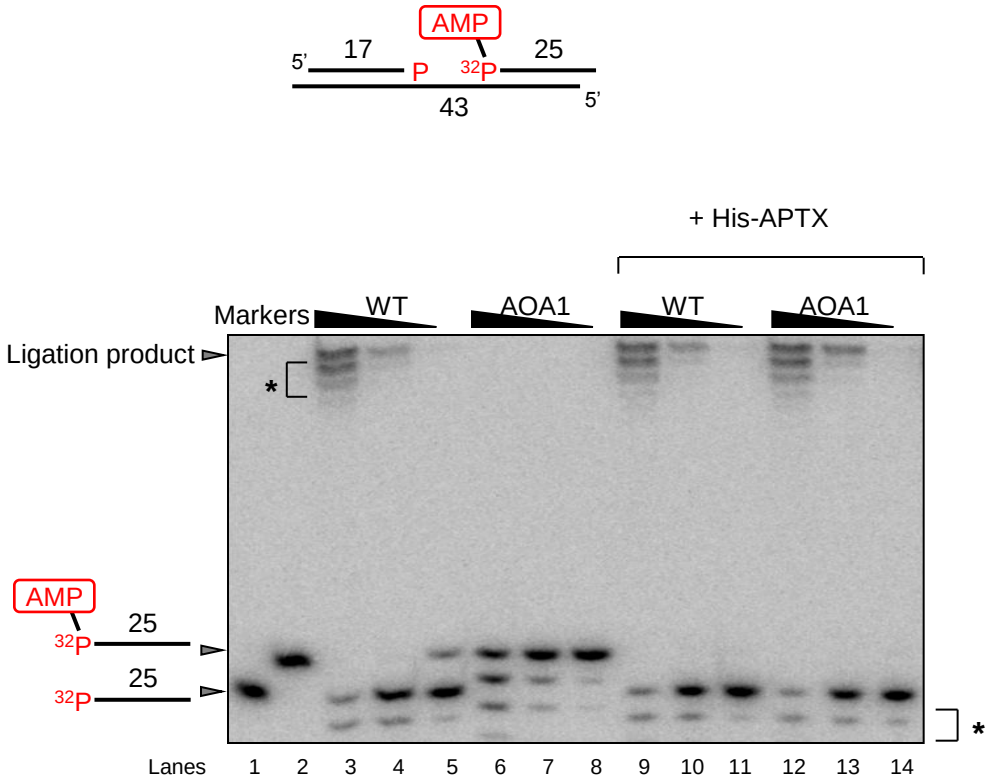

Figure 3.7 – ***Defective short-patch SSBR of abortive ligation intermediates by AOA1 whole cell extracts*** **in vitro** ***is rescued by complementation with recombinant His-APTX***

An adenylated oxidative SSB containing a 1 nucleotide gap with a 3'-P terminus and a 5'-AMP terminus was incubated with a titration of WT and AOA1 whole cell extracts (5μg, 1μg, 0.1μg) in the presence or absence of 100nM His-APTX at 30°C for 60min. A cartoon of the substrate is displayed (top). The reaction products were fractionated by denaturing PAGE and detected by phosphorimaging. Gel extracted AMP-^{32}P-25mer and ^{32}P-25mer were included as markers (Lanes 1 and 2). As seen before cell-extracts from lymphoblastoid cell lines had high levels of non-specific nuclease activity (*) which was supressed by addition of an 1000x fold molar excess of competitor oligonucleotide. Note that this experiment was performed four independent times with a representative experiment presented here.

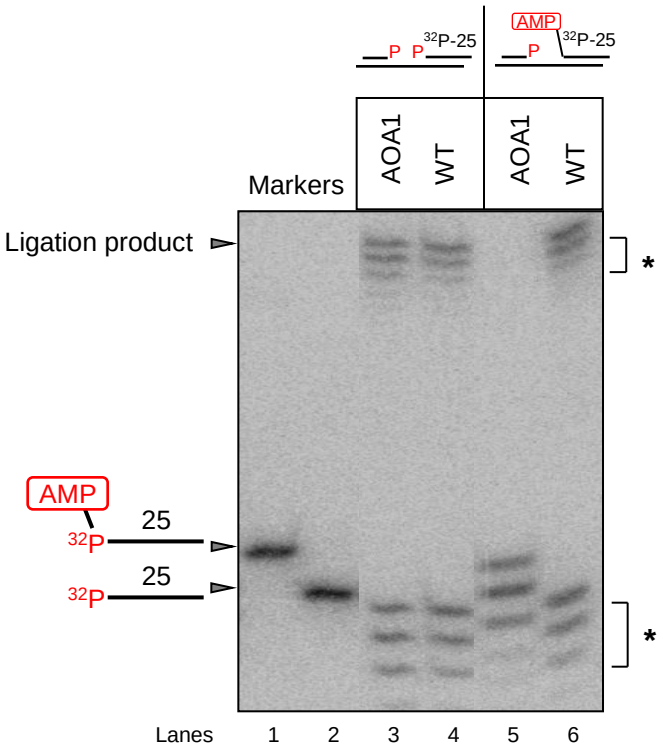

Figure 3.8 – *AOA1 extracts are proficient in the repair of a non-adenylated oxidative SSB*

5μg of WT and AOA1 whole cell extract were incubated with 25nM of an mock-adenylated or adenylated oxidative SSB, containing a 1 nucleotide gap, a 3'P and a 5'P or a 5'AMP, at 30°C for 60min. The reaction products were fractionated by denaturing PAGE and detected by phosphorimaging. Cartoons of the substrates are displayed. Gel extracted AMP-^{32}P-25mer and ^{32}P-25mer were included as markers (Lanes 1 and 2). As seen previously reactions containing cell-extracts from lymphoblastoid cell lines exhibited high levels of non-specific nuclease activity (*) which was supressed by addition of an 1000x fold molar excess of competitor oligonucleotide. Note that this experiment was performed two independent times with a representative experiment presented here.

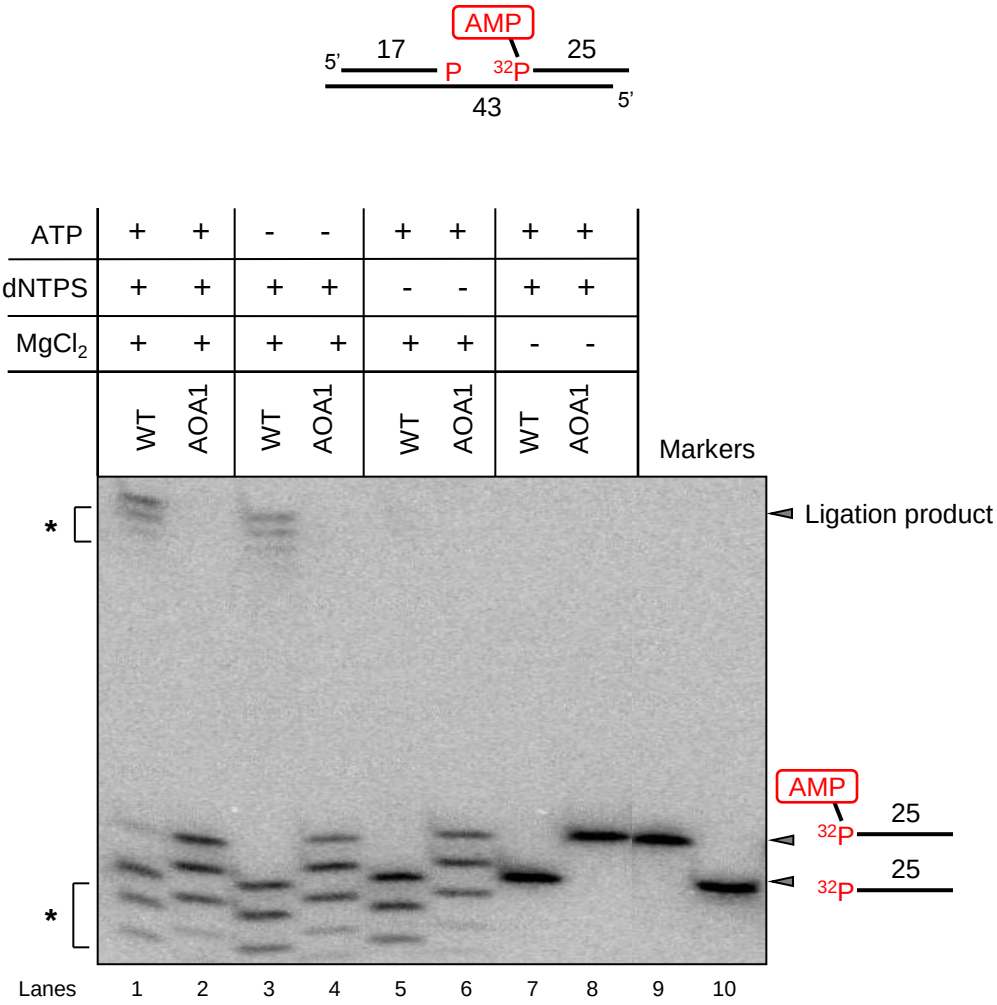

Figure 3.9 – *Short-patch SSBR of an abortive ligation intermediate* in vitro *by whole cell extracts is dNTP dependant*

An abortive ligation intermediate (25nM) consisting of a 1 nucleotide gap, a 3'P and a 5'AMP was incubated with 5µg of WT and AOA1 whole cell extract and ATP, dNTPs and $MgCl_2$ were separately dropped out of the reaction mix. Gel extracted AMP-^{32}P-25mer and ^{32}P-25mer were included as markers (Lanes 9 and 10). As seen reactions containing cell-extracts from lymphoblastoid cell lines exhibited non-specific nuclease activity (*) which was supressed by addition of an 1000x fold molar excess of competitor oligonucleotide. Note that this experiment was performed three independent times with a representative experiment presented here.

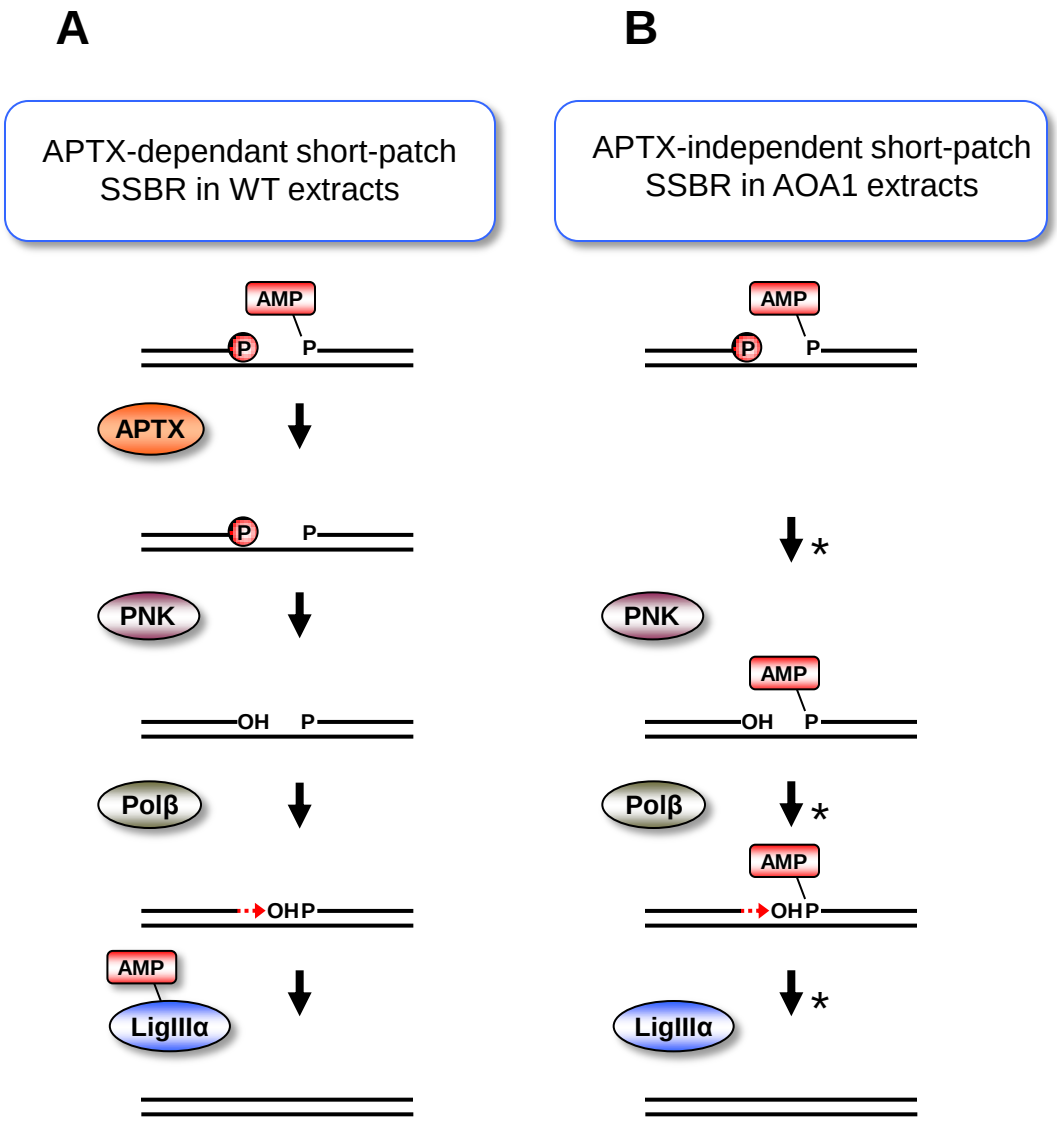

Figure 4.1 – *Model of short-patch SSBR of an abortive ligation intermediate occurring in WT and AOA1 whole cell extracts*

A Model for APTX-dependent short-patch SSBR of an abortive ligation intermediate in WT whole cell extracts. During end-processing, APTX cleaves the 5'-AMP, restoring a 5'-P and PNK converts the 3'P to a 3'OH. Polβ inserts a single nucleotide to fill the gap and the resulting nick is ligated by an adenylated LigIIIα molecule

B Model for APTX-independent short-patch SSBR of an abortive ligation intermediate in AOA1 whole cell extracts. Note that there are three potential points in which the short-patch SSBR of an abortive ligation intermediate can stall in the absence of APTX (asterisk). The presence of the 5'-AMP could prevent access of either PNK or Polβ to the 3' termini, blocking repair at the early steps, or the ligation of the adenylated nick could fail.

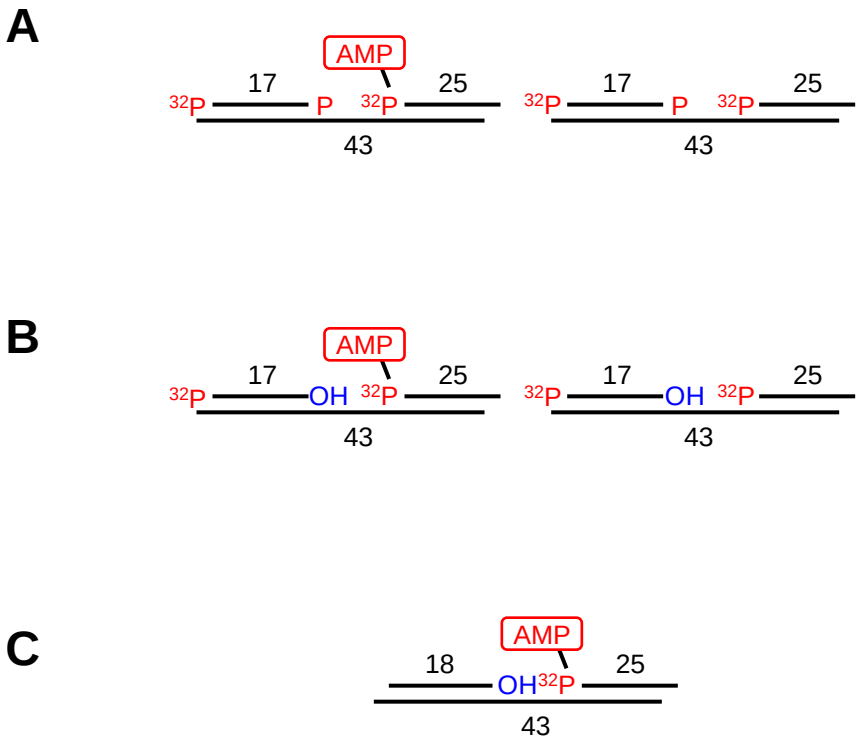

Figure 4.2 - ***Details of the SSB substrates employed in this chapter***

A Adenylated and mock adenylated SSB substrates used to directly measure PNK dependent repair of 3'- phosphate termini. The substrates contain a 1 nucleotide gap possessing a 3'-phosphate and either a 5'-AMP or 5'-P. Note the position of ^{32}P radiolabels on the 5' termini of both the 17mer and the 25mer oligonucleotides.

B Adenylated and mock adenylated SSB substrates used to directly measure gap-filling by Polβ. The substrates contain a 1 nucleotide gap possessing a 3'-hydroxyl and either a 5'-AMP or 5'-P. Note position of ^{32}P radiolabels on the 5' termini of both the 17mer and the 25mer oligonucleotides.

C An adenylated SSB substrate used to measure the direct ligation of an adenylated nick. The substrate contains a nick with a 3'-hydroxyl and a 5'-AMP. Note that unlike the substrates in **A** and **B**, this substrate possesses a ^{32}P radiolabel on the 5' termini of the 25mer oligonucleotide only.

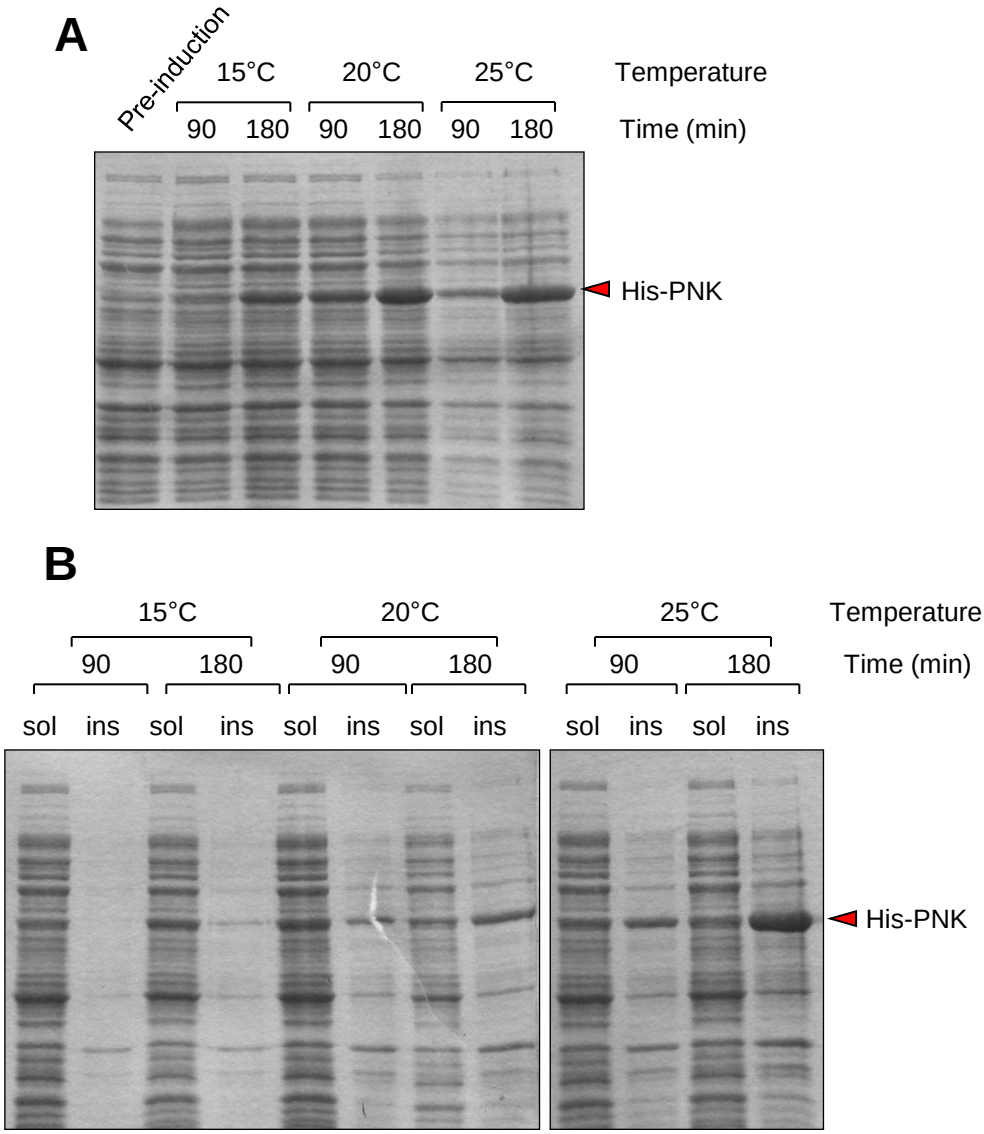

Figure 4.3 – *Optimising overexpression conditions for recombinant human His-PNK*

A To determine optimal expression conditions for His-PNK, six small scale cultures with three different growth temperatures (15°C, 20°C and 25°C) and two incubation times (90min and 180min) were set up. 1ml pre-induction and post-induction samples were taken, normalised for cell density of the culture and aliquots were analysed by 10% SDS-PAGE. His-PNK migrates at approximately 57kDa by SDS PAGE (red arrow). Total levels of recombinant His-PNK increased as the growth temperature and incubation time increased

B The cultures described above were harvested and sonicated and the soluble and insoluble fractions were separated by centrifugation. 10µl aliquots of the soluble and insoluble fractions were compared by 10% SDS-PAGE. The ratio of soluble His-PNK to insoluble His-PNK decreased as incubation time and growth temperature increased. Optimal conditions for the production of high levels of soluble His-PNK were considered to be incubation at 20°C for 90min.

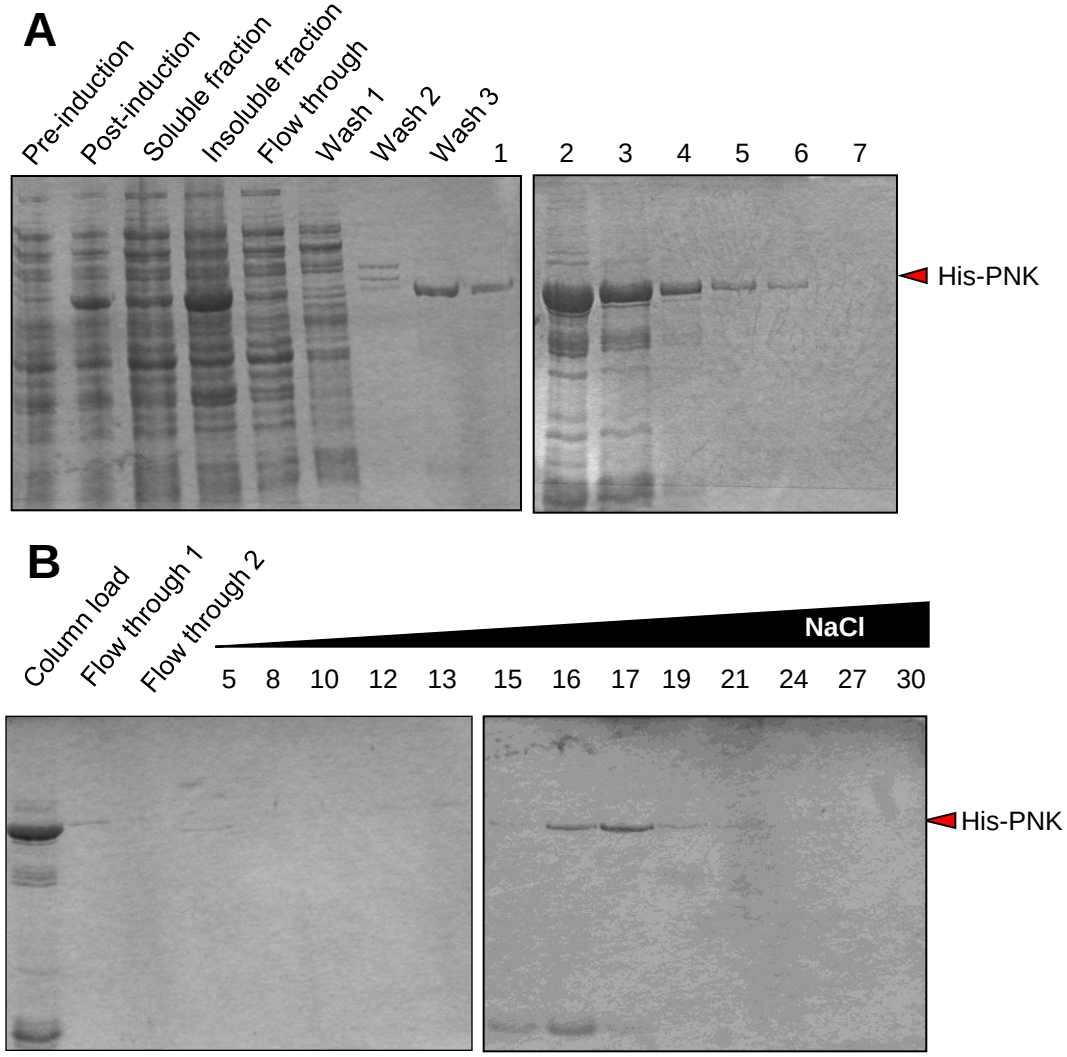

Figure 4.4 – *Overexpression and purification of recombinant His-tagged PNK in* E.coli

A His-PNK protein expression was induced in a 500ml bacterial culture by addition of 1mM IPTG and incubation at 20°C for 90min. 1ml pre-induction and post-induction samples were taken and normalised for the cell density. The bacterial cells were harvested, resuspended in 20ml buffer and lysed by sonication. The soluble fraction was separated from the insoluble material by centrifugation, and the insoluble material was resuspended in 20ml buffer. The clarified extract was loaded onto a 0.5ml Ni-NTA IMAC column, washed three times with 10 column volumes of buffer containing 10mM, 20mM and 40mM imidazole respectively and eluted in buffer containing 250mM imidazole. 10µl aliquots of each of the different fractions were analysed by 10% SDS PAGE and staining with coomassie blue. His-PNK runs at approximately 57kDa (red arrow). His-PNK co-eluted with a significant amount of contaminating proteins necessitating a second purification step; delete this sentence.

B Elution fractions 2 and 3 from Ni-NTA IMAC were pooled and loaded onto a cation exchange column at pH7.5. His-PNK was eluted from the column with a salt gradient from 0.1M to 1M NaCl. 10µl aliquots of the column load, flow through samples and selected elution fractions were analysed by 10% SDS-PAGE. Elution fraction 17 was chosen for use in experiments.

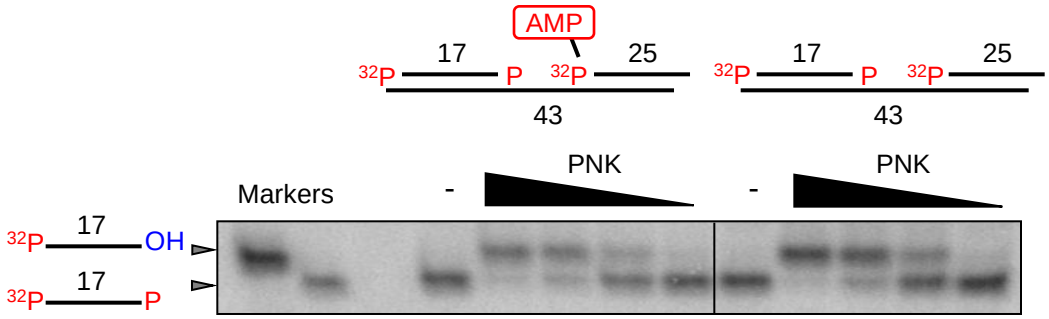

Figure 4.5 - ***A 5'-AMP terminus does not block PNK mediated 3' end processing***

A titration of His-PNK (250nM, 100nM, 50nM and 25nM) was incubated with an adenylated or mock-adenylated SSB substrate (25nM) containing a 1 nucleotide gap, a 3'-P terminus, and a 5'-AMP terminus for 1 hr at 30°C. The products were fractionated by 15% denaturing PAGE and detected by phosphoimaging. The substrate was ^{32}P-radiolabelled on the 5' termini of the 17mer oligonucleotide to directly visualise processing of the 3' termini. Cartoons of the substrates are shown above.

Repair of the 3'-phosphate terminus is indicated by reduced mobility of the radiolabelled 17mer. ^{32}P-17mer-P and ^{32}P-17mer-OH oligonucleotides were included as markers. Note that this experiment was performed three independent times with a representative experiment presented here.

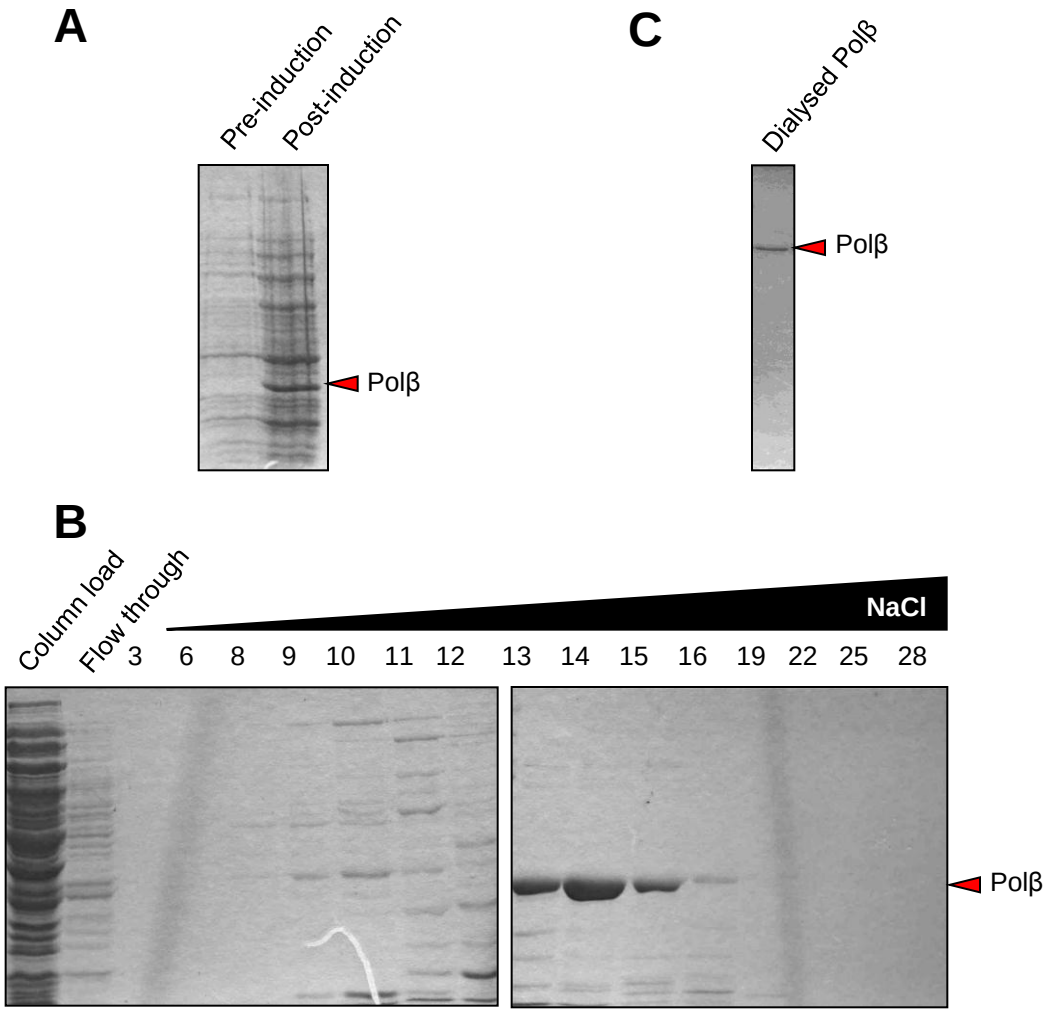

Figure 4.6 - *Overexpression and purification of recombinant human Polβ from* E.coli *by cation exchange chromatography*

A Expression of recombinant human Polβ was induced by incubation at 42°C for 4 hours. 1ml pre-induction and post-induction samples were taken and aliquots were analysed by 10% SDS PAGE.

B After induction of Polβ, the cells from 500ml of culture were harvested, resuspended in 20ml buffer and lysed by sonication. The soluble material was separated from the insoluble fraction by centrifugation. Clarified extract was then loaded onto a consequtive anion and cation exchange columns in series. Following extensive washing the anion exchange column was removed and Polβ was eluted from the cation exchange column with a salt gradient of 0.1M to 1M NaCl. 10µl aliquots of the column load, flow through and selected elution fractions from 6 to 31 were analysed by 10% SDS PAGE. Polβ eluted in a sharp peak between elution fractions 13 and 15. Elution fraction 14 was chosen for use in experiments.

C 500ng of the final dialysed preparation of Polβ was analysed by 10% SDS-PAGE.

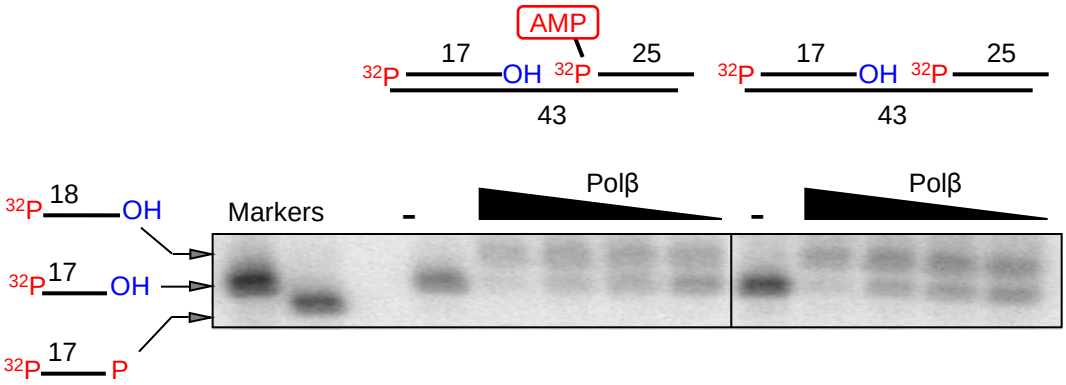

Figure 4.7 - *A 5'-AMP terminus does not block Polβ mediated 3' gap-filling*

A titration of Polβ (5nM, 15nM, 30nM, or 100nM) was incubated with an adenylated or mock-adenylated SSB substrate (25nM) containing a 1 nucleotide gap, a 3'-OH terminus and a 5'-AMP terminus for 1hr at 30°C. The products were fractionated by 15% denaturing PAGE and detected by phosphoimaging. The substrate was ^{32}P-radiolabelled on the 5' termini of the 17mer oligonucleotide to directly measure gap-filling. Cartoons of the substrates are shown above.

Incorporation of a single nucleotide into the SSB resulted in an increase conversion of the ^{32}P-17mer-OH to an ^{32}P-18mer-OH. ^{32}P-17mer-P and ^{32}P-17mer-OH oligonucleotides were included as markers. Note that this experiment was performed four independent times with a representative experiment presented here.

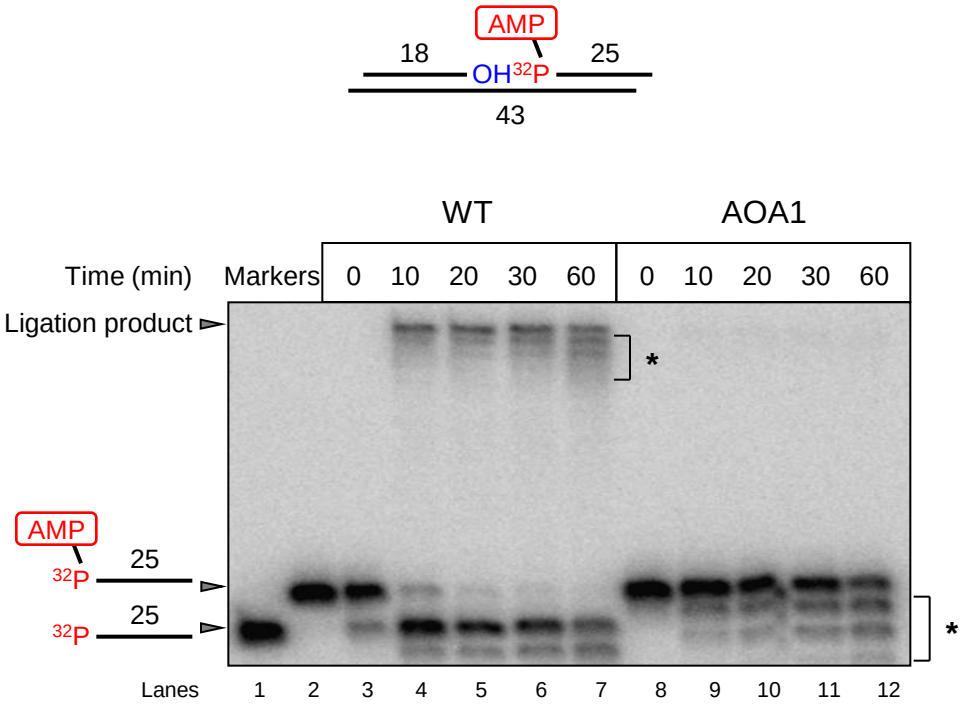

Figure 4.8 - *AOA1 whole cell extracts are unable to repair an adenylated nick*

6.25µg of whole cell extracts prepared from WT and AOA1 LCLs was incubated at 30°C for the indicated times with 25nM of an adenylated nick. The substrate was ^{32}P radiolabelled on the 5' termini of the 25mer oligonucleotide. A cartoon of the substrate is displayed above. The reaction products were fractionated by 15% denaturing PAGE and detected by phosphorimaging. The AMP-^{32}P-25mer and ^{32}P-25mer were included as markers (lanes 1 and 2). Repair of the pre-adenylated is visualised by the appearance of a ligation product. Cell-extracts from lymphoblastoid cell lines have high levels of non-specific nuclease activity (asterisk) which was suppressed by the addition of 1000x fold molar excess of a competitor oligonucleotide of unrelated sequence.

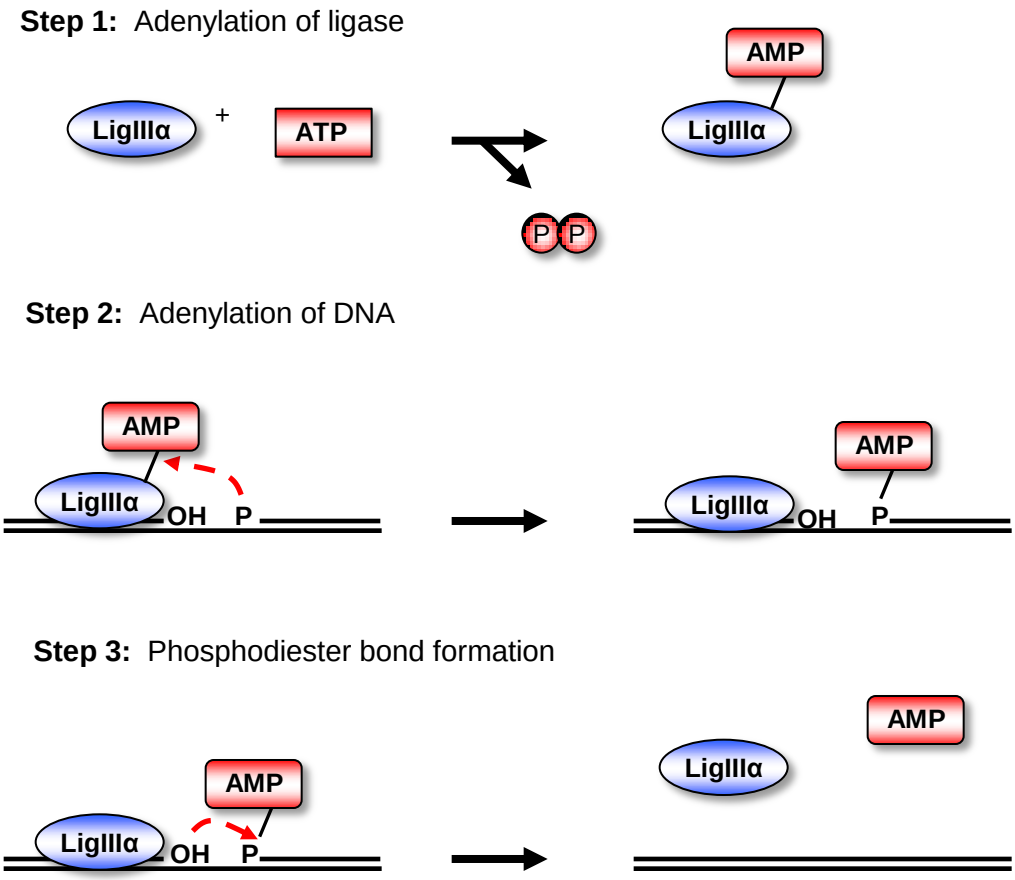

Figure 5.1 – *Reaction mechanism of mammalian ligases*

DNA ligases are nucleotidyltransferases (NTases) that utilise a high energy cofactor to catalyse phosphodiseter bond formation in a universal three-step reaction mechanism.

Step 1: In the first step of DNA ligation reacts with ATP to form a ligase-adenylate intermediate in which AMP is covalently linked to the active-site lysine. This reaction is very energetically favourable and the ligase-adenylate intermediate is stable in the absence of a DNA substrate. Therefore this reaction can be seen as essentially irreversible, meaning that the majority of ligase in the cell is likely to be in the adenylated form.

Step 2: The second step of ligation is the activation of the 5'P by adenylation of the DNA. During this step the oxygen of the 5'P attacks the phosphorus of the AMP, dispelling the lysine and transferring the adenylate group onto the 5'P, forming an AMP-DNA intermediate.

Step 3: The final step of ligation is the reformation of the phosphodiester backbone. During this step the non-adenylated ligase catalyses the nucleophilic attack of the 5'AMP by the 3'OH, displacing the AMP and joining the two polynucleotides by formation of a phosphodiester bond

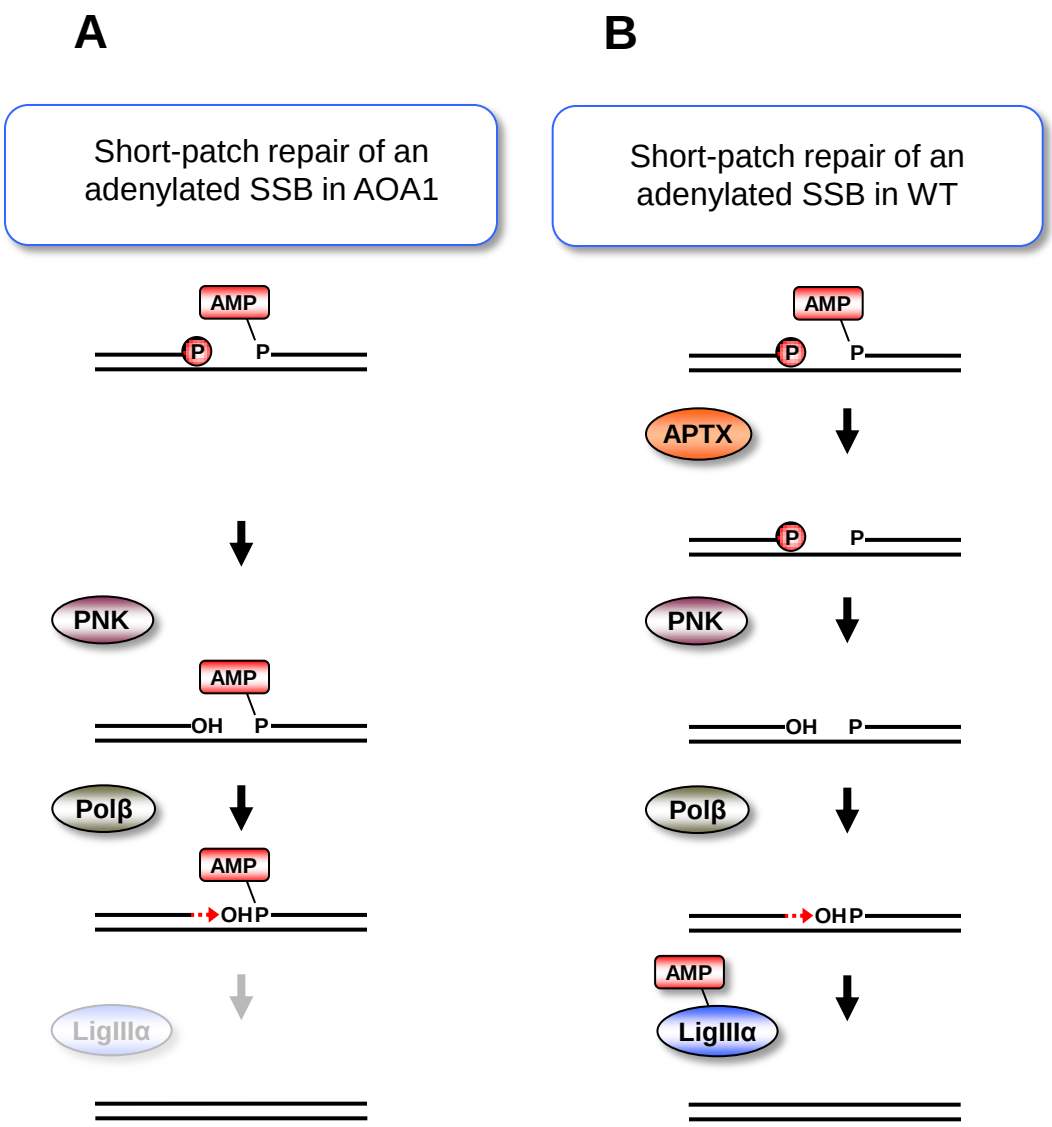

Figure 5.2 – *Model for the failure of APTX-independent repair of an adenylated nick due to limiting levels of non-adenylated DNA ligase*

DNA ligases exist within two forms in the cell. The first form is a non-adenylated ligase. This non-adenylated ligase can repair an pre-adenylated nick *in vitro* (**A**). The second form is an adenylated ligase which can repair a conventional nick *in vitro*, during which the ligase will become de-adenylated (**B**)**.**

The predominant form of ligase in the cell is likely to be the adenylated ligase and it is therefore possible that there are insufficient levels of non-adenlyated available to ligate a pre-adenylated nick in the absence of APTX (**B**).

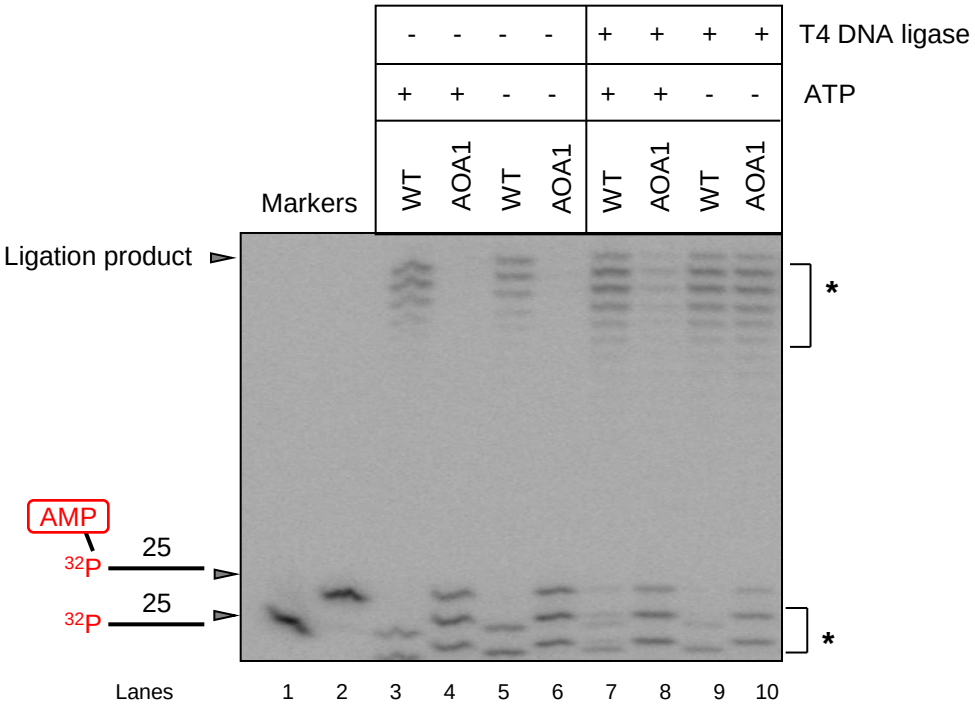

Figure 5.3 – *Short-patch repair of an adenylated 1nt gap is rescued in AOA1 independently of APTX by addition of recombinant DNA ligase in the absence of ATP*

An abortive ligation intermediate (25nM) consisting of a 1 nucleotide gap, a 3'-P terminus, and a 5'-AMP terminus, was incubated for 1hr at 30°with 5µg of WT or AOA1 whole cell extract in the presence or absence of 1mM ATP and/or absence T4 DNA ligase. The substrate was ^{32}P-radiolabelled on the 25mer oligonucleotide. A cartoon of the substrate is displayed above. The reaction products were fractionated by 15% denaturing PAGE and detected by phosphorimaging. AMP-^{32}P-25mer and ^{32}P-25mer were included as markers (Lanes 1 and 2). Cell-extracts from lymphoblastoid cell lines have high levels of non-specific nuclease activity (asterisk) which was suppressed by the addition of 1000x fold excess of a competitor oligonucleotide of unrelated sequence. Note that this experiment was performed eight independent times with a single representative experiment presented here.

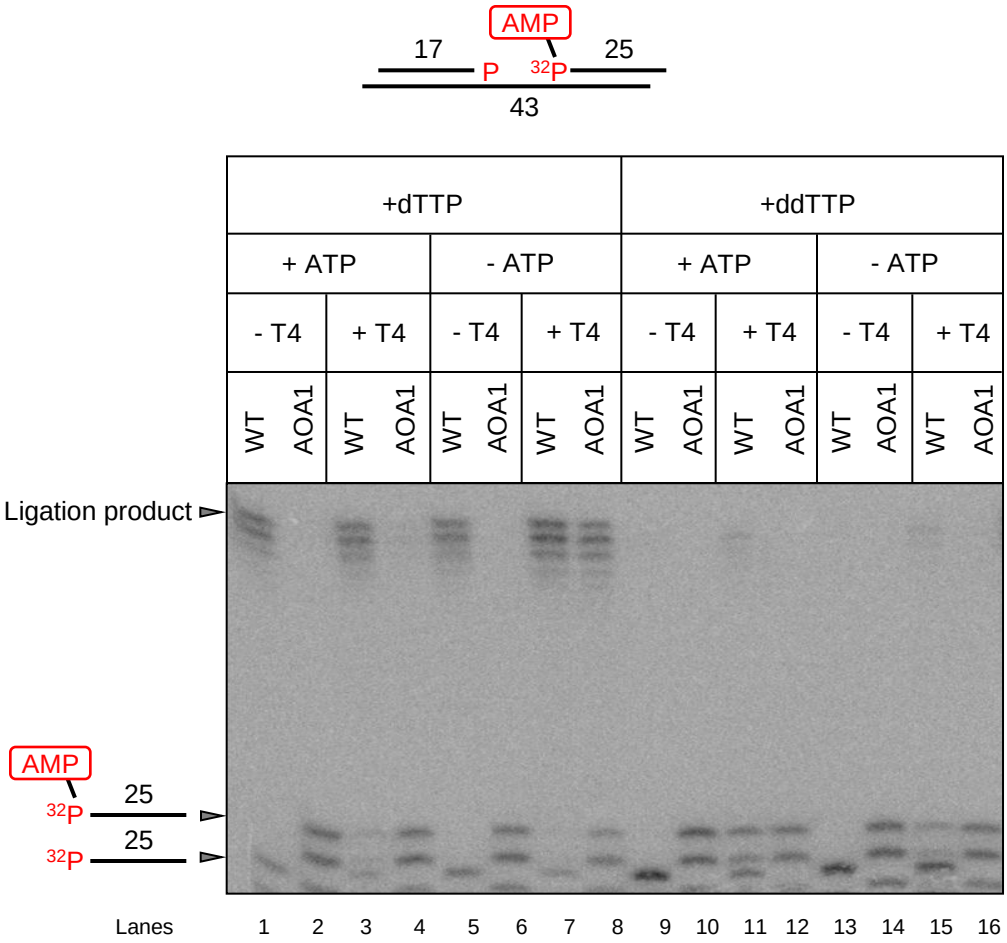

Figure 5.4 – *Short-patch SSBR of an abortive ligation intermediate in whole cell extracts* in vitro *is 'poisoned' by the addition of dideoxythymidine triphosphate*

An adenylated 1nt gap (25nM) consisting of a 1 nucleotide gap, a 3'-P and a 5'-AMP was incubated at 30°C for 1 hour with 5µg of WT and AOA1 whole cell extract in the presence or absence of 1mM ATP, 1U of T4 DNA ligase and 100µM dNTPs containing either dTTP or ddTTP. The substrate was ^{32}P radiolabelled on the 5' terminus of the 25mer oligonucleotide (^{32}P-25mer). A cartoon of the substrate is displayed above. The reaction products were fractionated by 15% denaturing PAGE and detected by phosphorimaging.

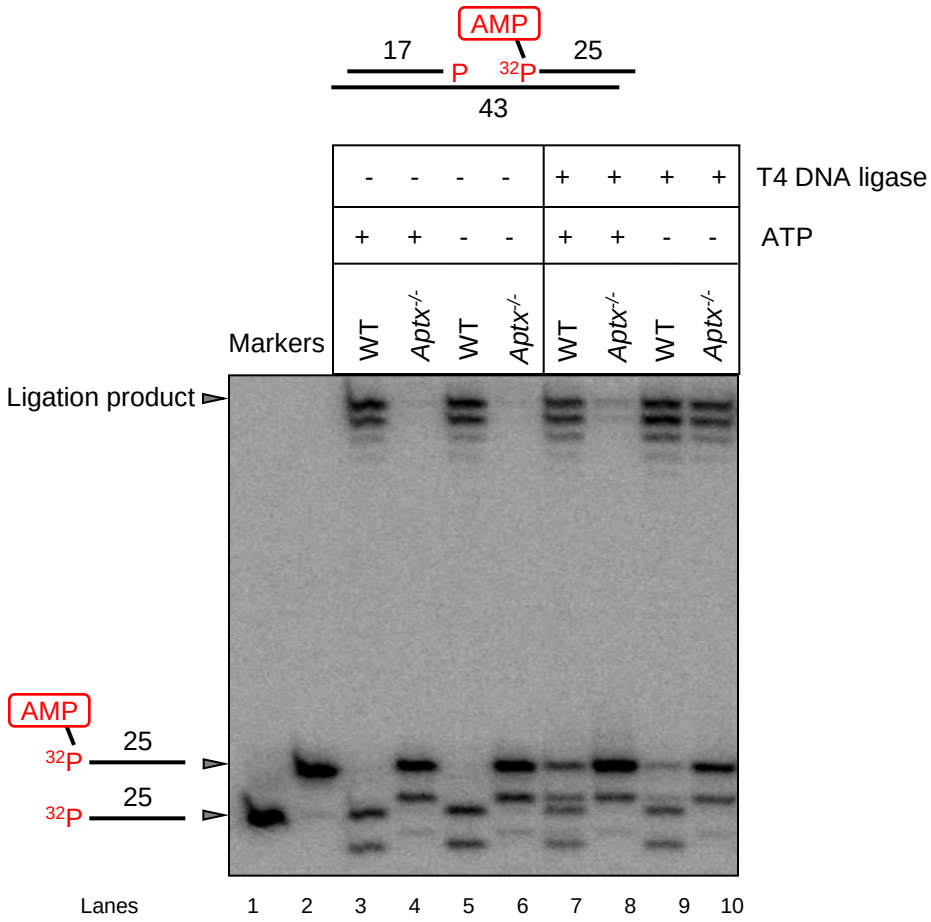

Figure 5.5 – *Short-patch SSBR of an adenylated 1nt gap by whole cell extracts prepared from quiescent* Aptx$^{-/-}$ *mouse neural astrocytes is rescued by addition of recombinant T4 DNA ligase in the absence of ATP*

An abortive ligation intermediate (25nM) consisting of a 1 nucleotide gap, a 3'P and a 5'AMP was incubated with 5µg of whole cell extracts from WT and *Aptx*$^{-/-}$ quiescent mouse astrocytes in the presence orabsence of 1mM ATP and/or 1U of T4 DNA ligase at 30°C for 1 hour. The substrate was ^{32}P radiolabelled on the 5' of the 25mer oligonucleotide. A cartoon of the substrate is displayed above. The reaction products were fractionated by 15% denaturing PAGE and detected by phosphorimaging. AMP-^{32}P-25mer and ^{32}P-25mer were included as markers (Lanes 1 and 2).

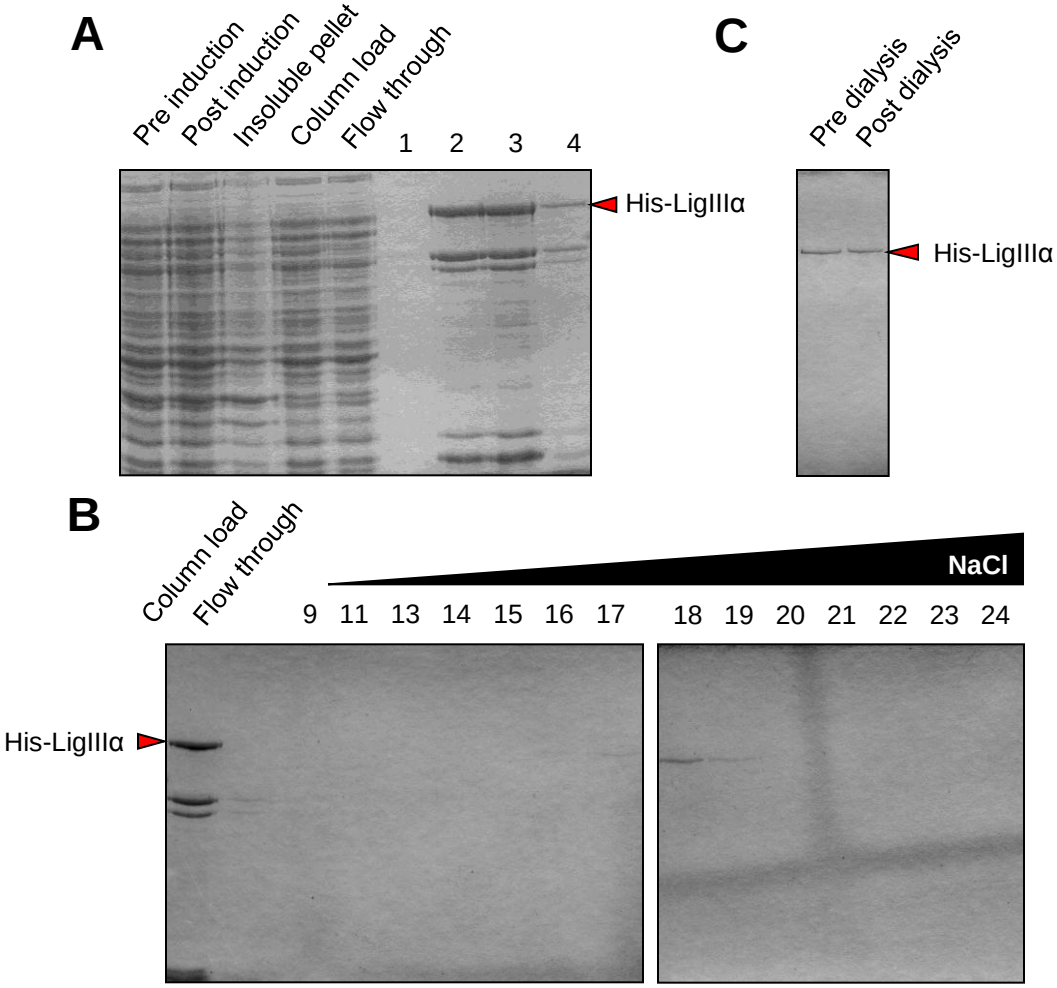

Figure 5.6 – *Overexpression and purification of recombinant human His-tagged LigIIIα*

A His-LigIIIα protein expression was induced in a 500ml bacterial culture by addition of 1ml IPTG and incubation at 20°C for 90min. 1ml pre-induction and post-induction samples were taken and normalised for the cell density. The bacterial cells were harvested, resuspended in 20ml buffer and lysed by sonication. The soluble fraction was separated from the insoluble material by centrifugation, and the insoluble material was resuspended in 20ml buffer. The clarified extract was loaded onto a 0.5ml Ni-NTA IMAC column, washed three times with buffer containing 10mM, 20mM and 40mM imidazole respectively and eluted in buffer containing 250mM imidazole. 10µl aliquots of each of the different purification stages were analysed by 10% SDS PAGE.

B Elution fractions 2 and 3 from Ni-NTA IMAC were pooled and the LigIIIα in these fractions further purified by cation exchange chromatography at pH7. His-LigIIIα was eluted from the column with a salt gradient from 0.1M to 1M NaCl. 10µl aliquots of the column load, flow through samples, and indicated elution fractions were analysed by 10% SDS-PAGE and staining with coomassie blue.

C Elution fraction 18 was dialysed into storage buffer and 500ng of LigIIIα was analysed by 10% SDS-PAGE.

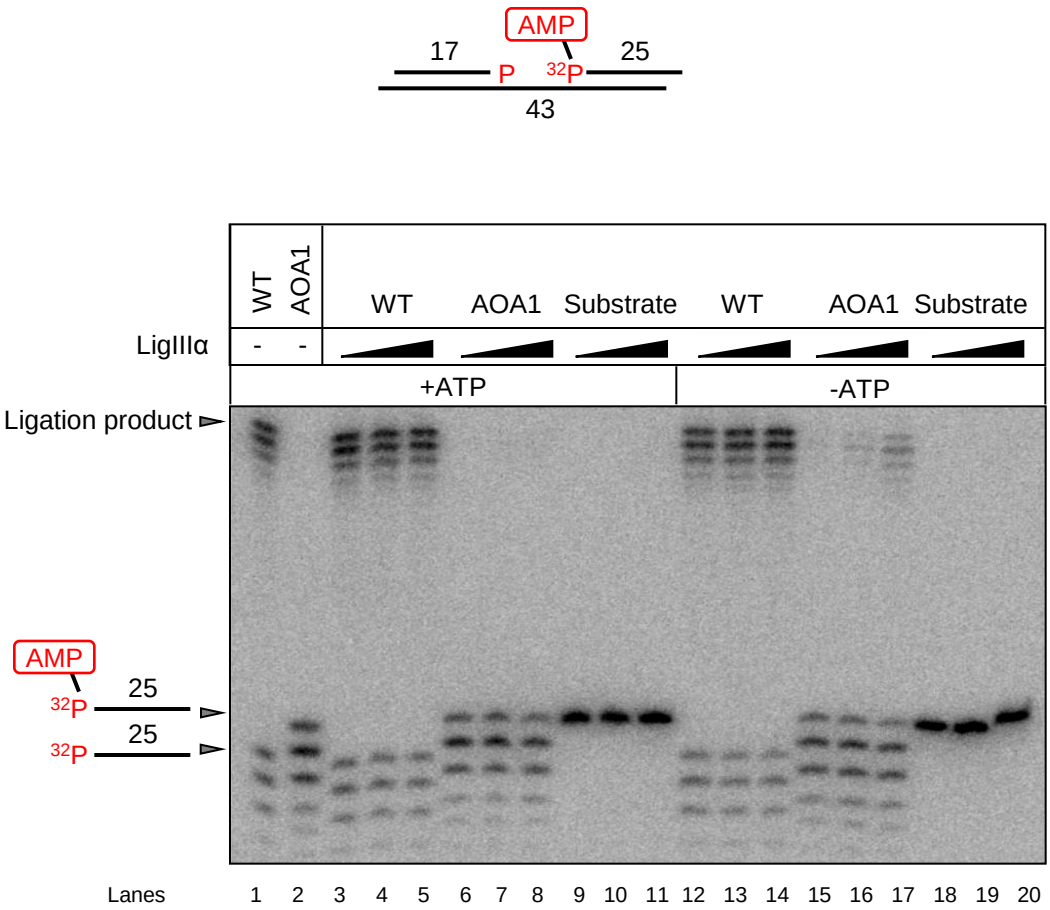

Figure 5.7 – *Complementation of the short-patch SSBR defect in AOA1 whole cell extracts with recombinant human LigIIIα in the absence of ATP*

An adenylated 1nt gap (100nM) harbouring 3'-P and 5'-AMP termini (top cartoon) was incubated 5µg of WT or AOA1 whole cell extract and 8nM, 24nM, or 72nM of His-LigIIIα in the presence or absence of 1mM ATP at 30°C for 1 hour, as indicated. His-LigIIIα was also incubated with the substrate in the absence of whole cell extract as a control (lanes 9-11 and 18-20). The substrate was ^{32}P radiolabelled on the 5' of the 25mer oligonucleotide (^{32}P-25mer). A cartoon of the substrate is displayed (top). The reaction products were fractionated by 15% denaturing PAGE and detected by phosphorimaging. Note that this experiment was performed two independent times with a single representative experiment presented here.

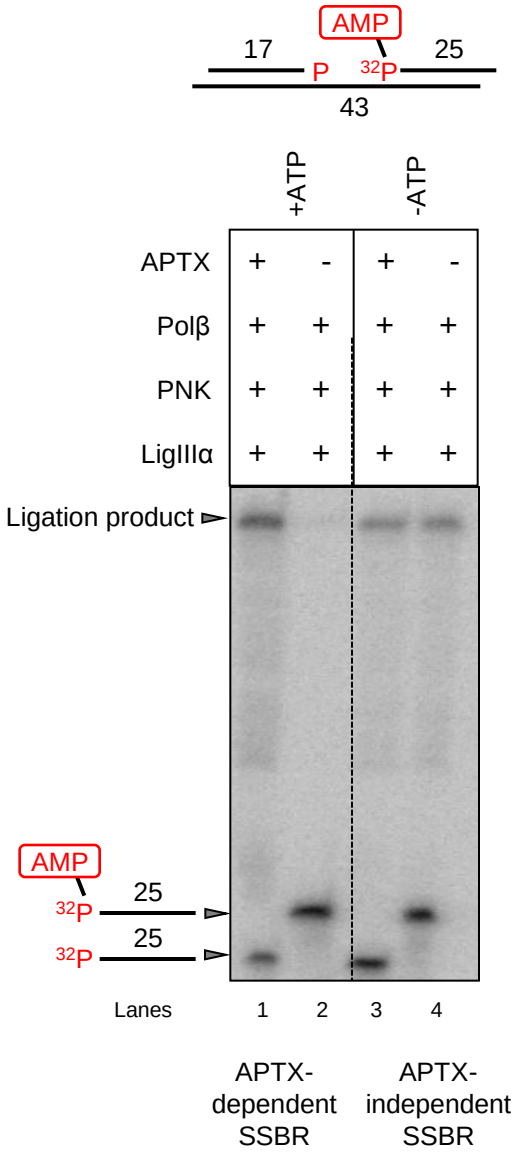

Figure 5.8 – *Reconstitution of APTX-independent SSBR by purified recombinant human proteins*

An adenylated 1nt gap (60nM) harbouring 3'-P and 5'-AMP termini was incubated at 30°C for 1 hour with 250nM His-PNK, 100nM Polβ and 80nM LigIIIα in the presence or absence of 100nM His-APTX and 1mM ATP. The substrate was ^{32}P radiolabelled on the 5' of the 25mer oligonucleotide (^{32}P-25mer). A cartoon of the substrate is displayed (top). The reaction products were fractionated by 15% denaturing PAGE and detected by phosphorimaging. Note that this experiment was performed two independent times with a single representative experiment presented here.

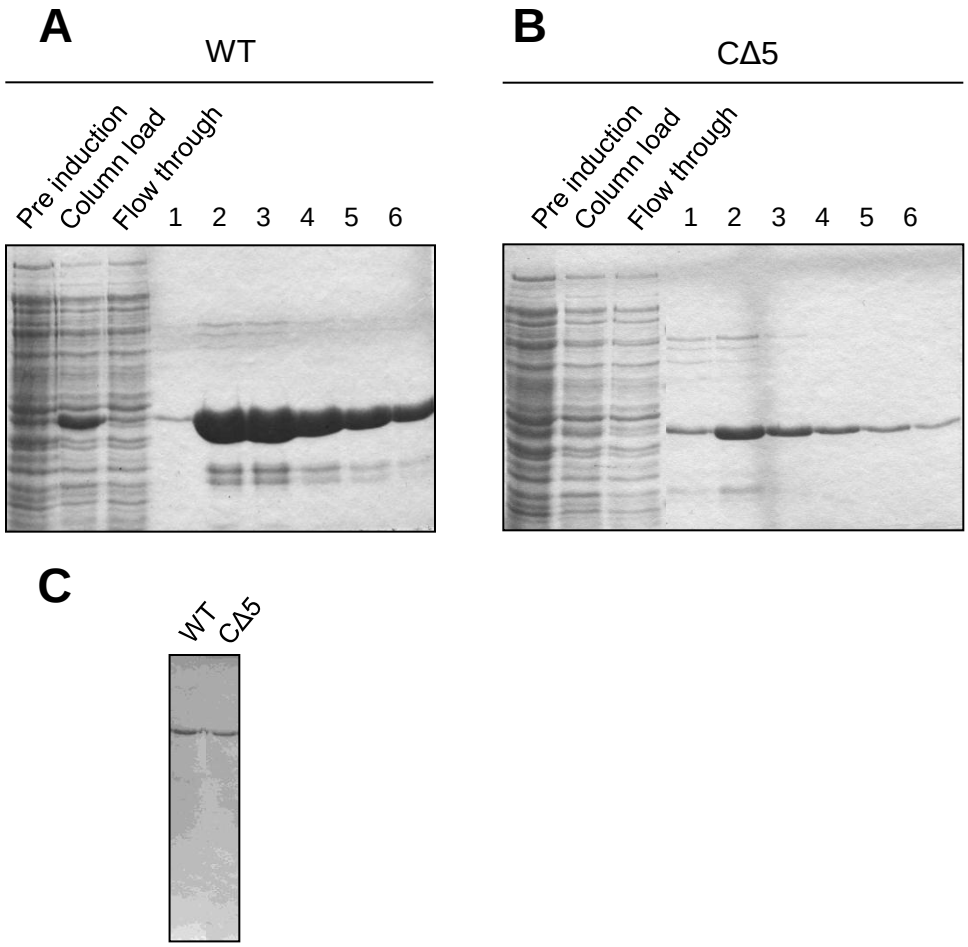

Figure 5.9 – ***Overexpression and purification of recombinant His-tagged Chlorella Virus DNA Ligases by Ni-NTA IMAC***

Expression of wild type CV DNA ligase (**A**) and mutant CΔ5 CV DNA ligase (**B**) was induced in a 500ml bacterial culture by addition of IPTG and incubation at 20°C for 90min. 1ml pre-induction and post-induction samples were taken and normalised for the cell density. The bacterial cells were harvested, resuspended in 20ml buffer and lysed by sonication. The soluble fraction was separated from the insoluble material by centrifugation, and the insoluble material was resuspended in 20ml buffer. The clarified extracts were loaded onto two Ni-NTA IMAC columns, washed three times with buffer containing 10mM, 20mM and 40mM imidazole respectively and eluted in buffer containing 250mM imidazole. 10µl aliquots of different purification stages were analysed by 10% SDS PAGE. WT CV DNA ligase migrates during SDS-PAGE at approximately 28kDa while CΔ5 CV DNA ligase migrates slightly faster (red arrow).

C Elution fraction 2 from each purification was dialysed and 500ng of protein analysed by 10% SDS-PAGE and coomassie blue staining.

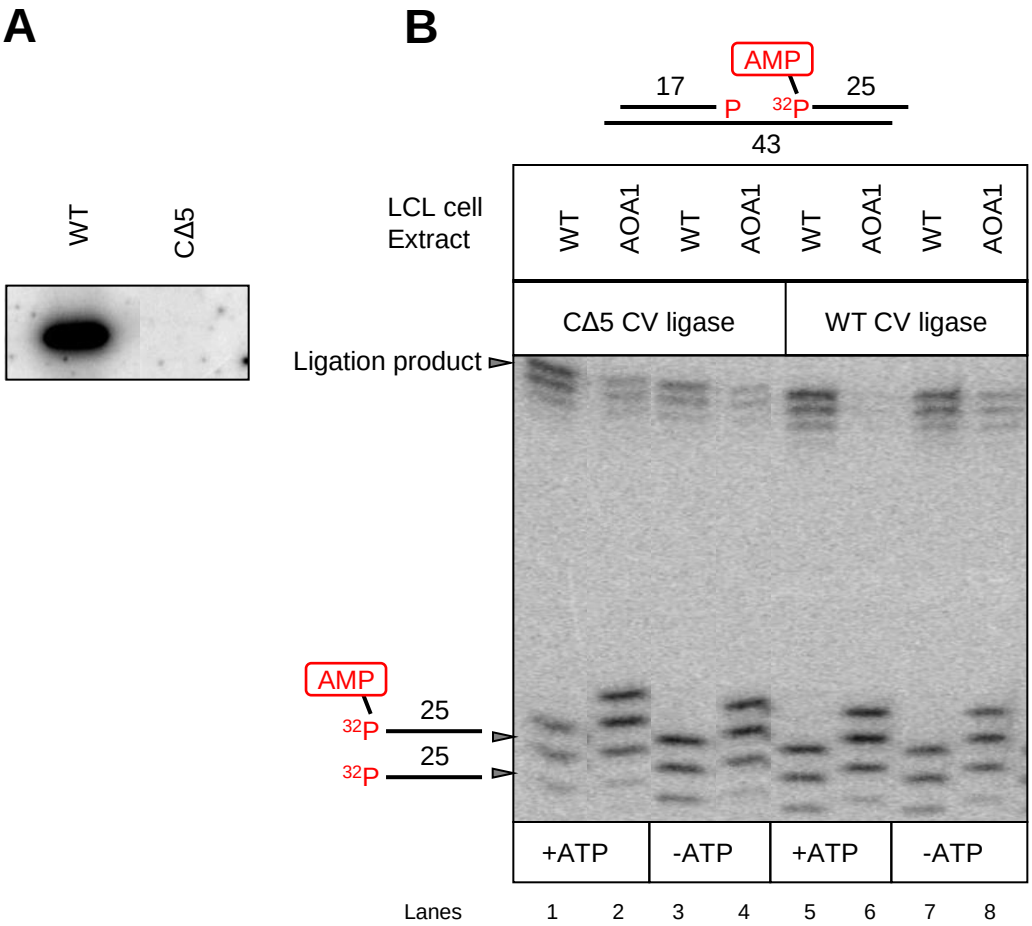

Figure 5.10 – *Short-patch SSBR of an abortive ligation intermediate can be restored in AOA1 extracts independently of ATP by addition of a non-adenylatable DNA ligase mutant*

A 100ng (280nM) of WT chlorella virus DNA ligase or CΔ5 chlorella virus DNA ligase was incubated with α^{32}P ATP and 10nM cold ATP at 30°C for 5min. Reactions were stopped by addition of formamide loading buffer, fractionationated by 10% SDS PAGE and detected by phosphorimaging. There was a very strong ^{32}P signal in the lane containing reaction products from the WT CV ligase adenylation reaction which ran at the expected size for WT CV ligase

B An adenylated 1nt gapped substrate (25nM) harbouring a 3'-P terminus was incubated at 30°C for 1 hour with 5µg of WT or AOA1 whole cell extract in the presence or absence of 1mM ATP and either 500nM WT chlorella virus DNA ligase or CΔ5 chlorella virus DNA ligase . The substrate was ^{32}P radiolabelled on the 5' of the 25mer oligonucleotide. A cartoon of the substrate is displayed above. The reaction products were fractionated by 15% denaturing PAGE and detected by phosphorimaging. Note that this experiment was performed two independent times with a single representative experiment presented here.

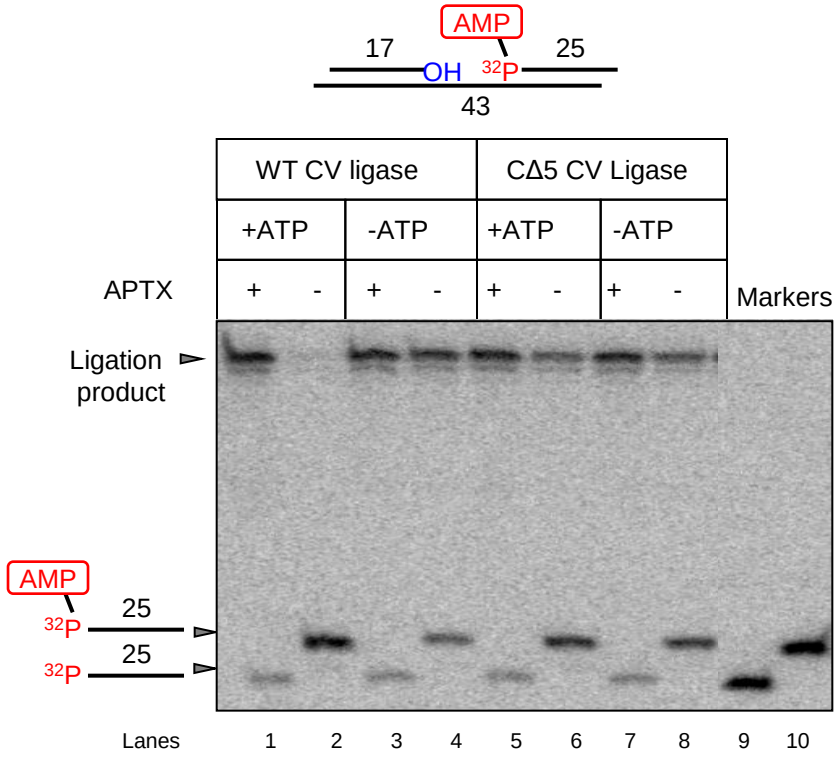

Figure 5.11 – Reconstitution of *APTX-independent SSBR using recombinant SSBR proteins and chlorella virus DNA ligases*

An adenylated 1nt gapped substrate (25nM) harbouring a 3'-OH terminus was incubated at 30°C for 1 hour with 100nM Polβ and either 500nM WT CV DNA ligase, 500nM CΔ5 CV DNA ligase or 1U T4 DNA ligase in the presence or absence of 100nM His-APTX and 1mM ATP. The substrate was ^{32}P radiolabelled on the 5' of the 25mer oligonucleotide (^{32}P-25mer). A cartoon of the substrate is displayed (top). The reaction products were fractionated by 15% denaturing PAGE and detected by phosphorimaging. Note that this experiment was performed two independent times with a single representative experiment presented here.

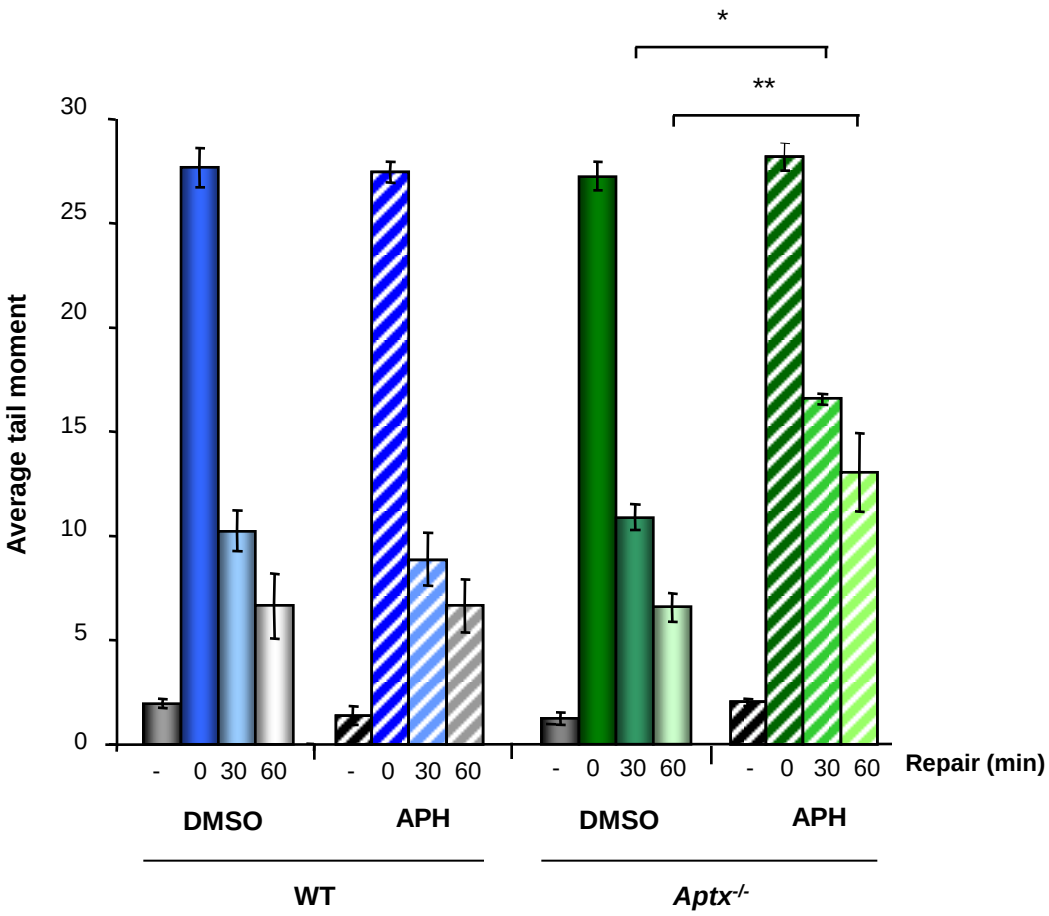

Figure 6.1 – A SSBR defect is uncovered in quiescent mouse* APTX$^{-/-}$ *astrocytes treated with aphidicolin

Astrocytes obtained from *APTX*$^{-/-}$ and WT littermate mice were cultured and made quiescent by contact inhibition and subsequent serum starvation. After a week in serum starvation media, the cells were harvested and pre-treated with 50μM APH or DMSO in suspension at 37°C for 30min. The cells were then washed with DPBS to remove any trace of media, and then incubated with 75μM H_2O_2 for 10min on ice. After damage induction, the cells were washed with ice cold DPBS three times and then allowed to repair at 37°C in media containing either APH or DMSO. Samples were taken at the indicated time points and comet tail moments were determined for 100 cells per sample using the Comet Assay IV software. The data from three independent experiments was averaged (+/- SEM). Asterisks indicate statistically significant differences as determined using SPSS software (*, $P \leq 0.05$; ** $P \leq 0.01$). These experiments were carried out by Sherif El-Khamisy and are presented here with kind permission.

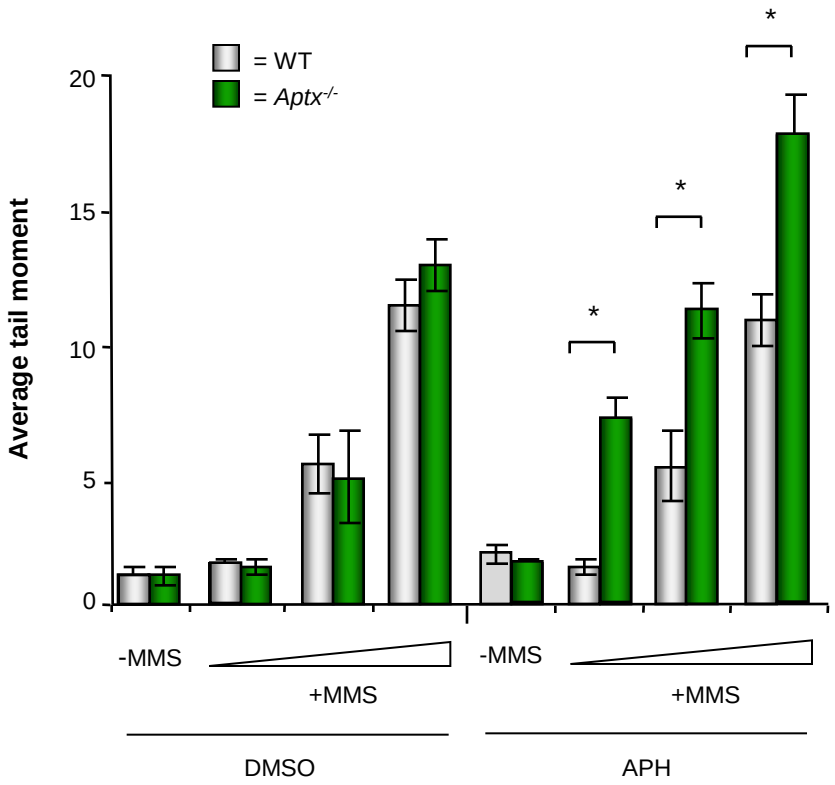

Figure 6.2 – A BER defect is uncovered in quiescent mouse* APTX$^{-/-}$ *astrocytes treated with aphidicolin

Astrocytes obtained from *APTX*$^{-/-}$ and WT littermate mice were cultured and made quiescent by contact inhibition and subsequent serum starvation. After a week in serum starvation media, the cells were harvested and pre-treated with 50μM APH or DMSO in suspension at 37°C for 30 min. The cells then incubated with 25, 50 or 100μM MMS for 10 min at 37°C in drug containing media. Samples were taken and comet tail moments were determined for 100 cells per sample using the Comet Assay IV software. The data from three independent experiments was averaged (+/- SEM). Asterisks indicate statistically significant differences as determined using SPSS software (*, $P \leq 0.05$). These experiments were carried out by Sherif El-Khamisy and are presented here with kind permission.

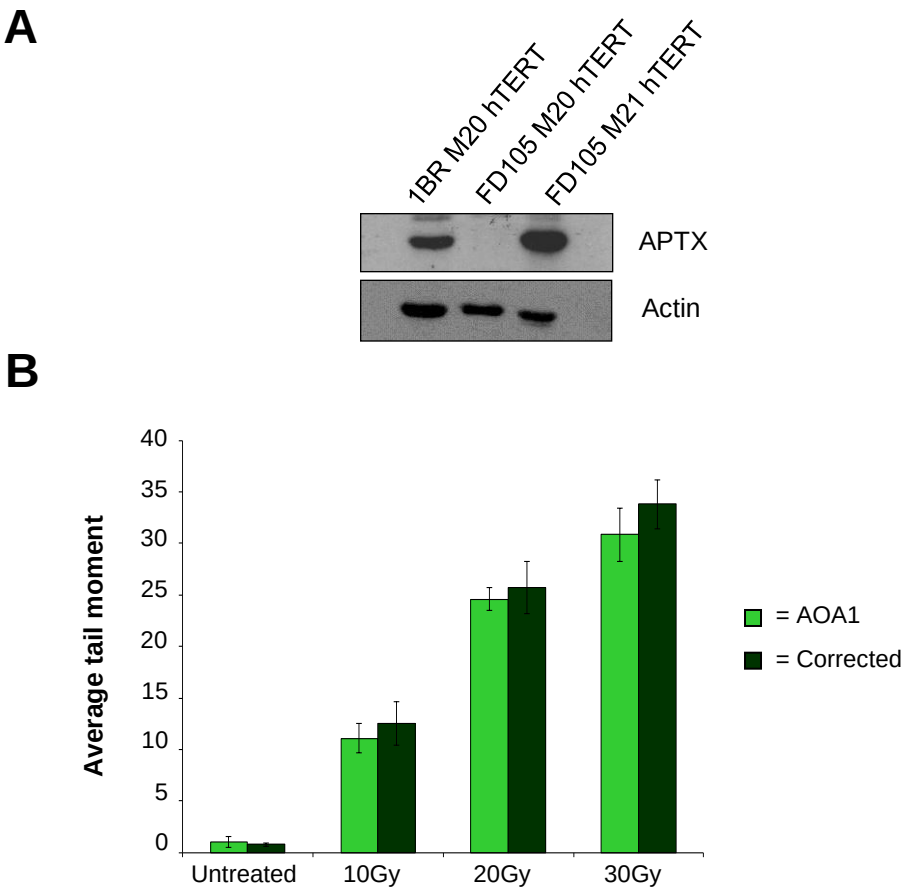

Figure 6.3 – Dose response of FD105 hTERT human fibroblasts to γ-irradiation

A An hTERT immortalised fibroblast cell line derived from an AOA1 individual that had been corrected by stable expression of human APTX (FD105 M21 hTERT) using a retroviral expression system and a control cell line consisting of the same parental AOA1 hTERT fibroblast cell line containing the empty expression vector (FD105 M20 hTERT) were cultured in parallel and immunoblotted for APTX protein. These cell lines were compared to a WT hTERT fibroblast cell line containing the empty expression vector (1BR M20 hTERT). These cell lines were originally created by Limei Ju.

B FD105 M20 hTERT (AOA1) (light green bars) and FD105 M21 hTERT (corrected) (dark green bars) cell lines were cultured, harvested and treated with increasing doses of γ-irradiation
in suspension. Comet tail moments were determined for 100 cells per sample using the Comet Assay IV software. The data from 3 independent experiments was averaged (+/- SEM).

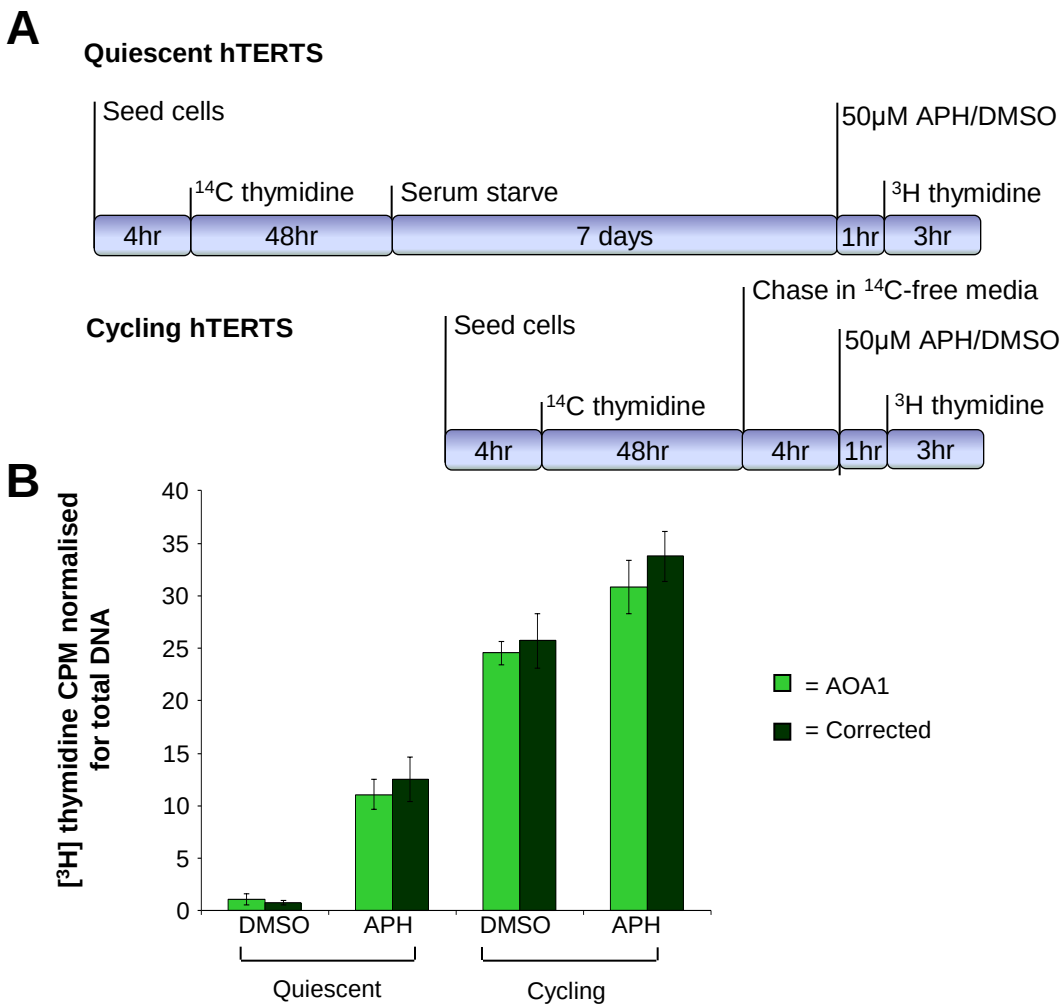

Figure 6.4 – Levels of DNA synthesis in cycling and quiescent hTERT fibroblasts treated with APH or DMSO

Levels of DNA synthesis in cycling and quiescent hTERT fibroblasts treated with APH or DMSO were determined using a [^{3}H] thymidine uptake assay. To normalise for total DNA content, all [^{3}H] counts were normalised to [^{14}C].

A Schematic detailing the incubation times for the DNA synthesis assay. 1x10^{5} cells of AOA1 (FD105 M20) and WT (corrected) (FD105 M21) were seeded into a 6 well dish. Two wells per cell line were seeded. The hTERTs were allowed to adhere for 4hrs and were then incubated with 0.02µCi/ml [^{14}C] thymidine for 48hrs before washing in 3x PBS and serum starving for 7 days. 56hrs before these quiescent cells were to be incubated with APH/DMSO, 0.5x10^{5} cells of AOA1 and corrected were seeded into a second 6 well dish and allowed to adhere for 4hrs. These cycling cells were then incubated with 0.02µCi/ml [^{14}C] thymidine for 48hrs before washing in 3x PBS and incubating in [^{14}C] thymidine free media for 4 hours. Both the quiescent and cycling cell lines were pre-treated with either 50µM APH or DMSO for 1hr and then incubated with 20µCi/ml [^{3}H] thymidine for 3hrs in the presence of drug. The cells were harvested and the ^{3}H and ^{14}C counts were measured using a scintillation counter.

B Measurement of DNA synthesis is presented as [^{3}H] count per minute (CPM) normalised for total DNA content using the [^{14}C] CPM. The data from two independent experiments were averaged (+/- SEM).

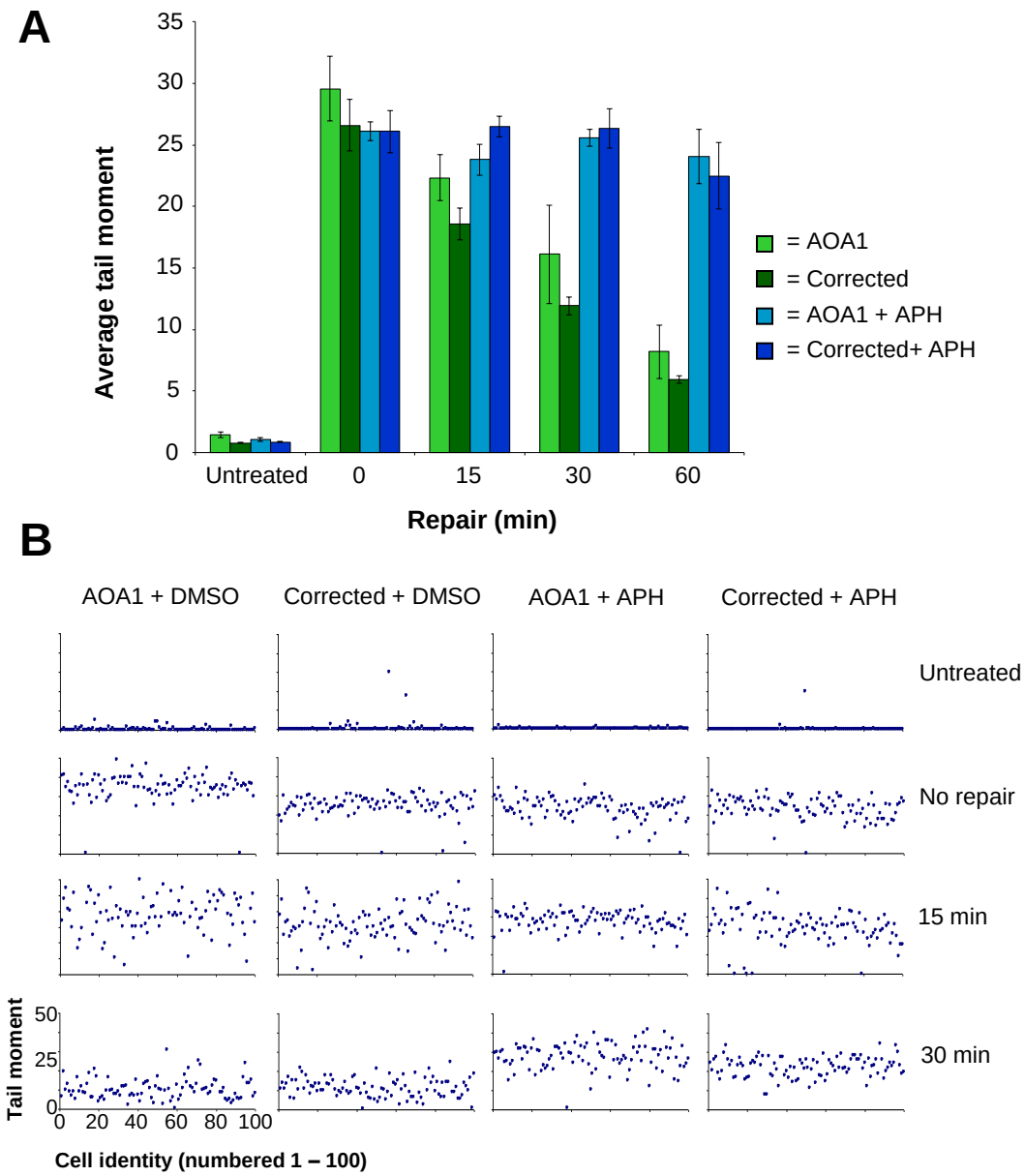

Figure 6.5 – Repair kinetics of γ-irradiation induced breaks in quiescent hTERT fibroblasts pre-treated with APH

Human hTERT fibroblast cell lines from an AOA1 patient stably corrected with either human APTX ORF (FD105 M21 hTERT) or containing empty vector (FD105 M20 hTERT) were made quiescent by contact inhibition and serum starvation for seven days, incubated with 50μM APH or DMSO in suspension for 1 hour at 37°C and irradiated on ice with γ-rays (30Gy). The cells were allowed to repair in media containing APH or DMSO at 37°C for the indicated time periods. Comet tail moments were determined for 100 cells per sample using the Comet Assay IV software.

A The data from 4 independent experiments was averaged (+/- SEM). The difference in repair between FD105 M20 and FD105 M21 treated with DMSO at the 15min, 30min and 60min repair time points was found not to be significant using the two-way anova test (p=0.062890865).
B Representative scatter graphs from selected time points from one experiment.

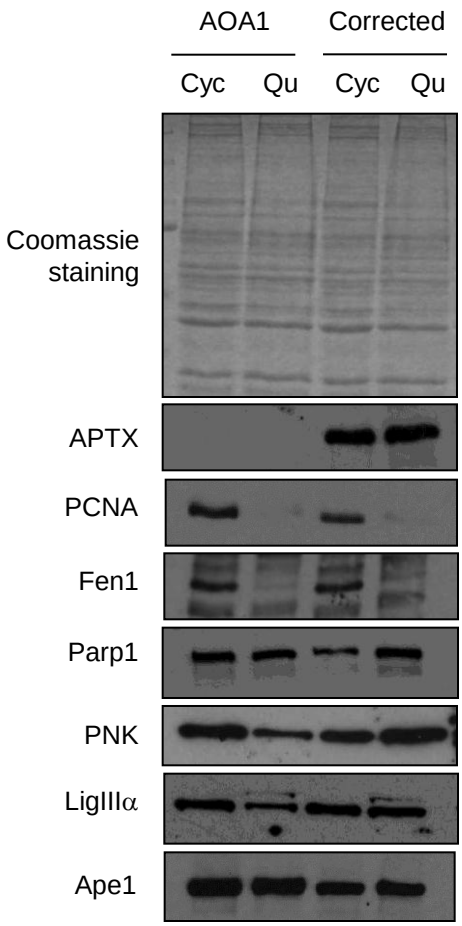

Figure 6.6 Total levels of SSBR proteins in cycling vs non-cycling AOA1 fibroblasts as determined by western blotting

FD105 M20 (AOA1) and FD105 M21 (corrected) hTERT fibroblast cell lines were cultured and were made quiescent by contact inhibition and serum starvation for a week. Separate flasks of the cell lines were kept cycling in parrallel. After a week the quiescent (Qu) and cycling fibroblasts (Cyc) were harvested and resuspended to a concentration of $2x10^4$ cells/ml in SDS loading buffer and $4x10^5$ cells were immunoblotted for various SSBR proteins. Samples were separately run on a protein gel and stained with coomassie blue for use as a loading control.

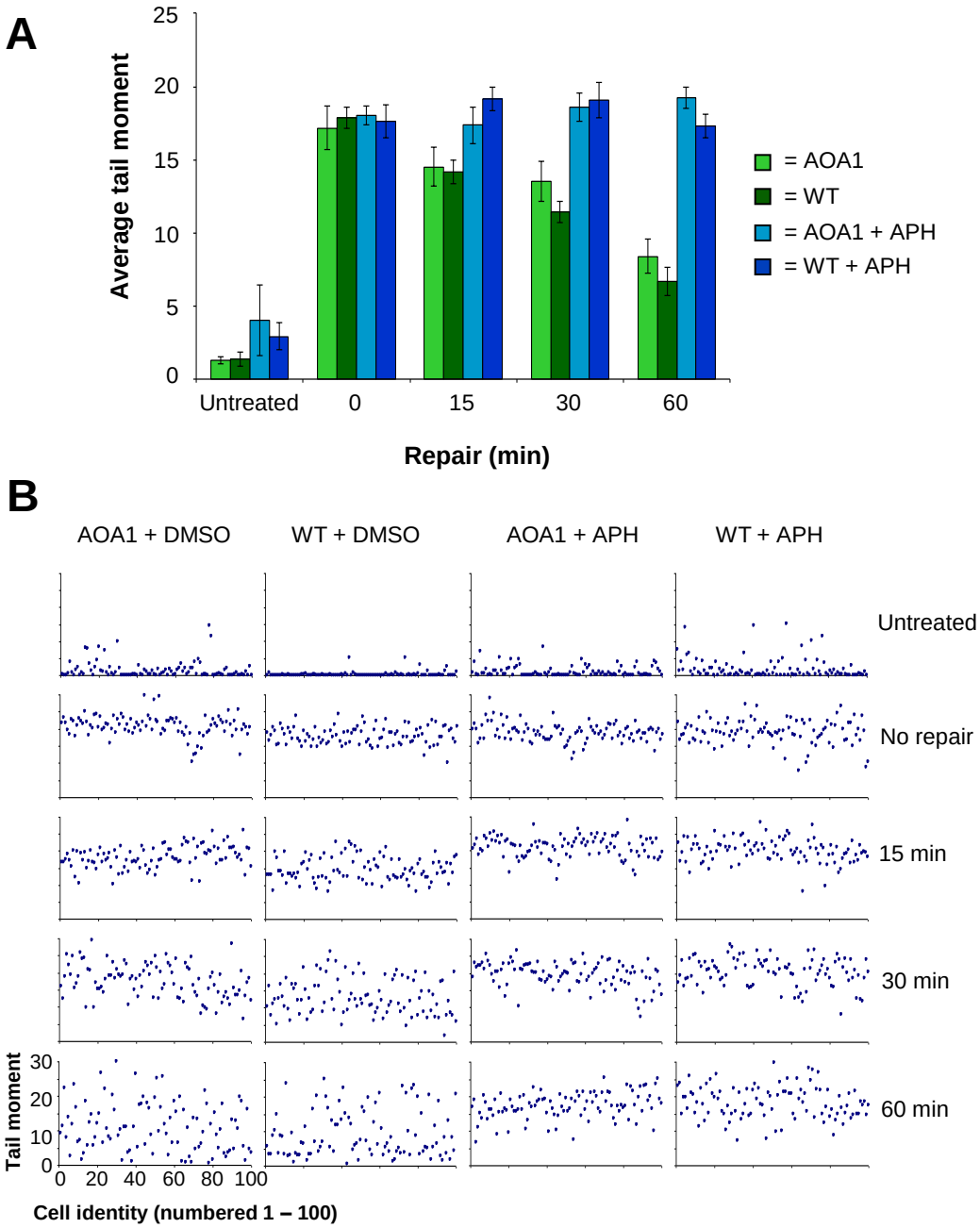

Figure 6.7 – Repair kinetics of γ-irradiation induced breaks in quiescent primary human AOA1 fibroblasts pre-treated with APH

Human primary fibroblast cell lines from an AOA1 patient (FD105) and an unrelated WT individual (1BR) were made quiescent by contact inhibiting and serum starving for 30 days. The cell lines were then incubated with 50μM APH or DMSO in suspension for 1 hour at 37°C and irradiated on ice with 30Gy γ-rays. The cells were allowed to repair in media containing APH or DMSO at 37°C for the indicated time periods. Comet tail moments were determined for 100 cells per sample using the Comet Assay IV software. **A** The data from 4 independent experiments was averaged (+/- SEM). Primary fibroblast cell lines with passage numbers of 4 – 8 were used in the experiments. The passage numbers of the WT and AOA1 cell lines were matched in each experiment. **B** Representative scatter graphs from one experiment.

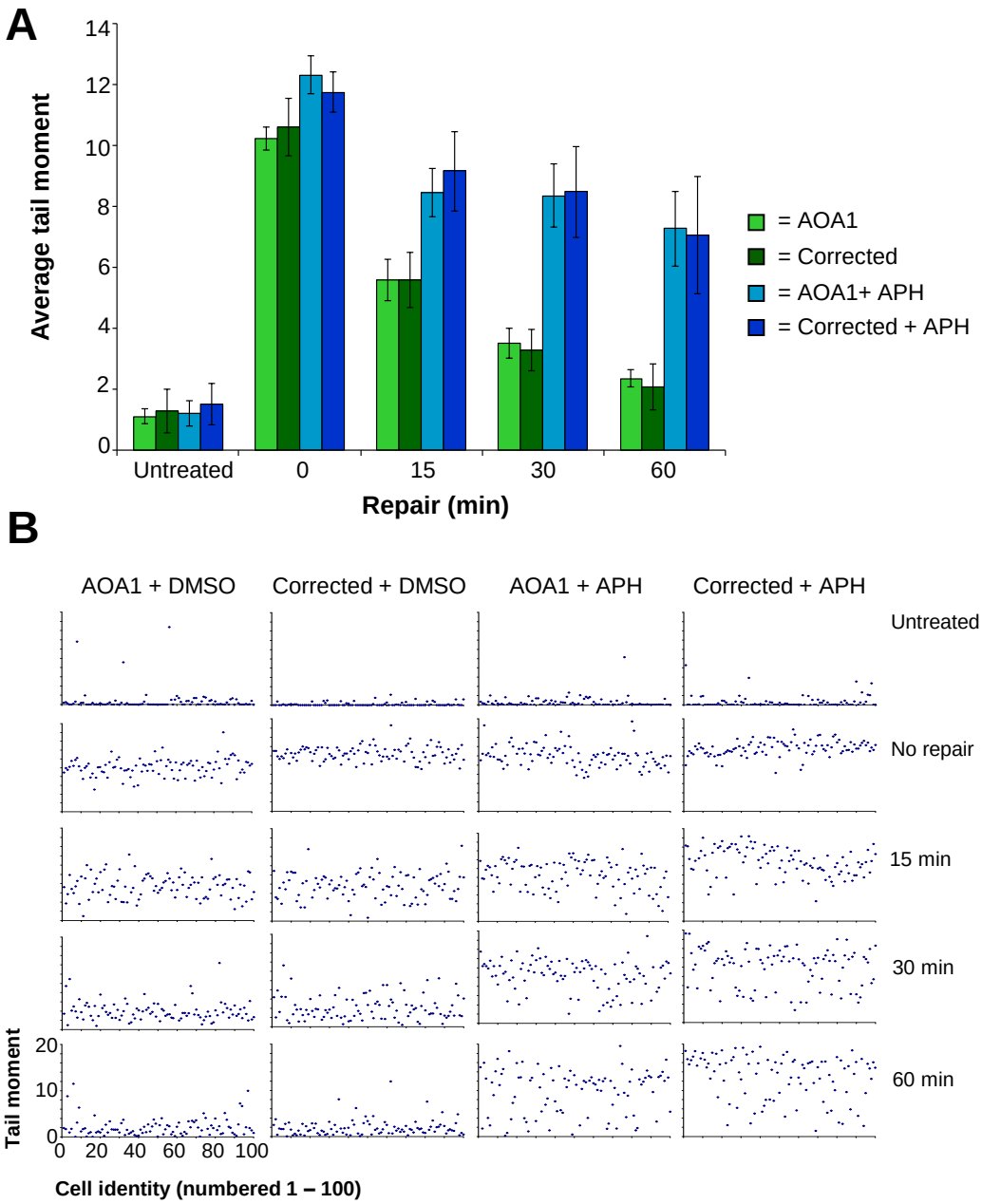

Figure 6.8 – Repair kinetics of γ-irradiation induced breaks in cycling hTERT fibroblasts pre-treated with APH

Cycling human hTERT fibroblast cell lines from an AOA1 patient (FD105) stably corrected with either human APTX ORF (FD105 M21) or containing empty vector (FD105 M20) were incubated with 50μM APH or DMSO in suspension for 1 hour at 37°C and irradiated on ice with 30Gy γ-rays. The cells were allowed to repair in media containing APH or DMSO at 37°C for the indicated time periods. Comet tail moments were determined for 100 cells per sample using the Comet Assay IV software. **A** The data from 4 independent experiments was averaged (+/- SEM).
B Representative scatter graphs from one experiment.

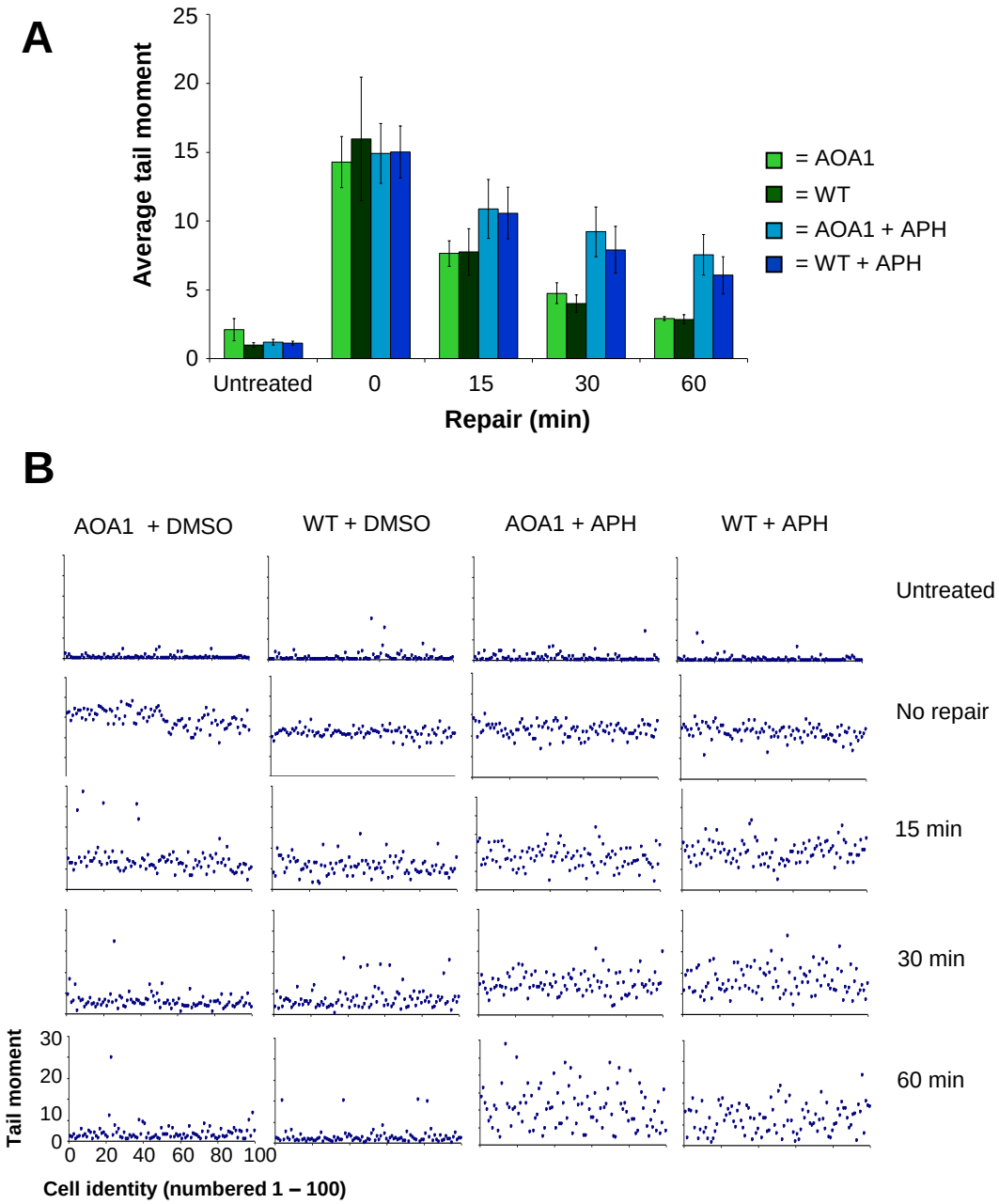

Figure 6.9 – Repair kinetics of γ-irradiation induced breaks in cycling primary human AOA1 fibroblasts pre-treated with APH

Cycling human primary fibroblast cell lines from an AOA1 patient (FD105) and an unrelated WT individual (1BR) were incubated with 50μM APH or DMSO in suspension for 1 hour at 37°C and irradiated on ice with 30Gy γ-rays. The cells were allowed to repair in media containing APH or DMSO at 37°C for the indicated time periods. Comet tail moments were determined for 100 cells per sample using the Comet Assay IV software. **A** The data from 4 independent experiments was averaged (+/- SEM). Primary fibroblast cell lines with passage numbers of 5 – 9 were used in the experiments. The passage numbers of the WT and AOA1 cell lines were matched in each experiment. **B** Representative scatter graphs from one experiment.

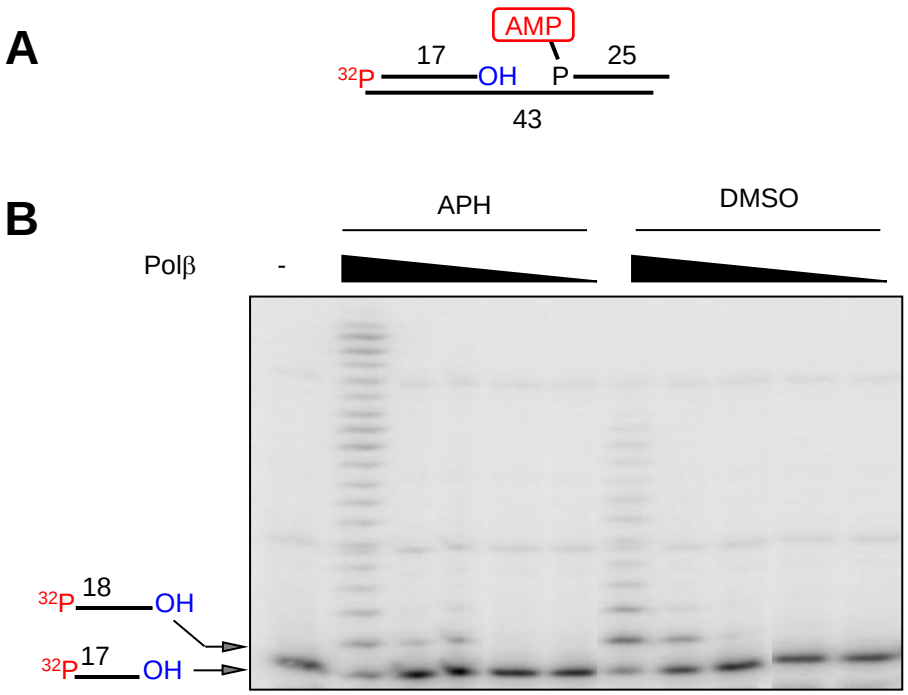

***Figure 6.10 APH does not inhibit the gap-filling activity of Polβ* in vitro**

A Cartoon of the substrate used in the experiments. The oligonucleotide duplex contains a 1 nucleotide gap with a 3'-OH and 5'-P. The substrate is ^{32}P radiolabelled on the 5' terminus of the 17mer.

B A titration of recombinant human Polβ (25nM, 10nM, 5nM, 2.5nM, 1nM) was pre-incubated with 50µM APH or DMSO for 15min at room temperature and then incubated with 25nM substrate at 30°C for 45min.

Reactions were stopped by addition of formamide loading buffer and the products fractionated by 15% denaturing PAGE and detected by phosphorimaging.

Name	Type	Preferred substrate
Uracil- N-glycosylase (UNG)	Monofunctional	Uracil
Single-strand- elective monofunctional uracil DNA glycosylase (SMUG1)	Monofunctional	Uracil
Methyl-CpG-binding domain protein 4 (MBD4)	Monofunctional	U and T opposite G
Thymine-DNA glycosylase (TDG)	Monofunctional	U and T opposite G
N-methylpurine-DNA glycosylase (MPG)	Monofunctional	3'-methyladenine, 3'-methylguanine
MutY homolog (MYH)	Monofunctional	A opposite 8-oxoG
Endonuclease III homolog (NTH1)	Bifunctional (β)	Thymine glycol, 5'- formyluracil
8-oxoguanine DNA glycosylase (OGG1)	Bifunctional (β)	8-oxoG, formamidoguanine
Endonuclease VIII-like 1 (NEIL1)	Bifunctional (βδ)	Formamidoadenine, thymine glycol, 5'-hydroxyuracil
Endonuclease VIII-like 2 (NEIL2)	Bifunctional (βδ)	Spiriminohydantoin, guanidinohydantoin, 5'-hydroxyuracil

Table 1.1 – *Mammalian DNA glycosylases*

Names and substrates of mammalian DNA glycosylases (Adapted from (Robertson et al., 2009))

Types of damaged termini at a SSB	Sources	Processed by
3’ – phosphate	Sugar fragmentation following ROS damage; cleavage of an AP site by a bifunctional DNA glycosylase (βδ elimination); repair of a Top1-SSB generated by ROS or topoisomerase poisons	PNK
3’ – phosphoglycolate	Sugar fragmentation following ROS damage	APE1
3’ – αβ unsaturated aldehyde	Cleavage of an AP site by a bifunctional DNA glycosylase (β elimination).	APE1
3’ - Top1 peptide	Abortive Top1 activity induced by ROS or topoisomerase inhibitors	Tdp1
5’ – hydroxyl	Sugar fragmentation following damage by ROS; repair of a Top1-SSB generated by ROS or topoisomerase poisons	PNK
5’ – aldehyde	Sugar fragmentation following ROS damage;	?
5’ – dRP	Cleavage of an AP site by APE1 generated by ROS or alkylating damage	Polβ
5’ – AMP	Premature ligation of an oxidative break.	APTX

Table 1.2 – *Types of damaged DNA termini at found at SSBs*

Chemistries of common damaged termini found at SSBs and the enzymes that repair them (Adapted from (Caldecott, 2008)).

Disease or syndrome	Gene	Neurological Symptoms	Extraneurological symptoms
DNA SSB repair deficiency			
Ataxia oculomotor apraxia 1 (AOA1)	*APTX*	Ataxia, neurodegeneration, oculomotor apraxia and peripheral neuropathy	Hypercholesterolaemia and hypoalbuminaemia
Spinocerebellar ataxia with axonal neuropathy 1 (SCAN1)	*TDP1*	Ataxia, neurodegeneration, peripheral axonal motor and sensory, and muscle weakness	Hypercholesterolaemia and hypoalbuminaemia
Microcephaly, early-onset, intractable seizures and developmental delay (MCSZ)	*PNK*	Microcephaly, infantile-onset seizures, developmental delay and variable behavioral problems, especially hyperactivity	Absent
DNA damage response or DNA DSB repair deficiency			
Ataxia telangiectasia (AT)	*ATM*	Ataxia, neurodegeneration, telangiectasia and dysarthia	Immunological defects, malignancy and sterility
Ataxia telangiectasia – like disorder (ATLD)	*MRE11*	Ataxia, neurodegeneration, dysarthia, oculomotor apraxia or microcephaly	Mild immunological defects
RAD50 deficiency	*RAD50*	Microcephaly and mental retardation	Short stature
Nijmegen breakage syndrome (NBS)	*NBS1*	Microcephaly	Immunological defects and lymphoid malignancy, growth retardation
ATR – Seckel syndrome	*ATR*	Microcephaly	Severe growth defects
LIG4 syndrome	*LIG4*	Microcephaly	Developmental/growth delay, severe combined immunodeficiency and lymphoma
Human immunodeficiency with microcephaly	*Cernunnos/XLF*	Microcephaly	Immunodeficiency
Radiosensitivity, immunodeficiency, dysmorphic features and learning difficulties (RIDDLE)	*RNF168*	Learning difficulties and slightly ataxic gait	Radiosensitivity, immunodeficiency and cancer predisposition
Bloom syndrome	*BLM*	Absent	Proportional dwarfism and cancer
Werner syndrome	*WRN*	Absent	Severe progeria and

			cancer
Fanconi anaemia	*BRCA2*	Microcephaly and medulloblastoma	Bone marrow defects, hypoplastic thumbs with radial defects
Ataxia oculomotor apraxia 2 (AOA2)	*SETX*	Cerebellar atrophy, axonal sensorimotor neuropathy, oculomotor apraxia	Elevated serum alpha-fetoprotein
Severe combined immunodeficiency and increased cellular radiosensitivity (RS-SCID)	*ARTEMIS*	Absent	Severe combined immunodeficiency and lymphoma
Nucleotide excision repair deficiency			
Xeroderma pigmentosum (XP)	*XPA–XPG*	Neurodegeneration and microcephaly	UV sensitivity and skin cancer
Cockayne syndrome (CS)	*CSA, CSB, XPB, XPD and XP*	Microcephaly and dysmyelination	Progeria and otherwise variable presentation
Trichothiodystroph (TTD)	*XPD, XPB and TTD-*	Neurodevelopmental defects and dysmyelination	Brittle hair and otherwise variable presentation

Table 1.3 – *Human syndromes associated with defects in the DNA damage response and repair pathways*

A list of human diseases associated with mutations in proteins involved in DNA SSB and DSB repair (Adapted from (McKinnon, 2009))

Plasmid DNA construct	Source/Reference
pB352-hAPTX	Caldecott Laboratory (Clements et al., 2004)
pET16b-hPNK	Caldecott Laboratory (Whitehouse et al., 2001)
pLW11-hPolβ	Wilson Laboratory (Sobol et al., 1996)
pET16b-hLigIIIα	Caldecott Laboratory (Taylor et al., 1998)
pET16b- PBCV-1 ligase	Shuman Laboratory (Sriskanda and Shuman, 1998)
pET16b- PBCV-1 CΔ5	Shuman Laboratory (Sriskanda and Shuman, 1998)

Table 2.1 – *Bacterial expression plasmid DNA constructs*

Plasmid DNA constructs used in this thesis for the overexpression of recombinant proteins in *E.coli* and their sources

Antibody	Type	Source	Conditions for immunoblotting
Anti-APTX	Rabbit polyclonal	Malcolm Taylor (Collaborator)	1:1000 5% milk 1 hour at RT
Anti-PNK	Rabbit polyclonal	Caldecott Laboratory	1:1000 1% milk ON at 4°C
Anti-XRCC1	Rabbit polyclonal	Caldecott Laboratory	1:100 5% milk ON at 4°C
Anti-Polβ	Mouse monoclonal	Abcam	1:100 1xTBST 1 hour at RT
Anti-LigIIIα	Rabbit polyclonal	Caldecott Laboratory	1:1500 3% milk ON at 4°C
Anti-PARP1	Mouse monoclonal	Serotec	1:500 5% milk 1 hour at RT
Anti-FEN1	Mouse monoclonal	Abcam	1:1000 5% milk 1 hour at RT
Anti-APE1	Mouse monoclonal	Abcam	1:2000 5% milk 1 hour at RT
Anti-PCNA	Mouse monclonal	CRUK	1:500 1% milk 1 hour at RT
Anti-β-Tubulin	Rabbit polyclonal	Bethyl Antibodies	1:3000 1xTBST 1 hour at RT
Anti-Actin	Mouse monoclonal	Sigma	1:2000 5% milk 1 hour at RT

Table 2.2 – *Primary antibodies*

Source, type and conditions for primary antibodies used for immunoblotting.

Antibody	Source	Conditions for immunoblotting
Anti-Rabbit HRP conjugated	DAKO	1:5000 1xTBST 1 hour at RT
Anti-Mouse HRP conjugated	DAKO	1:5000 1xTBST 1 hour at RT

Table 2.3 – *Secondary antibodies*

Source and conditions for secondary antibodies used for immunoblotting.

Recombinant protein	Expression vector	Incubation time	Incubation temperature
APTX	pB352-hAPTX	3 hours	30°C
PNK	pET16b-hPNK	90 min	20°C
LigIIIα	pET16b-hLigIIIα	90 min	20°C
Chlorella Virus DNA ligase	pET16b- PBCV- Ligase/ pET16b- PBCV- CΔ5	3 hours	30°C
Polβ	pLW11-hPolβ	4 hours	42°C

Table 2.4 – *Incubation conditions for the overexpression of different recombinant proteins in* E.coli

Details of the bacterial expression vectors and incubation conditions employed in this thesis for the overexpression of recombinant proteins in *E.coli.*

Recombinant protein	Isoelectric point (pI) of protein	pH of cation exchange chromatography buffers
APTX	9.27	8
PNK	8.73	7.5
LigIIIα	9.03	7.0
Polβ	9.01	7.5

Table 2.5 – ***pH of the buffers used during the purification of recombinant proteins by cation exchange chromatography***

Details of the pH of the buffers employed in the cation exchange purification steps.

Oligonucleotide	Sequence
25-mer	5’- GACATACTAACTTGAGCGAAACGGT – 3’
17-mer	5’- TCCGTTGAAGCCTGCTT – 3’
18-mer	5’- TCCGTTGAAGCCTGCTTT – 3’
43-mer	5’- CCGTTTCGCTCAAGTTAGTATGTCAAAGCAGGCTTCAACGGAT – 3’
Competitor oligonucleotide	5’- P-TCTGCTAGCATCGATCCATG – 3’

Table 2.6 – *Sequences of the oligonucleotides used to prepare model SSB substrates*

Sequences of the oligonucleotides used to prepare model SSB substrates *in vitro*. All oligonucleotides were ordered from Eurofins MWG Operon.

Cell lines	Cell type	Disease	Genotype	Source
MT1	LCL	WT	WT	Malcolm Taylor
MT6	LCL	AOA1	Homozygous for a genomic deletion of *APTX*	Malcolm Taylor
1BR	Fibroblast	WT	WT	Malcolm Taylor
FD105	Fibroblast	AOA1	Homozygous for W279X	Malcolm Taylor
1BR M20 hTERT	Fibroblast	WT	WT	Created by Limei Ju
FD105 M20 hTERT	Fibroblast	AOA1	Homozygous for W279X	Created by Limei Ju
FD105 M21 hTERT	Fibroblast	AOA1 (corrected)	Homozygous for W279X; corrected with stable integration of human APTX cDNA	Created by Limei Ju

Table 2.7 – *Details of the mammalian cell lines used in this study*

Details of the names, genotypes and sources of the mammalian cell lines employed in this thesis.

Published Work

MOLECULAR AND CELLULAR BIOLOGY, Mar. 2009, p. 1354–1362 Vol. 29, No. 5
0270-7306/09/$08.00+0 doi:10.1128/MCB.01471-08

Defective DNA Ligation during Short-Patch Single-Strand Break Repair in Ataxia Oculomotor Apraxia 1[▽]

John J. Reynolds,[1]† Sherif F. El-Khamisy,[1,2]† Sachin Katyal,[3] Paula Clements,[1] Peter J. McKinnon,[3] and Keith W. Caldecott[1]*

Genome Damage and Stability Centre, University of Sussex, Science Park Road, Falmer, Brighton BN1 9RQ, United Kingdom[1]; Biochemistry Department, Faculty of Pharmacy, Ain Shams University, Cairo, Egypt[2]; and Department of Genetics and Tumor Cell Biology, St. Jude Children's Research Hospital, Memphis, Tennessee[3]

Received 19 September 2008/Returned for modification 22 October 2008/Accepted 12 December 2008

Ataxia oculomotor apraxia 1 (AOA1) results from mutations in aprataxin, a component of DNA strand break repair that removes AMP from 5′ termini. Despite this, global rates of chromosomal strand break repair are normal in a variety of AOA1 and other aprataxin-defective cells. Here we show that short-patch single-strand break repair (SSBR) in AOA1 cell extracts bypasses the point of aprataxin action at oxidative breaks and stalls at the final step of DNA ligation, resulting in the accumulation of adenylated DNA nicks. Strikingly, this defect results from insufficient levels of nonadenylated DNA ligase, and short-patch SSBR can be restored in AOA1 extracts, independently of aprataxin, by the addition of recombinant DNA ligase. Since adenylated nicks are substrates for long-patch SSBR, we reasoned that this pathway might in part explain the apparent absence of a chromosomal SSBR defect in aprataxin-defective cells. Indeed, whereas chemical inhibition of long-patch repair did not affect SSBR rates in wild-type mouse neural astrocytes, it uncovered a significant defect in *Aptx*$^{-/-}$ neural astrocytes. These data demonstrate that aprataxin participates in chromosomal SSBR in vivo and suggest that short-patch SSBR arrests in AOA1 because of insufficient nonadenylated DNA ligase.

Oxidative stress is an etiological factor in many neurological diseases, including Alzheimer's disease, Parkinson's disease, and Huntington's disease. One type of macromolecule damaged by reactive oxygen species is DNA, and oxidative damage to DNA has been suggested to be a significant factor in these and other neurological conditions (2). In particular, a number of rare hereditary neurodegenerative disorders have provided direct support for the notion that unrepaired DNA damage causes neural dysfunction. Not least of these are the recessive spinocerebellar ataxias, a number of which are associated with mutations in DNA damage response proteins (17). The archetypal DNA damage-associated spinocerebellar ataxia is ataxia-telangiectasia (A-T), in which mutations in ATM protein result in defects in the detection and signaling of DNA double-strand breaks (DSBs) (3). A-T-like disorder is a related disease that exhibits neurological features similar to those of A-T, resulting from mutation of Mre11, a component of the MRN complex that operates in conjunction with ATM during DSB detection and signaling (28).

Two additional spinocerebellar ataxias are spinocerebellar ataxia with axonal neuropathy 1 (SCAN1) and ataxia oculomotor apraxia 1 (AOA1), in which the TDP1 and aprataxin proteins are mutated, respectively (9, 19, 27). Both TDP1 and aprataxin are components of the DNA strand break repair machinery (recently reviewed in references 6 and 24). Whereas SCAN1 is currently limited to nine individuals from a single family, AOA1 is one of the commonest recessive spinocerebellar ataxias. Aprataxin is a member of the histidine triad superfamily of nucleotide hydrolases/transferases and has been reported to remove phosphate and phosphoglycolate moieties from the 3′ termini of DNA strand breaks (26). Aprataxin can also remove AMP from a variety of ligands in vitro, including adenosine polyphosphates, AMP-lysine, AMP-NH_2 (adenine monophosphoramidate), and adenylated DNA in which AMP is covalently attached to the 5′ terminus of a DNA single-strand break (SSB) or DSB (1, 16, 23, 25). To date, aprataxin activity is greatest on AMP-DNA, suggesting that this may be the physiological substrate of this enzyme.

In vitro, DNA strand breaks with 5′-AMP termini can arise from premature DNA ligase activity. DNA ligases adenylate 5′ termini at DNA breaks to enable nucleophilic attack of the resulting pyrophosphate bonds by 3′-hydroxyl termini, thereby resealing the breaks. However, DNA adenylation by DNA ligases can occur prematurely, before a 3′-hydroxyl terminus is available. Aprataxin reverses these premature DNA adenylation events, in vitro at least, effectively "resetting" the DNA ligation reaction to the beginning (1). Whether or not 5′-AMP arises in DNA in vivo or is a physiological substrate of aprataxin, however, is unknown. Moreover, attempts to measure DNA strand break repair rates in vivo are conflicting and have failed to identify a consistent defect in DNA SSB repair (SSBR) or DSB repair (DSBR) in AOA1 cells (14, 15, 20). It is thus not clear whether or not defects in DNA strand break repair can account for this neurodegenerative disease.

Here we have resolved the discrepancy between the requirements for aprataxin in vitro and in vivo by identifying the stage at which SSBR reactions fail in vitro and by carefully analyzing chromosomal SSBR rates in vivo. We show that short-patch SSBR reactions are defective in AOA1 cell extracts at the final step of DNA ligation, resulting in the accumulation of adeny-

* Corresponding author. Mailing address: Genome Damage and Stability Centre, University of Sussex, Science Park Road, Falmer, Brighton BN1 9RQ, United Kingdom. Phone: 44 (0) 1273 877519. Fax: 44 (0) 1273 678121. E-mail: k.w.caldecott@sussex.ac.uk.
† J.J.R. and S.F.E.-K. contributed equally to this work.
▽ Published ahead of print on 22 December 2008.

lated DNA nicks, and that this defect can be rescued in AOA1 extracts independently of aprataxin by addition of recombinant DNA ligase. We also find that treatment with aphidicolin, an inhibitor of DNA polymerase δ (Pol δ) and Pol ε, unveils a measurable defect in chromosomal SSBR in *Aptx*$^{-/-}$ primary neural astrocytes, suggesting that the adenylated nicks that arise from the short-patch repair defect can be channeled into long-patch repair in vivo. These data demonstrate that aprataxin participates in chromosomal SSBR and suggest that this process arrests in AOA1, at oxidative SSBs, due to insufficient levels of nonadenylated DNA ligase.

MATERIALS AND METHODS

Preparation of adenylated DNA substrates. Oligonucleotide duplexes containing an SSB with a 5′-AMP terminus and either a 1-bp gap with a 3′-phosphate terminus or a nick with a 3′-hydroxyl terminus were prepared as follows. A 25-mer (5′-GACATACTAACTTGAGCGAAACGGT) was labeled by phosphorylation with T4 PNK and [γ-^{32}P]ATP and was annealed with a 43-mer (5′-CCG TTTCGCTCAAGTTAGTATGTCAAAGCAGGCTTCAACGGAT) and a 17-mer with a 3′-phosphate terminus (17-mer-P) (5′-TCCGTTGAAGCCTGCT T-P). The labeled 25-mer in this duplex was then either adenylated at the 5′ terminus by incubation with 1 U T4 DNA ligase at 30°C for 1 h in ligation buffer (50 mM Tris-HCl [pH 7.5], 10 mM $MgCl_2$, 5 mM dithiothreitol [DTT], 25 μg/μl bovine serum albumin, 1 mM ATP) or mock adenylated in the absence of T4 DNA ligase. The labeled adenylated 25-mer was then separated from the labeled nonadenylated 25-mer (and from the 17-mer and 43-mer) on a 15% denaturing polyacrylamide gel electrophoresis (PAGE) gel, excised, and eluted from the crushed gel in elution buffer (0.5 M ammonium acetate, 10 mM magnesium acetate, 1 mM EDTA [pH 8.0]) overnight at room temperature. The eluted DNA was then ethanol precipitated. The labeled mock-adenylated 25-mer was purified in parallel. The labeled adenylated 25-mer was then reannealed with the 43-mer and either the 17-mer-P (containing a 3′ phosphate) or an 18-mer (5′-TCCGT TGAAGCCTGCTTT) to produce oligonucleotide duplexes harboring an adenylated SSB with either a 1-bp gap and a 3′-phosphate terminus or a nick with a 3′-hydroxyl terminus, respectively. To measure the repair of 3′ termini by PNK or gap filling by Pol β, the 17-mer-P or a 17-mer oligonucleotide lacking a 3′ phosphate, respectively, was labeled with T4 PNK (phosphatase dead) and [γ-^{32}P]ATP and was annealed to the 25-mer and 43-mer. The substrate was either mock adenylated or adenylated as described above and was purified on a 15% native PAGE gel. The final substrate contained a 1-bp gap with a 5′ AMP and either a 3′ P or a 3′ OH.

Purification of recombinant human SSBR proteins. Pol β was expressed in *Escherichia coli* and purified by anion and cation exchange as previously described (29), using a 1.6-ml Poros column on a Biocad Sprint chromatography system (Applied Biosystems, United Kingdom). His-tagged PNK and His-tagged DNA ligase IIIα (Lig3α) were expressed in the *E. coli* strain BL21(DE3) for 90 min at 20°C following addition of 1 mM isopropyl-β-D-thiogalactopyranoside (IPTG). PNK was purified by cation-exchange chromatography followed by immobilized metal chelate affinity chromatography (IMAC) as previously described (30). Lig3α was purified by IMAC as described previously (7), followed by cation exchange as described previously for PNK. His-tagged aprataxin was expressed from pB352 (8) in BL21(DE3) by addition of 1 mM IPTG and incubation at 30°C for 3 h. Aprataxin was purified by IMAC followed by cation exchange as described above for PNK and Lig3α.

Preparation of human lymphoblastoid cell extracts. Total-cell extracts were prepared from 5×10^6 ConR2 (wild type [WT]) or Ap5 (AOA1) lymphoblastoid cells or from *Aptx*$^{+/+}$ and *Aptx*$^{-/-}$ primary quiescent mouse astrocytes by lysis in 0.2 ml 20 mM Tris-HCl (pH 7.5), 10 mM EDTA, 1 mM EGTA, 100 mM NaCl, 1% Triton X-100, and 1/100 dilution of protease inhibitor cocktail (Sigma). The extracts were clarified by centrifugation, quantified with a Bio-Rad DC protein assay kit using bovine serum albumin as a standard, and then aliquoted and snap-frozen.

In vitro repair of adenylated SSB substrates by recombinant proteins. For reactions employing recombinant human proteins, a 25 nM concentration of the indicated ^{32}P-labeled substrate was incubated with the indicated concentrations of recombinant protein for 1 h at 30°C in 25 mM HEPES (pH. 8.0), 130 mM KCl, 1 mM DTT, 10 mM $MgCl_2$, 100 μM deoxynucleoside triphosphates (dNTPs), and 1 mM ATP unless otherwise indicated. Reactions were stopped by addition of 1/3 volume of formamide gel loading buffer, and reaction products were fractionated on 15% denaturing PAGE gels and analyzed by a phosphorimager.

For reactions employing cell extracts, 5 μg of extract from WT lymphoblastoid cells (ConR2) or AOA1 lymphoblastoid cells (Ap5) or from *Aptx*$^{+/+}$ and *Aptx*$^{-/-}$ primary quiescent mouse astrocytes was incubated with a 100 nM concentration of the indicated ^{32}P-labeled substrate for 1 h at 30°C in 25 mM HEPES (pH 8.0), 130 mM KCl, 1 mM DTT, and, unless otherwise indicated, 10 mM $MgCl_2$, 100 μM dNTPs, and 1 mM ATP. A 1,000-fold excess of a competitor oligonucleotide with an unrelated sequence and a 5′ phosphate (5′-P-TCTGCTAGCATCGAT CCATG-3′) was added to reduce degradation of the labeled substrate by nonspecific nucleases. Reactions were stopped and products analyzed as described above.

Cell culture. (i) Human cells. 1BR3 cells are primary human fibroblasts, and ConR and ConR2 cells are lymphoblastoid cells, all from unrelated normal individuals. fAp1 and fAp4 cells are AOA1 primary fibroblasts, and Ap3 and Ap5 cells are AOA1 lymphoblasts. ConR, Con R2, fAp1, fAp4, Ap3, and Ap5 cells were kindly provided by Malcolm Taylor and, except for Ap5 and ConR2, have been described previously (8). Ap1, Ap3, and Ap4 cells harbor the homozygous *APTX* mutation W279X, which results in little or no aprataxin protein or activity (1, 8), and Ap5 cells harbor a genomic deletion of *APTX* (M. Taylor, unpublished data). Cells were cultured as described previously (8).

(ii) Primary mouse astrocytes. *Aptx*$^{-/-}$ mice have been described previously (1). The generation and characterization of nestin-Cre conditional *Xrcc1*$^{-/-}$ mice will be described elsewhere. All animals were housed in individually ventilated cabinets and were maintained in accordance with the guidelines of the institutional animal care and ethical committee at the University of Sussex. Mouse astrocytes were prepared from postnatal day 3 (P3) to P4 brains. Cortices were dissociated by passage through a 5-ml pipette, and cells were resuspended in Dulbecco's modified Eagle's medium and Ham's F-12 nutrient mixture (1:1; Gibco-BRL) supplemented with 10% fetal bovine serum, 1× Glutamax, 100 U/ml penicillin, 100 μg/ml streptomycin, and 20 ng/ml epidermal growth factor (Sigma). Primary astrocytes were established in Primeria T-25 tissue culture flasks (Falcon) at 37°C in a humidified oxygen-regulated (9%) incubator. The culture medium was changed after 3 days, and astrocyte monolayers reached confluence 3 days later. The purity of the astrocyte cultures was confirmed by immunofluorescence using an anti-GFAP antibody (Sigma).

Alkaline comet assays. Cells ($\sim 3 \times 10^5$/sample) were incubated with 75 μM (mouse astrocytes), 50 μM (human lymphoblastoid cells), or 75 μM (primary human fibroblasts) H_2O_2 for 10 min on ice or with the indicated doses of methyl methanesulfonate (MMS) for 10 min at 37°C. Where indicated, cells were then incubated in complete medium for the indicated repair periods at 37°C. To inhibit long-patch DNA polymerases, cells were incubated with 50 μM aphidicolin (Sigma) in complete medium for 30 min at 37°C. Cells were then either mock treated or treated with H_2O_2 or MMS as described above in the continued presence or absence of aphidicolin, as appropriate. Chromosomal DNA strand breaks were then measured using alkaline comet assays as previously described (5). Statistical analyses were performed using SPSS software.

RESULTS

Aprataxin interacts with the SSBR scaffold protein XRCC1, raising the possibility that a defect in chromosomal SSBR underlies the neuropathology of this disease. However, evidence for a defect in SSBR in aprataxin-defective AOA1 cells is conflicting (14, 15, 20). To resolve this issue, we employed alkaline comet assays to compare chromosomal SSBR rates in a variety of different aprataxin-defective cell types. It should be noted that while alkaline comet assays measure both SSBs and DSBs, these assays primarily measure SSBs following short periods of treatment with H_2O_2 or MMS, because these agents induce several orders of magnitude more SSBs than DSBs (4, 18). In contrast to the findings of a previous report (15), we failed to observe a significant difference in chromosomal SSBR rates between either lymphoblastoid cells (Fig. 1A) or primary fibroblasts (Fig. 1B) from AOA1 patients and those from normal individuals following H_2O_2-induced oxidative stress. Because individual genetic variability might mask differences in SSBR rates, we also compared chromosomal SSBR in quiescent primary astrocytes from *Aptx*$^{-/-}$ mice and isogenic *Aptx*$^{+/+}$ littermate controls. Astrocytes were chosen because

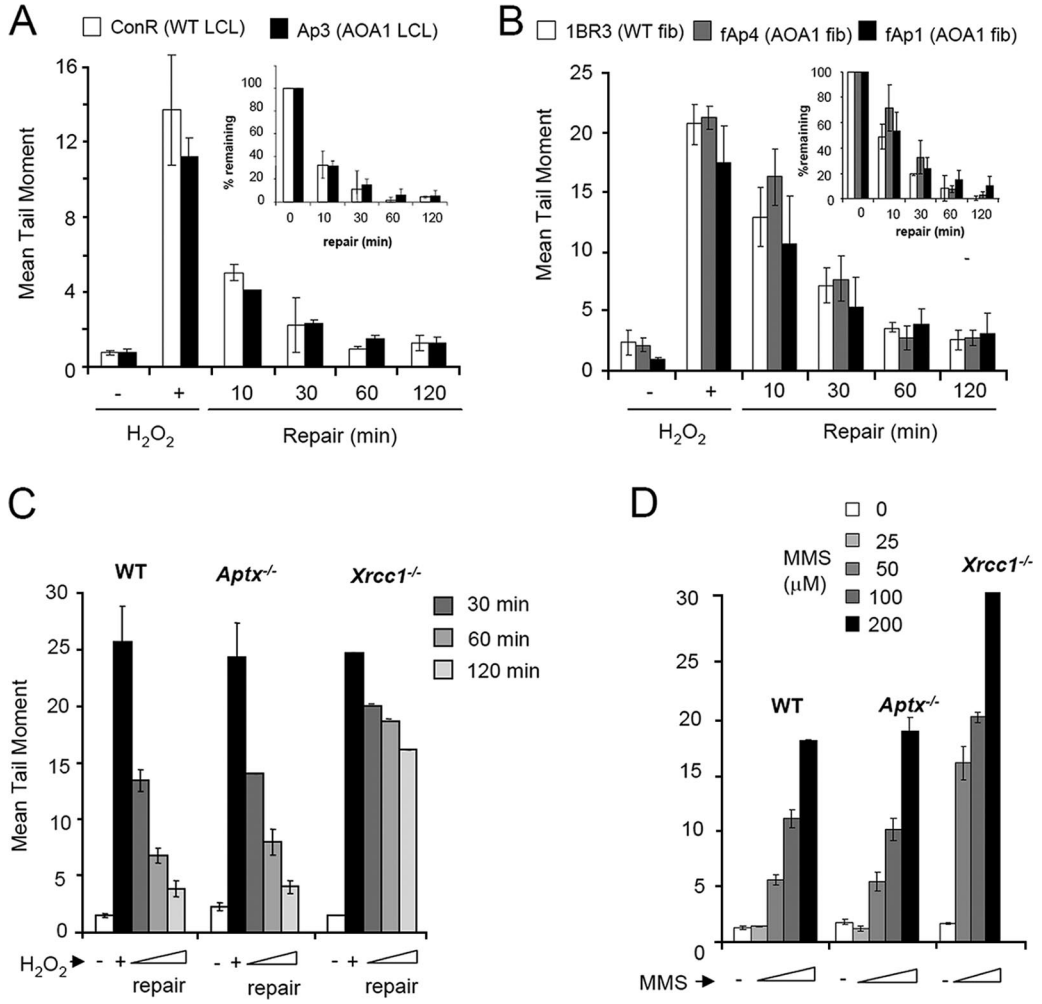

FIG. 1. Normal rates of chromosomal SSBR in cells lacking aprataxin. (A) AOA1 lymphoblastoid cells were incubated in the absence (−) or presence (+) of 50 μM H_2O_2 (15 min on ice), followed by incubation in a drug-free medium for the indicated repair period at 37°C. Chromosomal DNA strand breaks were then measured by alkaline comet assays. (B) AOA1 primary fibroblasts were treated in the absence (−) or presence (+) of 75 μM H_2O_2 (15 min on ice) and processed as described for panel A. Insets in panels A and B contain the same data as in the main panels but plotted as percent damage remaining. (C) WT, *Aptx*$^{-/-}$, and *Xrcc1*$^{-/-}$ primary quiescent astrocytes were incubated in the absence (−) or presence (+) of 75 μM H_2O_2 (10 min on ice), followed by incubation in a drug-free medium for the indicated repair period at 37°C. Chromosomal DNA strand breaks were then measured by alkaline comet assays. (D) WT, *Aptx*$^{-/-}$, and *Xrcc1*$^{-/-}$ primary quiescent astrocytes were incubated in the absence (−) or presence of the indicated concentration of MMS (10 min at 37°C). Chromosomal DNA strand breaks were then measured by alkaline comet assays.

they are neural in origin and thus better reflect the type of cells affected in AOA1. However, SSBR rates were similar in *Aptx*$^{+/+}$ and *Aptx*$^{-/-}$ astrocytes following treatment with H_2O_2 (Fig. 1C). *Aptx*$^{+/+}$ and *Aptx*$^{-/-}$ astrocytes also accumulated SSBs at similar rates during incubation with the alkyating agent MMS, suggesting that the rate of SSB rejoining during DNA base excision repair is also normal in *Aptx*$^{-/-}$ cells (Fig. 1D). In contrast, astrocytes lacking the core SSBR factor Xrcc1 exhibited greatly reduced SSBR rates following treatment with either H_2O_2 or MMS (Fig. 1C and D). It should be noted that we also observed normal SSBR kinetics in *Aptx*$^{-/-}$ postmitotic cerebellar granule neurons (data not shown). We conclude from these experiments that AOA1 and other aprataxin-defective cells lack a measurable defect in the global rate of chromosomal SSBR.

In contrast to the findings of cellular SSBR assays, protein extracts from *Aptx*$^{-/-}$ astrocytes and *Aptx*$^{-}$ chicken DT40 cells are unable to support short-patch repair of adenylated oxidative SSBs in vitro (1). To resolve this discrepancy, we examined whether this was also true in AOA1 lymphoblastoid cell extracts. To measure short-patch SSBR, we employed an oligonucleotide duplex harboring a 1-bp gap with 3′-phosphate termini, a substrate that mimics one of the commonest types of oxidative SSB arising in cells (Fig. 2A, top). The SSB also possesses a 5′ AMP and is therefore a substrate for aprataxin. In agreement with previous experiments with neural extracts (1), WT extracts efficiently removed AMP from 5′ termini and repaired the SSBs, as indicated by the respective appearance of the ^{32}P-labeled 25-mer and the ^{32}P-labeled 43-mer (Fig. 2A, lanes 6 to 8). In contrast, AOA1 extracts did not (Fig. 2A, lanes 3 to 5). Importantly, SSBR was proficient in AOA1 extracts if the initial SSB lacked 5′ AMP (Fig. 2B). A number of trun-

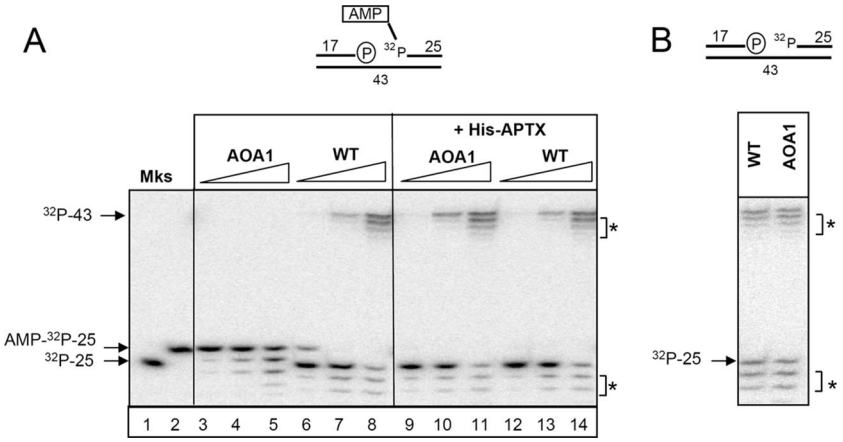

FIG. 2. Aprataxin-dependent short-patch SSBR of 5′-AMP SSBs in AOA1 lymphoblastoid extracts. (A) Defective short-patch SSBR in AOA1 extracts and its complementation by recombinant aprataxin. (Top) Cartoon of the oligonucleotide duplex employed for these experiments, containing a 1-bp gap, a 3′-phosphate terminus, and a 5′-AMP terminus. The 5′ phosphate to which AMP is covalently linked is labeled with ^{32}P. The position of this label restricts the assay to measurements of short-patch repair events only. Nucleotide lengths are shown. (Bottom) Portions (0.1 μg, 1.0 μg, or 5.0 μg) of either WT (ConR2) or AOA1 (Ap5) cell extracts were incubated for 60 min at 30°C with a ^{32}P-labeled 5′-AMP SSB substrate (25 nM) in the absence (left) or presence (right) of recombinant human aprataxin (APTX) (100 nM). Reaction products were fractionated and detected as described in Materials and Methods. The ^{32}P-labeled 25-mer containing (AMP-^{32}P-25) or lacking (^{32}P-25) 5′ AMP was fractionated in parallel for size markers (Mks). The position of the repaired ^{32}P-labeled 43-mer is also indicated. Asterisks indicate nonspecific nucleolytic products. (B) Normal short-patch repair of SSBs lacking 5′ AMP in AOA1 cell extracts. (Top) Cartoon of the oligonucleotide duplex employed for these experiments, containing a 1-bp gap, a 3′-phosphate terminus, and a normal ^{32}P-labeled 5′-phosphate terminus. WT (ConR2) or AOA1 (Ap5) cell extracts (5 μg) were incubated for 60 min at 30°C with a ^{32}P-labeled SSB substrate lacking 5′ AMP (100 nM). Reaction products were fractionated and detected as described in Materials and Methods.

cated oligonucleotide fragments were generated by nonspecific nucleolytic activity in these experiments, which represented degradation of the 3′ terminus of the ^{32}P-labeled 25-mer. However, this activity did not account for the short-patch repair defect in AOA1 cell extracts, which was fully complemented by the addition of recombinant aprataxin (Fig. 2A, lanes 9 to 11). The appearance of ligated product in these experiments was dependent on the presence of dNTPs, confirming that these experiments measured gap repair rather than ligation across the 1-bp gap (data not shown).

The predicted pathway for short-patch repair of SSBs harboring 5′ AMP in WT cells is depicted in Fig. 3A. It was considered likely that this pathway arrests in AOA1 extracts at the very beginning, prior to 3′-DNA end processing by PNK and/or DNA gap filling by Pol β, because the presence of AMP at the 5′ terminus might occlude access to the 3′ terminus. Surprisingly, however, the 3′-phosphatase activity of PNK was similar irrespective of whether the SSB possessed 5′ AMP or not, under conditions in which PNK was limiting (Fig. 3B). Similar results were observed for DNA gap filling by Pol β, with similar amounts of the ^{32}P-labeled 17-mer converted into a ^{32}P-labeled 18-mer irrespective of the presence or absence of 5′ AMP (Fig. 3C). These experiments suggested that neither PNK nor Pol β activity is affected by the presence of 5′ AMP at these time points, and thus short-patch SSBR might fail in AOA1 extracts at the final step of DNA ligation, resulting in the accumulation of adenylated DNA nicks (Fig. 3D).

To confirm this hypothesis, we compared WT and AOA1 extracts for their abilities to ligate adenylated nicks. Indeed, whereas adenylated nicks were efficiently ligated by extracts from WT cells, they remained largely unligated in reaction mixtures containing AOA1 cell extracts (Fig. 4A). The finding that short-patch repair in AOA1 arrests during DNA ligation is surprising, because adenylated nicks are normal intermediates of DNA ligation and are normally rapidly resealed by nonadenylated DNA ligase (11). Normally, the nonadenylated DNA ligase required for this purpose is created during, and tightly coupled with, adenylation of the 5′ terminus of the break by an adenylated DNA ligase (Fig. 4B). However, in the absence of aprataxin, DNA nicks may accumulate in a preadenylated state and therefore require preexisting pools of nonadenylated DNA ligase. While both nonadenylated and adenylated DNA ligases exist in cells, the former may be very limited because the readenylation of DNA ligases by cellular ATP is very rapid. Consequently, we reasoned that the DNA ligation defect in AOA1 may reflect insufficient cellular levels of nonadenylated DNA ligase. To test this hypothesis, we examined the impact of supplementing short-patch SSBR reaction mixtures in AOA1 cell extracts and *Aptx*$^{-/-}$ mouse neural astrocyte extracts with recombinant DNA ligase. Strikingly, addition of T4 ligase restored short-patch SSBR efficiency in both AOA1 cell extracts and *Aptx*$^{-/-}$ neural cell extracts to a level similar to that observed in WT extracts (Fig. 4C and D, compare lanes 6 and 10). Importantly, complementation was more efficient in the absence of ATP than in its presence, supporting the notion that it was the nonadenylated subfraction of T4 ligase that was responsible for complementation (Fig. 4C and D, compare lanes 8 and 10). Similar results were observed for AOA1 cell extracts if T4 ligase was replaced with human DNA ligase 3α, albeit to a lesser extent (Fig. 5A).

The data described above suggest that short-patch repair of some adenylated SSBs can occur independently of aprataxin if sufficient nonadenylated DNA ligase is available. To confirm this idea, we attempted to reconstitute this aprataxin-independent SSBR pathway using recombinant proteins. As expected, the repair of adenylated gaps by PNK, Pol β, and Lig3α was

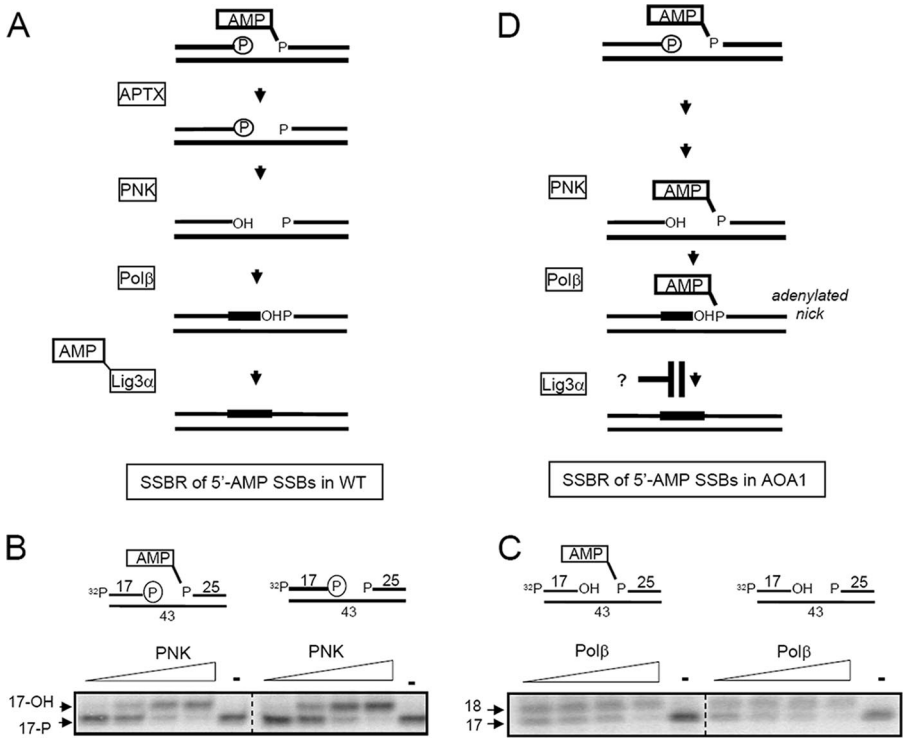

FIG. 3. Removal of 5′ AMP by aprataxin is not required for end processing by PNK or gap filling by Pol β. (A) Cartoon of aprataxin-dependent short-patch repair of adenylated SSBs in WT cells. (B) 5′ AMP does not affect processing of 3′-phosphate termini by PNK. An SSB substrate (25 nM) lacking or containing 5′ AMP as indicated (top) was incubated either with 25 nM, 50 nM, 125 nM, or 250 nM recombinant human PNK or without PNK (−) for 1 h at 30°C. Reaction products were fractionated by denaturing PAGE and detected by phosphorimaging. Note that the 5′ terminus of the 17-mer is labeled with ^{32}P in these experiments to allow detection of 3′ end processing. The position of the 17-mer harboring 3′ phosphate (17-P) or 3′ hydroxyl (3′-OH) is indicated. (C) 5′ AMP does not affect gap filling by Pol β. An SSB substrate (25 nM) lacking or containing 5′ AMP as indicated (top) was incubated either with 5 nM, 15 nM, 30 nM, or 100 nM purified recombinant human Pol β or without Pol β (−) for 1 h at 30°C. Reaction products were fractionated by denaturing PAGE and detected by phosphorimaging. The positions of the 17-mer and 18-mer are indicated as markers. (D) Cartoon depicting APTX-independent repair of adenylated SSBs in AOA1. Note the hypothetical blockage of this process at the final step of DNA ligation.

dependent on aprataxin in the presence of ATP, conditions under which Lig3α is largely adenylated (Fig. 5B). However, in the absence of ATP, short-patch repair of 5′-AMP SSBs occurred independently of aprataxin. Taken together, these experiments indicate that short-patch repair arrests in AOA1 cell extracts at the final step of DNA ligation, due to insufficient levels of nonadenylated DNA ligase.

Importantly, the finding that short-patch repair failed during DNA ligation provides a possible explanation for the absence of a measurable defect in chromosomal SSBR in AOA1, following oxidative stress. This is because adenylated DNA nicks might be channeled into long-patch SSBR reactions, during which the adenylated 5′ terminus is displaced by extended DNA gap filling and then clipped off nucleolytically, avoiding the requirement for either aprataxin or preexisting pools of nonadenylated DNA ligase. While our in vitro assay was not capable of measuring long-patch repair reactions, this process might operate efficiently at adenylated nicks within a chromosomal context. To examine this possibility, we compared chromosomal SSBR rates in WT and *Aptx*$^{-/-}$ quiescent mouse neural astrocytes in the presence and absence of aphidicolin, an inhibitor of the DNA polymerases Pol δ and Pol ε, which are implicated in long-patch repair reactions (10, 13, 22). Strikingly, whereas aphidicolin did not measurably reduce SSBR rates in WT astrocytes following H_2O_2 treatment, it significantly slowed SSBR in *Aptx*$^{-/-}$ astrocytes (Fig. 6A). Aphidicolin also selectively slowed short-patch base excision repair in AOA1 cells, as indicated by the accumulation of higher steady-state levels of chromosomal DNA strand breaks in *Aptx*$^{-/-}$ astrocytes than in WT astrocytes during short incubations with the DNA-alkylating agent MMS (Fig. 6B). The fact that SSBR in *Aptx*$^{-/-}$ cells was slowed rather than prevented by aphidicolin most likely reflects the fact that only a subset of H_2O_2- and MMS-induced SSBs possess adenylated 5′ termini. Nevertheless, the presence of a measurable defect in chromosomal SSBR in *Aptx*$^{-/-}$ cells indicates that a significant fraction of endogenous SSBs arising from oxidative stress and DNA base damage are substrates for aprataxin.

In summary, we demonstrate here that aprataxin is required for SSBR in vivo and suggest that short-patch SSBR is defective in AOA1 cells, at oxidative SSBs, due to insufficient levels of nonadenylated DNA ligase.

DISCUSSION

AOA1 is one of the commonest recessive hereditary spinocerebellar ataxias identified to date. This disease results from mutations in aprataxin, a component of the DNA strand break

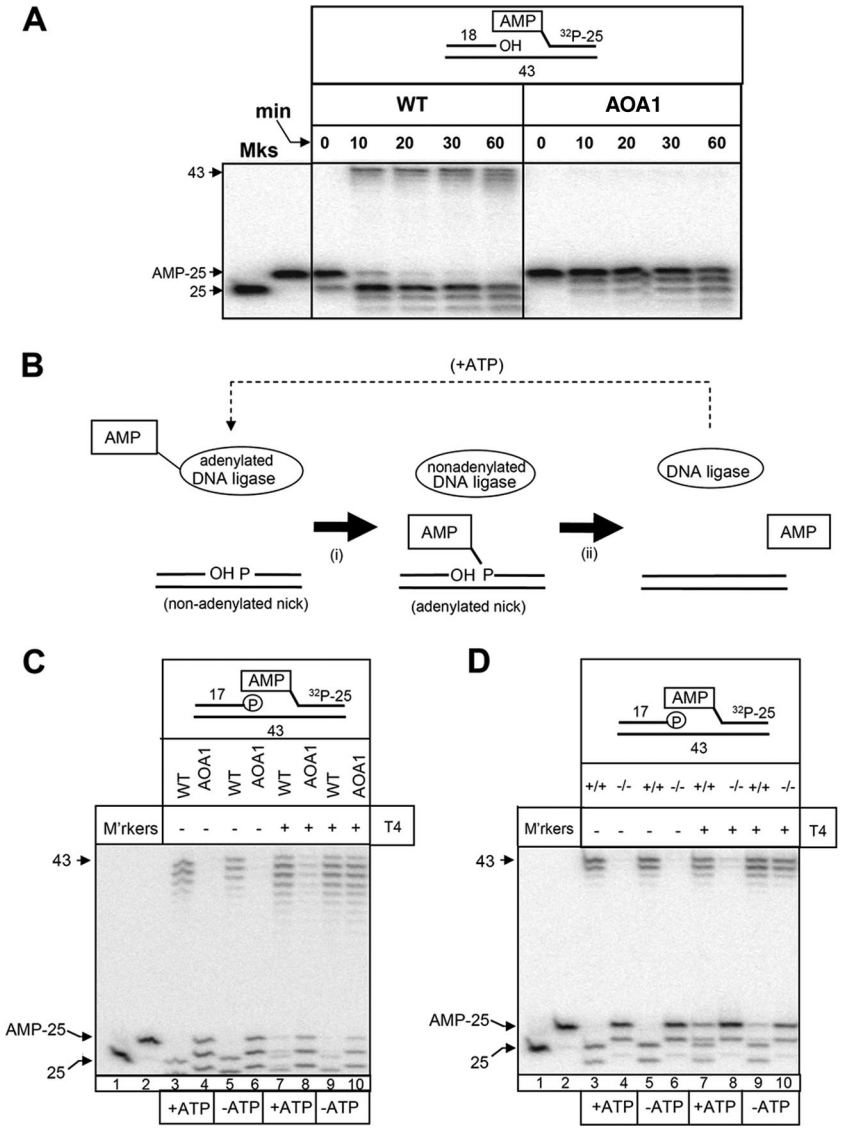

FIG. 4. Short-patch SSBR fails in AOA1 due to insufficient levels of nonadenylated DNA ligase. (A) AOA1 cell extracts cannot efficiently ligate adenylated DNA nicks. Total WT (ConR2) or AOA1 (Ap5) lymphoblastoid cell extracts (6.25 μg) were incubated with a ^{32}P-labeled adenylated nicked substrate (25 nM) (top) for the indicated times at 30°C. Reaction products were fractionated by denaturing PAGE and detected by phosphorimaging. A ^{32}P-labeled 25-mer containing 5′ AMP (AMP-25) and one lacking 5′ AMP were fractionated for size markers (Mks). The position of the 43-mer ligated product is indicated. (B) Cartoon depicting ligation of a nonadenylated DNA nick by DNA ligase. (i) An adenylated DNA ligase molecule transfers AMP to the 5′-phosphate terminus of a DNA nick, resulting in an adenylated nick and a nonadenylated ligase molecule. (ii) The nonadenylated DNA ligase molecule rapidly catalyzes a nucleophilic attack of the pyrophosphate bond linking AMP to DNA, resulting in nick ligation and the release of AMP. The nonadenylated DNA ligase molecule is readenylated (dashed arrow) in readiness for the next ligation event. (C) Complementation of the SSBR defect in AOA1 lymphoblastoid extracts by recombinant T4 DNA ligase. Total WT (ConR2) or AOA1 (Ap5) lymphoblastoid cell extracts (5 μg) were incubated with a ^{32}P-labeled 5′-AMP SSB substrate (25 nM) for 1 h at 30°C in the presence or absence of 1 mM ATP and/or 2 U of T4 DNA ligase, as indicated. Reaction products were fractionated by denaturing PAGE and detected by phosphorimaging. The positions of the ^{32}P-labeled 43-mer reaction product and the ^{32}P-labeled 25-mer containing or lacking 5′ AMP are indicated. M'rkers, markers. (D) Complementation of the SSBR defect in *Aptx*$^{-/-}$ primary astrocyte extracts by recombinant T4 DNA ligase. *Aptx*$^{+/+}$ (+/+) or *Aptx*$^{-/-}$ (−/−) mouse astrocyte extracts (5 μg) were incubated with a ^{32}P-labeled 5′-AMP SSB substrate (25 nM) for 1 h at 30°C in the presence or absence of 1 mM ATP and/or 2 U of T4 DNA ligase, as indicated. Reaction products were fractionated by denaturing PAGE and detected by phosphorimaging. The positions of the ^{32}P-labeled 43-mer reaction product and the ^{32}P-labeled 25-mer containing or lacking 5′ AMP are indicated.

repair machinery that removes AMP from 5′ termini during short-patch SSBR reactions in vitro (1, 9, 19). However, whether or not aprataxin is required for chromosomal DNA strand break repair in vivo is unclear. This is because the occurrence of DNA strand breaks with 5′ AMP has not yet been demonstrated. Moreover, attempts to detect a chromosomal DNA repair defect in AOA1 cells have proved conflicting and unclear (14, 15, 20). To resolve the latter issue, we carefully measured chromosomal SSBR rates in a variety of aprataxin-defective cell lines, including genetically matched

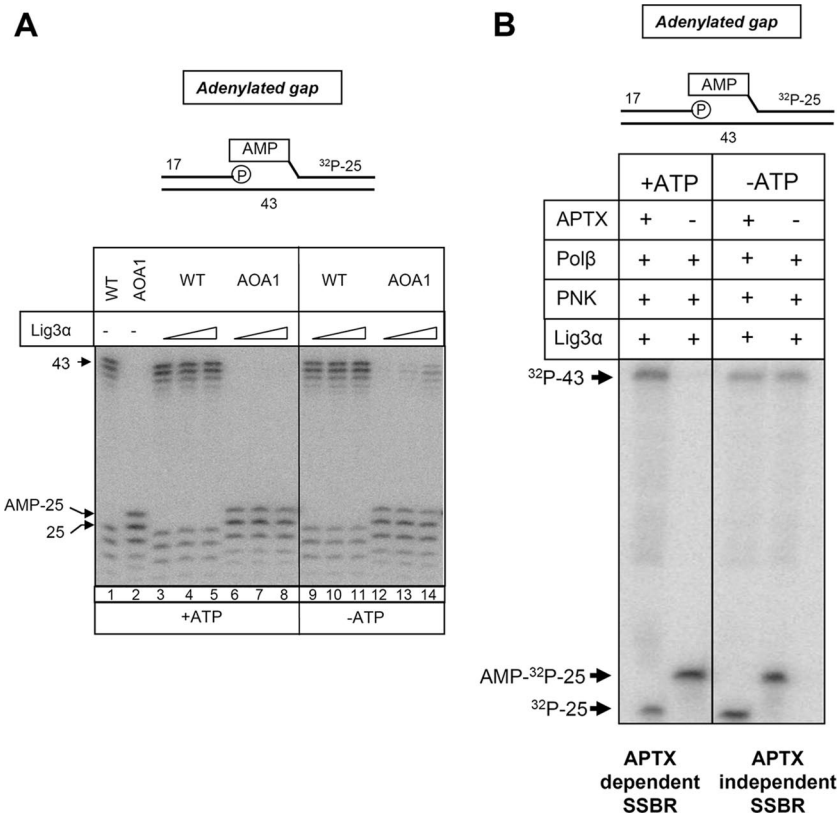

FIG. 5. Complementation of the SSBR defect in AOA1 lymphoblastoid cell extracts by recombinant human Lig3α and reconstitution of aprataxin-independent SSBR with recombinant human proteins. (A) Complementation of the SSBR defect in AOA1 lymphoblastoid cell extracts by recombinant DNA ligase IIIα (Lig3α). Total WT or AOA1 lymphoblastoid cell extracts (5 μg) were incubated with a ^{32}P-labeled 5′-AMP SSB (100 nM) substrate for 1 h at 30°C in the presence or absence of 1 mM ATP and/or 8 nM, 24 nM, or 72 nM Lig3α, as indicated. (B) Reconstitution of aprataxin-independent SSBR with recombinant human proteins. A 5′-AMP SSB substrate (60 nM) was incubated with 250 nM recombinant PNK, 100 nM Pol β, and 80 nM Lig3α in the presence or absence of 100 nM aprataxin (APTX) and 1 mM ATP, as indicated, for 1 h at 30°C. Reaction products were fractionated by denaturing PAGE and detected by phosphorimager.

WT and *Aptx*$^{-/-}$ quiescent neural cells. These experiments revealed that the overall rate of SSBR is normal in aprataxin-defective cells. Notably, we also failed to detect reduced rates of DSBR in AOA1 (unpublished observations).

To resolve the discrepancy between the requirement for aprataxin for SSBR in vitro versus that in vivo, we identified the stage at which short-patch SSBR fails in AOA1 in vitro. Notably, 3′-DNA end processing and DNA gap filling occurred normally during SSBR in the absence of aprataxin, despite the persistence of AMP on the 5′ terminus. However, SSBR reactions subsequently stalled at the final step of DNA ligation, resulting in the accumulation of adenylated DNA nicks. This was surprising, because adenylated DNA nicks are normal, indeed prerequisite, intermediates of DNA ligation reactions, requiring only nonadenylated DNA ligase to reseal the breaks. We therefore reasoned that DNA ligation might fail in AOA1 cell extracts because of insufficient levels of nonadenylated DNA ligase. This would be consistent with the notion that while DNA ligases exist in both adenylated and nonadenylated states, the former predominates in cells because of the cellular ATP concentration. This would not pose a problem in WT cells, in which aprataxin activity ensures that DNA nicks arising during SSBR are not preadenylated and thus are substrates for adenylated DNA ligase. However, in AOA1 cells, DNA nicks can arise in a preadenylated state during SSBR which thus require nonadenylated DNA ligase. In short, we propose that while all cells possess low levels of nonadenylated ligase, due to the rapid adenylation of free ligase molecules by cellular ATP, only in aprataxin-defective cells do preadenylated nicks arise at a level that exceeds the availability of nonadenylated ligase.

Confirmation that short-patch SSBR fails in AOA1 due to insufficient levels of nonadenylated DNA ligase emerged from our finding that addition of recombinant T4 DNA ligase or human Lig3α restored short-patch SSBR in AOA1 extracts and *Aptx*$^{-/-}$ quiescent astrocyte extracts in the absence of aprataxin. Importantly, complementation was more efficient if ATP was omitted from the reaction mixtures, supporting the notion that the complementing factor was nonadenylated DNA ligase. This may also explain the apparent difference between the abilities of T4 DNA ligase and Lig3α to complement the defect (compare Fig. 4C and 5A), since it is likely that the relative amounts of nonadenylated ligase present in the two DNA ligase preparations were different.

The finding that adenylated nicks accumulate during short-patch SSBR in AOA1 provides a possible explanation for the normal rate of chromosomal SSBR observed in this disease. This is because adenylated nicks can be channeled into long-

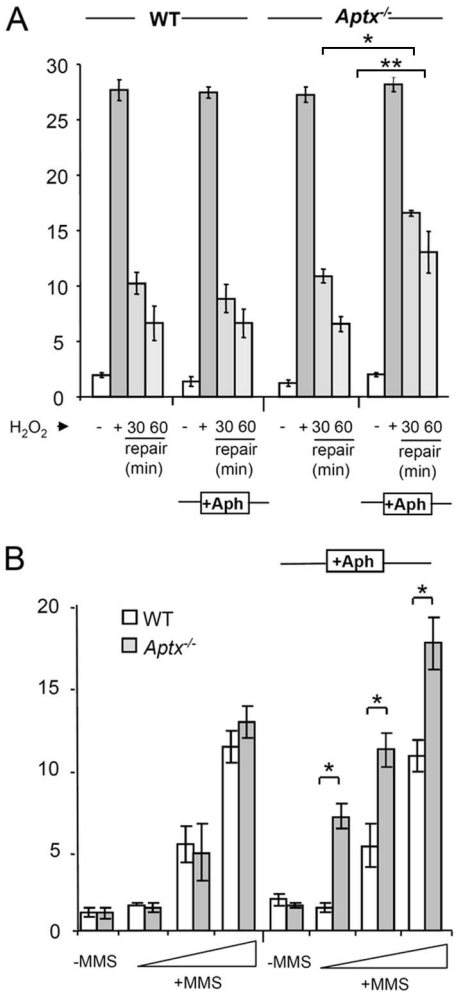

FIG. 6. Defective short-patch SSBR in quiescent primary $Aptx^{-/-}$ mouse neural cells. (A) Quiescent WT and $Aptx^{-/-}$ mouse astrocytes were either left untreated (−) or treated with 75 μM H_2O_2 for 10 min on ice (+) and, where indicated, then incubated in drug-free medium for 30 or 60 min. Where indicated (+Aph), cells were preincubated with 50 μM aphidicolin for 30 min at 37°C, and repair was conducted in the continued presence of aphidicolin. Chromosomal DNA strand breaks were then quantified by alkaline comet assays. Each bar represents the average mean tail moment from three independent experiments (error bars, ±1 standard deviation). Asterisks indicate statistically significant differences (*, $P \leq 0.05$; **, $P \leq 0.01$). (B) Quiescent WT and $Aptx^{-/-}$ mouse astrocytes were either left untreated (−) or treated with 25, 50, or 100 μM MMS for 10 min at 37°C with (+Aph) or without preincubation with 50 μM aphidicolin. Chromosomal DNA strand breaks were then quantified by alkaline comet assays. Each bar represents the average mean tail moment from three independent experiments (error bars, ±1 standard deviation). Asterisks indicate statistically significant differences (*, $P \leq 0.05$; **, $P \leq 0.01$).

patch SSBR. In this pathway, damaged 5′ termini are displaced as a single-stranded flap during gap filling from the 3′ terminus and cleaved off by Flap endonuclease 1 (FEN1) (reviewed in reference 12). This process would not be detected by the short-patch repair assays employed in the current work, because oligonucleotide duplexes of the type employed here are not good substrates for long-patch repair reactions and because cleavage of the single-strand flap would remove the ^{32}P label in our substrates. However, to determine whether long-patch repair might compensate for the loss of short-patch repair in aprataxin-defective cells, we exploited the observation that long-patch SSBR employs the aphidicolin-sensitive DNA polymerases Pol δ and/or Pol ε (10, 13, 22). Because inhibition of Pol δ and/or Pol ε also prevents DNA replication during S phase and can thus impact DNA metabolism independently of long-patch SSBR, we employed quiescent primary astrocytes for these experiments. Strikingly, whereas preincubation with aphidicolin did not affect SSBR rates in WT cells, it revealed a significant chromosomal SSBR defect in $Aptx^{-/-}$ primary quiescent astrocytes following treatment with either H_2O_2 or MMS. SSBR was slowed rather than prevented by aphidicolin, perhaps reflecting the fact that only a subset of DNA strand breaks induced by these agents possess 5′-AMP termini. Alternatively, it is possible that $Aptx^{-/-}$ quiescent astrocytes possess additional, partially overlapping SSBR pathways. Nevertheless, these data demonstrate, for the first time, the involvement of aprataxin in chromosomal SSBR in vivo.

It remains to be determined whether long-patch repair can also compensate for defective short-patch repair in AOA1 cells, as appears to be the case in $Aptx^{-/-}$ mouse neural cells. However, if this is the case, why do aprataxin mutations result in disease? One possibility is that a subset of SSBs arise at which long-patch repair cannot operate. For example, it is possible that aprataxin is also required to repair specific types of damaged 3′ termini (26). Long-patch repair would be unable to operate at such breaks, because no 3′-hydroxyl primer terminus is available for DNA gap filling. Alternatively, since aprataxin is associated with the DSBR machinery (8), it is possible that unrepaired DSBs might account for AOA1. It should be noted, however, that we have so far failed to detect a DSBR defect in AOA1 or $Aptx^{-/-}$ cells (unpublished observations). Finally, it is possible that long-patch repair is not operative or is attenuated in the specific cell types that are affected in AOA1. For example, a number of replication-associated proteins, including several of those implicated in long-patch repair, are downregulated in certain differentiated cell types (21). Thus, it will now be of interest to expand the experiments described in this study to other cell types, including those neural cell types most likely affected in AOA1.

ACKNOWLEDGMENTS

We thank LiMei Ju and Poorvi Patel for technical assistance and Malcolm Taylor for the provision of AOA1 lymphoblastoid cells.

This work was funded by MRC, BBSRC, and European Community (Integrated Project DNA repair [LSHG-CT-2005-512113]) grants to K.W.C. P.J.M. is funded by grants from the NIH and ALSAC of SJCRH. S.F.E.-K. is funded by the Wellcome Trust (grant 085284).

REFERENCES

1. **Ahel, I., U. Rass, S. F. El-Khamisy, S. Katyal, P. M. Clements, P. J. McKinnon, K. W. Caldecott, and S. C. West.** 2006. The neurodegenerative disease protein aprataxin resolves abortive DNA ligation intermediates. Nature **443:**713–716.
2. **Barzilai, A., S. Biton, and Y. Shiloh.** 2008. The role of the DNA damage response in neuronal development, organization and maintenance. DNA Repair (Amsterdam) **7:**1010–1027.
3. **Biton, S., A. Barzilai, and Y. Shiloh.** 2008. The neurological phenotype of ataxia-telangiectasia: solving a persistent puzzle. DNA Repair (Amsterdam) **7:**1028–1038.
4. **Bradley, M. O., and K. W. Kohn.** 1979. X-ray induced DNA double strand break production and repair in mammalian cells as measured by neutral filter elution. Nucleic Acids Res. **7:**793–804.

5. **Breslin, C., P. M. Clements, S. F. El-Khamisy, E. Petermann, N. Iles, and K. W. Caldecott.** 2006. Measurement of chromosomal DNA single-strand breaks and replication fork progression rates. Methods Enzymol. **409:**410–425.
6. **Caldecott, K. W.** 2008. Single-strand break repair and genetic disease. Nat. Rev. Genet. **9:**619–631.
7. **Caldecott, K. W., S. Aoufouchi, P. Johnson, and S. Shall.** 1996. XRCC1 polypeptide interacts with DNA polymerase β and possibly poly(ADP-ribose) polymerase, and DNA ligase III is a novel molecular 'nick-sensor' in vitro. Nucleic Acids Res. **24:**4387–4394.
8. **Clements, P. M., C. Breslin, E. D. Deeks, P. J. Byrd, L. Ju, P. Bieganowski, C. Brenner, M. C. Moreira, A. M. Taylor, and K. W. Caldecott.** 2004. The ataxia-oculomotor apraxia 1 gene product has a role distinct from ATM and interacts with the DNA strand break repair proteins XRCC1 and XRCC4. DNA Repair (Amsterdam) **3:**1493–1502.
9. **Date, H., O. Onodera, H. Tanaka, K. Iwabuchi, K. Uekawa, S. Igarashi, R. Koike, T. Hiroi, T. Yuasa, Y. Awaya, T. Sakai, T. Takahashi, H. Nagatomo, Y. Sekijima, I. Kawachi, Y. Takiyama, M. Nishizawa, N. Fukuhara, K. Saito, S. Sugano, and S. Tsuji.** 2001. Early-onset ataxia with ocular motor apraxia and hypoalbuminemia is caused by mutations in a new HIT superfamily gene. Nat. Genet. **29:**184–188.
10. **DiGiuseppe, J. A., and S. L. Dresler.** 1989. Bleomycin-induced DNA repair synthesis in permeable human fibroblasts: mediation of long-patch and short-patch repair by distinct DNA polymerases. Biochemistry **28:**9515–9520.
11. **Ellenberger, T., and A. E. Tomkinson.** 2008. Eukaryotic DNA ligases: structural and functional insights. Annu. Rev. Biochem. **77:**313–338.
12. **Fortini, P., and E. Dogliotti.** 2007. Base damage and single-strand break repair: mechanisms and functional significance of short- and long-patch repair subpathways. DNA Repair (Amsterdam) **6:**398–409.
13. **Goscin, L. P., and J. J. Byrnes.** 1982. DNA polymerase delta: one polypeptide, two activities. Biochemistry **21:**2513–2518.
14. **Gueven, N., O. J. Becherel, A. W. Kijas, P. Chen, O. Howe, J. H. Rudolph, R. Gatti, H. Date, O. Onodera, G. Taucher-Scholz, and M. F. Lavin.** 2004. Aprataxin, a novel protein that protects against genotoxic stress. Hum. Mol. Genet. **13:**1081–1093.
15. **Gueven, N., P. Chen, J. Nakamura, O. J. Becherel, A. W. Kijas, P. Grattan-Smith, and M. F. Lavin.** 2007. A subgroup of spinocerebellar ataxias defective in DNA damage responses. Neuroscience **145:**1418–1425.
16. **Kijas, A. W., J. L. Harris, J. M. Harris, and M. F. Lavin.** 2006. Aprataxin forms a discrete branch in the HIT (histidine triad) superfamily of proteins with both DNA/RNA binding and nucleotide hydrolase activities. J. Biol. Chem. **281:**13939–13948.
17. **Lavin, M. F., N. Gueven, and P. Grattan-Smith.** 2008. Defective responses to DNA single- and double-strand breaks in spinocerebellar ataxia. DNA Repair (Amsterdam) **7:**1061–1076.
18. **Lundin, C., M. North, K. Erixon, K. Walters, D. Jenssen, A. S. Goldman, and T. Helleday.** 2005. Methyl methanesulfonate (MMS) produces heat-labile DNA damage but no detectable in vivo DNA double-strand breaks. Nucleic Acids Res. **33:**3799–3811.
19. **Moreira, M. C., C. Barbot, N. Tachi, N. Kozuka, E. Uchida, T. Gibson, P. Mendonca, M. Costa, J. Barros, T. Yanagisawa, M. Watanabe, Y. Ikeda, M. Aoki, T. Nagata, P. Coutinho, J. Sequeiros, and M. Koenig.** 2001. The gene mutated in ataxia-ocular apraxia 1 encodes the new HIT/Zn-finger protein aprataxin. Nat. Genet. **29:**189–193.
20. **Mosesso, P., M. Piane, F. Palitti, G. Pepe, S. Penna, and L. Chessa.** 2005. The novel human gene aprataxin is directly involved in DNA single-strand-break repair. Cell. Mol. Life Sci. **62:**485–491.
21. **Narciso, L., P. Fortini, D. Pajalunga, A. Franchitto, P. Liu, P. Degan, M. Frechet, B. Demple, M. Crescenzi, and E. Dogliotti.** 2007. Terminally differentiated muscle cells are defective in base excision DNA repair and hypersensitive to oxygen injury. Proc. Natl. Acad. Sci. USA **104:**17010–17015.
22. **Niranjanakumari, S., and K. P. Gopinathan.** 1993. Isolation and characterization of DNA polymerase epsilon from the silk glands of *Bombyx mori*. J. Biol. Chem. **268:**15557–15564.
23. **Rass, U., I. Ahel, and S. C. West.** 2007. Actions of aprataxin in multiple DNA repair pathways. J. Biol. Chem. **282:**9469–9474.
24. **Rass, U., I. Ahel, and S. C. West.** 2007. Defective DNA repair and neurodegenerative disease. Cell **130:**991–1004.
25. **Seidle, H. F., P. Bieganowski, and C. Brenner.** 2005. Disease-associated mutations inactivate AMP-lysine hydrolase activity of aprataxin. J. Biol. Chem. **280:**20927–20931.
26. **Takahashi, T., M. Tada, S. Igarashi, A. Koyama, H. Date, A. Yokoseki, A. Shiga, Y. Yoshida, S. Tsuji, M. Nishizawa, and O. Onodera.** 2007. Aprataxin, causative gene product for EAOH/AOA1, repairs DNA single-strand breaks with damaged 3′-phosphate and 3′-phosphoglycolate ends. Nucleic Acids Res. **35:**3797–3809.
27. **Takashima, H., C. F. Boerkoel, J. John, G. M. Saifi, M. A. Salih, D. Armstrong, Y. Mao, F. A. Quiocho, B. B. Roa, M. Nakagawa, D. W. Stockton, and J. R. Lupski.** 2002. Mutation of TDP1, encoding a topoisomerase I-dependent DNA damage repair enzyme, in spinocerebellar ataxia with axonal neuropathy. Nat. Genet. **32:**267–272.
28. **Taylor, A. M., A. Groom, and P. J. Byrd.** 2004. Ataxia-telangiectasia-like disorder (ATLD)—its clinical presentation and molecular basis. DNA Repair (Amsterdam) **3:**1219–1225.
29. **Taylor, R. M., C. J. Whitehouse, and K. W. Caldecott.** 2000. The DNA ligase III zinc finger stimulates binding to DNA secondary structure and promotes end joining. Nucleic Acids Res. **28:**3558–3563.
30. **Whitehouse, C. J., R. M. Taylor, A. Thistlethwaite, H. Zhang, F. Karimi-Busheri, D. D. Lasko, M. Weinfeld, and K. W. Caldecott.** 2001. XRCC1 stimulates human polynucleotide kinase activity at damaged DNA termini and accelerates DNA single-strand break repair. Cell **104:**107–117.

Biochemical Society Annual Symposium No. 76

transactions

Biochemical Society Transactions www.biochemsoctrans.org

Short-patch single-strand break repair in ataxia oculomotor apraxia-1

John J. Reynolds*, Sherif F. El-Khamisy*† and Keith W. Caldecott*[1]

*Genome Damage and Stability Centre, University of Sussex, Science Park Road, Falmer, Brighton BN1 9RQ, U.K., and †Biochemistry Department, Faculty of Pharmacy. Ain Shams University, Cairo, Egypt

Abstract

AOA1 (ataxia oculomotor apraxia-1) results from mutations in aprataxin, a component of DNA strand break repair that removes AMP from 5′-termini. In the present article, we provide an overview of this disease and review recent experiments demonstrating that short-patch repair of oxidative single-strand breaks in AOA1 cell extracts bypasses the point of aprataxin action and stalls at the final step of DNA ligation, resulting in accumulation of adenylated DNA nicks. Strikingly, this defect results from insufficient levels of non-adenylated DNA ligase and short-patch single-strand break repair can be restored in AOA1 extracts, independently of aprataxin, by addition of recombinant DNA ligase.

AOA1 (ataxia oculomotor apraxia-1)

AOA1 is an autosomal recessive spinocerebellar ataxia syndrome that resembles Friedreich's ataxia and A-T (ataxia telangiectasia) neurologically, but which lacks extraneurological features such as immunodeficiency and telangiectasia. A recent study of 14 French, Italian and Algerian AOA1 patients from nine families supports the likelihood that, although cerebellar atrophy, ataxia and sensorimotor axonal neuropathy are common to most AOA1 patients, the presence and severity of other features is more variable (~85% of patients in the case of oculomotor apraxia) [1]. Variation in clinical impact and/or severity of AOA1 is suggested further by reported clinical overlap with other neurological diseases/conditions, such as MSA (multiple system atrophy) and ataxia with coenzyme Q10 deficiency [2–4]. AOA1 accounts for 5–10% of all autosomal recessive cerebellar ataxias and has variable age of onset (typically 1–18 years), with a mean of ~5 years [1,5]. Unlike A-T cells, AOA1 cells are only mildly sensitive, if at all, to ionizing radiation and other genotoxins, and exhibit normal cell-cycle-checkpoint control and chromosome stability following ionizing radiation [6]. Consistent with these observations, elevated cancer incidence has not been reported in AOA1 patients. The gene mutated in AOA1 is designated *APTX* [7,8], and the protein product of *APTX* is designated aprataxin.

Aprataxin contains a central HIT (histidine triad) domain and is a member of the HIT domain superfamily of nucleotide hydrolases/transferases. The N-terminus of aprataxin exhibits homology with PNK (polynucleotide kinase) [8], and like PNK encodes a divergent FHA (forkhead-associated) domain [9]. The FHA domains of both aprataxin and PNK facilitate constitutive interactions with protein kinase CK2-phosphorylated XRCC1 (X-ray repair complementing defective repair in Chinese-hamster cells 1) [6,9–14]. It is noteworthy that a third member of this divergent FHA domain family has been identified [denoted APLF (aprataxin- and PNK-like factor)/PALF (PNK and aprataxin-like FHA protein)/Xip1] and shown to bind CK2-phosphorylated XRCC1 [15–17]. In fact, all three FHA domain proteins are also sequestered into the DSBR (double-strand break repair) machinery, via FHA domain-mediated interaction with CK2-phosphorylated XRCC4 [6,15,18]. It is thus highly likely that aprataxin, PNK and APLF play roles both in SSBR (single-strand break repair) and DSBR. Aprataxin also associates with PARP-1 [poly(ADP–ribose) polymerase 1] and p53, and additionally with the nucleolar proteins nucleolin, nucleophosmin and UBF-1 (upstream binding factor 1) [12,19]. The association and partial co-localization of aprataxin with nucleolar proteins is also mediated by the FHA domain, although whether these associations are direct or indirect (e.g. via another protein) remains to be determined. Nevertheless, the association of aprataxin with nucleolar proteins may indicate that SSBR and/or DSBR is particularly important at sites of high transcriptional activity, perhaps to prevent SSBs (single-strand breaks) from blocking gene expression.

Most of the mutations identified in AOA1 to date are located within the HIT domain or just upstream of the C-terminal zinc-finger motif, consistent with a critical requirement for the HIT domain for normal neurological function. Many of these mutations greatly reduce the stability and/or cellular level of aprataxin and may thus be functionally null alleles [12,20,21]. Some mutations appear to be associated with later disease onset and/or milder clinical features [8,22–24], which, in some cases, appear to have less impact on aprataxin stability and/or activity [20]. On the basis of sequence comparisons and substrate specificity, aprataxin appears to

Key words: aprataxin, ataxia oculomotor apraxia, short-patch repair, single-strand break repair, spinocerebellar ataxia.

Abbreviations used: AOA1, ataxia oculomotor apraxia-1; APLF, aprataxin- and polynucleotide kinase-like factor; A-T, ataxia telangiectasia; DSBR, double-strand break repair; FHA, forkhead-associated; HIT, histidine triad; Lig3α, DNA ligase IIIα; Polβ, polymerase β; PNK, polynucleotide kinase; SSB, single-strand break; SSBR, single-strand break repair; WT, wild-type; XRCC1, X-ray repair complementing defective repair in Chinese-hamster cells 1.

[1]To whom correspondence should be addressed (email k.w.caldecott@sussex.ac.uk).

represent a discrete branch of the HIT domain superfamily [25]. Indeed, although aprataxin can hydrolyse substrates typical of either the Fhit or Hint branch of HIT domain proteins, releasing AMP from diadenosine tetraphosphate or AMP-lysine respectively, its catalytic activity is very low (k_{cat} <0.03 s^{-1}) [20,25]. Aprataxin has also been reported to process two types of damaged 3′-terminus arising at oxidative DNA breaks, 3′-phosphate and 3′-phosphoglycolate termini, raising the possibility that it is an end-processing factor. However, the activity of aprataxin on such substrates is also very low (k_{cat} ~0.0003–0.003 s^{-1}). A more likely physiological substrate for aprataxin are 5′-AMP termini, at which AMP is covalently linked to 5′-phosphate through a pyrophosphate bond [26,27]. DNA strand breaks in which the 5′-terminus is linked to AMP are normal intermediates of DNA ligation, but if they arise before 3′-DNA end processing has occurred, ligation is inhibited. Aprataxin can remove AMP from the 5′-terminus of DNA breaks at such 'abortive' DNA ligation events, effectively 'proofreading' the DNA ligase reaction [26]. In addition to the HIT domain, the C-terminal zinc finger is important for aprataxin activity on 5′-AMP, probably to increase the affinity and/or specificity of aprataxin for 5′-AMP substrates [27]. Although the ability to process 5′-AMP termini is a very elegant activity, it remains to be determined whether or not this type of terminus arises *in vivo*.

AOA1 and short-patch SSBR

To clarify the nature of the SSBR defect in AOA1, we recently reconstituted AOA1-dependent short-patch SSBR assays *in vitro* with human and rodent cell extracts [26,28]. To measure short-patch SSBR, we employed an oligonucleotide duplex harbouring a 1-bp gap with 3′-phosphate termini, a substrate that mimics one of the commonest types of oxidative SSB arising in cells (Figure 1A). The SSB also possesses a 5′-AMP and is therefore a substrate for aprataxin. WT (wild-type) extracts efficiently removed AMP from 5′-termini and repaired the SSBs, as indicated by the respective appearance of ^{32}P-labelled 25-mer and 43-mer (Figure 1A, lanes 6–8). In contrast, however, AOA1 extracts did not (Figure 1A, lanes 3–5). It should be noted that SSBR is proficient in AOA1 extracts if the initial SSB lacks 5′-AMP ([28] and results not shown). A number of truncated oligonucleotide fragments were generated by non-specific nucleolytic activity in these experiments (see asterisks in Figure 1A), which is common in lymphoblastoid extracts, and which represent degradation of the 3′-terminus of the ^{32}P-labelled 25-mer. However, this activity did not account for the short-patch repair defect in AOA1 extracts, which was fully complemented by addition of recombinant aprataxin (Figure 1A, lanes 9–11). The appearance of ligated product in these experiments was dependent upon the presence of dNTPs, confirming that these experiments measured gap repair rather than ligation across the 1-bp gap (results not shown).

The predicted pathway for short-patch repair of SSBs harbouring 5′-AMP in WT cells is depicted in Figure 1(B). It was considered likely that this pathway arrests in AOA1 extracts at the very beginning, before 3′-DNA end-processing by PNK and/or DNA gap-filling by Polβ (polymerase β), because the presence of AMP at the 5′-terminus might occlude access to the 3′-terminus. Surprisingly, however, the 3′-phosphatase activity of PNK was similar irrespective of whether or not the SSB possessed 5′-AMP, under conditions

Figure 1 | Aprataxin-dependent short-patch SSBR of 5′-AMP SSBs in AOA1 lymphoblastoid extracts

(**A**) Defective short-patch SSBR in AOA1 extracts and its complementation by recombinant aprataxin. Upper panel: cartoon of the oligonucleotide duplex employed for these experiments containing a 1-bp gap, 3′-phosphate terminus and 5′-AMP terminus. The 5′-phosphate to which AMP is covalently linked is labelled with ^{32}P. The position of this label restricts the assay to measurements of short-patch repair events only. Numbers denote nucleotide lengths. Lower panel: 0.1, 1.0 or 5.0 μg of either WT (ConR2) or AOA1 (Ap5) extracts were incubated for 60 min at 30°C with ^{32}P-labelled 5′-AMP SSB substrate (25 nM) in the absence (left) or presence (right) of recombinant human aprataxin (APTX) (100 nM). Reaction products were fractionated and detected as described above. ^{32}P-labelled 25-mer containing (AMP-^{32}P-25) or lacking (^{32}P-25) 5′-AMP was fractionated in parallel for size markers (Mks). The position of repaired ^{32}P-labelled 43-mer (^{32}P-43) is also indicated. Non-specific nucleolytic products are indicated by an asterisk. (**B**) Cartoon of aprataxin-dependent short-patch repair of adenylated SSBs in WT cells. Reproduced from Molecular and Cellular Biology (2009), **29**, 1354–1362, doi:10.1128/MCB.01471-08 [28], with permission © 2009 American Society for Microbiology.

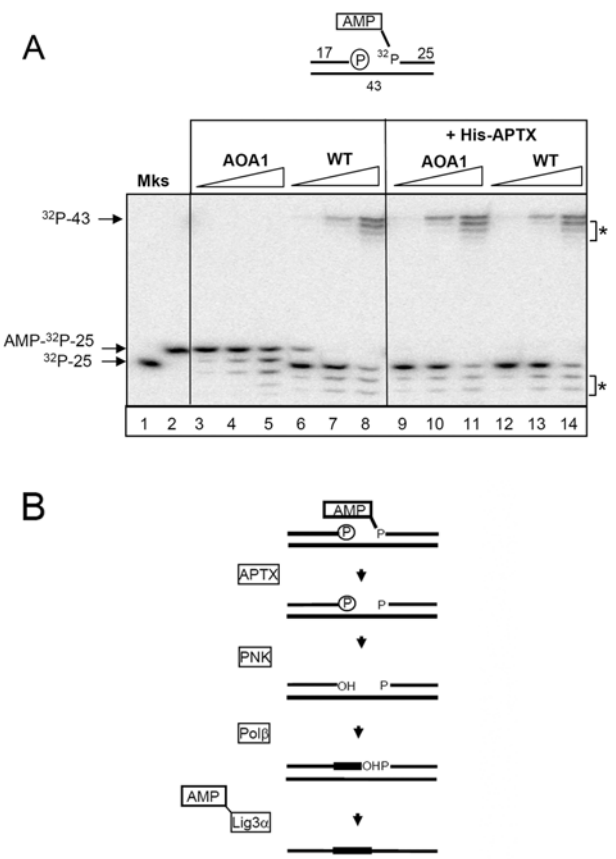

Figure 2 | Removal of 5′-AMP by aprataxin is not required for end-processing by PNK or gap-filling by Polβ

(**A**) 5′-AMP does not affect processing of 3′-phosphate termini by PNK. SSB substrate (25 nM) lacking or containing 5′-AMP as indicated (upper panel) was incubated with 25, 50, 125 or 250 nM recombinant human PNK, or without PNK (-), for 1 h at 30 °C. Reaction products were fractionated by denaturing PAGE and detected by phosphorimaging. Note that the 5′-terminus of the 17-mer is labelled with ^{32}P in these experiments to allow detection of 3′-end processing. The position of the 17-mer harbouring the 3′-phosphate (17-P) or 3′-hydroxy group (3′-OH) is indicated. (**B**) 5′-AMP does not affect gap-filling by Polβ. SSB substrate (25 nM) lacking or containing 5′-AMP as indicated (upper panel) was incubated with 5, 15, 30 or 100 nM purified recombinant human Polβ, or without Polβ (-), for 1 h at 30 °C. Reaction products were fractionated by denaturing PAGE and detected by phosphorimaging. The positions of 17-mer and 18-mer are included as markers. Reproduced from Molecular and Cellular Biology (2009), **29**, 1354–1362, doi:10.1128/MCB.01471-08 [28], with permission © 2009 American Society for Microbiology.

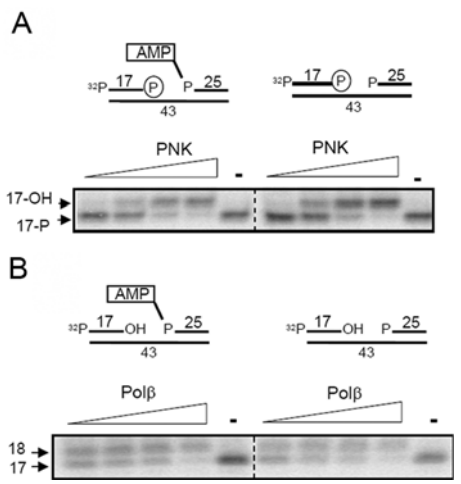

in which PNK was limiting (Figure 2A). Similar results were observed for DNA gap-filling by Polβ, with similar amounts of ^{32}P-labelled 17-mer converted into ^{32}P-labelled 18-mer, irrespective of the presence or absence of 5′-AMP (Figure 2B). These experiments suggested that neither PNK nor Polβ activity is affected by the presence of 5′-AMP at these time points, and thus short-patch SSBR might fail in AOA1 extracts at the final step of DNA ligation, resulting in the accumulation of adenylated DNA nicks. This was surprising, because adenylated DNA nicks are normal, indeed prerequisite, intermediates of DNA-ligation reactions, requiring only non-adenylated DNA ligase to reseal the breaks. We considered that DNA ligation might fail in AOA1 cell extracts because of insufficient levels of non-adenylated DNA ligase. This would be consistent with the notion that, although DNA ligases exist in both adenylated and non-adenylated states, the former predominates in cells because of the cellular concentration of ATP. This would not be a problem in WT cells, in which aprataxin activity ensures that DNA nicks arising during SSBR are not pre-adenylated and are thus substrates for adenylated DNA ligase. However, in AOA1 cells, DNA nicks arise in a pre-adenylated state during SSBR and thus require non-adenylated DNA ligase. We thus suggest that, whereas all cells possess low levels of non-adenylated ligase, because of the rapid adenylation of free ligase molecules by cellular ATP, only in aprataxin-defective cells do pre-adenylated nicks arise at a level sufficient to exceed the availability of non-adenylated ligase.

Evidence in support of this hypothesis arose when we compared WT and AOA1 extracts for their ability to ligate adenylated nicks. Whereas adenylated nicks were efficiently ligated by cell extract from WT cells, they remained largely unligated in reactions containing AOA1 cell extract (Figure 3A). To test our hypothesis further, we examined the impact of supplementing short-patch SSBR reactions in AOA1 cell extracts and *Aptx*$^{-/-}$ mouse neural astrocyte extracts with recombinant DNA ligase. Addition of T4 ligase restored short-patch SSBR efficiency in both AOA1 and *Aptx*$^{-/-}$ neural cell extract to a level similar to that observed in WT extract (Figure 3B, compare lanes 6 and 10). Importantly, complementation was more efficient in the absence of ATP than in its presence, supporting the notion that it was the non-adenylated subfraction of T4 ligase that was responsible for complementation (Figure 3B, compare lanes 8 and 10). The experiments described above suggested that short-patch repair of some adenylated SSBs can occur independently of aprataxin if sufficient non-adenylated DNA ligase is available. To confirm this idea, we also attempted to reconstitute this aprataxin-independent SSBR pathway using recombinant proteins. As expected, the repair of adenylated gaps by PNK, Polβ and Lig3α (DNA ligase IIIα) was dependent on aprataxin in the presence of ATP, conditions under which Lig3α is largely adenylated (Figure 4). However, in the absence of ATP, short-patch repair of 5′-AMP SSBs occurred independently of aprataxin. Taken together, these experiments indicate that short-patch repair arrests in AOA1 cell extracts at the final step of DNA ligation, owing to insufficient levels of non-adenylated DNA ligase.

The finding that adenylated nicks accumulate during short-patch SSBR in AOA1 provides a possible explanation for the normal rate of chromosomal SSBR observed in AOA1. This is because adenylated nicks can be channelled into long-patch SSBR. In this pathway, damaged 5′-termini are displaced as a single-stranded flap during gap-filling from the 3′-terminus and cleaved off by FEN1 (flap endonuclease-1) (reviewed in [29]). This process would not be detected by the short-patch repair assays employed in our recent work [28], because oligonucleotide duplexes of the type employed here are not good substrates for long-patch repair reactions and because cleavage of the single-strand flap would remove the ^{32}P label in our substrates. However, if long-patch repair can compensate for defective short-patch repair in AOA1 cells, then why do aprataxin mutations result in disease? One possibility is that a subset of SSBs arise at which long-patch repair cannot operate. For example, it is possible that aprataxin is also required to repair specific types of damaged 3′-terminus [30]. Long-patch repair would be unable to operate at such breaks, because a 3′-hydroxy primer terminus is not available for

Figure 3 | Short-patch SSBR fails in AOA1 due to insufficient levels of non-adenylated DNA ligase

(**A**) AOA1 extracts cannot efficiently ligate adenylated DNA nicks. Total WT (ConR2) or AOA1 (Ap5) lymphoblastoid cell extracts (6.25 μg) were incubated with ^{32}P-labelled adenylated nicked substrate (25 nM) (shown schematically in the upper panel) for the indicated time period at 30 °C. Reaction products were fractionated by denaturing PAGE and detected by phosphorimaging. ^{32}P-labelled 25-mer containing (AMP-25) or lacking (25) 5′-AMP were fractionated for size markers (Mks). The position of 43-mer ligated product (43) is indicated. (**B**) Complementation of the SSBR defect in AOA1 lymphoblastoid extracts by recombinant T4 DNA ligase. Total WT (ConR2) or AOA1 (Ap5) lymphoblastoid cell extracts (5 μg) were incubated with ^{32}P-labelled 5′-AMP SSB substrate (25 nM) (shown schematically in the upper panel) for 1 h at 30°C in the presence or absence of 1 mM ATP and/or 2 units of T4 DNA ligase, as indicated. Reaction products were fractionated by denaturing PAGE and detected by phosphorimaging. The positions of ^{32}P-labelled 43-mer reaction product (43) and ^{32}P-labelled 25-mer containing (AMP-25) or lacking (25) 5′-AMP are indicated. Reproduced from Molecular and Cellular Biology (2009), **29**, 1354–1362, doi:10.1128/MCB.01471-08 [28], with permission © 2009 American Society for Microbiology.

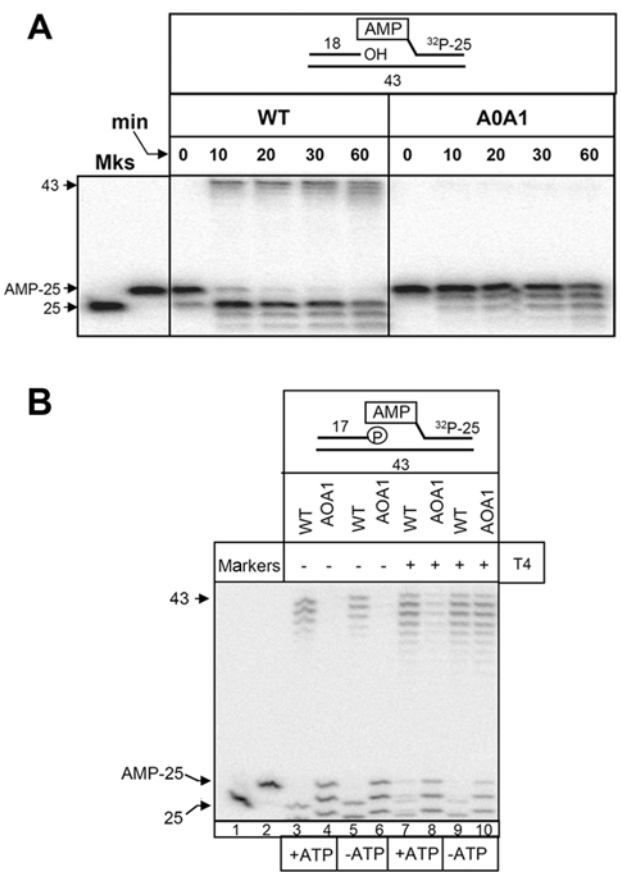

Figure 4 | Reconstitution of aprataxin-independent SSBR with recombinant human proteins

Reconstitution of aprataxin-independent SSBR with recombinant human proteins. 5′-AMP SSB substrate (60 nM) (shown schematically above the gel) was incubated with 250 nM recombinant PNK, 100 nM Polβ and 80 nM Lig3α in the presence or absence of 100 nM aprataxin (APTX) and 1 mM ATP, as indicated, for 1 h at 30 °C. Reaction products were fractionated by denaturing PAGE and detected by phosphorimaging. Reproduced from Molecular and Cellular Biology (2009), **29**, 1354–1362, doi:10.1128/MCB.01471-08 [28], with permission © 2009 American Society for Microbiology.

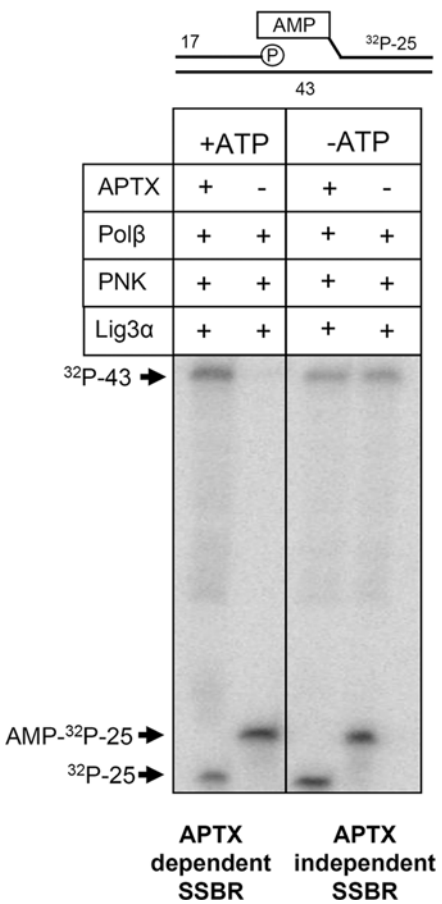

DNA gap-filling. Alternatively, since aprataxin is associated with the DSBR machinery [6], it is possible that unrepaired double-strand breaks might account for AOA1. It should be noted, however, that we have so far failed to detect a DSBR defect in AOA1 or *Aptx*$^{-/-}$ cells (S. F. EI-Khamisy and K.W. Caldecott, unpublished work). Finally, it is possible that long-patch repair is not operative or is attenuated in the specific cell types that are affected in AOA1. For example, a number of replication-associated proteins, including several of those implicated in long-patch repair, are down-regulated in certain differentiated cell types [31].

Funding

This work was funded by the Medical Research Council [grant numbers G0600776 and G0400959], the Biotechnology and Biological Sciences Research Council [grant number C516595] and the European Community [Integrated Project DNA repair grant LSHG-CT-2005-512113] (to K.W.C.). S.F.E. was funded partly by the Wellcome Trust [grant number 085284].

References

1 Le Ber, I., Moreira, M.C., Rivaud-Pechoux, S., Chamayou, C., Ochsner, F., Kuntzer, T., Tardieu, M., Said, G., Habert, M.O., Demarquay, G. et al. (2003) Cerebellar ataxia with oculomotor apraxia type 1: clinical and genetic studies. Brain **126**, 2761–2772

2 Baba, Y., Uitti, R.J., Boylan, K.B., Uehara, Y., Yamada, T., Farrer, M.J., Couchon, E., Batish, S.D. and Wszolek, Z.K. (2006) Aprataxin (*APTX*) gene mutations resembling multiple system atrophy. Parkinsonism Relat. Disord. **13**, 139–142

3 Quinzii, C.M., Kattah, A.G., Naini, A., Akman, H.O., Mootha, V.K., DiMauro, S. and Hirano, M. (2005) Coenzyme Q deficiency and cerebellar ataxia associated with an aprataxin mutation. Neurology **64**, 539–541

4 Le Ber, I., Dubourg, O., Benoist, J.F., Jardel, C., Mochel, F., Koenig, M., Brice, A., Lombes, A. and Durr, A. (2007) Muscle coenzyme Q10 deficiencies in ataxia with oculomotor apraxia 1. Neurology **68**, 295–297

5 Moreira, M.C., Barbot, C., Tachi, N., Kozuka, N., Mendonca, P., Barros, J., Coutinho, P., Sequeiros, J. and Koenig, M. (2001) Homozygosity mapping of Portuguese and Japanese forms of ataxia-oculomotor apraxia to 9p13, and evidence for genetic heterogeneity. Am. J. Hum. Genet. **68**, 501–508

6 Clements, P.M., Breslin, C., Deeks, E.D., Byrd, P.J., Ju, L., Bieganowski, P., Brenner, C., Moreira, M.C., Taylor, A.M. and Caldecott, K.W. (2004) The ataxia-oculomotor apraxia 1 gene product has a role distinct from ATM and interacts with the DNA strand break repair proteins XRCC1 and XRCC4. DNA Repair **3**, 1493–1502

7 Date, H., Onodera, O., Tanaka, H., Iwabuchi, K., Uekawa, K., Igarashi, S., Koike, R., Hiroi, T., Yuasa, T., Awaya, Y. et al. (2001) Early-onset ataxia with ocular motor apraxia and hypoalbuminemia is caused by mutations in a new HIT superfamily gene. Nat. Genet. **29**, 184–188

8 Moreira, M.C., Barbot, C., Tachi, N., Kozuka, N., Uchida, E., Gibson, T., Mendonca, P., Costa, M., Barros, J., Yanagisawa, T. et al. (2001) The gene mutated in ataxia-ocular apraxia 1 encodes the new HIT/Zn-finger protein aprataxin. Nat. Genet. **29**, 189–193

9 Caldecott, K.W. (2003) DNA single-strand break repair and spinocerebellar ataxia. Cell **112**, 7–10

10 Luo, H., Chan, D.W., Yang, T., Rodriguez, M., Chen, B.P., Leng, M., Mu, J.J., Chen, D., Songyang, Z., Wang, Y. and Qin, J. (2004) A new XRCC1-containing complex and its role in cellular survival of methyl methanesulfonate treatment. Mol. Cell. Biol. **24**, 8356–8365

11 Date, H., Igarashi, S., Sano, Y., Takahashi, T., Takahashi, T., Takano, H., Tsuji, S., Nishizawa, M. and Onodera, O. (2004) The FHA domain of aprataxin interacts with the C-terminal region of XRCC1. Biochem. Biophys. Res. Commun. **325**, 1279–1285

12 Gueven, N., Becherel, O.J., Kijas, A.W., Chen, P., Howe, O., Rudolph, J.H., Gatti, R., Date, H., Onodera, O., Taucher-Scholz, G. and Lavin, M.F. (2004) Aprataxin, a novel protein that protects against genotoxic stress. Hum. Mol. Genet. **13**, 1081–1093

13 Sano, Y., Date, H., Igarashi, S., Onodera, O., Oyake, M., Takahashi, T., Hayashi, S., Morimatsu, M., Takahashi, H., Makifuchi, T. et al. (2004) Aprataxin, the causative protein for EAOH is a nuclear protein with a potential role as a DNA repair protein. Ann. Neurol. **55**, 241–249

14 Loizou, J.I., El-Khamisy, S.F., Zlatanou, A., Moore, D.J., Chan, D.W., Qin, J., Sarno, S., Meggio, F., Pinna, L.A. and Caldecott, K.W. (2004) The protein kinase CK2 facilitates repair of chromosomal DNA single-strand breaks. Cell **117**, 17–28

15 Iles, N., Rulten, S., El-Khamisy, S.F. and Caldecott, K.W. (2007) APLF (C2orf13) is a novel human protein involved in the cellular response to chromosomal DNA strand breaks. Mol. Cell. Biol. **27**, 3793–3803

16 Kanno, S., Kuzuoka, H., Sasao, S., Hong, Z., Lan, L., Nakajima, S. and Yasui, A. (2007) A novel human AP endonuclease with conserved zinc-finger-like motifs involved in DNA strand break responses. EMBO J. **26**, 2094–2103

17 Bekker-Jensen, S., Fugger, K., Danielsen, J.R., Gromova, I., Sehested, M., Celis, J., Bartek, J., Lukas, J. and Mailand, N. (2007) Human Xip1 (C2orf13) is a novel regulator of cellular responses to DNA strand breaks. J. Biol. Chem. **282**, 19638–19643

18 Koch, C.A., Agyei, R., Galicia, S., Metalnikov, P., O'Donnell, P., Starostine, A., Weinfeld, M. and Durocher, D. (2004) Xrcc4 physically links DNA end processing by polynucleotide kinase to DNA ligation by DNA ligase IV. EMBO J. **23**, 3874–3885

19 Becherel, O.J., Gueven, N., Birrell, G.W., Schreiber, V., Suraweera, A., Jakob, B., Taucher-Scholz, G. and Lavin, M.F. (2006) Nucleolar localization of aprataxin is dependent on interaction with nucleolin and on active ribosomal DNA transcription. Hum. Mol. Genet. **15**, 2239–2249

20 Seidle, H.F., Bieganowski, P. and Brenner, C. (2005) Disease-associated mutations inactivate AMP-lysine hydrolase activity of Aprataxin. J. Biol. Chem. **280**, 20927–20931

21 Hirano, M., Asai, H., Kiriyama, T., Furiya, Y., Iwamoto, T., Nishiwaki, T., Yamamoto, A., Mori, T. and Ueno, S. (2007) Short half-lives of ataxia-associated aprataxin proteins in neuronal cells. Neurosci. Lett. **419**, 184–187

22 Criscuolo, C., Mancini, P., Menchise, V., Sacca, F., De Michele, G., Banfi, S. and Filla, A. (2005) Very late onset in ataxia oculomotor apraxia type I. Ann. Neurol. **57**, 777

23 Criscuolo, C., Mancini, P., Sacca, F., De Michele, G., Monticelli, A., Santoro, L., Scarano, V., Banfi, S. and Filla, A. (2004) Ataxia with oculomotor apraxia type 1 in Southern Italy: late onset and variable phenotype. Neurology **63**, 2173–2175

24 Tranchant, C., Fleury, M., Moreira, M.C., Koenig, M. and Warter, J.M. (2003) Phenotypic variability of aprataxin gene mutations. Neurology **60**, 868–870

25 Kijas, A.W., Harris, J.L., Harris, J.M. and Lavin, M.F. (2006) Aprataxin forms a discrete branch in the HIT (histidine triad) superfamily of proteins with both DNA/RNA binding and nucleotide hydrolase activities. J. Biol. Chem. **281**, 13939–13948

26 Ahel, I., Rass, U., El-Khamisy, S.F., Katyal, S., Clements, P.M., McKinnon, P.J., Caldecott, K.W. and West, S.C. (2006) The neurodegenerative disease protein aprataxin resolves abortive DNA ligation intermediates. Nature **443**, 713–716

27 Rass, U., Ahel, I. and West, S.C. (2007) Actions of aprataxin in multiple DNA repair pathways. J. Biol. Chem. **282**, 9469–9474

28 Reynolds, J.J., El-Khamisy, S.F., Katyal, S., Clements, P., McKinnon, P.J. and Caldecott, K.W. (2009) Defective DNA ligation during short-patch single-strand break repair in ataxia oculomotor apraxia-1. Mol. Cell. Biol. **29**, 1354–1362

29 Fortini, P. and Dogliotti, E. (2007) Base damage and single-strand break repair: mechanisms and functional significance of short- and long-patch repair subpathways. DNA Repair **6**, 398–409

30 Takahashi, T., Tada, M., Igarashi, S., Koyama, A., Date, H., Yokoseki, A., Shiga, A., Yoshida, Y., Tsuji, S., Nishizawa, M. and Onodera, O. (2007) Aprataxin, causative gene product for EAOH/AOA1, repairs DNA single-strand breaks with damaged 3′-phosphate and 3′-phosphoglycolate ends. Nucleic Acids Res. **35**, 3797–3809

31 Narciso, L., Fortini, P., Pajalunga, D., Franchitto, A., Liu, P., Degan, P., Frechet, M., Demple, B., Crescenzi, M. and Dogliotti, E. (2007) Terminally differentiated muscle cells are defective in base excision DNA repair and hypersensitive to oxygen injury. Proc. Natl. Acad. Sci. U.S.A. **104**, 17010–17015

Received 13 February 2009
doi:10.1042/BST0370577

nature genetics

Mutations in *PNKP* cause microcephaly, seizures and defects in DNA repair

Jun Shen[1,12], Edward C Gilmore[2,3,12], Christine A Marshall[1], Mary Haddadin[4,11], John J Reynolds[5], Wafaa Eyaid[6], Adria Bodell[1], Brenda Barry[1], Danielle Gleason[2], Kathryn Allen[1], Vijay S Ganesh[1], Bernard S Chang[1], Arthur Grix[7], R Sean Hill[2], Meral Topcu[8], Keith W Caldecott[5], A James Barkovich[9] & Christopher A Walsh[1,2,10]

Maintenance of DNA integrity is crucial for all cell types, but neurons are particularly sensitive to mutations in DNA repair genes, which lead to both abnormal development and neurodegeneration[1]. We describe a previously unknown autosomal recessive disease characterized by microcephaly, early-onset, intractable seizures and developmental delay (denoted MCSZ). Using genome-wide linkage analysis in consanguineous families, we mapped the disease locus to chromosome 19q13.33 and identified multiple mutations in *PNKP* (polynucleotide kinase 3′-phosphatase) that result in severe neurological disease; in contrast, a splicing mutation is associated with more moderate symptoms. Unexpectedly, although the cells of individuals carrying this mutation are sensitive to radiation and other DNA-damaging agents, no such individual has yet developed cancer or immunodeficiency. Unlike other DNA repair defects that affect humans, *PNKP* mutations universally cause severe seizures. The neurological abnormalities in individuals with MCSZ may reflect a role for PNKP in several DNA repair pathways.

We identified the autosomal recessive disorder MCSZ with the following features: microcephaly, infantile-onset seizures, developmental delay and variable behavioral problems, especially hyperactivity. MCSZ was observed in multiple pedigrees of Middle Eastern and European origin (**Fig. 1**). The first three pedigrees were Arabic Palestinians living in Jordan and the United States. Three other families with similar manifestations were Arabic (Kingdom of Saudi Arabia), Turkish and of mixed European ancestry (United States). We later found less severely affected individuals with MCSZ from family 7, which is also mixed European heritage and from the United States. Brain magnetic resonance imaging scans (MRIs) consistently show microcephaly with preserved brain structures, without apparent neuronal migration or other structural abnormalities, and with no evidence of degeneration (**Fig. 2**). The affected individuals did not develop ataxia or other neurological symptoms. Routine clinical genetic and metabolic screening showed no abnormalities. Despite careful inquiry, individuals with MCSZ were not found to have a higher frequency of common or uncommon infections, offering no clinical evidence of immunodeficiency. Cells from one affected individual showed sensitivity to irradiation in a standard colony-survival assay[2,3]. However, no affected person has developed cancer by age 21, and heterozygous carriers have not developed early-onset cancer or any sign of immunodeficiency (**Supplementary Note**, Clinical Information, **Supplementary Table 4** and Summary).

Genome-wide linkage screens suggested a single common homozygous region on chromosome 19q in all six individuals with MCSZ in the consanguineous families 1–3. This same locus showed homozygosity in the two affected individuals from family 4 and in the single one from family 5 whose parents were not known to be related. We observed no other regions of linkage, including at known primary microcephaly loci. Notably, all six affected individuals in the three Palestinian families (families 1–3) were homozygous for the same 3-cM (1.5-Mb) haplotype (between markers D19S879 and D19S907) at chromosome 19q13.33, suggesting a common ancestor (**Supplementary Fig. 1**). Further investigation revealed a common town of origin for these families. Linkage analysis of families 1–4 and family 6 generated a combined maximum two-point lod score of 5.60 at D19S867 with $\theta = 0$ (**Supplementary Table 1**) and a maximum multipoint lod score of 7.12 (**Supplementary Fig. 2**).

We sequenced 41 genes within the minimal region (**Supplementary Fig. 2** and **Supplementary Table 2**), and only the *PNKP* gene contained mutations. We found homozygous mutations in families 1–5

[1]Howard Hughes Medical Institute, Department of Neurology, Beth Israel Deaconess Medical Center and Program in Neuroscience, [2]Division of Genetics and The Manton Center for Orphan Disease Research, Department of Medicine, Children's Hospital Boston, and [3]Division of Child Neurology, Department of Neurology, Massachusetts General Hospital, Harvard Medical School, Boston, Massachusetts, USA. [4]Department of Pathology, Cytogenetics Laboratory, Al-Bashir Hospital, Ministry of Health, Amman, Jordan. [5]Genome Damage and Stability Centre, University of Sussex, Falmer, Brighton, UK. [6]Genetics & Endocrinology, Department of Pediatrics, King Fahad National Guard Hospital, King Abdul Aziz Medical City, Saudi Arabia. [7]Department of Medical Genetics, Kaiser-Permanente Point West Medical Offices, Sacramento, California, USA. [8]Hacettepe University, Medical Faculty, Ihsan Dogramaci Children's Hospital, Department of Pediatrics, Section of Pediatric Neurology, Ankara, Turkey. [9]Department of Radiology, Department of Neurology and Department of Pediatrics, University of California at San Francisco, San Francisco, California, USA. [10]Broad Institute of Massachusetts Institute of Technology and Harvard University, Cambridge, Massachusetts, USA. [11]Present address: Quest Diagnostics, Nichols Institute, San Juan Capistrano, California, USA. [12]These authors contributed equally to the work. Correspondence should be addressed to C.A.W. (Christopher.Walsh@childrens.harvard.edu).

Received 6 August 2009; accepted 23 December 2009; published online 31 January 2010; doi:10.1038/ng.526

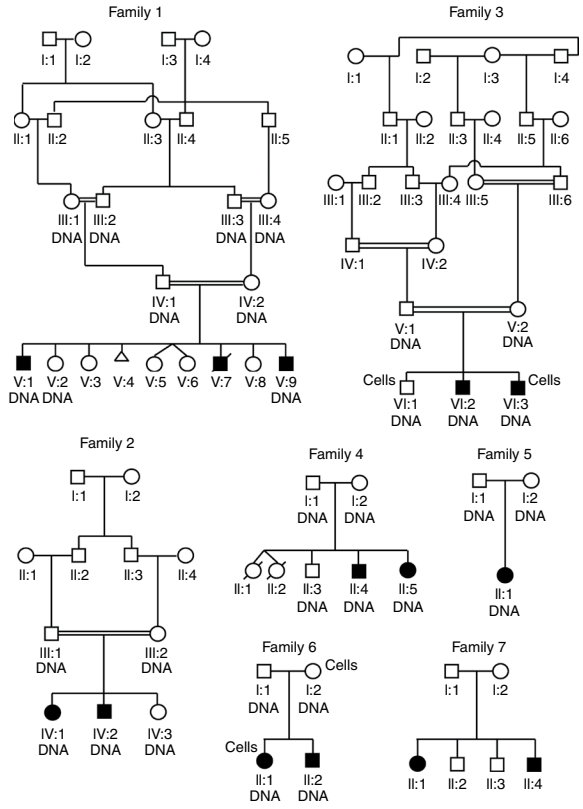

Figure 1 Pedigrees of MCSZ families. Family 1 represents a consanguineous Palestinian pedigree in Jordan. Family 2 shows another consanguineous Palestinian pedigree that is reportedly unrelated to family 1, also in Jordan. Family 3 is also consanguineous and Palestinian, but the family now resides in the United States. Family 4 is from the Kingdom of Saudi Arabia, and the parents were not known to be consanguineous. Family 5 is from Turkey, and the parents were not known to be related. Family 6 is of mixed European descent from the United States (German-Irish). Family 7 is also of mixed European (Swedish, Italian, Irish and English) heritage, from the United States. The individuals from whom samples were obtained are indicated by the label 'DNA'. The individuals from whom we established lymphoid cell lines are indicated by the label 'Cells'. Cells and DNA were available for all members of family 7.

and compound heterozygous mutations in families 6 and 7 (see **Fig. 3** and **Supplementary Fig. 3** for detailed analyses of all mutations). The three Palestinian families (families 1–3) shared a homozygous base pair substitution in exon 11 (G975A), resulting in the nonconservative amino acid change E326K. The families from the Saudi Arabia (family 4) and Turkey (family 5) had the same homozygous 17-bp duplication (17-bp dup) in exon 14 (1250_1266dup), resulting in a frameshift, T424GfsX48. Family 6 (European) had two heterozygous mutations: the same 17-bp duplication in exon 14 as the Saudi and Turkish families and a point mutation in exon 5 (C526T) that results in L176F. The moderately affected members of family 7 (European) showed compound heterozygosity, carrying the 17-bp duplication mutation in exon 14 and a 17-bp deletion in intron 15 that disrupts proper mRNA splicing.

To confirm that these mutations were pathogenic, we analyzed Epstein-Barr virus (EBV)-transformed lymphocytes derived from affected individuals from families 3 (E326K substitution) and 7 (17-bp duplication and intron 15 deletion). The samples from the severely affected individual (family 3) and mildly affected individuals (family 7) had much lower concentrations of PNKP protein than did those from unaffected or heterozygous family members (**Fig. 3b**). RT-PCR analysis showed that the intron 15 deletion in family 7 disrupts mRNA splicing and causes skipping of exon 15; a barely detectable level of properly spliced mRNA remains (**Fig. 3c**). The low concentrations of PNKP protein and the indistinguishable phenotype among severely affected individuals from families 1–6 suggest that all of these mutations impair PNKP severely or completely; in contrast, the individuals from family 7, who have a slightly milder phenotype and carry one noncoding mutation, may retain some PNKP activity.

Unexpectedly, despite their diverse ancestries (Saudi, Turkish and mixed European), all chromosomes with the 17-bp duplication mutation seem to share the same haplotype for 18 SNPs in or near the *PNKP* locus (**Supplementary Fig. 4a**). The low frequency of this mutated haplotype (**Supplementary Fig. 4b**) suggests that the 17-bp

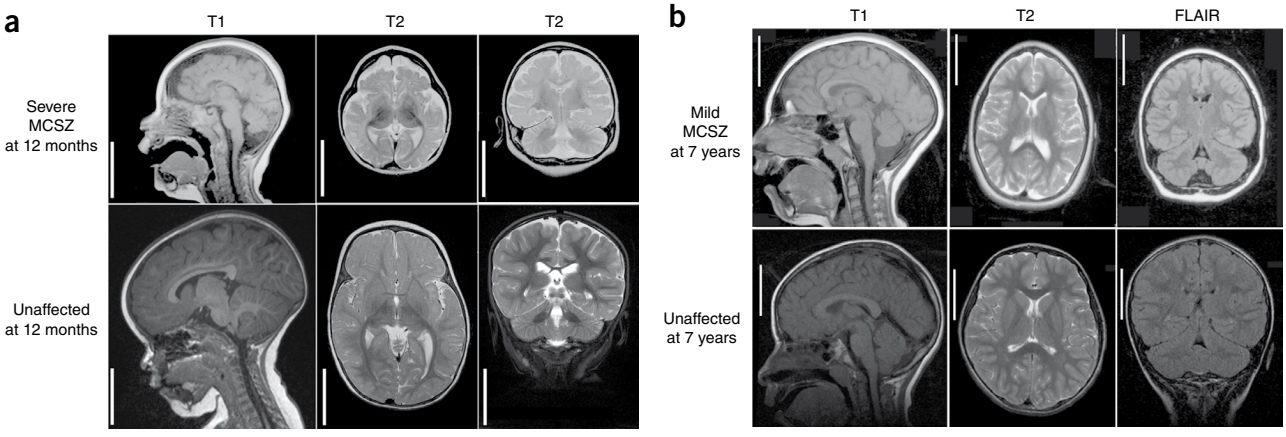

Figure 2 Brain MRIs of individuals with MCSZ. Representative MRI images are shown from families 4 (**a**; severely affected) and 7 (**b**; moderately affected) with aged-matched controls. MRIs of severely affected individuals from other families were similar to the representative images in **a**. Sagittal images are shown on the left (T1), axial images in the middle (T2) and coronal images on the right (T2 (**a**) and FLAIR (**b**)), with the MRI sequence noted above the image. The MRIs show that, despite the microencephaly (small brain), the gyral pattern is not clearly abnormal, indicating an absence of visible neuronal migration abnormality. The cerebellum is proportionately small compared to the cerebrum, and the subpallium (basal ganglia or ventral cerebrum) is proportionate to the pallium (dorsal cerebrum). There is no evidence of atrophy or glial scarring. Scale bar indicates 5 cm for both unaffected and MCSZ images.

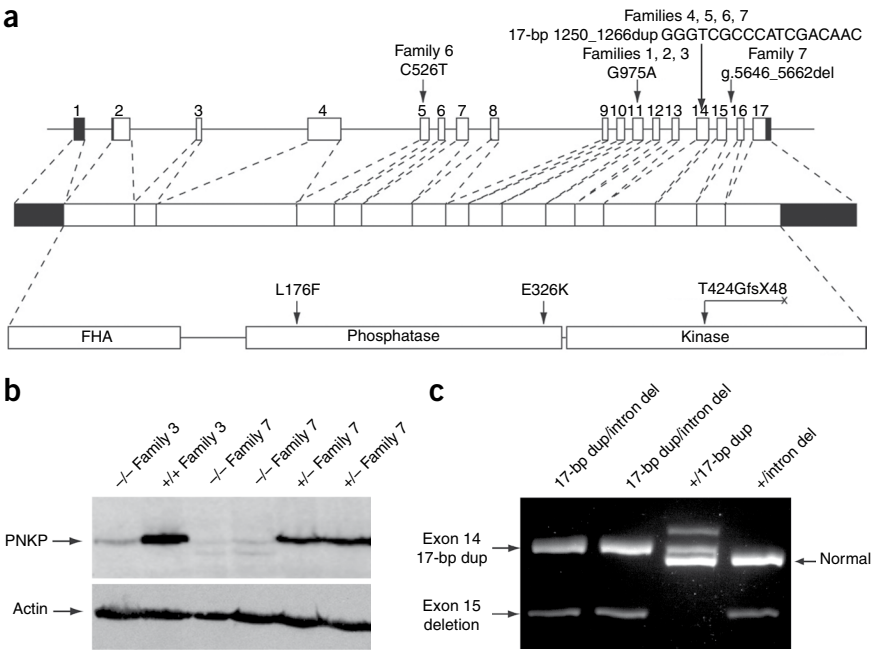

Figure 3 *PNKP* mutations in individuals with MCSZ. (**a**) The diagram shows four different mutations identified in human *PNKP* genomic DNA, mRNA and protein, including protein domains (forkhead is indicated by 'FHA'). The human *PNKP* gene consists of 17 exons (boxes) and encodes a peptide of 521 amino acids. Filled boxes represent untranslated regions and open boxes represent coding regions. Lines connecting the exons represent introns. (**b**) Protein blot for PNKP. Lanes 1 and 2 show samples from an individual with MCSZ (VI:3 with the E326K mutation) and an unaffected brother (VI:1), respectively, from family 3. Lanes 3 and 4 represent individuals with MCSZ (II:1 and II:4, with both a 17-bp duplication (dup) and a 17-bp intron 15 deletion (del)) from family 7. In contrast, lanes 5 and 6 represent the father (I:1) and brother (II:3) from this family, who are both heterozygous for the 17-bp intron 15 del. The band indicates a molecular weight of ~60 kDa (predicted size 57 kDa). Anti–β-actin is a loading control. (**c**) RT-PCR products of mRNA from members of family 7 show the expected size from the normal copy of *PNKP* cDNA (636 bp), seen in lanes 3 and 4 from unaffected carriers. The 17-bp dup results in a 653-bp fragment, seen in lanes 1, 2 and 3. The band in lanes 1, 2 and 4 corresponding to a size of 548 bp is found in samples with the intron 15 deletion lacking exon 15 (determined from sequencing; data not shown). A small amount of normal-sized transcript is seen in lanes 1 and 2 with higher exposure (data not shown), indicating that a small amount of normal PNKP mRNA can be produced.

duplication in exon 14 is probably of shared origin and very old in all or most of these families. Nonetheless, the mutation shows an extremely low carrier frequency in the general population, as the 17-bp duplication mutation was absent in 1,080 Middle Eastern or European-descended control chromosomes, and all other mutations were absent in all 280 control chromosomes screened.

The PNKP protein has been implicated in repair of both double-strand breaks (DSBs) and single-strand breaks (SSBs)[4,5], because its phosphatase domain removes 3′-phosphates and its kinase domain phosphorylates 5′-hydroxyl groups, steps that are required for DNA ligation[6]. PNKP's forkhead domain mediates interaction with the non-homologous end-joining (NHEJ) complex via XRCC4 or with the SSB and base-excision repair (BER) pathways via XRCC1 (**Supplementary Fig. 5**)[4–8]. *PNKP* has been further implicated in the repair pathway disrupted in an ataxic neurodegenerative disease, spinocerebellar ataxia with axonal neuropathy (denoted SCAN1 and involving a

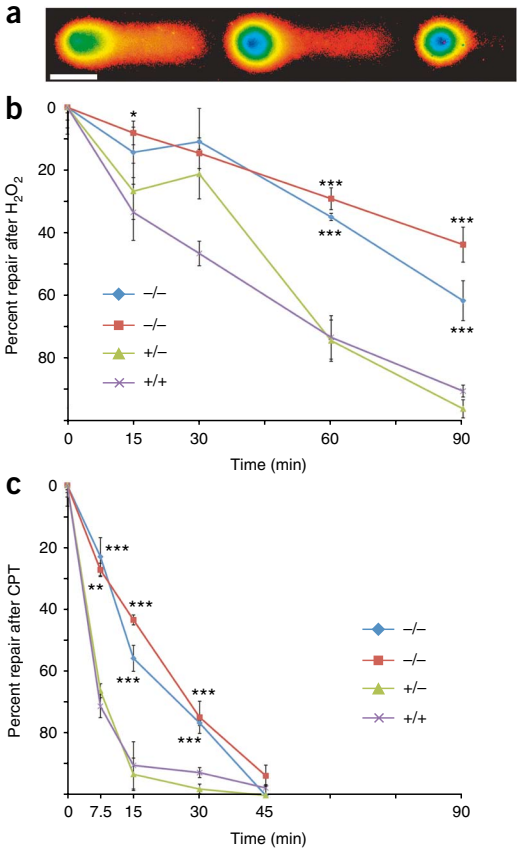

Figure 4 Lymphocytes from individuals with MCSZ show abnormal DNA repair. (**a**) Examples of comet assay results. The intensity of the fluorescence is represented in pseudocolor, as the electrical field drives damaged, loose DNA from left to right. The image at left shows a cell with 50% tail DNA with the body of the nucleus (green) on the left and the tail of the comet derived from the damaged DNA extending to the right. The images middle and right show progressively less damage, with 29% and 11% tail DNA, respectively. (**b**) After hydrogen peroxide treatment with 0 min for recovery, cells show their maximum damage. Cells derived from individuals with MCSZ (blue and red) show significant impairment in their ability to repair DNA after hydrogen peroxide was removed, whereas cells derived from unaffected family members were able to repair DNA much more efficiently. (**c**) After camptothecin (CPT) treatment, there was also statistically significantly slower repair in cells derived from individuals with MCSZ compared with those from unaffected family members (green and purple). However, after 45 min, the MCSZ-derived cells were able to repair all CPT damage, in contrast to hydrogen peroxide–treated cells. All cells were derived from family 7. Blue diamonds and red squares indicate cells from individuals with MCSZ carrying the exon 14 17-bp duplication and the intron 15 17-bp deletion (II:1 and II:4, respectively); green triangles represent an unaffected parent who is heterozygous for the intron 15 17-bp deletion (I:1); purple crosses represent an unaffected sibling with no mutation (II:2). $*P = 0.05$; $**P < 0.005$; $***P < 0.0005$. Scale bar, 50 μm.

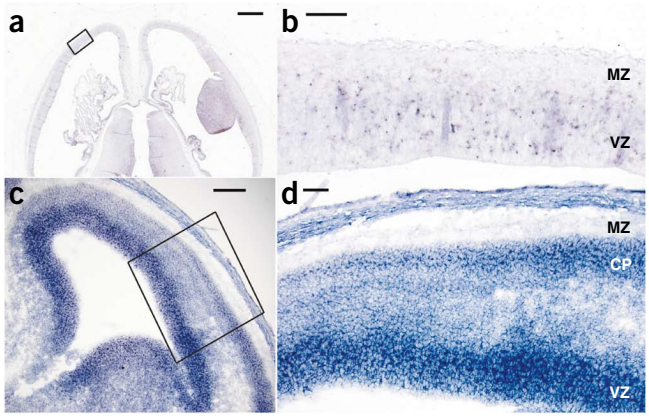

Figure 5 *PNKP in situ* hybridization. (**a**,**b**) *In situ* hybridization of Carnegie Stage 22 human embryos (~54 postovulatory days) with an antisense probe to human *PNKP* (**a**). The sense strand (not shown) showed no specific hybridization. A higher-magnification image of the boxed area in the developing cerebral cortex is shown (**b**). The ventricular zone (VZ), containing proliferating cells, shows PNKP mRNA expression, whereas the cell-sparse marginal zone (MZ) has no staining. (**c**,**d**) Mouse embryonic day 14 cerebral cortex (**c**) (with high-magnification view of the boxed region (**d**)) shows a similar staining pattern, with high expression within the proliferating VZ and lower but maintained expression within differentiated neurons of the cortical plate (CP). **a** and **b** are in the transverse plane, and **c** and **d** are coronal. Scale bars indicate 1 mm (**a**), 100 μm (**b**), 150 μm (**c**) and 75 μm (**d**).

mutation in *TDP1*) (see **Supplementary Fig. 5** for additional details). The abnormalities in a clinical irradiation–sensitivity test already reflect deficiencies in NHEJ, which is required to repair radiation-induced DSBs. Because PNKP potentially has roles in additional repair pathways, we tested cells in response to other DNA-damaging agents.

We examined the response of cells from individuals with MCSZ to free radical damage from hydrogen peroxide, which predominately requires BER, and camptothecin, which requires TDP1 via its activity on topoisomerase I, using an alkaline comet assay that detects both SSBs and DSBs by quantifying the amount of DNA that moves from a nucleus after electrophoresis. Typical nuclei with various degrees of DNA damage are shown in **Figure 4a**. We determined the relative amount of DNA damage by measuring the 'Percent tail DNA' (DNA that has moved out of the nucleus). The relative amount of DNA damage repair was quantified as the percent tail DNA after toxin exposure at various times of recovery (see **Supplementary Table 2** for all data) and normalized to the maximum and minimum damage for each cell line in each experiment. MCSZ-derived cell lines were significantly impaired in their ability to repair hydrogen peroxide–induced damage (**Fig. 4b**) and were also delayed in repairing camptothecin-induced damage (**Fig. 4c**). MCSZ-derived cells were eventually able to repair the camptothecin-induced damage after 45 min, but they could not repair all hydrogen peroxide–induced damage even after 90 min. These data suggest that camptothecin-induced damage may be easier to repair than free radical damage in the setting of *PNKP* mutations. Although individuals with MCSZ do not develop the ataxia that characteristically results from *TDP1* mutations that also cause camptothecin sensitivity[9,10], it may be that those we studied are too young (oldest 21 years) to show this characteristic, or there may be some mechanism compensating for the loss of PNKP.

Microcephaly can result from failure to produce enough neurons during development (primary microcephaly) or from degeneration after normal development. Individuals with MCSZ have no evidence of brain atrophy or clinical regression, making degeneration unlikely (see the **Supplementary Note**, Clinical Information, for further details). *In situ* hybridization indicated that human and mouse *PNKP* mRNAs are expressed in both dividing neuronal precursors in the cerebral cortical ventricular zone (VZ, **Fig. 5a–c**) and in postmitotic neurons of the cortical plate (CP, **Fig. 5d**), which is consistent with potential roles in both dividing and postmitotic neurons. In addition, we found that when we used RNAi to reduce levels of Pnkp in dissociated mouse neurons *in vitro*, there was a small but statistically significant increase in apoptosis in both neuronal precursors and differentiated neurons (**Supplementary Figs. 6** and **7** and **Supplementary Table 3**) compared to cells transfected with control plasmids. This indicates that microcephaly could result from apoptosis of precursors, differentiated neurons or both cell types.

Disruption of genes encoding NHEJ repair proteins can lead to microcephaly in humans and/or mice, as occurs in LIG4 syndrome, which involves mutations in *Lig4* (refs. 11–13), in severe combined immunodeficiency with microcephaly, or as a result of mutations in *NHEJ1* (encoding Cernunnos)[14], *Xrcc4* (ref. 15), *Xrcc6* (encoding Ku70) and *Xrcc5* (encoding Ku80)[16] and *Prkdc* (encoding DNA-PKcs)[17]. However, disruption of NHEJ function is not known to cause seizures, which are a prominent clinical feature of MCSZ. In contrast, disruption of the BER and SSB pathways by deletion of *Xrcc1* in mice produced normal brain size, but the mutant mice developed ataxia, loss of interneurons within the cerebellum and seizure-like behavior[18]. The intriguing similarity of phenotypes between humans with MCSZ who carry mutations in *PNKP* and mice with targeted deletion of *Xrcc1* does suggest a potential common mechanism, demonstrating the requirement for the BER and SSB pathways in the prevention of seizures, potentially via an interneuron-specific requirement of the BER and SSB pathway. Therefore, the unique pattern of neurological symptoms of MCSZ may reflect a requirement for PNKP activity in multiple DNA repair pathways.

METHODS

Methods and any associated references are available in the online version of the paper at http://www.nature.com/naturegenetics/.

Note: Supplementary information is available on the Nature Genetics website.

ACKNOWLEDGMENTS

J.S. was supported by the Victoria and Stuart Quan Fellowship. Research was supported by grants from the US National Institute of Neurological Disorders and Stroke to E.C.G. (5K08NS059673-02) and to C.A.W. (NSR01-35129), the Fogarty International Center (R21 NS061772), the Manton Center for Orphan Disease Research, the Simons Foundation and by Dubai Harvard Foundation for Medical Research. E.C.G. was also supported by a K12 Child Health Research Center award to Children's Hospital Boston (1 K12 HD052896-01A1) and a Research in Training Award from the Child Neurology Foundation. J.J.R. and K.W.C. are supported by the UK Medical Research Council (G0600776 & G0400959). C.A.W. is an Investigator of the Howard Hughes Medical Institute. We thank S. Lindsay and S. Lisgo from the Medical Research Council–Wellcome Trust Human Developmental Biology Resource (HDBR), Institute of Human Genetics, International Centre for Life, Newcastle upon Tyne, UK, for performing human *in situ* hybridizations. We are grateful for genotyping services provided by the Center for Inherited Disease Research (CIDR). CIDR is fully funded through a federal contract from the US National Institutes of Health to The Johns Hopkins University, contract number HHSN268200782096C and NIH N01-HG-65403. Genotyping at Children's Hospital Boston is supported by the Intellectual and Developmental Disabilities Research Centers (CHB MRDDRC, P30 HD18655).

AUTHOR CONTRIBUTIONS

J.S. helped to characterize MCSZ syndrome, identified the MCSZ locus and calculated lod scores, sequenced genes in the MCSZ locus to identify *PNKP* mutations and wrote the manuscript; E.C.G. helped to characterize MCSZ syndrome,

identified the moderately affected MCSZ family, performed RT-PCR on moderately affected family samples, performed comet assays, organized and analyzed Sequenom experiments, did analysis of PNKP mutation, performed mouse RNAi experiments, helped perform mouse *in situ* hybridizations and wrote the manuscript; C.A.M. sequenced genes in the MCSZ locus to identify *PNKP* mutations and helped perform human *in situ* hybridizations; M.H. identified affected patients and provided clinical information; J.J.R. performed PNKP protein blots and confirmatory comet assays; W.E. identified affected patients and provided clinical information; A.B. organized clinical information and patient samples; B.B. organized clinical information and patient samples; D.G. organized patient samples and helped perform Sequenom experiments; K.A. organized patient samples and helped perform sequencing experiments; V.S.G. helped analyze Sequenom experiments; B.S.C. helped organize clinical information to identify MCSZ syndrome; A.G. identified affected patients and provided clinical information; R.S.H. helped organize genetic data and calculate lod scores; M.T. identified affected patients and provided clinical information; K.W.C. advised on comet assays, supervised PNKP protein blotting and edited the manuscript; A.J.B. characterized MRIs for patient classification; C.A.W. directed the overall research and wrote the manuscript.

The genetic study was approved by Beth Israel Deaconess Medical Center and Children's Hospital Boston Institutional Review Boards. Appropriate informed consent was obtained from all involved human subjects. All animal work was approved by Harvard Medical School, Beth Israel Deaconess Medical Center and Children's Hospital Boston Institutional Animal Care and Use Committees.

COMPETING INTERESTS STATEMENT

The authors declare no competing financial interests.

Published online at http://www.nature.com/naturegenetics/.
Reprints and permissions information is available online at http://npg.nature.com/reprintsandpermissions/.

1. McKinnon, P.J. DNA repair deficiency and neurological disease. *Nat. Rev. Neurosci.* **10**, 100–112 (2009).
2. Huo, Y.K. *et al.* Radiosensitivity of ataxia-telangiectasia, X-linked agammaglobulinemia, and related syndromes using a modified colony survival assay. *Cancer Res.* **54**, 2544–2547 (1994).
3. Sun, X. *et al.* Early diagnosis of ataxia-telangiectasia using radiosensitivity testing. *J. Pediatr.* **140**, 724–731 (2002).
4. Jilani, A. *et al.* Molecular cloning of the human gene, *PNKP*, encoding a polynucleotide kinase 3′-phosphatase and evidence for its role in repair of DNA strand breaks caused by oxidative damage. *J. Biol. Chem.* **274**, 24176–24186 (1999).
5. Karimi-Busheri, F. *et al.* Molecular characterization of a human DNA kinase. *J. Biol. Chem.* **274**, 24187–24194 (1999).
6. Chappell, C., Hanakahi, L.A., Karimi-Busheri, F., Weinfeld, M. & West, S.C. Involvement of human polynucleotide kinase in double-strand break repair by non-homologous end joining. *EMBO J.* **21**, 2827–2832 (2002).
7. Whitehouse, C.J. *et al.* XRCC1 stimulates human polynucleotide kinase activity at damaged DNA termini and accelerates DNA single-strand break repair. *Cell* **104**, 107–117 (2001).
8. Ali, A.A., Jukes, R.M., Pearl, L.H. & Oliver, A.W. Specific recognition of a multiply phosphorylated motif in the DNA repair scaffold XRCC1 by the FHA domain of human PNK. *Nucleic Acids Res.* **37**, 1701–1712 (2009).
9. Takashima, H. *et al.* Mutation of TDP1, encoding a topoisomerase I–dependent DNA damage repair enzyme, in spinocerebellar ataxia with axonal neuropathy. *Nat. Genet.* **32**, 267–272 (2002).
10. El-Khamisy, S.F. *et al.* Defective DNA single-strand break repair in spinocerebellar ataxia with axonal neuropathy-1. *Nature* **434**, 108–113 (2005).
11. Frank, K.M. *et al.* Late embryonic lethality and impaired V(D)J recombination in mice lacking DNA ligase IV. *Nature* **396**, 173–177 (1998).
12. Barnes, D.E., Stamp, G., Rosewell, I., Denzel, A. & Lindahl, T. Targeted disruption of the gene encoding DNA ligase IV leads to lethality in embryonic mice. *Curr. Biol.* **8**, 1395–1398 (1998).
13. O'Driscoll, M. *et al.* DNA ligase IV mutations identified in patients exhibiting developmental delay and immunodeficiency. *Mol. Cell* **8**, 1175–1185 (2001).
14. Buck, D. *et al.* Cernunnos, a novel nonhomologous end-joining factor, is mutated in human immunodeficiency with microcephaly. *Cell* **124**, 287–299 (2006).
15. Gao, Y. *et al.* A critical role for DNA end-joining proteins in both lymphogenesis and neurogenesis. *Cell* **95**, 891–902 (1998).
16. Gu, Y. *et al.* Defective embryonic neurogenesis in Ku-deficient but not DNA-dependent protein kinase catalytic subunit-deficient mice. *Proc. Natl. Acad. Sci. USA* **97**, 2668–2673 (2000).
17. Vemuri, M.C., Schiller, E. & Naegele, J.R. Elevated DNA double strand breaks and apoptosis in the CNS of *scid* mutant mice. *Cell Death Differ.* **8**, 245–255 (2001).
18. Lee, Y. *et al.* The genesis of cerebellar interneurons and the prevention of neural DNA damage require XRCC1. *Nat. Neurosci.* **12**, 973–980 (2009).

ONLINE METHODS

Genetic screening. Family 1 underwent a genome-wide linkage screen using about 400 microsatellite markers in the ABI linkage mapping set MD v2.5 at an average density of 10 cM (Applied Biosystems) at the Children's Hospital in Boston (Genotyping Core facility). We performed genome-wide screens for families 3 and 4 at the Center for Inherited Disease Research using microsatellite markers that were also at an average spacing of 10 cM. We carried out fine mapping using polymorphic microsatellite markers from the ABI linkage mapping set HD v2.5 at an average density of 5 cM (Applied Biosystems) along with additional microsatellite markers identified using the UCSC Human Genome Browser[19] and synthesized primers (Sigma-Genosys). Two point and multipoint lod scores calculated using Allegro[20] assumed recessive inheritance, full penetrance and a disease allele frequency of 0.0001. All nucleotide numbers are in reference to cDNA, in which A (of the ATG start site) is +1, except for the intronic deletion, which is in reference to the genomic sequence, in which A of ATG of the translational start site is +1 (all from UCSC genome browser, NCBI Build 36.1).

***PNKP* protein blotting.** For *PNKP*, we grew EBV-transformed lymphocytes in DMEM with 15% (vol/vol) FCS plus normocin. We lysed 2×10^5 cells in SDS loading buffer at 90 °C and fractionated them by SDS-PAGE. We transferred the proteins to Hybond-C Extra Nitrocellulose (GE Healthcare), stained them with Ponceau S solution (Sigma) and washed them in TBST (25 mM Tris base, 150 mM NaCl, 2.7 mM KCl, 0.1% Tween-20) before carrying out immunoblotting with anti-PNK (SK3195)[21] at a dilution of 1:1,000 in 5% (wt/vol) nonfat dried milk. We then washed the blots and probed them with goat anti-rabbit IgG–horseradish peroxidase (HRP) secondary antibody (DakoCytomation), which we detected with ECL detection reagents (GE Healthcare). The blot was then washed in TBST and re-probed with monoclonal anti–β-actin (Sigma) using rabbit anti-mouse IgG HRP (DakoCytomation) as a secondary antibody.

***PNKP* reverse transcriptase polymerase chain reaction.** We grew EBV-transformed lymphocytes as described above. We isolated the RNA using the RNeasy Mini Kit (Qiagen). We used 5 μg of total RNA for first-strand synthesis with oligo(dT) primers using the SuperScript III First-Strand Synthesis SuperMix (Invitrogen). We then used 1 μl of the product of the reverse transcriptase reaction was used in PCR with primers from Exon 10 to Exon 17.

Comet assays. We carried out alkaline comet assays using the protocol from CometAssay ES unit (Trevigen). Briefly, we grew affected individual–derived EBV-transformed lymphocytes as described above. Cells were obtained before treatment or exposed to 100 μM hydrogen peroxide (Sigma) or 10 μM camptothecin (Sigma) for 30 and 60 min, respectively, at 37 °C. After exposure, we immediately collected the cells for the 0 min recovery time point or washed them once, resuspended them in growth medium and incubated at 37 °C. Cells were subsequently at the times indicated. We then embedded the cells in low-melt agarose, plated them on microscope slides, lysed them, treated them with alkaline solution and then electrophoresed the slides in alkaline solution at 1 V cm^{-1} (21 V) with ~300 mA for 30 min. We washed and dried the slides were washed and stained the DNA with SYBR green. Images of nuclei and tails were taken with a Nikon TE2000-E fluorescent microscope with CCD camera, and we determined the percent tail DNA with CometScore 1.5 software (TriTek).

***In situ* hybridization.** We performed human *in situ* hybridizations at the Human Developmental Biology Resource (Institute of Human Genetics, International Centre for Life, UK) with probes to antisense human *PNKP* cDNA (nucleotides +488–1500). We carried out mouse *in situ* hybridizations as described[22], with an antisense probe derived from mouse *Pnkp* cDNA (+386–1566).

We calculated statistics using Microsoft Excel unless otherwise described. The 'Percent DNA repair' values in **Figure 4** were determined by measuring the mean of the percent tail DNA in three separate wells (raw data are presented in **Supplementary Fig. 5**), using the combined percent tail DNA at 0 min recovery (maximum damage) and the minimum damage measured as full recovery for each individual cell line. We determined *P* values by comparing the baseline adjusted DNA repair level from three separate wells using a *t*-test that "compared" each MCSZ-deficient line to two normal control cell lines with a two-tailed distribution and homoscedastic test.

***PNKP* mutation analysis.** We performed PNKP protein alignments using MegAlign (Lasergene). We examined the three-dimensional structure of mouse Pnkp in MacPyMOL from previously published information[23]. The Branch Point analysis was done with Human Splicing Finder version 2.3 (http://www.umd.be/HSF/)

Determination of the 17-bp duplication haplotype in exon 14. We determined Sequenom SNP genotypes in samples from affected and control individuals at the Molecular Genetics Core Facility at Children's Hospital Boston. We determined haplotypes were determined with Mendelian inheritance patterns for parents and offspring and with Phase haplotype-determining software[24–26] for control samples.

PNKP RNA interference studies. pSilencer 1.0 GFP had RNAi oligos targeted to mouse *Pnkp* mRNA identified via the Broad Institute RNAi Consortium shRNA Library, ligated into EcoRI and ApaI sites (Mo-Pnkp RNAi primers, **Supplementary Table 3**; Invitrogen). We dissected the cerebral cortices from embryonic day 13.5 Swiss-Webster mice and dissociated them using the Papain Dissociation System (Worthington Biochemical). We washed the cells twice in HBSS buffer (HyClone, Thermo Scientific) and transfected them using the Amaxa Nucleofactor 96 well shuttle system (Amaxa Biosystems) with either pSilencer mouse *Pnkp*-RNAi GFP or pSilencer GFP with or without pSport-human *PNKP* (Open Biosystems, Entrez clone ID BC057659). We grew the cells on poly-L-ornithine–treated (Sigma-Aldrich) Lab-Tek chamber slides with Permox (Nalge Nunc International) in DMEM with 10% (vol/vol) FBS for the Pax6 studies. For the NeuN studies, we changed the medium of the cultures to Neurobasal complete medium after 4 h. We fixed the cultures with 4% (vol/vol) paraformaldehyde 24 h after transfection. We carried out immunostaining in PBS with 0.2% (wt/vol) Triton X-100 and 10% (vol/vol) goat serum with chick anti-GFP (Abcam), rabbit anti-cleaved caspase 3 (Asp175) (Cell Signaling Technology), mouse anti-Pax6 (The Developmental Studies Hybridoma Bank) or mouse anti-NeuN (Chemicon). We detected the primary antibodies with anti-chicken IgG Alexa 488 (Invitrogen) and donkey anti-mouse IgG Cy3 or donkey anti-rabbit IgG Cy5 (Jackson ImmunoResearch). Images were obtained by looking for GFP-positive cells with a Nikon TE2000-E fluorescent microscope and Metamorph imaging software. We counted the cells from digital images with the counter blinded as to whether the cultures were derived from *Pnkp*-RNAi or control transfections. We calculated the *P* values in **Supplementary Figure 7** using a *G*-test of goodness of fit with 5 degrees of freedom, a two-tailed *P* value and no Williams correction[27].

Mouse *Pnkp* RNA interference testing. We tested the mouse (Mo) *Pnkp* RNAi construct Mo-*Pnkp*-DsRed or the human construct Hu-*PNKP*-DsRed, both expressed by the pCAG-DsRed vector[28]. We transfected the RNAi control vector (empty vector)/Mo-*Pnkp*-DsRed fusion protein, Mo-*Pnkp*-RNAi/Mo-*Pnkp*-DsRed, RNAi-control/Hu-*PNKP*-DsRed fusion and Mo-*Pnkp*-RNAi/Hu-*PNKP*-DsRed into NIH-3T3 cells with Lipofectamine 2000 (Invitrogen) according to the manufacturer's protocol. We counted the cells after 24 h in culture. Random fields were chosen by the level of GFP expression, and the number of cells with high GFP expression was counted, followed by the number of cells expressing the Ds-Red fusion protein. DsRed expression was nuclear, as expected from PNKP localization (data not shown). For protein blot analysis, we transfected NIH-3T3 cells as described above. After 24 h of culture, we lysed the cells using the protocol described above for PNKP protein blotting. After quantifying the protein using the BCA assay, we separated 25 μg of protein per lane by PAGE. We transferred the protein to a membrane, blocked it with Odyssey blocking buffer (Li-Cor Biosciences) and probed with mouse anti-actin (AC-15), rabbit anti-GFP (Molecular Probes) and rabbit anti-DsRed (Clontech). Primary antibody was detected with anti-mouse labeled with IRDye 700 or anti-rabbit IRDye 800 (Li-Cor Biosciences) and detected with Li-Cor imaging system. In the bar graph, protein amounts are normalized to RNAi control conditions.

doi:10.1038/ng.526

19. Karolchik, D. *et al*. The UCSC Genome Browser Database: 2008 update. *Nucleic Acids Res.* **36**, D773–D779 (2008).
20. Gudbjartsson, D.F., Jonasson, K., Frigge, M.L. & Kong, A. Allegro, a new computer program for multipoint linkage analysis. *Nat. Genet.* **25**, 12–13 (2000).
21. Breslin, C. & Caldecott, K.W. DNA 3′-phosphatase activity is critical for rapid global rates of single-strand break repair following oxidative stress. *Mol. Cell. Biol.* **29**, 4653–4662 (2009).
22. Berger, U.V. & Hediger, M.A. Differential distribution of the glutamate transporters GLT-1 and GLAST in tanycytes of the third ventricle. *J. Comp. Neurol.* **433**, 101–114 (2001).
23. Bernstein, N.K. *et al.* The molecular architecture of the mammalian DNA repair enzyme, polynucleotide kinase. *Mol. Cell* **17**, 657–670 (2005).
24. Stephens, M., Smith, N.J. & Donnelly, P. A new statistical method for haplotype reconstruction from population data. *Am. J. Hum. Genet.* **68**, 978–989 (2001).
25. Stephens, M. & Donnelly, P. A comparison of Bayesian methods for haplotype reconstruction from population genotype data. *Am. J. Hum. Genet.* **73**, 1162–1169 (2003).
26. Stephens, M. & Scheet, P. Accounting for decay of linkage disequilibrium in haplotype inference and missing-data imputation. *Am. J. Hum. Genet.* **76**, 449–462 (2005).
27. McDonald, J.H. *Handbook of Biological Statistics* (Sparky House, Baltimore, 2008).
28. Matsuda, T. & Cepko, C.L. Electroporation and RNA interference in the rodent retina *in vivo* and *in vitro*. *Proc. Natl. Acad. Sci. USA* **101**, 16–22 (2004).